The regulation of circadian rhythms by the natural light environment

Laura Steel

Magdalen College

Sleep and Circadian Neuroscience Institute

Nuffield Department of Clinical Neuroscience

A thesis submitted to the University of Oxford for the degree of Doctor of Philosophy (PhD)

Trinity 2024

Declaration of authorship

I declare that all the work presented here is my own, except where otherwise stated. This work has not been submitted for any other degree or professional qualification.

Word count (excluding tables, figure legends, appendices and references): 49617

Laura Steel, Trinity term 2024

This thesis is dedicated in loving memory of my four wonderful grandparents

Acknowledgements

I feel immensely lucky to have had the opportunity to complete a PhD. I would like to thank the people who have made my PhD so rewarding, and my time in Oxford so happy.

First and foremost, an enormous thank you to my primary supervisor, Professor Stuart Peirson. Thank you for always bringing enthusiasm and a thoughtful perspective to a situation, and for being so very generous with your time and advice. Your patience and encouragement have motivated me through the challenging moments of this PhD and as such, have really developed my confidence as a scientist – thank you.

Thank you to my secondary supervisor, Professor Russell Foster - your insightful and enthusiastic advice on papers has been so appreciated. To my colleagues, thank you for so generously and patiently sharing your expertise. In particular, to Dr Eric Tam, Dr Laurence Brown, Dr Takuma Morimoto, Dr Carrie Pothecary, Dr Ma'ayan Semo, Professor Mark Hankins, Professor David Bannerman, Professor Manuel Spitschan, Professor Hannah Smithson, Kieran Foster and to all the animal technicians. A big thank you to Selma, Shiwen and Marissa – your company in the lab and field (and beyond) made work so much more fun! Finally, thank you to my sixth-form Biology teacher, Mrs Ballard, whose lessons made me so excited about Biology.

There are many people who have made my PhD such a happy period, but I must thank a few in particular. Maisie, Frances and Ashna - thank you for being such kind, fun and supportive friends (and housemates) for the last four years. To Hannah and Jack, and to my wonderful friends beyond Oxford – James, Calla, Aine, Ellie, Georgia, Lottie and Drewe. To Winston, thank you for your constant support – for celebrating little PhD wins so enthusiastically and keeping me going through the "final push". Finally, thank you to my wonderful family – immediate and extended, to whom I owe so very much. In particular, to my parents, grandparents and Isabella. Thank you for your unwavering love, care, and understanding; and for all of the many ways you have supported and prioritised my education. To you all, thank you for sharing the highs and lows of life and the PhD with me - doing this without you would have been so much harder and a lot less fun!

Thank you to those who made this project possible - the DTP and BBSRC for funding this project, and to Magdalen College for providing a beautiful haven in which to recharge in throughout my PhD. Finally, to the animals which died to produce this work – thank you.

Abstract

Almost all life on Earth has evolved under ~24hr cycles in environmental conditions such as light and temperature. Consequently, virtually all organisms have evolved internally generated near-24hr cycles in physiology and behaviour, known as circadian rhythms. However, these rhythms rarely have a period of exactly 24hrs. As such, daily adjustment by external time cues is required to align the phase of internal circadian rhythms with the external environment. This enables organisms to anticipate predictable daily changes in environmental conditions, and optimise physiology and behaviour to the varying demands of day and night. In mammals, the primary time cue is light, and therefore this process is referred to as photoentrainment. In nature, light is a complex and dynamic stimulus – changing in intensity and spectrum across the 24hr period. In addition, the timing of an organism's activity can significantly influence the light available for photoentrainment. Despite these complexities, the vast majority of our knowledge of photoentrainment has been generated using rodent models under highly simplified laboratory conditions. The circadian system is very plastic, and as such, the disparity between laboratory and natural light environments is highly relevant for our understanding of photoentrainment. Therefore, in this thesis I take an ecologically guided approach to the study of photoentrainment, by incorporating two key elements of the natural light environment into laboratory studies. Firstly, the opportunity for behaviour to regulate light exposure, and secondly, the dynamic changes in both light intensity and spectrum that occur across the day/night cycle.

I initially characterise how mice are exposed to light under standard laboratory conditions, before developing a method to allow mice to self-modulate their light exposure. Under this paradigm mice sample their light environment most extensively at twilight, identifying an important role for behaviour in determining the timing of light exposure in naturalistic environments. We show that crepuscular light sampling is abolished in mice lacking a circadian clock, suggesting a feedback loop between light, the circadian clock and behaviour. The relative contribution of classical photoreceptors and melanopsin in driving this pattern of behaviour is then considered using knockout mouse models. Next, we extend our behavioural paradigm by simulating the experience of daylight and twilight on the mouse retina, and demonstrate that the spectral changes associated with twilight alters mouse behaviour. Finally, we consider reflectance as a further source of directional and seasonal variation in intensity and spectrum in the natural light environment, which has rarely been considered in previous studies. Collectively, our data highlight the important role of behaviour and naturally-occurring changes in intensity and spectrum in regulating photoentrainment. This thesis extends our understanding of circadian photoentrainment beyond

simplified laboratory conditions, to naturalistic conditions comparable to those under which circadian rhythms evolved.

Contents

Chapter 3. Light sampling behaviour regulates circadian entrainment

Chapter 4. The role of melanopsin and classical photoreceptors in regulating light sampling behaviour

Chapter 5. Effects of natural light spectra on light sampling behaviour and circadian entrainment

Chapter 6. Characterising the light environment of a natural woodland using hyperspectral imaging

Chapter 7. General Discussion

Appendix. The effect of nestbox availability on behavioural anxiety levels

References

Abbreviations

ANOVA – analysis of variance

Bmal1 / BMAL1 – brain and muscle ARNT-Like 1 gene / protein

Clock / CLOCK – circadian locomotor output cycles kaput gene / protein

cry / CRY – cryptochrome gene / protein

CT – circadian time

DD – constant dark

hr(s) – hour(s)

IF – image forming

ipRGC – intrinsically photosensitive retinal ganglion cell

IRC – irradiance response curve

IS – interdaily stability

IV – intradaily variability

LD – light:dark

LED – light emitting diode

LL – constant light

MEA – multi-electrode array

NIF – non-image forming

Opn4 / OPN4 – melanopsin gene / protein

per / PER – period gene / protein

PLR – pupillary light response

PRC – phase response curve

RA – relative amplitude

(R)SPD – (relative) spectral power distribution

SCN – suprachiasmatic nuclei

TTFL – transcriptional translational feedback loop

ZT – zeitgeber time

λmax – wavelength of peak sensitivity

Chapter 1. Introduction

1.1 Circadian rhythms and photoentrainment

1.1.1 Features of circadian rhythms

Due to the rotation of the earth on its axis, almost all organisms have evolved under predictable ~24hr cycles in environmental conditions such as light and temperature. As a result, many organisms have evolved circadian rhythms (Edgar et al., 2012). These are endogenous rhythms in physiology and behaviour with a period (known as tau, τ) of near 24hrs. Circadian rhythms occur at multiple levels of biological organisation – from rhythms in gene expression (Zhang et al., 2014) to sleep (Beersma and Gordijn, 2007), and have several defining features. Firstly, they persist under constant conditions, which provides evidence for an internally generated biological clock (Pittendrigh, 1960). Secondly, circadian rhythms are temperature compensated, meaning that period length does not change as a function of temperature (Sweeney and Hastings, 1960); and finally, circadian rhythms can be aligned, or entrained, to external stimuli (Pittendrigh, 1960).

1.1.2 Circadian entrainment

Circadian rhythms rarely have a period of precisely 24hrs, hence the term 'circadian' coming from the Latin for 'around a day'. In fact, the exact period length shows both between-species (interspecific) and within-species (intraspecific) variation. Therefore, under constant conditions organisms will still display robust circadian rhythms, but the onset of the rhythms will drift, or 'free run'. For example, mice have an average period of 23.7hrs (Jud et al., 2005), which means that the active phase (known as alpha, α) will begin slightly earlier each day under constant darkness (DD). An adjustment, or 'phase-shift', of the circadian clock by external time cues (termed zeitgebers, from the German for 'time-giver') is therefore necessary to maintain appropriate alignment between the internal clock and the external environment (Roenneberg et al., 2003). This process is known as entrainment, and a system is considered entrained when the period of the entraining stimulus (T) is equal to that of the endogenous period (τ).

Whilst there is evidence that food availability (Brinkhof et al., 1998) and temperature (Sweeney and Hastings, 1960) are important zeitgebers, light is the primary time cue in mammals and this process is therefore referred to as photoentrainment. Light influences the phase of the clock differently across the 24hr period, with light at dawn advancing the clock (a positive phase shift, $+\Delta\varphi$), light at dusk delaying the clock (a negative phase shift, $-\Delta\varphi$), and light during the subjective

day having little effect (the 'dead zone'). These time-dependent effects of light on the phase of the clock are summarised by the Phase Response Curve (PRC) (Fig1.1) (Foster et al., 2020; Pittendrigh and Minis, 1964). Entrainment by discrete phase-shifts to light is referred to as the discrete, or non-parametric, model of entrainment (Pittendrigh, 1958). Whilst the shape of PRCs are broadly comparable across organisms (DeCoursey, 1960; Hoban and Sulzman, 1985; Khalsa et al., 2003), the exact shape can show both interspecific (Pittendrigh and Daan, 1976) and intraspecific (DeCoursey, 1960) variation. This depends on period length, with fast clocks (periods <24hrs) such as those possessed by nocturnal species (DeCoursey, 1960) showing larger delays and smaller advances than diurnal species (Brown, 2016; Khalsa et al., 2003). These phase shifts by light are intensity-dependent, exhibiting sigmoidal irradiance response curves (IRC) (Foster et al., 2020). The creation of multiple IRCs for different monochromatic light stimuli enable action spectra for non-image forming (NIF) responses to light to be generated, such as the pupillary light response (PLR) (Lucas et al., 2001) and circadian phase shifting (Hattar et al., 2003; Provencio and Foster, 1995; Yoshimura and Ebihara, 1996). The peak sensitivity of an action spectra can be useful in characterising the photoreceptors mediating a response to light (Peirson et al., 2005a).

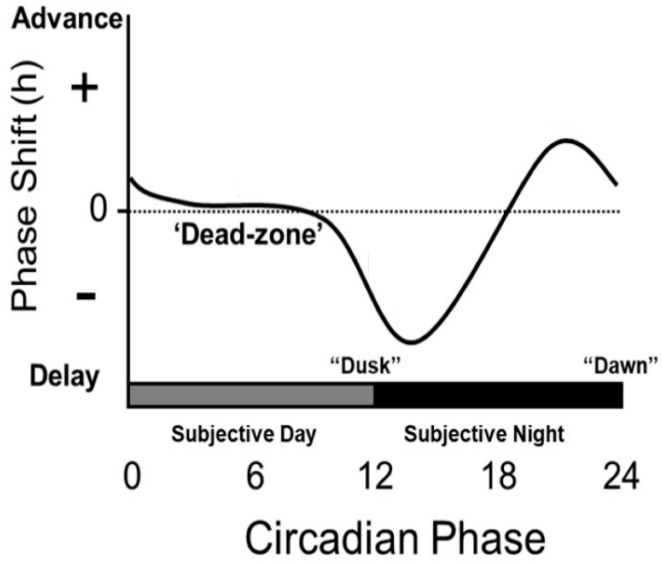

Figure 1.1 – The Phase Response Curve (PRC) for a nocturnal rodent, e.g. a mouse, characterising the phase shifting effect of light delivered at different timepoints of the circadian phase. Circadian phase can be expressed on a circadian timescale (CT), where subjective day is defined as CT0-12, and subjective night CT12-24. Figure reproduced from Foster et al (2020).

In addition to generating discrete phase-shifts, light is thought to alter the clock via a continuous (or parametric) model – with light altering the velocity of the oscillator so that it approximates its period to that of the entraining light:dark (LD) cycle (Aschoff, 1979). The intensity-dependent

change in period in response to constant light supports this idea (Daan, 2000; Eckel-Mahan and Sassone-Corsi, 2015). The direction of change differs between diurnal and nocturnal species, with period length decreasing with increasing light intensity in diurnal species, and increasing in length in nocturnal species (Roenneberg and Foster, 1997); a concept referred to as Aschoff's Rule.

1.1.3 Direct effects of light

Light can also directly modulate behaviour and physiology. If delivered during the night, the direct effects of light on nocturnal rodents include a pronounced reduction in activity levels known as negative masking (Mrosovsky, 1999; Thompson et al., 2008) an increase in sleep (Lupi et al., 2008; Tsai et al., 2009) and alterations to body temperature (Rupp et al., 2019) and mood (LeGates et al., 2014; Milosavljevic, 2019). In diurnal species, light can increase arousal (Cajochen et al., 2005) and cognitive performance (Chellappa et al., 2011).

1.2 Photic input to the mammalian clock

1.2.1 The dual function of the mammalian eye

Photic input in mammals is exclusively ocular. This is in contrast to non-mammalian vertebrates, many of which also possess extra-retinal photoreceptors located in the hypothalamus, pineal gland and parietal eye (Menaker, 1968; Peirson et al., 2009; Shand and Foster, 1999; Tamotsu and Morita, 1986; Underwood et al., 2001; Underwood and Calaban, 1987). The loss of extra-retinal photoreceptors in mammals is thought to have resulted from a period of nocturnality in the early evolution of eutherian mammals, due to diurnal competition from dinosaurs (Gerkema et al., 2013; Walls and Walls, 1942). Nocturnality may have rendered deep-brain photoreceptors unnecessary in mammals, and therefore light for photoentrainment is detected exclusively by retinal photoreceptors in mammals. As such, the mammalian eye performs both image-forming (IF) and non-image forming (NIF) functions.

1.2.2 Structure of the retina

Light enters the mammalian eye through the cornea and travels through the aqueous humour, lens and vitreous humour, before reaching the photosensitive and highly stratified retina at the back of the eye (Fig1.2). The retina is comprised of five neuronal cell types (Fig1.2) - photoreceptor cells, bipolar cells, horizontal cells, amacrine cells and finally retinal ganglion cells (RGCs), the axons of which form the optic nerve (Baden et al., 2018; Hatori and Panda, 2010). These are organised into five layers - three of which contain cell bodies (the outer nuclear layer (OPL, or photoreceptor layer), the inner nuclear layer (INL), and the ganglion cell layer (GCL)) and are themselves

separated by two synaptic layers (the inner and outer plexiform layers (IPL; OPL)) (Baden et al., 2020). The mammalian retina is inverted and therefore light reaches the inner retina first. However, most light continues through the retina to the photoreceptor layer, where light is converted into changes in membrane potential during the phototransduction cascade (Goldberg et al., 2016). Put simply, light information from photoreceptors is then passed to bipolar cells, which connect the OPL to the IPL and transmit information to the RGCs. This pathway is more complex in rods than cones, with rods synapsing onto a specific type of bipolar cell, the rod bipolar cell, which signal to RGCs indirectly via AII amacrine cells (Demb and Singer, 2015). From RGCs, information is relayed to different image-forming and non-image forming centres of the brain via the optic nerve (Dhande and Huberman, 2014; Euler et al., 2014). Horizontal and amacrine cells provide lateral interactions within the outer and inner plexiform layers, respectively (Demb and Singer, 2015). The reality is unsurprisingly far more complex, and further information can be found in reviews on the topic (Baden et al., 2018; Demb and Singer, 2015).

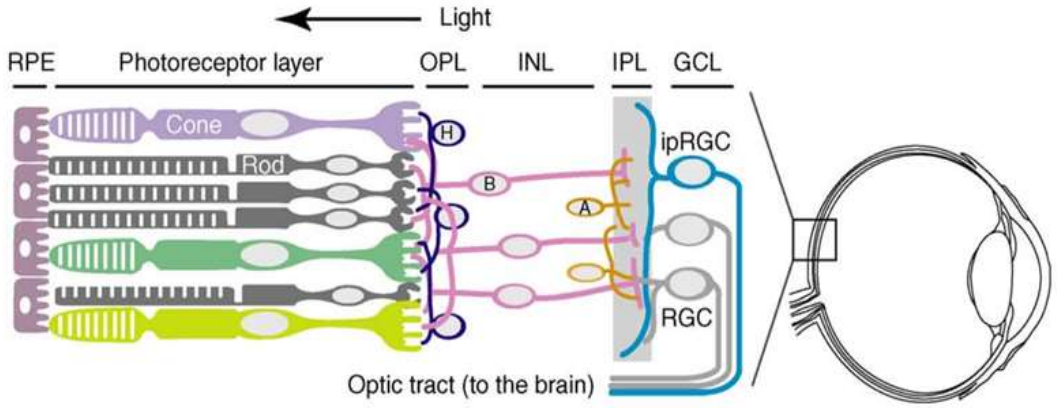

Figure 1.2 Structure of the mammalian retina. Layers from the back of the retina to the front: retinal pigment epithelial (RPE), photoreceptor layer, outer plexiform layer (OPL), inner nuclear layer (INL), inner plexiform layer (IPL), ganglion cell layer (GCL). Cell types: cones (lilac, green, yellow), rods (dark grey), horizontal cells (dark purple, 'H'), bipolar cells (pink, 'B'), amacrine cells (orange, 'A'), retinal ganglion cells (light grey, 'RGC'), intrinsically photosensitive retinal ganglion cell (blue, 'ipRGC'). The mouse tapetum sits behind the RPE. Figure reproduced from Hatori and Panda (2010).

1.2.3 Photoreceptors and phototransduction

The photoreceptor layer contains rod and cone cells. Both of these photoreceptor cell types have a specialised photosensory organelle known as the outer segment (OS), which express visual pigments specific to the photoreceptor type – rod opsins (OPN2) and cone-opsins (OPN1)

(Goldberg et al., 2016). Visual pigments are transmembrane proteins formed of an opsin protein bound to a photosensitive vitamin-A derived chromophore, 11-*cis* retinal. The absorption of photons by 11-*cis* retinal drives its isomerisation to the all-*trans* state, and initiates the phototransduction cascade (Fig1.3). This begins with a conformational change in the opsin protein within 1ms, which activates the G-protein transducin. From here, phosphodiesterase is activated resulting in the hydrolysation of cGMP to GMP. This causes cyclic nucleotide gated ion channels in the OS plasma membrane to close (3-5% of channels by a single photon (Fain et al., 2010)), leading to the hyperpolarisation of the photoreceptor cell and a fall in the release of glutamate at the synaptic terminal (Peirson et al., 2018). In this way, photoreceptors are unusual neurons since they are depolarised in the absence of a stimulus (i.e. the dark) - producing a constant release of glutamate via ribbon synapses. This is known as the 'dark current' (Wang and Kefalov, 2011). Eventually, the opsin decays to its inactive form, whilst the isomerised chromophore is recycled to 11-*cis* retinal in the retinal pigment epithelium (RPE) via the visual cycle (Wang and Kefalov, 2011; and reviewed in Strauss, 2005).

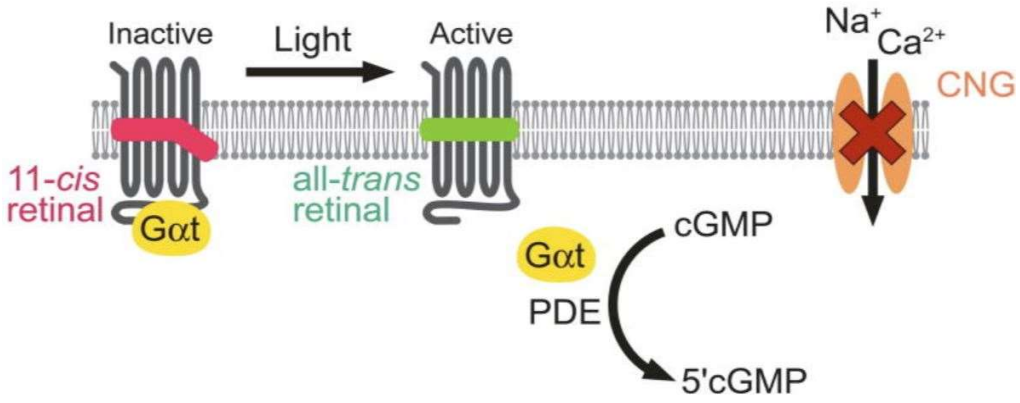

Figure 1.3 Simplified schematic of the vertebrate phototransduction cascade. Gαt (transducin), PDE (phosphodiesterase), cGMP (cyclic guanosine monophosphate), CNG (cyclic nucleotide gated). Figure reproduced from Hatori and Panda (2010).

1.2.3 Specialisations of rods and cones

Whilst both rod and cone cells perform this phototransduction cascade, these photoreceptors differ in several ways. These specialisations allow rods to mediate scotopic vision (low light, ~7-11 log quanta), whilst cones mediate photopic (bright light, ~10-15 log quanta) and colour vision (Ingram et al., 2016; Lamb, 2016; Peirson et al., 2018). Structural differences between rods and cones may be particularly relevant. In the rod OS, visual pigment is located in internal membrane

discs, and therefore separated from the plasma membrane. In contrast, visual pigment in cones is located within stacked invaginations of the plasma membrane. As such, there is a much larger surface area for the rapid movement of substances. This includes chromophore transfer for pigment regeneration and faster calcium feedback, enabling cones to function more effectively in photopic conditions (Fu and Yau, 2007; Yau, 1994). Secondly, in contrast to cones, multiple rod cells converge onto individual rod bipolar cells, providing a higher signal to noise ratio and increased sensitivity, albeit at the cost of acuity (Euler et al., 2014; Völgyi et al., 2009).

Due to the specialisations of rods and cones, the organisation of the retina can differ between species with divergent visual environments, as a result of different selection pressures. Firstly, the relative abundance of rods and cones can vary between species. Predominantly nocturnal species such as the mouse, have a rod-dominated retina – with rods accounting for 97% of photoreceptors (6.4 million) and cones for only 3% (200,000) (Carter-Dawson and Lavail, 1979; Jeon et al., 1998; Leamey et al, 2008; Peirson et al., 2018). This is similar to the rat (Galindo-Romero et al., 2022). Secondly, regional specialisations of the retina differ between species (Baden et al., 2020). Unlike primates, mice do not possess a *fovea centralis* – a high acuity region in the central retina with high cone density and no rods or blood vessels present (Hendrickson, 2009). Therefore, the photoreceptor density of the mouse retina is most comparable to the primate peripheral retina (Peirson et al., 2018).

Interspecific specialisations also extend to the spectral sensitivity of cone opsins. Although all vitamin A-based photopigments have the same characteristic absorption spectrum when expressed on a wave number scale (Dartnall, 1953), their maximal sensitivity (λmax) can vary widely (from 360 to 620nm) (Peirson et al., 2009). This latter characteristic can be useful for determining the photopigment responsible for a given biological response (Govardovskii et al., 2000; Hattar et al., 2003; Peirson et al., 2005a). Opsins are G-protein-coupled receptors, formed of seven transmembrane domains. Key functional residues are involved in spectral tuning, in particular those within the retinal binding site – the extracellular cavity where the chromophore binds - with some motifs rendering an opsin more sensitive to long or short wavelength light (Hagen et al., 2023). Cone cells can express different opsins, each with differing spectral sensitivities, and it is the comparison of these which form the basis of colour vision. Mice express two cone opsins – a UV sensitive (UVS) and medium-wavelength sensitive (MWS) opsin, maximally sensitive to 360nm and 508nm, respectively (Jacobs et al., 1991; Sun et al., 1997). Interestingly, unlike in most mammalian species, mouse cone opsins display a dorsal-ventral gradient across the retina, with UVS opsin expressed most highly in the ventral retina and MWS opsin expressed most strongly in the dorsal retina (Röhlich et al., 1994). This renders the upper visual field very sensitive to UV light

which may aid detection of predators against the sky (Yilmaz and Meister, 2013). 95% of cones co-express both these opsins, although a small subset solely express UVS opsin (Peirson et al., 2018; Röhlich et al., 1994). In contrast, humans have three cone opsins – a SWS opsin (λmax = 420nm), MWS opsin (λmax = 534nm) and LWS opsin (λmax = 564nm) (Bowmaker and Dartnall, 1980). This means that mice are less sensitive to long-wavelength light than humans. However, due to the bell-shaped spectral sensitivity curve, wavelength and intensity are interchangeable in deciding the likelihood that a photon is absorbed (Do, 2019). Therefore, contrary to common perception, mice can still detect long-wavelength light if it is sufficiently bright. This has important implications for animal husbandry (Peirson et al., 2018).

1.2.4 Discovery of melanopsin

Since light was known to regulate circadian entrainment, and it was also known that the removal of the murine eye abolished all IF and NIF responses to light (Nelson and Zucker, 1981), an obvious question arose in the 1990s – do rods or cones mediate photoentrainment? However, a series of elegant studies, outlined below, demonstrated that neither rods or cones were necessary and identified a small subset (2-5%) of RGCs with intrinsically photosensitive properties - referred to as intrinsically photosensitive melanopsin-expressing retinal ganglion cell (ipRGCs; or pRGCs or mRGCs).

The dogma that rods and cones were the only photoreceptors in the mammalian eye was first challenged in 1991, when Foster et al (1991) demonstrated that mice lacking rods and cones (carrying the *rd/rd Pde6b*^{rd1} mutation; Pittler and Baehr, 1991) exhibit normal photoentrainment. Since a small number of cones (5%) may be retained in the *rd/rd* retina (Carter-Dawson et al., 1978), transgenic mice lacking all rods and cones were developed and shown to retain non-image forming responses to light, including circadian phase-shifting (*rdta/cl;* Freedman et al., 1999), suppression of pineal melatonin (*rd/rd cl;* Lucas et al., 1999) and the pupillary light response (*rd/rd cl;* Lucas et al., 2001). Interestingly, the spectral sensitivity of these responses peaked around 480nm (Lucas et al., 2001; Yoshimura and Ebihara, 1996), differing from that of rods (λmax = 498nm) and cones (λmax = 360nm and 508nm). These studies raised the intriguing possibility that the mammalian eye possessed a third class of photoreceptor. Subsequent studies demonstrated that a small subset of RGCs in the mouse retina express the photopigment melanopsin (Provencio et al., 2000) - an opsin encoded by the gene *Opn4*, with a peak sensitivity of 480nm, which was first identified in the African clawed frog, *Xenopus laevis* (Provencio et al., 1998). The distribution and anatomy of these cells was very similar to the RGCs forming the retinohypothalamic tract (RHT) – which conveys light information from the retina to the suprachiasmatic nuclei (SCN) (Hattar et al., 2002; Moore and Lenn, 1972). Melanopsin knockout studies demonstrated its importance for

circadian photoentrainment – with attenuated phase-shifting responses to light in mice lacking melanopsin (Panda et al., 2002b; Ruby et al., 2002), whilst triple knockout studies showed that rods, cones and melanopsin accounted for all retinal photoreception (Hattar et al., 2003; Panda et al., 2003). Berson (et al., 2002) and Sekaran et al (2003) demonstrated the intrinsic photosensitive properties of this subpopulation of RGCs, and Melyan et al (2005) and Panda et al (2005) provided the final link by showing that melanopsin could induce photosensitivity. Therefore, these studies collectively demonstrated that ipRGCs are a third class of photoreceptors in the mammalian eye, with a peak sensitivity around 480nm. The peak sensitivity of human melanopsin was confirmed in humans by Bailes and Lucas (2013) (λmax = 479nm).

1.2.5 Characteristics of melanopsin

Melanopsin differs to rod and cone opsins in several ways. Most notably, melanopsin actually shares greatest homology with invertebrate photopigments, such as those found in squid (Provencio et al., 1998), than vertebrate photopigments. This can explain the growing evidence that melanopsin is a bistable pigment – meaning that chromophore regeneration can occur endogenously by exposure to a certain wavelength of light, compared to vertebrate photopigments in which the RPE is needed to regenerate 11-*cis* retinal (Do, 2019; Mure et al., 2007). Melanopsin is also expressed at a much lower density than classical photoreceptors (~1/1000 of rods and cones, Do, 2019) which allows light to reach the photoreceptor layer in the inverted mammalian retina. As such, melanopsin primarily regulates photopic responses to light (~11-15 log quanta; Peirson et al., 2018). This low sensitivity to light is compensated for by a long integration time (x20 longer than rods and >100x longer than cones, Do, 2019); resulting in melanopsin responding slowly to light (Berson et al., 2002; Hattar et al., 2002; Mouland and Brown, 2022). This makes them well suited to act as circadian photoreceptors, which need to integrate light over relatively long durations whilst being less sensitive to temporary light stimuli not associated with the daily light-dark cycle (Mohawk et al., 2012).

Whilst the ability of mice lacking rods and cones to entrain to an LD cycle demonstrates that classical photoreceptors are not required for photoentrainment, it does not preclude them from contributing. Indeed, photoentrainment is only attenuated, not abolished, in mice lacking melanopsin (*Opn4*$^{-/-}$) (Panda et al., 2002b; Ruby et al., 2002), demonstrating that rods and cones can mediate entrainment in the absence of melanopsin (Hankins et al., 2008; Peirson et al., 2018; Van Oosterhout et al., 2012). Furthermore, the action spectra for phase shifting by light peaks at 480nm in *rd/rd cl* mice (Hattar et al., 2003), but peaks at 500nm in retinally-intact mice (Yoshimura and Ebihara, 1996). Thus, it is now well established that ipRGCs receive intrinsic signals from

melanopsin phototransduction, as well as extrinsic input from rods and cones (Aggelopoulos and Meissl, 2000; Güler et al., 2008; Lucas et al., 2012).

The description of the characteristics of melanopsin is complicated by the multiple subtypes of ipRGCs which have been defined. There are five, perhaps six, subtypes (M1-M6) which differ in melanopsin expression levels, soma size, dendritic stratification, and projections to the brain (Aranda and Schmidt, 2021; Hughes et al., 2016; Schmidt et al., 2011). M1 ipRGCs are arguably the most well defined. They have the highest levels of melanopsin expression (Hughes et al., 2016) and by using the Opn4tau-LacZ line, M1 ipRGCs have been shown to project primarily to the SCN for the photoentrainment of circadian rhythms, as well as other circadian centres such as the intergeniculate leaflet (IGL) and ventral lateral geniculate leaflet (vLGN) (Hattar et al., 2006; Schmidt et al., 2011). However, ipRGCs more broadly project to a wide range of brain regions beyond those regulated in circadian entrainment (Do, 2019; Morin and Allen, 2006), explaining their involvement in a range of IF and NIF responses to light. These include the regulation of the pupillary light reflex (PLR) (Lucas et al., 2001), light aversion (Johnson et al., 2010; Semo et al., 2010), sleep induction (Altimus et al., 2008; Hubbard et al., 2013; Lupi et al., 2008; Tsai et al., 2009) and mood and cognition (Legates et al., 2012; Tam et al., 2016); as well as more recently, in image formation (Brown et al., 2010; Ecker et al., 2010; Zele et al., 2018). Although the mechanisms by which ipRGCs mediate the acute effects of light remain less well characterised than that of the circadian system, recent work by Rupp et al (2019) identified that input to the SCN is not sufficient to regulate the acute effects of light on thermoregulation and sleep, and these are in fact driven by a distinct subset of ipRGCs that do not project to the SCN. Furthermore, melanopsin can also be expressed as either a long or short isoform, which have been shown to mediate different NIF responses to light – with the short isoform (OPN4S) mediating the PLR, the long isoform (OPN4L) mediating negative masking, and both isoforms regulating circadian phase shifting and light-mediated sleep induction (Jagannath et al., 2015).

1.3 Circadian clocks

1.3.1 Discovery of the suprachiasmatic nuclei (SCN)

ipRGCs project to the master clock in the SCN via the RHT. The discovery of the SCN as the mammalian pacemaker followed an extensive series of lesion studies by Curtis Richter who had observed periodic spontaneous activity in rats (Richter, 1922). Of all his studies, only a lesion to the anterior hypothalamus disrupted rhythmicity, albeit in a single rat (Richter, 1965; Weaver,

1998). From here, a paired nuclei in the anterior hypothalamus, known as the suprachiasmatic nuclei, was identified as a likely site of the pacemaker when lesions here resulted in the abolishment of circadian rhythms in activity patterns and drinking behaviour in rats (Stephan and Zucker, 1972), as well as in cortisol secretion (Moore and Eichler, 1972). The SCN was confirmed to receive photic input by the use of radioactive tracers to map the RHT from the optic nerve to the SCN (Moore and Lenn, 1972). From this work, it seemed likely that the SCN was important for the generation of circadian rhythms and their regulation by light. *In vivo* assessment of glucose consumption in the SCN (Schwartz et al., 1983; Schwartz and Gainer, 1977) and electrical activity (Inouye and Kawamura, 1979) confirmed the presence of oscillations – with SCN activity being high during the day and low at night. These traits were also observed *in vitro* (Gillette, 1986; Newman and Hospod, 1986). Interestingly, the electrical activity of neurons outside of the SCN were in antiphase to those within the SCN (Inouye and Kawamura, 1979). To examine this further, the SCN was isolated *in vivo* from the rest of the brain. It was observed that rhythmic neuronal activity continued in the SCN but was abolished in extra-SCN neurons (Inouye and Kawamura, 1979), demonstrating a role for the SCN in both generating and coordinating rhythmicity. Transplantation of the SCN between wildtype hamsters (with a period of ~24hrs) and homozygous *tau/tau* mutant golden hamsters (with a period of ~20hrs; Ralph and Menaker, 1988) demonstrated that the period of restored rhythmicity matched that of the SCN donor genotype (Ralph et al., 1990). Collectively, these studies provided evidence for the role of the SCN as the primary pacemaker in mammals (Ono et al., 2024; Weaver, 1998).

1.3.2 Features of the SCN

The SCN is a bilaterally paired nucleus containing ~20,000 neurons (Mohawk et al., 2012), which can be subdivided into two sections on the basis of connectivity and neuropeptide expression – a ventral (core) region and a dorsal (shell) region (Colwell, 2011; Hastings et al., 2018; Moore and Silver, 1998) A simplified version of the current working model is that vasoactive intestinal peptide (VIP) expressing neurons in the core region receive photic input from the retina, via the RHT, and signal to arginine vasopressin (AVP) expressing shell neurons (Colwell, 2011; Hastings et al., 2018), which subsequently regulate SCN outputs (Saper et al., 2005). However, in reality, this is more complex, with ipRGCs having been shown to additionally innervate neurons in the shell region (Fernandez et al., 2016). Interestingly, the SCN neurons of both diurnal (Sato and Kawamura, 1984) and nocturnal organisms show higher electrical activity during the day – indicating that the diurnal/nocturnal switch is downstream of the SCN. An important feature of SCN neurons is intercellular coupling which acts to create a coherent SCN output with a period of ~24hrs (Herzog et al., 2004) from individual neurons with a wide variation in period (22hr to 30hrs) (Welsh et al.,

1995). More recently, the recognition of season by the SCN has also been shown to be a network emergent property (Olde Engberink et al., 2020). The need for intercellular coupling also confirms that it must be a sub-cellular mechanism that is responsible for generating circadian oscillations – a molecular clock mechanism that is now known to be based on an intracellular transcriptional-translational feedback loop (TTFL), consisting of a number of core clock genes.

1.3.3 The molecular clock

The discovery of the molecular clock in eukaryotes was awarded the 2017 Nobel Prize in Physiology and Medicine (Callaway and Ledford, 2017). The molecular clock is hugely complex (Takahashi, 2017), but at its core the TTFL is composed of a positive and negative limb (Fig1.4; Fig1.5). In eukaryotes, the positive limb consists of the core clock proteins, CLOCK and BMAL1, which form a heterodimer that bind to the e-box enhancer regions of *Per1-2 and Cry1-2* genes to initiate transcription (Buhr and Takahashi, 2013) (Fig1.4). In the negative limb, the resulting PER and CRY proteins dimerize and translocate to the nucleus where they act on the CLOCK:BMAL1 complex to inhibit further transcription of *Per* and *Cry* genes (Buhr and Takahashi, 2013) (Fig1.4). As the amount of PER and CRY falls, transcription of *Per* and *Cry* by the CLOCK:BMAL1 complex increases again. In mice, CLOCK:BMAL1 activation occurs during the day, resulting in the accumulation of PER and CRY in the early evening (Takahashi, 2017). In addition to these core loops there are accessory loops. For example, the CLOCK:BMAL1 complex activates the *Rev-erba* and *Rora/β* genes. The resulting REV-ERB and ROR proteins compete for the RORE binding sites within the promotor of *Bmal1,* with REV-ERB proteins suppressing *Bmal1* transcription, and ROR proteins initiating transcription (Buhr and Takahashi, 2013) (Fig1.4). Casein kinase 1 (CK1) isoforms (α, δ, ε) are also involved via phosphorylating PER and thereby making PER a target for degradation (Mohawk and Takahashi, 2011) (Fig1.4). As such, the rate of PER and CRY degradation is critical for determining the period of the clock (Ralph and Menaker, 1988), and disruptions to this process by mutations can give rise to phenotypic differences in period length. For example, the *tau* mutant hamster has a period of ~20hrs as a result of a mutation in casein kinase 1ϵ (Ck1e) which reduces PER phosphorylation (Lowrey et al., 2000).

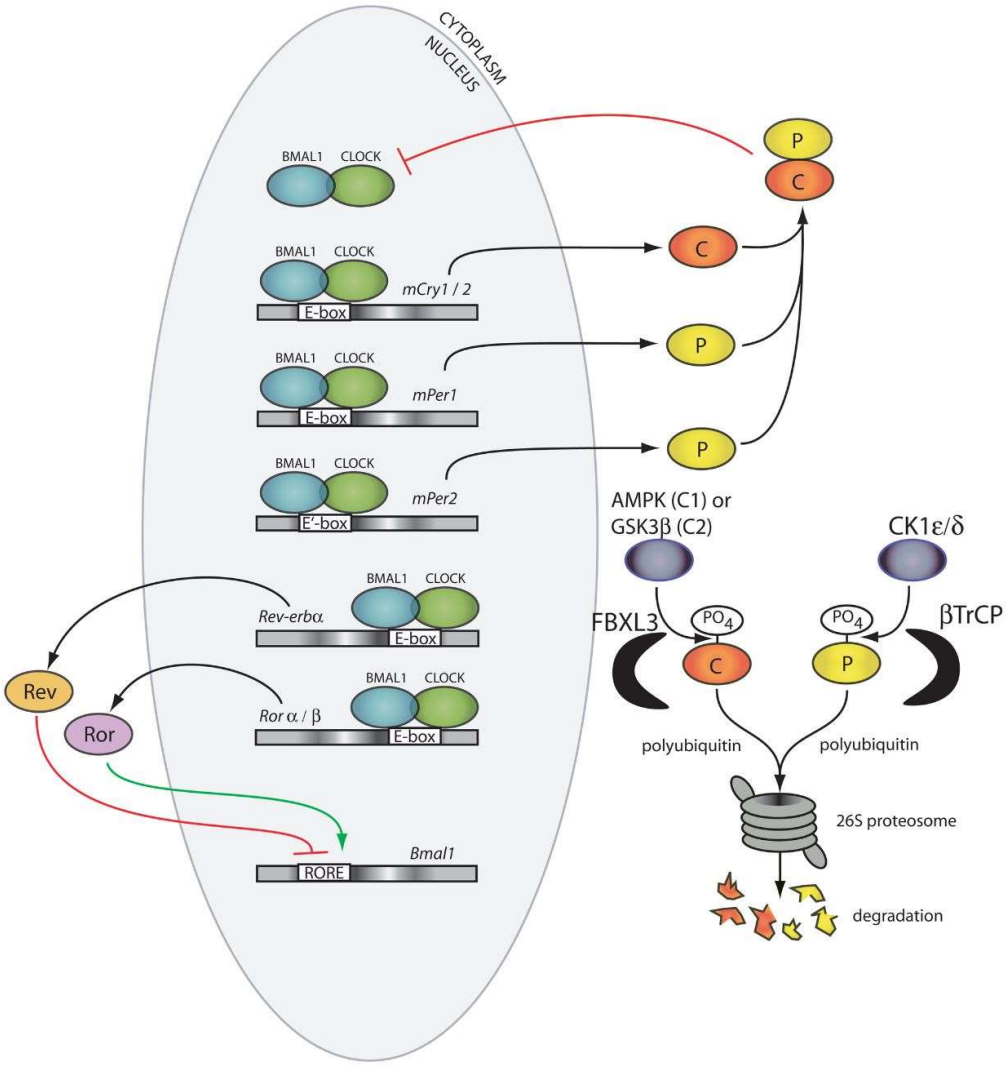

Figure 1.4 Schematic of the molecular clock in mammals. Positive limb: CLOCK:BMAL1 heterodimers (green and blue ovals, respectively) bind to the e-box regions of Cry1-2 and Per1-2 genes, initiating transcription. Negative limb: The resulting CRY and PER proteins (orange and yellow ovals, respectively) translocate back into the nucleus and inhibit transcription of Cry1-2 and Per1-2 genes. Accessory limb: The CLOCK:BMAL1 heterodimer also activates Rev-erbα and Rora/β genes, producing protein products REV (pale orange oval) and ROR (purple oval), respectively. REV inhibits Bmal1 transcription, whilst ROR initiates transcription. Phosphorylation of PER by casein kinase 1 (isoforms δ/ε) (grey oval) and phosphorylation of CRY by AMPK1 or GSK3β (grey oval), target the negative limb proteins for degradation. Figure reproduced from Buhr and Takahashi (2013).

1.3.4 The role of peripheral clocks

The discovery that almost every cell type in the body has a molecular circadian clock, and that many tissues continue to express circadian oscillations in isolation - including in fibroblasts (Balsalobre et al., 1998), the liver (Yamazaki et al., 2000; Yoo et al., 2004), the lung and skeletal muscle (Yamazaki et al., 2000), demonstrated the existence of 'peripheral clocks' (Dibner et al., 2010; Mohawk et al., 2012). This complicated the simple model of entrainment, which until this point had consisted of an input (light to the eye), an oscillator (the SCN) and outputs (rhythms in behaviour and physiology). Furthermore, it was not solely clock genes which were found to be rhythmic, but instead 3-10% of mRNA transcripts in peripheral tissues (Duffield et al., 2002; Hughes et al., 2009; Panda et al., 2002a; Storch et al., 2002; Ueda et al., 2002). Interestingly, most of the rhythmically transcribed genes were specific to the organ they were expressed in – suggesting the need to optimise physiology within each tissue to the varying demands of the activity-rest cycle.

Peripheral clocks become desynchronised at the organ level in the absence of the SCN (Sinturel et al., 2021; Yoo et al., 2004) indicating a need for SCN input for synchronisation. Whilst previous literature indicated that the SCN was also required for synchronisation within peripheral clocks at the cellular level (Guo et al., 2006), recent research argues that, as in the SCN, intercellular coupling also occurs in peripheral tissues, such as between hepatocytes (Finger and Kramer, 2021; Sinturel et al., 2021). The SCN provides output signals to synchronise peripheral clocks (Fig1.5) via the autonomic nervous system (Kalsbeek et al., 2010), body temperature (Brown et al., 2002) and humoral signals such as glucocorticoids (Kaneko et al., 1981; Mohawk et al., 2012). However, peripheral clocks can also entrain to cues independent of SCN derived timing - for example, on a restricted feeding schedule peripheral clocks in the liver entrain to meal times and uncouple from SCN-driven rhythms (Bechtold, 2008; Damiola et al., 2000; Saini et al., 2013). This ability of peripheral clocks to entrain independently is likely to be important for generating plasticity in the circadian system under natural and therefore less predictable environments (Van Der Veen et al., 2017).

To summarise – during photoentrainment, ipRGCs in the retina combine both intrinsic (from melanopsin) and extrinsic (from rods and cones) photic information and this is passed to the SCN in the anterior hypothalamus, via the RHT (Moore and Lenn, 1972; Stephan and Zucker, 1972). Whilst the SCN has traditionally been described as the master clock, it can arguably be more accurately described as a "master synchroniser" (Buhr and Takahashi, 2013) since most cell types possess a molecular clock and show circadian rhythms in gene expression when isolated from the SCN (Abe et al., 2002; Yamazaki et al., 2000). The SCN synchronises peripheral circadian clocks to appropriate phase (Dibner et al., 2010); although peripheral clocks can also entrain

independently to other zeitgebers (Damiola et al., 2000; Stokkan et al., 2001; Van Der Veen et al., 2017). Thus, the SCN and peripheral clocks act together to generate rhythmic outputs in physiology and behaviour (Fig1.5).

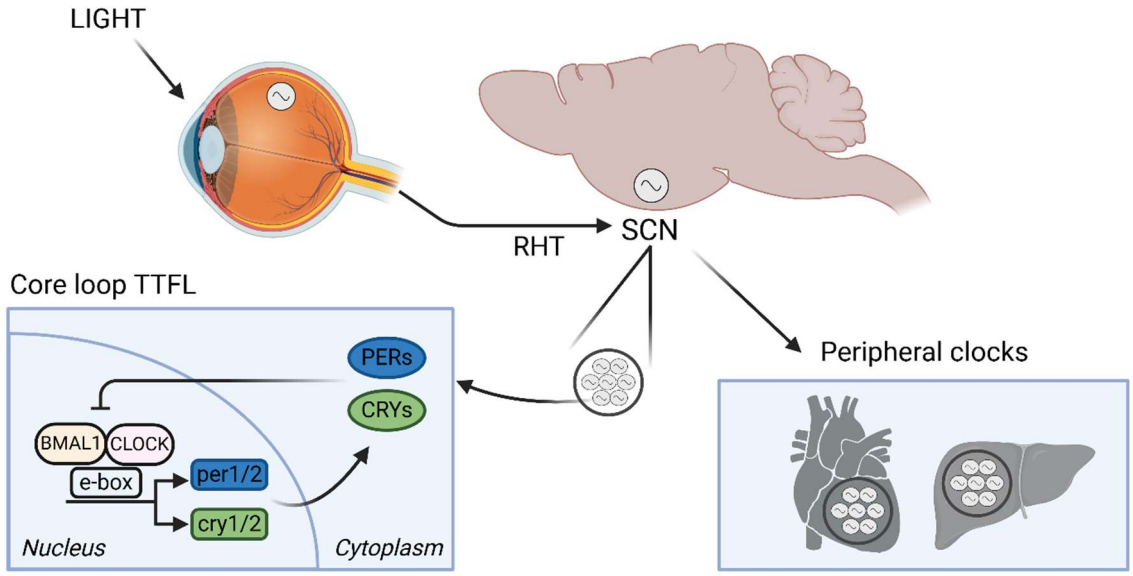

Figure 1.5 Summary schematic of photoentrainment. Light information from the retina is passed to the suprachiasmatic nuclei (SCN) via the retinohypothalamic tract (RHT), where it entrains an intracellular molecular clock. The SCN synchronises peripheral clocks in other tissues, although these can also entrain independently. Core loop TTFL based on Fisk et al (2018). Figure made in Biorender.

1.3.5 Are circadian rhythms adaptive?

The ubiquity of circadian clocks across the tree of life (Bell-Pedersen et al., 2005; Edgar et al., 2012; Johnson et al., 1996) suggest, although do not prove, that circadian rhythms provide a strong selective advantage to an organism. Whilst the specific components involved in the TTFL differ between species, the TTFL structure is shared between the three phylogenetic domains (Eukarya, Archaea and Bacteria) (Bell-Pedersen et al., 2005). As such, there has been debate as to how many times a circadian timekeeping mechanism evolved (Jones et al., 2010; Rosbash, 2009). Whilst the core clock proteins in mammals show no relationship to those in cyanobacteria (Rosbash, 2009), other shared markers of circadian rhythms have been identified across the phylogenetic domains, such as the oxidation-reduction cycles of perodiredoxin proteins (Edgar et al., 2012). Therefore, it appears that a circadian clock in cellular metabolism may have evolved in the last universal

common ancestor of the phylogenetic domains, before further mechanisms evolved in divergent phylogenetic branches.

Circadian rhythms could confer fitness benefits in two ways. Firstly, by enabling organisms to anticipate predictable daily changes in the external environment and align physiology and behaviour to the varied demands of the solar day (extrinsic adaptive value) (Roenneberg and Foster, 1997). This would occur via the optimisation of phase angle (Jabbur et al., 2024), or in other words, the accurate entrainment of the internal circadian clock to the external environment (Roenneberg and Merrow, 2002). Conversely, the ability of circadian clocks to coordinate internal processes may confer a second, and intrinsic, form of adaptive value. For example, being able to temporally separate mutually incompatible processes, such as nitrogen fixation and photosynthesis (Jabbur et al., 2024; Mitsui et al., 1986). Studies in which *D.melanogaster* retained functional circadian clocks after being housed in constant light for 600 (Sheeba et al., 1999) or 700 generations (Paranjpe et al., 2003) lend support to circadian rhythms providing intrinsic adaptive value. In addition, circadian rhythms are still present in the cave-dwelling Mexican blind cavefish, *Astyanax mexicanus*, albeit dampened compared to the surface population (Beale et al., 2013, 2016; Stemmer et al., 2015).

However, direct links between circadian rhythms and an increase in fitness have been difficult to establish, with different fitness testing paradigms having strengths and weaknesses (Jabbur et al., 2024; Sharma, 2003). For example, DeCoursey et al (2000) demonstrated that SCN-lesioned animals experienced higher predation rates compared to sham-operated controls, likely arising from the higher nocturnal activity exhibited by SCN-lesioned animals. However, this study occurred over a 80-day period, and so although it suggests that a circadian clock is beneficial for survival, it does not explicitly test reproductive success, and therefore fitness. Arguably, the most rigorous paradigms we have to assess fitness are competition assays performed under semi-natural environments (Jabbur et al., 2024). Competition assays were first established in microbes (Gause, 1934) and utilise the Principle of Competitive Exclusion – the idea that two species that compete for the same ecological niche cannot coexist. As such, the species with even the smallest advantage will outcompete the other (Hardin, 1960). This assay has since been used to assess the adaptive value of circadian rhythms in cyanobacteria (Ouyang et al., 1998; Woelfle et al., 2004), *Arabadopsis* (Dodd et al., 2005) and mice (Spoelstra et al., 2016). In all three of these organisms, alleles of clock genes which produced free running periods that were non-resonant with the environmental period (i.e. had non-optimal phase angles of entrainment) had decreased fitness (Jabbur et al., 2024). This supports the idea that natural selection is acting on entrainment (Jabbur et al., 2021; Roenneberg et al., 2010).

1.4 Light

1.4.1 The characteristics and measurement of light

Light is the primary cue for circadian entrainment in mammals. Therefore, it is important to consider what light is and how it can be measured. Light is often defined as electromagnetic radiation in the portion of the electromagnetic spectrum capable of generating a visual sensation in humans (typically wavelengths from ~350nm to 750nm) (Peirson et al., 2005a; Sliney, 2016). However, this anthropocentric definition ignores the diversity of opsins found across organisms (Peirson et al., 2009). Light is considered to possess characteristics of both particles (which are referred to as photons) and waves (Sliney, 2016), and can subsequently be measured in the number of photons intersecting a surface during a period of time, or in the amount of energy light imparts to a surface (in watts (W)) (Cronin et al., 2014).

When considering the biological responses to light, it is more intuitive to measure light in photons, since photoreceptors absorb light as photons. However, it is possible to convert watts to photons by first calculating the energy per photon (N_p) - defined by $N_p = hc/\lambda$; where h is Plank's constant and c is the speed of light in a vacuum, and λ is the wavelength of light. It is necessary to know the wavelength of light, because energy per photon is proportional to $1/\lambda$, so short wavelength photons are more energetic than photons at longer wavelengths (Johnsen, 2011; Peirson et al., 2005a). The irradiance (in watts) of the light source can then be divided by the energy per photon (N_p) to calculate photon flux (Peirson et al., 2005a), thereby converting units from watts to photons. The measurement of light can then be further characterised by the features of light being measured. This group of units are known as radiometric units and consist of radiance, irradiance and radiant flux - and can be defined in either photons or watts. Radiance (photons/s/m^2/sr or W/m^2/sr) measures directional intensity received from a light source and measured from a point in space. In contrast, irradiance (photons/s/m^2 or W/m^2) measures light intensity received by a surface, from all directions. Finally, radiant flux (W or photons/s) measures total light intensity output from a source, to all directions combined. The CIE e-ILV provides definitions of key terms and units.

Whilst radiometric units can be used to characterise light from any part of the electromagnetic spectrum, there is a comparable measuring system known as photometric units, which are used to measure visible light and are weighted to the human visual system (Cronin et al., 2014; Johnsen, 2011). The photometric units are luminance (cd/m^2), illuminance (lumens/m^2, 'lux') and luminous flux (lumen, lm); corresponding to radiance, irradiance and radiant flux, respectively. Photometric units account for the fact that light energy is distributed across wavelengths - a feature which can

be characterised by a spectral power distribution. Since humans are more sensitive to some wavelengths of light than others, calculating total energy across a spectrum does not predict how bright a light source will appear (Lucas et al., 2024). Therefore, radiometric units are weighted by a spectral efficiency function (the photopic sensitivity function, V(λ), for humans) to generate a unit of perceived brightness. However, the peak of V(λ) is at 555nm – which does not match peak sensitivity of animals with other opsin complements, such as rodents. As such, two light sources matched for brightness for a human observer, but with different spectral power distributions, could appear a very different brightnesses to a mouse (Fig1.6). In addition, perceived brightness does not indicate how a light source will influence NIF responses to light – such as circadian entrainment. Therefore, a new metric known as α-opic irradiance (or α-opic equivalent daylight illuminance (units: lux), if multiplied by the α-opic efficacy of luminous radiation (ELR)) have been developed, whereby radiometric light is weighted by the spectral sensitivity of individual photopigments, as defined by their intrinsic wavelength preference and pre-receptoral filtering (Lucas et al., 2024, 2014). The 'alpha' in α-opic lux is a place holder for the specific photopigment. For example, in mice there are four possible α-opic lux – S-cone opic lux, melanopic lux, rhodopic lux and M-cone opic lux (Lucas et al., 2024, 2014).

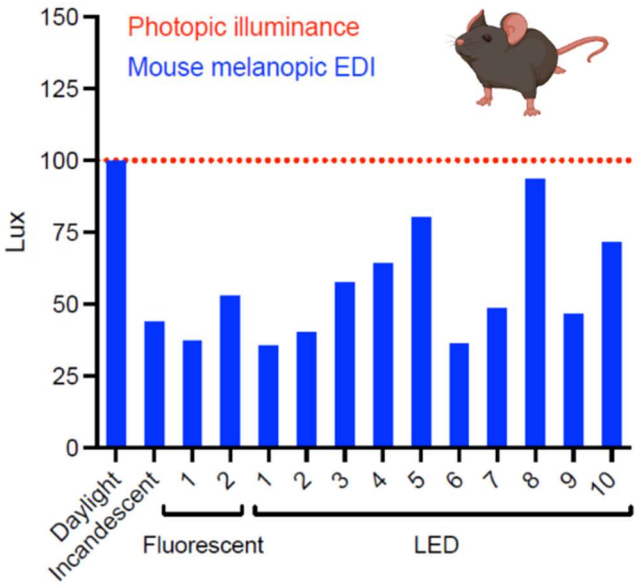

Figure 1.6 –Schematic to demonstrate that white light sources with the same photopic lux (red) can have highly variable mouse melanopic lux values (blue), depending on their spectrum. Figure taken from Lucas et al (2024).

1.4.2 The natural light environment

When studying the influence of light on circadian entrainment, it is particularly important to consider the key features of the natural light environment, under which photoentrainment evolved. In nature, light is a complex and dynamic environmental signal – with changes in intensity and spectrum across the 24hr cycle (Spitschan et al., 2016). As a result of predictable changes in the angle of solar elevation, light intensity can vary from 0.001 photopic lux on an clear moonless night to over 100,000 photopic lux on a clear, sunny day (Johnsen, 2011; Spitschan et al., 2016). Transient changes in cloud cover may further alter these values – with a moonless overcast night having a 10-fold lower intensity than a moonless clear night, and an overcast day having an 100-fold lower intensity than a clear, sunny day (Johnsen, 2011). These daily changes in light intensity occur particularly rapidly at twilight (Fig1.7A) – of which there are three stages, defined by the angle of solar elevation. Civil twilight occurs when the sun is between 0° and -6° below the horizon, and this is followed by nautical twilight (-6° to -12°) and subsequently astronomical twilight (-12° to -18°) (Spitschan et al., 2016). The length of twilight varies with time of year and latitude – due to the changing angle of the setting or rising sun's path with respect to the horizon.

These changes in light intensity occur concomitantly with changes in spectrum. The spectrum of daylight has been well characterised – initially by Judd et al (1964) in which a set of 622 daylight spectral power distributions were analysed, with the majority of variance shown to be explained by three functions. This work was incorporated into the CIE standard illuminant D65 (CIE, 2022) (Fig1.7B, green). The sky during the day appears blue as a result of the scattering of sunlight, known as Rayleigh scattering. This is the phenomenon by which light waves scatter in various directions when they interact with particles that are smaller than the wavelength of light. Light is scattered more strongly when the wavelength is closer in size to that of the scattering particle; therefore, since most atmospheric particles are much smaller than the wavelength of light, blue light is scattered more strongly than red light as it has a shorter-wavelength (Rayleigh, 1899). Twilight is even more short-wavelength enriched compared to that of daylight (Fig1.7B, blue). This is due the addition of the Chappius effect (Hulburt, 1953) - in which the lower position of the sun in the sky during twilight means that light travels a longer distance through the atmosphere than during the day, and as such, is subject to greater absorption of light by ozone, which has a maximum absorption at ~603nm. The light detected by an organism's photopigments is further modified by the differential absorbance, transmission and reflectance of materials in the local environment (Cronin et al., 2014; Morimoto et al., 2019; Shiwen et al., 2021), as well as properties of pre-receptor filtering including lens transmission, which can vary between species and individuals (Douglas and Jeffery, 2014).

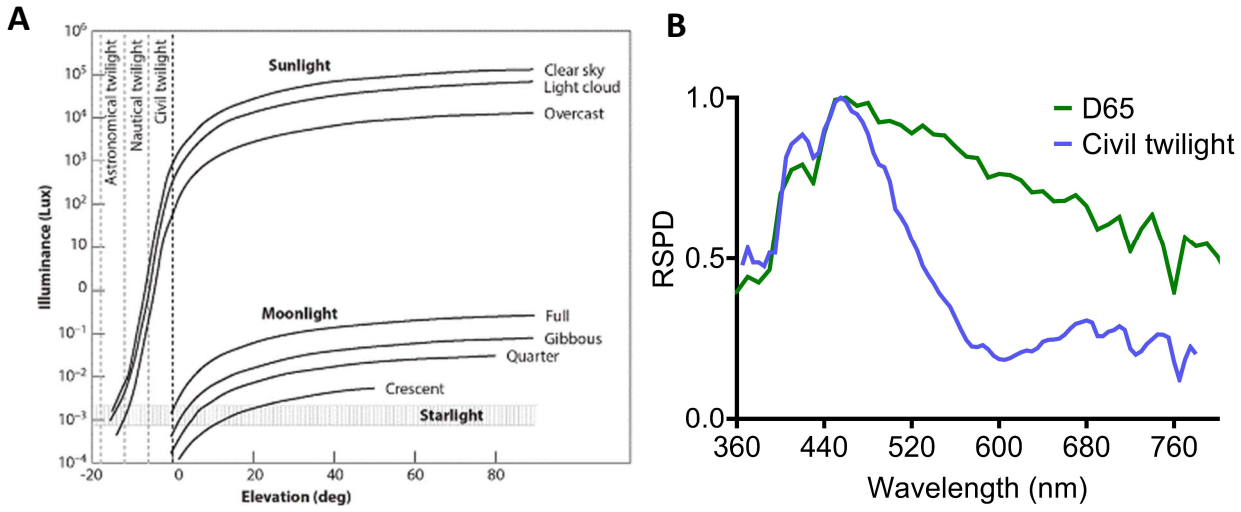

Figure 1.7 Features of the natural light environment. **(A)** Changes in illuminance as a function of solar elevation. Figure taken from Cronin et al., 2014 (originally from Bond and Henderson, 1963). **(B)** Relative spectral power distribution (RSPD) of the CIE D65 standard illuminant (representative of daylight) and civil twilight (measured at -6 degrees of solar elevation, data from Spitschan et al, 2016). Figure made in GraphPad Prism.

Beyond the complexity of the light environment itself, the pattern of an organism's behaviour can directly modulate the timing and duration of light exposure; a concept referred to as light sampling behaviour (DeCoursey, 1986; Decoursey and Menon, 1991). This adds an additional layer of complexity in regulating the light available to an organism for photoentrainment, especially in natural environments where the intensity and spectrum of light change as a function of time. The influence of light sampling behaviour on light exposure will vary between animals with different life histories (Fig1.8; (Kenagy, 1976; Roenneberg and Foster, 1997)). Whilst the schematic in Fig1.8 is a simplification, it demonstrates that diurnal organisms are likely to be exposed to light during the day (Fig1.8,A,B), whilst nocturnal organisms may be exposed to light at twilight (Fig1.8,C,D); with burrowing and roosting habits playing an important role in determining the precise shape of light exposure (e.g. Fig1.8C versus D). The role of behaviour in modulating light exposure may be particularly relevant for predominantly nocturnal burrow-dwelling species such as kangaroo rats (Kenagy, 1976; Lockard and Owings, 1974) and the flying squirrel (Decoursey and Menon, 1991), or nocturnal bats which roost in dark locations (DeCoursey and DeCoursey, 1964; John W. Twente, 1955; Voûte et al., 1974), since these environments enable more control over light exposure.

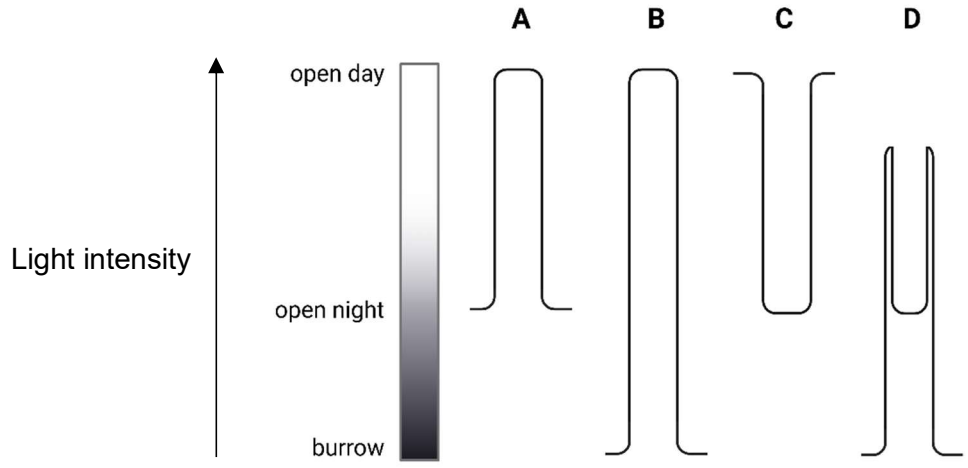

Figure 1.8 Schematic demonstrating how life history differences can modulate light sampling patterns, and subsequent light exposure for photoentrainment. Light intensity is represented by the bar on the left hand side, with higher light intensity at the top. Each curve (A-D) is centred around the organism's activity midpoint. **(A)** Diurnal non-burrowing organisms. **(B)** Diurnal burrowing organisms. **(C)** Nocturnal non-burrowing organisms. **(D)** Nocturnal burrowing organisms. Figure adapted from Roenneberg and Foster (1997), and made in Biorender.

1.5 Thesis rationale

1.5.1 Laboratory environments are highly simplified

Light is the primary cue for circadian photoentrainment in mammals. In natural environments both light itself, and the way organisms interact with it, can be very complex. Despite this, the majority of our knowledge of photoentrainment originates from experiments performed on rodents under highly simplified laboratory conditions. The house mouse (*Mus musculus),* commonly referred to as the laboratory mouse, is a key model species for circadian entrainment (Peirson et al., 2018; Tir et al., 2022), having been established as a general model organism in the early 1900s following the trade of fancy mice (Phifer-Rixey and Nachman, 2015). The ancestral range of the laboratory mouse was likely modern day India (Phifer-Rixey and Nachman, 2015) and they seek vegetated, sheltered areas to nest (Latham and Mason, 2004). However, in the laboratory they are usually housed under 12:12hr LD cycles of broad spectrum white light sources, which are short-wavelength depleted relative to daylight, and are generally simple on/off square-wave cycles, or may involve very short ramped transitions (Peirson et al., 2018). In addition, under standard laboratory conditions, there is no opportunity for mice to escape from the light and therefore exhibit light sampling behaviour. Mice exhibit strong nocturnal rhythms in activity in the laboratory environment and are known to build burrows in natural (Sutherland and Singleton,

2003), semi-natural (Schmid-Holmes et al., 2001) and laboratory (Adams and Boice, 1981; Bouchard and Lynch, 1989) environments. Therefore, the ability to regulate their light exposure may be an important, and generally overlooked, aspect of photoentrainment. Although shelter enrichment such as red plastic or cardboard houses are often used, these reduce but do not abolish light exposure, and are unlikely to reduce light intensity below the threshold for entrainment (0.01 photopic lux in C57Bl6 mice) (Butler and Silver, 2011; Ebihara and Tsuji, 1980; Foster and Helfrich-Förster, 2001; Peirson et al., 2018; Steel et al., 2022). Finally, beyond light, further environmental conditions are also simplified – such as the provision of *ad libitum* food and water, constant temperatures, and a lack of social cues.

1.5.2 Why is this a problem?

Simplified laboratory conditions are, to an extent, necessary - to control for variables and subsequently assess the contribution of different experimental factors. Indeed, experiments under these reductionist conditions have generated a huge body of knowledge on circadian entrainment. However, it has been frequently demonstrated that animals can behave very differently under laboratory conditions and natural environments (Calisi and Bentley, 2009). The adaptive flexibility of the circadian system (Shemesh et al., 2007; Van Der Veen et al., 2017) may mean that this is a particular problem for this field. For example, many studies have shown that although mice exhibit strictly nocturnal patterns of activity in the laboratory, diurnal activity is common under more naturalistic environments - such as low night time temperatures (Daan et al., 2011; van der Vinne et al., 2014) or conditions of limited food availability (Hut et al., 2011; Northeast et al., 2019). Similar temporal niche switching to nocturnality when in captivity has been observed in other rodent species such as the cururos (*Spalacopus cyanus*) (Rezende et al., 2003), the tuco-tuco (*Ctenomys sociabilis*) (Tomotani et al., 2012) and the golden hamster (Gattermann et al., 2008). Therefore, in a similar way to how over-standardisation of experimental conditions can lead to local truths with little external validity (Richter et al., 2009), over-simplification of environmental cues in the laboratory may be limiting our understanding of circadian entrainment to how it works under a set of specific conditions.

1.5.3 How can this problem be addressed?

This problem has been previously identified (Enright, 1970) and the integration of behavioural ecology and evolution with neurophysiology has been proposed as a solution; both in the study of circadian rhythms (Helm et al., 2017; Schwartz et al., 2017; Van Der Veen et al., 2017) and sleep (Aulsebrook et al., 2016; Rattenborg et al., 2017; Siegel, 2020). This more naturalistic approach to research is referred to as increasing "ecological validity", and is gaining traction not only in neuroscience (Smith, 2023) but other fields such as molecular biology (Heard, 2022). Whilst studies

have investigated activity patterns in the wild across a range of species (Halle and Stenseth, 2000; Schlaich et al., 2017; Schwartz et al., 2017; Sutherland and Singleton, 2003), it is challenging to control for multiple variables or investigate mechanisms of circadian entrainment. Therefore, this thesis takes the approach of bringing elements of the natural environment into the laboratory environment – one by one, to assess their relative effect on circadian entrainment, using the house mouse (*Mus musculus*) as a model species. In the studies previously mentioned which showed differences in the timing of activity under laboratory and naturalistic conditions, multiple factors were changing e.g. light, temperature and social cues (Daan et al., 2011; Hut et al., 2011; Northeast et al., 2019; van der Vinne et al., 2014). However, this thesis focuses specifically on light – in particular the role of behaviour in regulating light exposure, and the importance of natural spectral changes for photoentrainment. The key literature in these areas of research will be outlined in the next section. Finally, these topics are also relevant for understanding circadian entrainment in humans and its frequent disruption (Biller et al., 2024; Roenneberg and Merrow, 2016; West et al., 2017; West and Bechtold, 2015) – as summarised by the 'spectral diet' concept which shows how human behaviour can directly impact the intensity and spectrum of light available for entrainment (Webler et al., 2019).

1.5.4 Key literature - the role of behaviour in photoentrainment

The role of behaviour in regulating light exposure was first investigated in wild bats, which were shown to sample the external light environment at dusk prior to leaving their roost (John W. Twente, 1955; Voûte et al., 1974). Along with the observation that one or two pulse skeleton photoperiods (LD cycles with light delivered only in a brief pulse at dawn, dusk, or dawn and dusk; Pittendrigh and Daan, 1976) were sufficient for entrainment in golden hamsters (Earnest and Turek, 1983) and flying squirrels (DeCoursey, 1972), these data drove curiosity as to how burrow or cave-dwelling organisms receive light cues in natural conditions. This question was investigated in the laboratory in Syrian hamsters (Boulos et al., 1996; Pratt and Goldman, 1986), flying squirrels (DeCoursey, 1986), and most recently in mice (Refinetti, 2004), by simulating dark nests in which the nest entrance was monitored by a motion sensor. Activation of this motion sensor was referred to as 'burrow emergence' by Pratt and Goldman (1986) and as 'light sampling behaviour' by DeCoursey (1986). Total light exposure in the presence of a dark nestbox was not quantified in Syrian hamsters (Pratt and Goldman, 1986) or mice (Refinetti, 2004), but was reduced to 0.4-3.5% of the light phase in flying squirrels (Decoursey and Menon, 1991) and 2.5-12.5% of the light phase in hamsters (Boulos et al., 1996).

These studies disagree on whether being able to self-modulate light exposure has a significant effect on photoentrainment, or the model by which this might occur. DeCoursey demonstrated

that on some days flying squirrels exposed themselves to no light at all, and free ran until activity onset advanced into the light phase (DeCoursey, 1986). In addition, animals housed with a dark nest appeared to have an abrupt arousal time at which point they sampled the outside light environment. If it was dark, wheel running began immediately; but if it was still light outside, animals returned to the nestbox and activity was phase shifted by a 40min delay. Similarly, hamsters housed with dark nestboxes reduced light exposure in the morning, generating differences in entrainment (Boulos et al., 1996). However, Refinetti (2004) argued that nestbox availability does not have a major effect on photoentrainment, with variability in activity onset increasing slightly but otherwise no observable differences, and no evidence of free-running as in the flying squirrel (DeCoursey, 1986).

Despite these striking results on the effect of nestbox availability on light exposure the literature on the role of behaviour in photoentrainment is limited and has not been recently updated in model organisms. However, in non-model organisms some exciting research is currently being carried out in the subterranean rodent, the tuco-tuco (*Ctenomys* aff.*knighti)* (Flôres et al., 2016; Jannetti et al., 2023; Oda and Valentinuzzi, 2024). Light sensitive loggers fixed to neck collars demonstrated that tuco-tucos expose themselves to an irregular pattern of brief episodes of light each day in semi-field enclosures, primarily driven by foraging trips (Flôres et al., 2016). Furthermore, animals in the laboratory were able to entrain to a simplified representation of this light exposure pattern – consisting of 1hr of light (fluorescent light, 1000 photopic lux) delivered at a random time within a day-length time period of up to 14hrs (Flôres et al., 2016). Interestingly, the single light pulses did not result in a zig-zagging of activity onset, which would be expected if entrainment was being driven exclusively by discrete phase shifts. Instead, it is likely that continuous changes to the velocity of the clock are also involved. Similarly, the ground squirrel has been shown to entrain without exposure to any light at dawn or dusk in natural environments (Hut et al., 1999) and instead is thought to integrate subtle changes in irradiance across the light phase across multiple days, rather than simple daily phase shifts (Beersma et al., 1999; Hut et al., 1999). The research in the tuco-tuco emphasises that the discrete and continuous models of entrainment, whilst useful, are neither fully accurate or mutually exclusive (Oda and Valentinuzzi, 2024), and highlights the importance of studying the role of behaviour in regulating light exposure for promoting our understanding of photoentrainment.

1.5.5 Key literature – the role of naturalistic light environments in photoentrainment

The most common efforts to simulate naturalistic lighting environments in the laboratory have involved modulating photoperiods (Boulos and Macchi, 2005; Comas and Hut, 2009) or ramping white light sources to simulate changes in light intensity at twilight (Boulos et al., 2002, 1996;

Boulos and Macchi, 2005; Comas and Hut, 2009; Schlichting et al., 2015; Usui et al., 2000). Aschoff and Wever predicted an increase in zeitgeber strength with increasing twilight duration (Aschoff and Wever, 1965; Wever, 1964), and indeed, studies in hamsters (Boulos et al., 2002, 1996) and rats (Usui et al., 2000) suggest that twilight does enable entrainment to LD cycles with a wider range of periods and results in less variation in activity onset. However, when twilight length was changed in combination with photoperiod length, differences between hamsters (Boulos and Macchi, 2005) and mice (Comas and Hut, 2009) became apparent. Hamsters successfully entrained to a short photoperiod (6hrs) with a long twilight (2hrs), but mice didn't start activity until 5.3hrs after lights off under the same conditions. The authors suggest these differences could relate to different intrinsic circadian periods in mice (<24hrs) and hamsters (>24hrs) and differences in the shape of their PRCs (Comas and Hut, 2009; Pittendrigh and Daan, 1976); emphasising that models of entrainment may differ between species and therefore the need for comparative studies (Roenneberg et al., 2010).

Using spectral changes to track twilight was suggested over 20 years ago (Roenneberg and Foster, 1997). However, whilst previous studies identified that UV light, which is more prevalent at twilight, may be an important entrainment cue in hamsters (Hut et al., 2000) and mice (Van Oosterhout et al., 2012); spectral changes at twilight have only recently been simulated in the laboratory (Walmsley et al., 2015) due to the technical challenges of separating colour and brightness. Walmsley demonstrated that the changes in UVS:MWS ratio across twilight (and therefore the apparent colour of light to the mouse visual system) were more predictive of the sun's position than irradiance, as a result of the greater effect of cloud cover on light intensity than spectrum (Mouland et al., 2019; Woelders et al., 2018). The next question of interest was whether the circadian clock can detect these changes in colour. Walmsley showed that a group of SCN neurons do in fact display cone-dependent spectral opponency, rendering them capable of tracking changes in spectrum across twilight. Furthermore, simulating spectral changes at twilight altered circadian phase in body temperature compared to an intensity-only twilight in wildtype, but not *Cnga3*$^{-/-}$ mice (lacking cone phototransduction) (Walmsley et al., 2015). These spectral changes may also be important for human photoentrainment. For example, human patients experiencing disrupted circadian rhythms as a result of brain injury, showed improved entrainment under simulated daylight conditions compared to standard electric lighting (Angerer et al., 2022). However, these two lighting conditions differed in both intensity and spectrum – making it hard to assess the relative contribution of each. However, mathematical analyses also support the hypothesis that the integration of spectral and intensity cues increases the reliability of time cues for human entrainment when cloud cover is present (Woelders et al., 2018).

1.6 Thesis aims

As laid out in the thesis rationale, the overall objective of this thesis is to further our understanding of how circadian photoentrainment is regulated under naturalistic light environments – in particular, the role of behaviour and naturalistic changes in spectral composition. Mice were used as a model organism throughout and the following aims were established to accomplish this objective.

Aim 1. Characterise how mice are exposed to light under standard laboratory conditions.
Identify how mice are exposed to light under standard housing conditions utilised in circadian neuroscience studies, and rodent laboratory research more widely. Assess whether these practices may be generating sufficient variation in light levels to drive differences in home cage activity and circadian entrainment (Chapter 2).

Aim 2. Design a paradigm to investigate the role of behaviour in regulating circadian photoentrainment.
Design a paradigm to enable mice to self-select their light exposure, from which light sampling behaviour and circadian entrainment metrics can be quantified (Chapter 3).

Aim 3. Investigate the mechanisms regulating light sampling behaviour and circadian entrainment.
Use transgenic mice to investigate:

3.1 The role of the circadian clock in regulating light sampling behaviour and circadian entrainment (Chapter 3).

3.2 The role of classical photoreceptors and melanopsin in regulating light sampling behaviour and circadian entrainment (Chapter 4).

Aim 4. Characterise and investigate the effects of naturally-occurring spectral changes in the light environment on light sampling behaviour and circadian entrainment.
4.1 Develop a multi-channel LED set-up to simulate natural daylight and the spectral changes occurring during twilight, to assess whether spectral cues are important for regulating light sampling behaviour and circadian entrainment (Chapter 5).

4.2 Characterise a natural light environment in a highly spectrally and spatially resolved way using hyperspectral techniques, to assess spectral reflectance as a source of variation in natural light environments (Chapter 6).

Chapter 2. Effects of cage position and light transmission on home cage activity and circadian entrainment

This chapter contains reproduced material from the following paper:

Steel et al., 2022. Effects of cage position and light transmission on home cage activity and circadian entrainment in mice, Frontiers in Neuroscience. DOI: 10.3389/fnins.2021.832535

Many thanks to Tecniplast for the provision of the Digital Ventilated Cage (DVC) system used in this study.

2.1 Abstract

Light is known to exert powerful effects on behaviour and physiology, including upon the amount and distribution of locomotor activity across the day/night cycle. Here we characterise variation in home cage light spectrum and intensity arising from cage position within an individually ventilated cage (IVC) rack and cage material. We then use home cage activity monitoring to measure the effect of this variation on key circadian entrainment metrics in mice. Due to the relative positioning of any IVC with regard to the animal facility lighting, notable differences in light intensity were observed across the IVC rack. Although all mice were found to be entrained, significant differences in the timing of activity onset and differences in activity levels were found between mice housed in standard versus red filtering cages. Furthermore, by calculating the effective irradiance based upon known mouse photopigments, a significant relationship between light intensity and key circadian entrainment metrics is shown. Perhaps unsurprisingly, given the important role of the circadian photopigment melanopsin in circadian entrainment, melanopic illuminance is shown to correlate more strongly with key circadian entrainment metrics than photopic lux. Collectively, our results suggest that differences in light intensity may reflect an uncharacterised source of variation in laboratory rodent research, with potential consequences for reproducibility. Room design and layout vary within and between facilities, and caging design and lighting location relative to cage position can be highly variable. We therefore suggest that cage position should be factored into experimental design, and wherever possible, experimental lighting conditions should be characterised as a way of accounting for this source of variation.

2.2 Introduction

Light mediates both acute and circadian effects on the regulation of locomotor activity in a dose-dependent manner, making light intensity a critical variable in rodent research. Studies on the threshold of circadian entrainment have shown that mice are remarkably sensitive to light, and are able to entrain to light levels of around 0.01 photopic lux (Butler and Silver, 2011; Ebihara and Tsuji, 1980); although there is some variation between strains of mice, with C57 mouse strains more sensitive than C3H (Foster and Helfrich-Förster, 2001). Increasing light intensities lead to greater activity suppression in response to light (Contreras et al., 2021; Mrosovsky, 1999; Thompson et al., 2008) and greater circadian phase shifts (Foster et al., 1991; Hattar et al., 2003; Provencio and Foster, 1995; Yoshimura et al., 1994). These responses are typically plotted as irradiance response curves (IRCs), with increasing light levels resulting in greater biological responses up to a point of saturation.

The effect of wavelength is to shift the relative position of these IRCs, requiring more or less light to evoke the same response (corresponding to lower or higher sensitivity, respectively). Such studies have shown that mice are most sensitive to light around 480-511nm (Hattar et al., 2003; Peirson et al., 2005b; Provencio and Foster, 1995; Yoshimura and Ebihara, 1996). Moreover, these studies clearly show that mice can respond to longer wavelength light, but since they lack a long-wavelength sensitive (LWS) cone like humans, they are relatively less sensitive to red light compared to humans (Peirson et al., 2018). Together these data illustrate that the use of photopic lux – a measurement of illuminance based upon human visual sensitivity which peaks around 555nm – are inappropriate for measuring the effects of light on mice (Lucas et al., 2014). However, to date, most guidance on light levels in animal facilities are given in photopic lux.

It is known that light levels differ markedly across mouse cage racks and reflect a source of potential experimental variability. These differences can be up to 80-fold between cages on the top and bottom of a cage rack in normal transparent cages (Clough, 1982; Weihe et al., 1969). IVCs are widely used in laboratory mouse husbandry, offering many advantages including increased biosecurity, stocking density, controlled environmental conditions and reduced exposure to laboratory animal allergens (Brandstetter et al., 2005). IVC design varies between distributors, with differences in materials as well as the spacing of cages within a rack. IVC racks house multiple rows of cages, and cages may be produced to reduce in-cage light exposure. As such, the light levels experienced by any animal within an IVC rack will depend upon the cage position as well as the cage material. Both the row and column of a cage may affect the light intensity, depending upon how the rack is positioned relative to the room lighting (Clough et al., 1995).

Although light is known to mediate both acute and circadian effects on the regulation of locomotor activity, to date no studies have systematically evaluated the effects of cage position on light and home cage activity. Here we describe the effects of cage position and filtering on cage light levels, and the effects of these systematic differences on home cage activity using the Digital Ventilated Cage (DVC) system (Tecniplast, Italy). We predicted that mice housed in cages with lower light levels would show less stable circadian entrainment and more daytime activity.

2.3 Materials and Methods

2.3.1 Animals

This study had an initial cohort of 12 WT (6 female and 6 male) mice of C57BL/6J background (Envigo, Blackthorn, UK, RRID: IMSR_ JAX:000664), aged 11-weeks at the start of the experiment. However, one male was culled prior to the start of experiments due to fighting injuries. All mice were singly housed in new cages (that had undergone minimal processing to meet the hygiene levels of the facility) and these cages were not changed for the duration of the experiment. All cages were placed in the Digital Ventilated Cage (DVC) rack (Tecniplast, Italy) at 20-24˚C and 45-65% ± 10% humidity, with food (Envigo 2916) and water available *ad libitum*. Mice were maintained under a cool white fluorescent light source with a ramped 13h 10-min/10h 50-min light-dark cycle [lights on at 07:50 and reaching full intensity (260 photopic lux) at 09:00, and fully off at 21:00]. Animals were housed in specific pathogen free (SPF) conditions, and the only prior reported positives on health screening in this unit were *Entamoeba muris, Enteromonas Sp* and *Trichomonas Sp;* though no positives were reported during the course of this study (Envigo, Alconbury UK). All experimental procedures were conducted at the University of Oxford, UK in accordance with the United Kingdom Animals (Scientific Procedures) Act 1986 under Project License PP0911346 and Personal License I82616702.

2.3.2 Experimental design

The cohort of 11 animals was randomly split into two groups. There was a control group of 5 mice (3 female and 2 male) which were housed in standard Green Line individually ventilated cages (IVC; Tecniplast GM500, polysulfone), and an experimental group of 6 mice (3 female and 3 male) which were housed in red individually ventilated cages (IVC; Tecniplast GM500, polysulfone). All mice were habituated in the central rows of the DVC rack for 1 week prior to the start of the experiment. Animals were then assigned to 'top', 'middle' and 'bottom' row positions within the DVC rack (Fig. S2.1), spending 1 week at each position. Mice were rotated through the different

rack positions in a counterbalanced order and were culled via cervical dislocation at the end of the 3 week experimental period.

2.3.3 Home cage activity monitoring

All mice were singly housed in a DVC rack (Tecniplast, Italy). This is an IVC rack which continuously measures activity via capacitance sensing technology (CST) (Iannello, 2019). A sensing board is installed below each IVC cage in the rack and is composed of 12 equally spaced electrodes, the electrical capacitance of which are measured every 250ms. Due to the high water content of animals, the capacitance of the electrodes is significantly influenced by the presence of mice. Therefore, animal movement can be recorded as changes in capacitance across electrodes (Iannello, 2019; Pernold et al., 2019). Capacitance measurements from adjacent electrodes are compared, and when the difference is larger than a fixed threshold the electrode is considered activated. From this, an animal locomotion index (ALI) is produced which is expressed in an arbitrary unit normalised between 0% and 100%. 0% represents no activity, and if all electrodes are simultaneously activated, a value of 100% is produced. For our analysis, we exported the animal locomotion index from DVC Analytics in 1 min bins across all 12 electrodes.

2.3.4 Light measurements

An XL-500 BLE Spectroradiometer (NanoLambda, Korea) was used to take power and photopic lux measurements of the internal light environment of the standard and red cages in positions across the DVC rack. Individual measurements were taken in the front, middle and back of each cage, in all columns across the top (row 10), middle (row 6) and bottom (row 1) of the DVC rack (Table S2.1). The mean of these within-cage values were taken, to produce a single measure of photopic lux for each cage type across the relevant positions of the DVC rack (Table 2.1). The spectral power distribution (SPD) of the room light where the DVC rack was located was measured at the height of the top row of the DVC rack using a calibrated Ocean Optics USB2000+ Spectrophotometer (Ocean Insight, Oxford, UK). Standard and red cage transmission measurements were taken under dark conditions, using a calibrated Ocean Optics Spectrometer and a broad-spectrum microscope light source (Photonic, Wein, Austria). The DVC room light SPD was corrected by these cage transmission measurements to produce relative spectral power distributions (RSPD). Linear interpolation was used to convert these RSPDs into 5nm bins, and α-opic irradiance values (CIE, 2018) for S-cones, M-cones, rods and melanopsin were then calculated for each cage position, using the Rodent Toolbox (Lucas et al., 2014). Due to the positioning of the room lights in relation to the DVC rack (Fig. 2.1A) the light intensity varied significantly across the DVC rack – showing, in general, a decrease in intensity from top left to bottom right of the rack (Fig. S2.2).

Standard Cage irradiance	A	B	C	D	E	F
Top - Photopic	177.5	145.5	122.9	46.5	54.1	29.7
Top – S-cone	19.0	15.6	13.2	5.0	5.8	3.2
Top - Melanopic	113.3	92.9	78.5	29.7	34.5	19.0
Top - Rhodopic	115.2	94.4	79.7	30.2	35.1	19.3
Top – M-cone	119.6	98.0	82.8	31.3	36.4	20.0
Middle - Photopic	39.6	70.4	69.6	57.7	44.6	20.3
Middle – S-cone	4.2	7.5	7.5	6.2	4.8	2.2
Middle - Melanopic	25.3	44.9	44.4	36.8	28.5	13.0
Middle - Rhodopic	25.7	45.7	45.2	37.4	28.9	13.2
Middle – M-cone	26.7	47.4	46.9	38.9	30.0	13.7
Bottom - Photopic	17.3	13.4	18.6	13.3	11.6	13.7
Bottom – S-cone	1.9	1.4	2.0	1.4	1.2	1.5
Bottom - Melanopic	11.0	8.6	11.9	8.5	7.4	8.7
Bottom - Rhodopic	11.2	8.7	12.1	8.6	7.5	8.9
Bottom – M-cone	11.7	9.0	12.5	9.0	7.8	9.2
Red Cage irradiance	**A**	**B**	**C**	**D**	**E**	**F**
Top - Photopic	19.1	16.9	13.5	6.2	6.5	3.3
Top – S-cone	0.7	0.6	0.5	0.2	0.2	0.1
Top - Melanopic	4.4	3.9	3.1	1.4	1.5	0.8
Top - Rhodopic	5.4	4.8	3.8	1.8	1.8	0.9
Top – M-cone	5.9	5.2	4.1	1.9	2.0	1.0
Middle - Photopic	6.0	8.8	7.9	6.9	5.3	2.6
Middle – S-cone	0.2	0.3	0.3	0.2	0.2	0.1
Middle - Melanopic	1.4	2.0	1.8	1.6	1.2	0.6
Middle - Rhodopic	1.7	2.5	2.2	2.0	1.5	0.7
Middle – M-cone	1.8	2.7	2.4	2.1	1.6	0.8
Bottom - Photopic	3.9	3.7	3.4	3.5	2.8	1.8
Bottom – S-cone	0.1	0.1	0.1	0.1	0.1	0.1
Bottom - Melanopic	0.9	0.9	0.8	0.8	0.6	0.4
Bottom - Rhodopic	1.1	1.0	1.0	1.0	0.8	0.5
Bottom – M-cone	1.2	1.1	1.9	1.1	0.9	0.6

Table 2.1 Light intensity in photopic lux and other α-opic irradiance, in each column (A-F) of the DVC rack across the top, middle and bottom rows. Reported for a standard cage (top table) and red cage (bottom table).

2.3.5 Circadian entrainment metrics

The animal locomotion index, for all 11 cages across the 3 week period, was exported from DVC Analytics in 1 minute bins and processed in MATLAB (R2021a). Following this, MATLAB and Actogram J (Schmid et al., 2011) were used to calculate several circadian entrainment metrics for each mouse in each position (Brown et al., 2019). These are described below. For all analyses, the light phase was defined as 07:50 to 20:59 and the dark phase from 21:00 to 07:49. ZT0 was defined as light onset (07:50 local clock time).

Light and dark phase activity (%). In the laboratory WT mice are nocturnal, with activity mainly limited to the dark phase. An increase in the proportion of activity carried out during the light phase is therefore considered a marker of circadian disruption (Oliver et al., 2012). Light and dark phase activity are expressed as a percentage of total activity across the 24h period (Brown et al., 2019).

Relative amplitude. The relative amplitude of a circadian rhythm is the difference in scale between periods of peak activity and rest across the 24h cycle (Brown et al., 2019; Van Someren et al., 1999). A low relative amplitude value is indicative of a weak and disrupted circadian rhythm, since it shows fewer distinct and consolidated periods of activity and rest. In our analysis, the active period was defined as the dark phase and the rest period defined as the light phase. The relative amplitude of every 24h period for each mouse was calculated and the mean taken across a week to output a single relative amplitude measure for each mouse in the top, middle and bottom DVC rack positions.

Activity onset. An animal with a normal circadian rhythm will begin locomotor activity around the same time each day. A small phase angle of entrainment and low variability in activity onset between days can therefore be a marker of circadian robustness (Brown et al., 2019). Activity onset for every 24h period for each mouse was calculated using Actogram J's inbuilt function, which first smooths the data, using the standard deviation of a smoothing Gaussian distribution. Following this, activities are considered 'active' if they exceed the threshold of the median of all activity values (Schmid et al., 2011). The mean and standard deviation of activity onset for each mouse in the top, middle and bottom DVC rack positions were calculated.

Regularity Disruption Index (RDI). The Regularity Disruption Index (RDI) was developed to quantitatively measure irregular activity patterns and is based on sample entropy (Golini et al., 2020). A high RDI is indicative of a more irregular rhythm, whilst a low RDI suggests reliable activity patterns. This measure can be exported directly from the DVC Analytics website, with separate analysis for the light and dark phase.

Activity bouts. Circadian disruption results in increased fragmentation of activity and rest (Brown et al., 2019), and is consequently associated with changes in the proportion of activity bouts of different lengths. Light and dark phase activity were analysed separately using MATLAB to categorise activity bouts into bins of different lengths (1, 2, 3, 4-5, 6-10, 11-21, 21-40 and >40 minutes). Time weighted frequency histograms were produced (based on analysis from Mochizuki et al., 2004) to explore changes in activity bout distribution.

Periodogram power. Periodogram power is a measure of the strength of a rhythm, with higher values reflecting more reliable rhythms and very low values indicating arrhythmicity (Brown et al., 2019). The power of the chi-squared periodogram (Qp) is particularly commonly used in circadian analysis – if the Qp value for a period exceeds that of the expected background value based on the chi-square distribution, the period is considered significant (Brown et al., 2019; Sokolove and Bushell, 1978). The Qp value for each mouse in each position was calculated using Actogram J's inbuilt chi-squared periodogram function (Schmid et al., 2011).

Inter-daily stability. Inter-daily stability (IS) is a measure of the day-to-day reproducibility of activity cycles. Activity patterns are highly reproducible in healthy animals, and so a low IS value suggests circadian disruption. IS was calculated as the variance of the average 24h activity pattern expressed as a ratio of total variance (Brown et al., 2019).

Intra-daily variability. Intra-daily variability (IV) is a measure of the number of transitions between activity and rest – with a higher IV value reflecting a more fragmented rhythm (Brown et al., 2019).

2.3.6 Statistical analysis

GraphPad Prism 9 was used to visualise the data and run statistical analysis. Statistical significance of differences in circadian measures across cage type and position were tested with two-way repeated-measures ANOVAs, with a Greenhouse-Geisser correction applied to adjust for lack of sphericity (Fig. 2.3). Similarly, the relationship between frequency of activity bouts of different lengths, with cage type and position, were also tested with two-way repeated-measures ANOVAs (Fig. 2.4). Irradiance measurements were log10 transformed and a simple linear regression was applied to investigate the relationship between light intensity and circadian entrainment metrics, for each mouse in each DVC rack position (Fig. 2.5).

2.4 Results

2.4.1 Room lighting and cage transmission

The SPD of the animal facility room light is shown in Fig. 2.1B. The peaks at ~435nm, ~545nm and ~610nm are typical for a modern cool white fluorescent lamp; confirming wavelength calibration. As expected, the standard cage (Fig. 2.1C) transmits light broadly across the spectrum from 375nm to 780nm, and therefore provides a comparable light environment to the external room (Fig. 2.1D). Conversely, the red cage (Fig. 2.1E) shows a gradual increase in long wavelength transmission, with transmission saturating at 93% from between 580nm to 780nm (Fig. 2.1F).

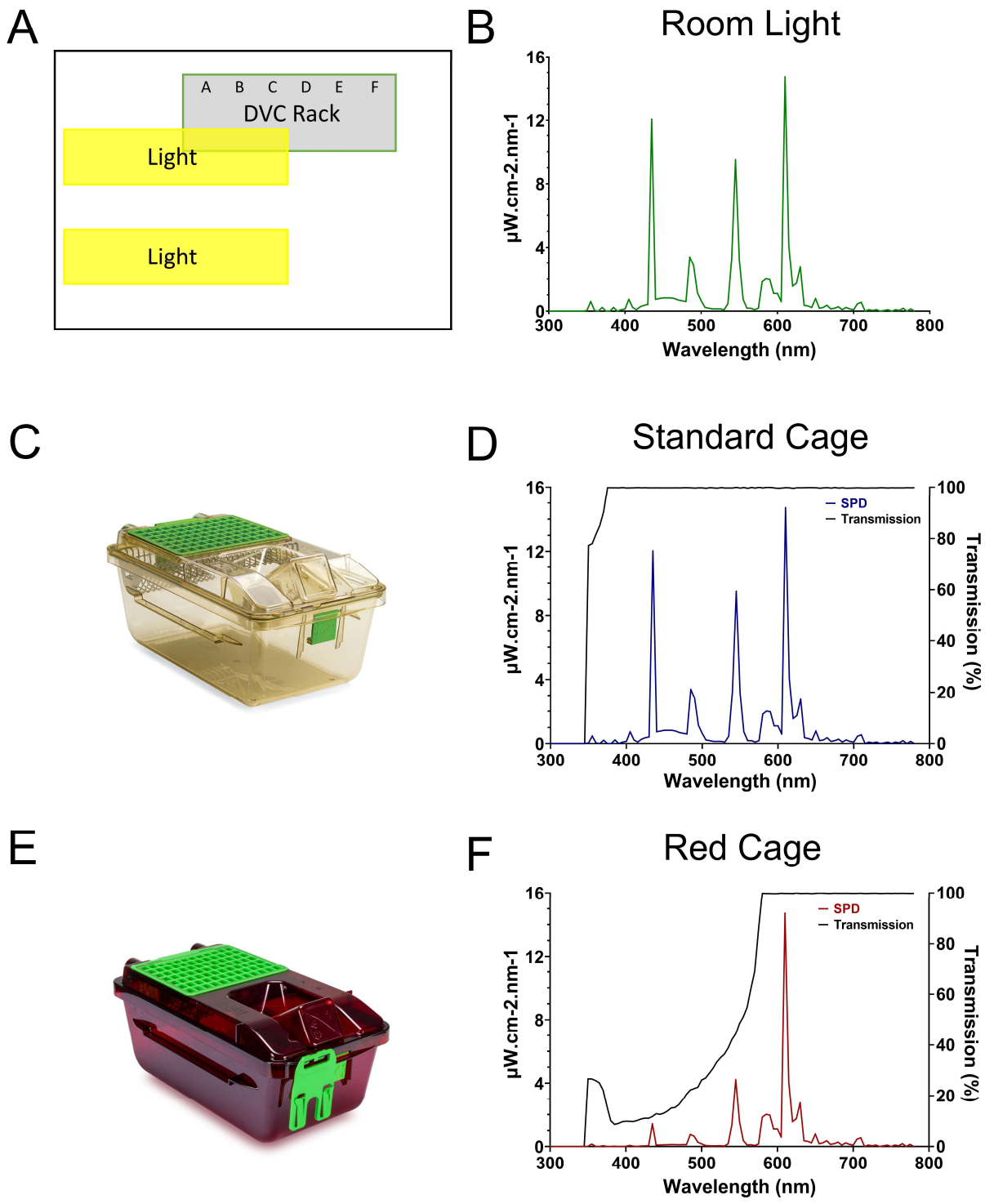

Figure 2.1 Room lighting and cage transmission. **(A)** Schematic of the relative positioning of the DVC rack and the room lights. **(B)** SPD of the DVC room light. **(C)** Standard Green Line individually ventilated cage (IVC; Tecniplast GM500). **(D)** SPD of the internal light environment, and the transmission, of a standard cage. **(E)** Red individually ventilated cage (IVC; Tecniplast GM500). **(F)** SPD of the internal light environment, and the transmission, of a red cage.

2.4.2 Activity across the DVC rack and cage type

Fig. 2.2A shows the mean animal locomotion index (ALI) of animals housed in standard (top panel) and red (bottom panel) cages in the top, middle and bottom rows of the DVC rack. The ALI is used as a measure of activity, and is plotted in Fig. 2.2A over the course of a week. In both standard and red cages, mice show clear dark phase activity and reduced activity levels during the light phase – in keeping with their nocturnal behaviour under laboratory conditions. The most obvious difference is the much higher levels of dark phase activity in mice housed in standard cages compared to red cages. Fig. 2.2B and Fig. 2.2C are representative actograms of a standard and red cage housed mouse, respectively. Each actogram shows 1 week of activity data, and activity onsets are marked with red triangles (calculated in Actogram J). Visual inspection of these actograms suggested that periods of activity and rest may be more consolidated in standard cages versus red cages.

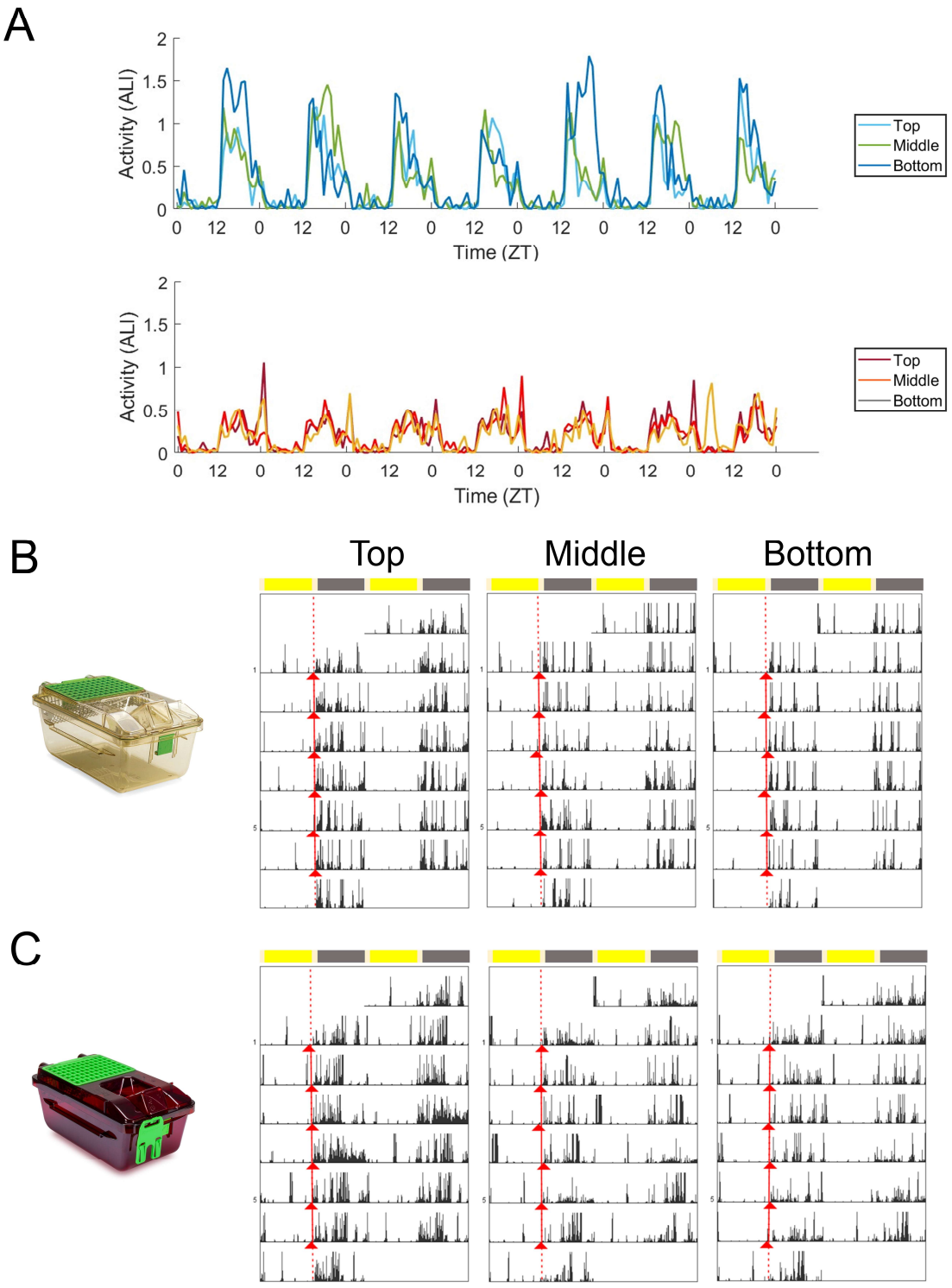

Figure 2.2 Activity plots and representative actograms. **(A)** Mean activity (measured as the animal locomotion index) of mice housed in standard cages (top panel) and red cages (bottom panel) across one week in the top, middle and bottom positions. **(B,C)** Double plotted actograms (Actogram J) of a representative standard cage housed mouse **(B)** and red cage housed mouse **(C)** in the one week spent in the top, middle and bottom positions of the DVC rack. Activity onsets are marked in red (Actogram J).

2.4.3 Circadian entrainment metrics

A range of standard circadian entrainment metrics are shown in Fig. 2.3. Two-way repeated-measures ANOVAs were used to test for significant effects of cage type (2 levels – standard and red) and cage position (3 levels – top, middle and bottom) on these key circadian disruption measures. Light phase activity (%) was higher in the red cages compared to the standard cages across all DVC rack positions, but this effect was not quite statistically significant [$F(1.0,9.0) = 4.196$, $p = 0.071$] (Fig. 2.3A). This is likely to be due to the high variance observed in light phase activity between animals and cage positions. There was no significant effect of cage position on light phase activity [$F(1.8,16.4) = 0.631$, $p = 0.530$], or a significant cage position by cage type interaction [$F(2.0,18.0) = 0.026$, $p = 0.975$] (Fig. 2.3A). Similarly, standard cage dark phase activity is consistently higher than red cage dark phase activity, but again fails to reach the level of significance [$F(1.0,9.0) = 4.196$, $p = 0.071$] (Fig. 2.3B). There was no significant effect of cage position on dark phase activity [$F(1.8,16.4) = 0.631$, $p = 0.530$], or a significant cage position by cage type interaction [$F(2.0,18.0) = 0.026$, $p = 0.975$] (Fig. 2.3B). Relative amplitude was higher in standard cages than red cages, across all positions (Fig. 2.3C). However, there was no significant effect of cage type [$F(1.0,9.0) = 4.151$, $p = 0.072$] or cage position [$F(1.8,16.3) = 0.629$, $p = 0.530$]. Similarly, there was no significant cage position by cage type interaction [$F(2.0,18.0) = 0.023$, $p = 0.975$] (Fig. 2.3C).

There was a significant main effect of cage type on activity onset (Fig. 2.3D), with mice housed in red cages starting their activity ~30 minutes earlier each day compared to mice housed in standard cages [$F(1.0,9.0) = 8.264$, $p = 0.018$]. There was no significant main effect of cage position on activity onset [$F(2.0,17.9) = 1.623$, $p = 0.225$] or significant cage type by cage position interaction [$F(2.0,18.0) = 0.074$, $p = 0.929$] (Fig. 2.3D); and similar patterns in cage position were seen for both red and standard cage activity onsets.

Finally, the RDI during the light phase was higher in red cage housed mice than in standard cage housed mice, suggesting more irregular activity rhythms, although this was not significant [$F(1.0,9.0) = 3.883$, $p = 0.080$] (Fig. 2.3E). Similarly, there was no significant effect of cage position [$F(1.9,17.2) = 0.407$, $p = 0.663$] or significant cage position by cage type interaction, [$F(2.0,18.0) = 0.991$, $p = 0.390$]. Fig. 2.3F shows the RDI calculated for the dark phase, in which there was a significant effect of cage position [$F(1.8,16.6) = 5.545$, $p = 0.016$], but no significant effect of cage type [$F(1.0,9.0) = 0.000$, $p = 0.994$], or cage position by cage type interaction [$F(2.0,18.0) = 1.41$, $p = 0.270$]. No significant effects of cage type or position were reported for periodogram power, period, inter-daily stability or intra-daily variability (data not shown).

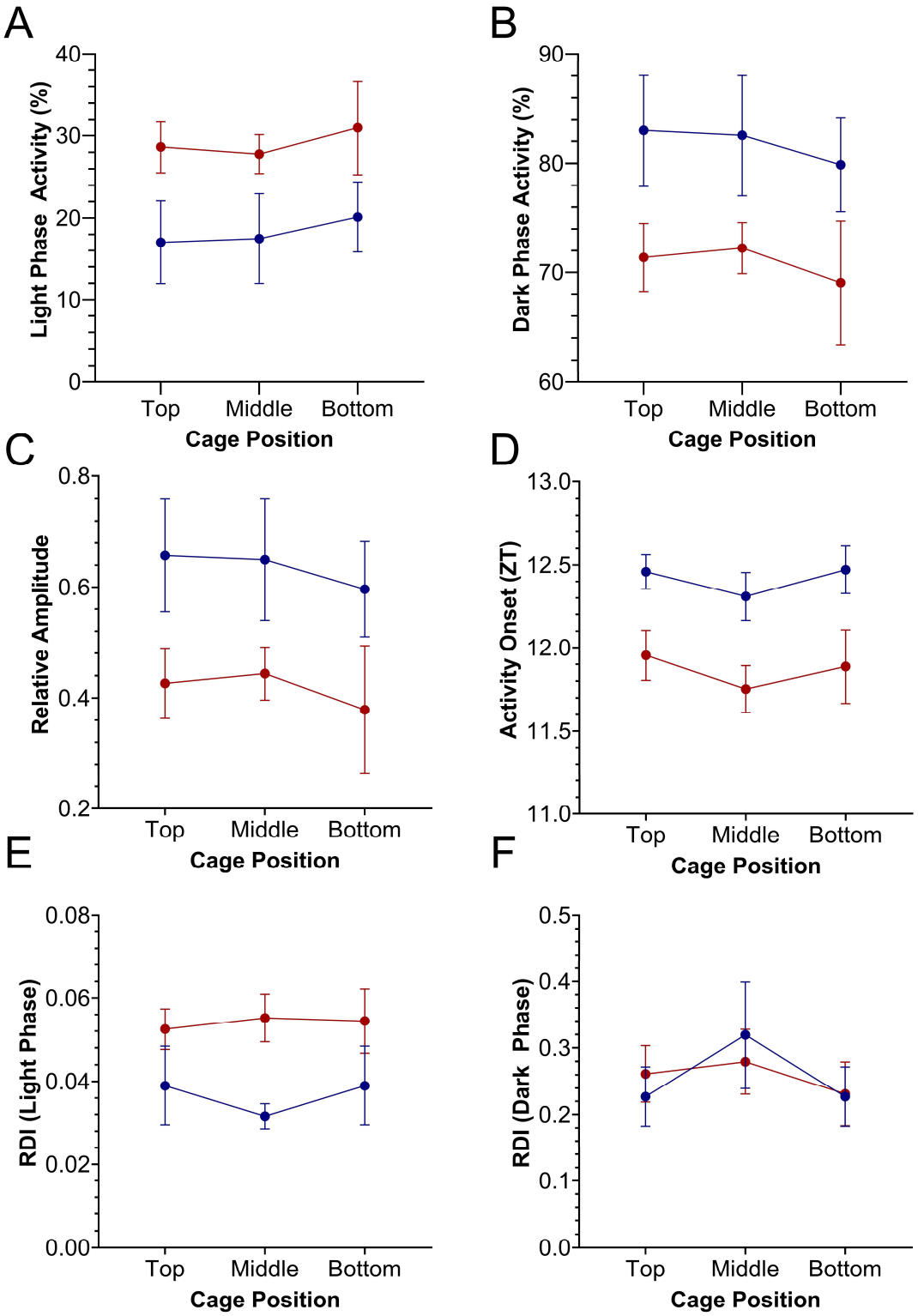

Figure 2.3 Key circadian entrainment metrics for standard (blue) and red (red) cages, across top, middle and bottom positions of the DVC rack. Two-way repeated-measures ANOVAs were used to test for significant effects of cage type and cage position. **(A)** Light phase activity (%). **(B)** Dark phase activity. **(C)** Relative amplitude. **(D)** Activity Onset (ZT). **(E)** Regularity disruption index (RDI) - light phase. **(F)** Regularity disruption index (RDI) – dark phase. Plotted as mean +/- SEM.

2.4.4 Activity bout distribution across the DVC rack and cage type

Time-weighted frequency histograms illustrating the distribution of activity bouts in standard and red cages across the DVC rack are presented in Fig. 2.4. Two-way repeated-measures ANOVAs were used to test for significant main effects of cage type (standard and red) and bout length (corresponding to activity bouts of 1, 2, 3, 4-5, 6-10, 11-20, 21-40, >40 mins) on the frequency of bouts across top, middle and bottom rack positions. Light phase (top panel, Fig. 2.4) and dark phase (bottom panel, Fig. 2.4) activity data were analysed separately due to the large differences in activity across the light/dark cycle.

In the light phase, a significant main effect of bout length on frequency of bouts occurred in the top position [$F(2.9,26.0) = 122.592$, $p = <0.0001$]; middle position [$F(2.1,19.3) = 58.549$, $p = <0.0001$] and bottom position [$F(1.5,13.9) = 47.561$, $p = <0.0001$]. Similarly, in the dark phase, there was a significant main effect of bout length on frequency of bouts across the DVC rack – top position [$F(1.6,15.8) = 22.943$, $p = <0.0001$]; middle position [$F(1.2,11.0) = 13.615$, $p = 0.001$]; bottom position [$F(1.6,14.1) = 17.297$, $p = 0.0003$]. This is clearly demonstrated in Fig. 2.4, with both standard and red cages across the DVC rack showing higher numbers of shorter activity bouts than longer activity bouts. No significant main effect of cage type on bout frequency was identified in any position, in either of the light or dark phase analyses. However, in the light phase there was a significant cage type by bout length interaction across the top position [$F(7.0,63.0) = 9.788$, $p = <0.0001$]; middle position [$F(7.0, 63.0) = 2.331$, $p = 0.035$] and bottom position [$F(7.0,63.0) = 3.457$, $p = 0.003$]. This cage type by bout length interaction was only found in the top position of the dark phase analysis [$F(7.0,63.0) = 3.080$, $p = 0.007$] and not in the middle position [$F(7.0,63.0) = 0.658$, $p = 0.707$] or the bottom position [$F(7.0,63.0) = 0.331$, $p = 0.937$]. As shown in Fig. 2.4, in all the light phase analyses, and the top position of the dark phase analysis, the frequency of short bouts in standard cages is higher than in the red cages. But as bout length increases, the frequency of bouts becomes higher in red cages than standard cages. This suggests that in the light phase brief bouts of quiet wakefulness predominate in standard cages, whereas longer periods of extended activity occur in red cages. This is consistent with more light phase activity in red cages in comparison with standard cages (Fig. 2.3A).

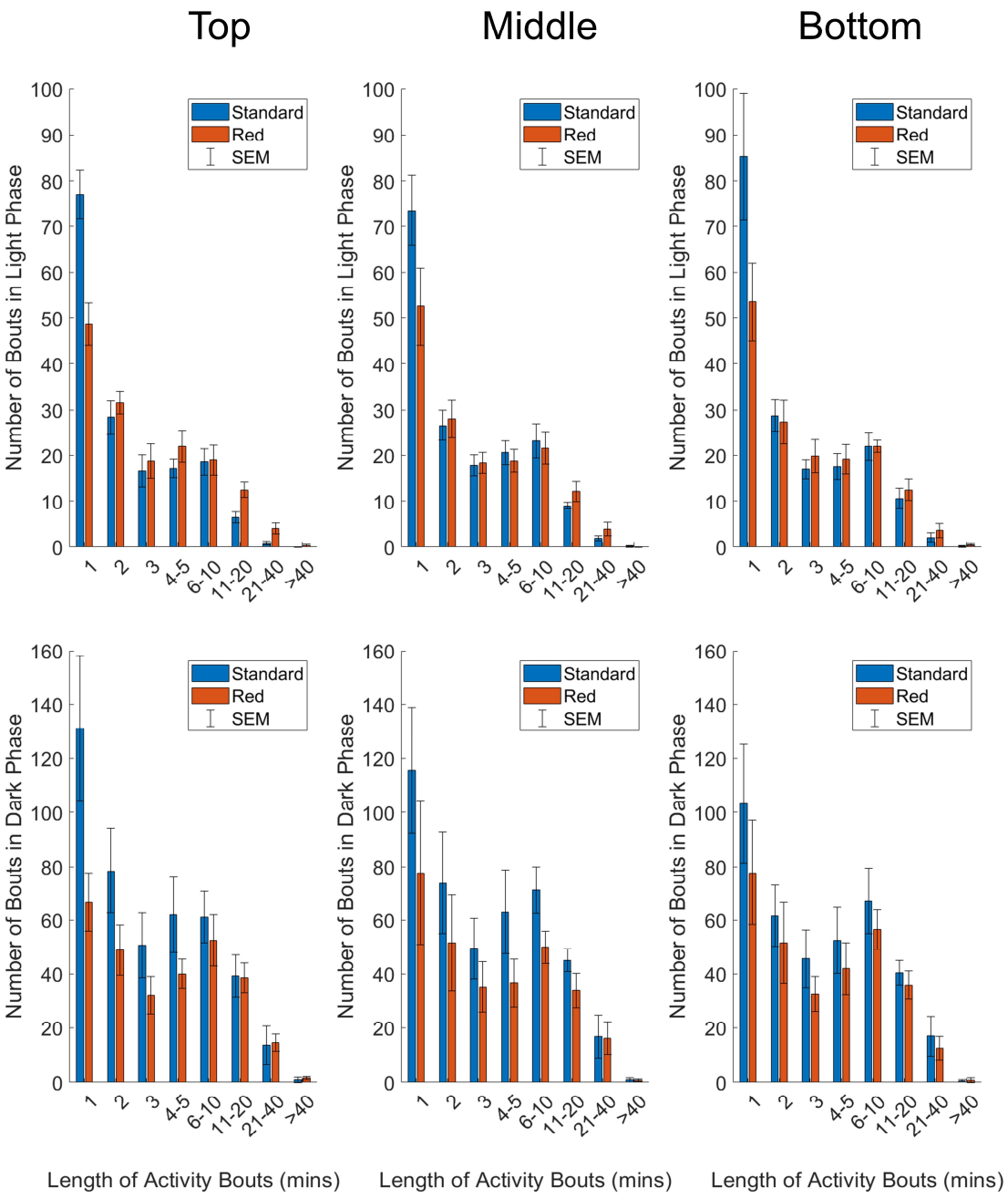

Figure 2.4 Number of activity bouts of different lengths in standard (blue) and red (red) IVCs, plotted as mean +/- SEM in time-weighted frequency histograms. Analysed separately for light phase (top panel) and dark phase (bottom panel) data, and separately by DVC rack position (top, middle and bottom).

2.4.5 Relationship between circadian entrainment metrics and light intensity

Light levels vary across a cage rack depending upon its positioning relative to the room lighting. Therefore, light levels for any given cage decrease from the top to the bottom of a cage rack, but also along any row depending upon its proximity to the overhead light (Fig 2.1A; Fig. S2.2). Therefore, light intensity can be more accurately viewed as a continuum across the DVC rack, rather than a categorical variable. Animals housed in the top, middle or bottom of the cage positions could be exposed to quite different ambient light levels (with a 6.0, 3.5 and 1.6-fold change within top, middle and bottom positions respectively in the standard cages, and a 6.0, 3.4 and 2.2-fold change in top, middle and bottom positions respectively in red cages; Table 2.1).

To account for this variation in home cage light levels, circadian entrainment metrics for every mouse in each position of the DVC rack were compared against the light intensity for the corresponding cage type and specific position. The relationship between circadian entrainment metrics and light intensity were then explored through a series of linear regression analyses (Fig. 2.5). The circadian disruption measures were correlated with both photopic lux (Fig. 2.5A,C,E,G) and melanopic equivalent daylight illuminance (EDI) (Fig. 2.5B,D,F,H). Not all data points are fully independent – there are 3 data points per mouse (a total of 33 measurements from 11 animals), representing their time in the top, middle and bottom positions of the DVC rack. However, each plotted value corresponds to a separate week of activity measurements under different lighting conditions.

A significant negative correlation was found between light phase activity (%) and photopic lux [$R^2 = 0.247$, $p = 0.003$] (Fig. 2.5A), as well as between light phase activity (%) and melanopic irradiance [$R^2 = 0.264$, $p = 0.002$] (Fig. 2.5B). This is expected since the proportion of total activity occurring during the light phase will be lower in those animals with more strongly entrained activity-wake rhythms (Brown et al., 2019). Interestingly, the intensity of light during the light phase not only influences light phase activity, but also the level of dark phase activity. As shown in Fig.5C a significant positive correlation was found between dark phase activity (%) and photopic lux [$R^2 = 0.247$, $p = 0.003$], as well as with melanopic irradiance [$R^2 = 0.264$, $p = 0.002$] (Fig. 2.5D). Relative amplitude is related to both light and dark phase activity. A significant positive correlation was found between relative amplitude and photopic lux [$R^2 = 0.243$, $p = 0.004$] (Fig. 2.5E) and melanopic irradiance [$R^2 = 0.260$, $p = 0.002$] (Fig. 2.5F). The correlations between light intensity and timing of activity onset are more significant than the other three measures, with a significant positive correlation found between timing of activity onset and photopic lux [$R^2 = 0.276$, $p = 0.002$] (Fig. 2.5G), and melanopic irradiance [$R^2 = 0.322$, $p = 0.001$] (Fig. 2.5H).

For all measures, the correlations between melanopic irradiance and circadian entrainment metrics are stronger than with photopic lux. This is expected given that photopic lux is based on cone-mediated vision (weighted to 555nm) in a standard human observer (Al Enezi et al., 2011) and therefore is not relevant to the mouse visual system, which only possesses an M-cone with a peak sensitivity at 508nm (Sun et al., 1997). Melanopic irradiance, with a peak sensitivity at ~480nm, has been widely proposed as a unit of circadian light intensity and is likely to be more strongly correlated to measures of entrainment due to the role of melanopsin ipRGCs in circadian entrainment (Al Enezi et al., 2011; Lucas et al., 2014).

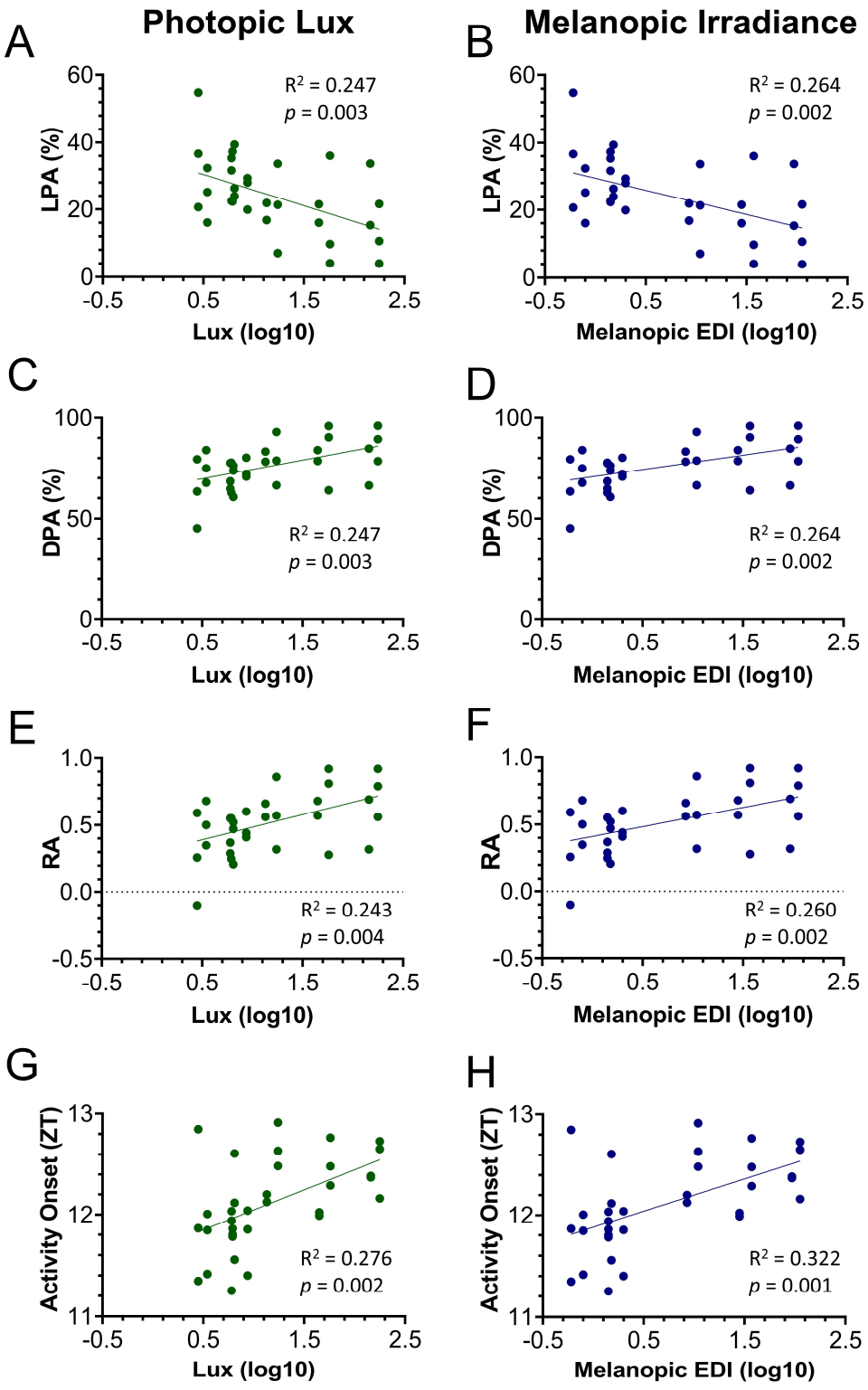

Figure 2.5 Relationship between key circadian entrainment metrics and photopic lux (**A,C,E,G**) or melanopic irradiance (**B,D,F,H**). All light intensity values have been log10 transformed. Light phase activity (LPA) (%) against photopic lux **(A)** and melanopic EDI **(B)**. Dark phase activity (DPA) (%) against photopic lux **(C)** and melanopic EDI **(D).** Relative amplitude (RA) against photopic lux **(E)** and melanopic EDI **(F).** Activity onset (ZT) against photopic lux **(G)** and melanopic EDI **(H)**. Linear regression was used to test for a relationship between the circadian entrainment metrics and light intensity.

2.5 Discussion

Here we show that light intensity varies markedly across a standard IVC rack, with over a 15-fold difference between highest and lowest intensities in standard cages and over a 10-fold lower intensity in red cages. This variation results from the relative positioning of light sources to the IVC rack, in addition to other features of the room layout. The light environment experienced by laboratory animals will therefore be influenced not only by the animal facility lighting, but by the specific position of the cage within any IVC rack. Similar phenomena have been reported before, such as in Weihe et al (1969) where an 83-fold difference in light intensity was shown between transparent cages at the top and bottom of a rack. Furthermore, we show that cage material can impact the spectrum of light reaching an animal. This effect has been explored previously in nude rats housed in transparent, blue and amber cages (Dauchy et al., 2013). Disrupted rhythms in measures of endocrine metabolism and physiology, such as plasma corticosterone levels, were reported for animals housed in blue and amber cages compared to clear cages (Dauchy et al., 2013).

There is an extensive literature showing the potent effects of light on physiology and behaviour. Therefore, we predicted that the differences in light environment across cage type and position in our study would impact key circadian entrainment metrics. Indeed, mice housed in red cages and therefore under a lower light intensity at each position, started their activity significantly earlier (~30 minutes) than mice housed in standard cages. Similarly, red-caged mice showed a higher level of light phase activity, lower level of dark phase activity as well as a lower relative amplitude than mice in standard cages. Whilst these latter differences were not significant, they are all features of less robust circadian entrainment (Brown et al., 2019). Furthermore, a significant interaction of cage type and bout length was seen in the light phase activity bout analysis, with red cages showing longer periods of extended activity, consistent with greater light phase activity in red cages than standard cages.

Our data also demonstrate that simply categorising light intensity by row height (top, middle and bottom) in the IVC rack may be overly simplistic, as substantial variation in light intensity within each row was also observed (Table 2.1; Fig. S2.2). Light intensity should be viewed as a continuum, and in this way, both standard and red cage data can be analysed together. Linear regression was used to test for a significant relationship between both photopic and melanopic irradiance and the key circadian measures (Fig. 2.5). The strength of circadian entrainment, as described by key measures, was found to increase with increasing light intensity. The slope of the linear regression line was significantly different from zero in all measures, reflecting that light intensity explained a greater proportion of the variation in the data than a horizontal line through the mean. Although

the R2 values are significant, they are quite low; indicating that light intensity does not explain all the variance seen in the key circadian measures. Interestingly, the R^2 values were higher for melanopic irradiance than photopic lux across all circadian measures, which is consistent with the key role of ipRGCs in circadian entrainment (Al Enezi et al., 2011).

Although mice housed in red cages showed earlier activity onsets, all mice in the IVC rack were still able to successfully entrain to the light dark cycle. This is not surprising given that previous work has shown that mice should be able to entrain to light levels as low as 0.01 photopic lux (Butler and Silver, 2011; Ebihara and Tsuji, 1980; Foster and Helfrich-Förster, 2001), whereas the lowest light intensity recorded in our IVC rack was only 1.8 photopic lux. As such, the light levels across an IVC rack should be well above the threshold for circadian entrainment. Furthermore, our data shows that, contrary to common perception, red cages are not equivalent to darkness for mice. Whilst mice lack a long-wave sensitive (red) cone, they are still able to detect and entrain to red light if the intensity is sufficiently high (Peirson et al., 2018).

The circadian measures shown in Fig. 2.5 were also analysed against α-opic irradiance values for the additional mouse retinal photoreceptors, including the UV-sensitive short-wavelength sensitive cones (S-cones), medium-wave sensitive cones (M-cones) and rods. As expected, based upon the known role of melanopsin in circadian entrainment, melanopic irradiance correlated most strongly with light phase activity, dark phase activity and relative amplitude (Table S2.2). Photopic lux correlated least strongly, which adds support to the argument that this measure is not as relevant as melanopic irradiance when studying mice - since it is based upon human visual sensitivity (Al Enezi et al., 2011; Brown et al., 2013). Interestingly, activity onset showed a slightly higher correlation with S-cone-opic irradiance values than melanopic irradiance (Table S2.2). As mice were housed under a light dark cycle with ramped light transitions, different photoreceptors may play a role in the timing of activity onset at the light to dark transition. Under these conditions, the dynamically changing light intensity may be a sensory task that favours cones. If this is indeed the case, it is intriguing that S-cone-opic irradiance correlates more strongly than M-cone-opic irradiance. Whilst previous work has shown that S-cones play a role in circadian entrainment (Van Oosterhout et al., 2012), M-cones can also contribute (Lall et al., 2010). In the current study, the greater correlation with S-cone-opic irradiance may reflect the dorsal-ventral gradient in cone opsin, with higher S-cone expression in the ventral retina, which will receive more light from the upper visual field (Hughes et al., 2013). However, these findings are preliminary and further research into the role of specific photoreceptors in different aspects of home cage activity is needed.

Our study has several important limitations. It was originally designed to be completely counterbalanced, however, the loss of one male mouse due to fighting injuries before the start of the experiment resulted in an unbalanced design. In addition, because of row and column effects on cage light levels and the use of males and females, greater variance was observed in circadian measures than under comparable studies in light-controlled chambers (Albrecht and Foster, 2002; Hughes et al., 2015; Jud et al., 2005). As a result, greater statistical power would be beneficial to detect more subtle changes. As is routine in circadian studies, animals were singly housed to allow activity monitoring to be attributed to a single animal. As the cage is the experimental unit in mouse studies, this reduced the number of animals used, but could potentially affect home cage behaviour and thermoregulation (Festing et al, 2016).

Light exerts potent effects on the physiology and behaviour of mice, including activity levels (Albrecht and Foster, 2002; Hughes et al., 2015; Jud et al., 2005), sleep and arousal (Pilorz et al., 2016), body temperature (McGuire et al., 1973), melatonin production (Brainard et al., 1984) and corticosterone secretion (Ishida et al., 2005). Therefore, differences in home cage light levels across experimental cages are a source of potential biological variability. This may be particularly relevant for tests of exploratory activity, anxiety and photophobia (Ueno et al., 2024); but also has the potential to affect cognitive performance (Tam et al., 2016) since this can vary with sleep history (Tam et al., 2021). If this is indeed the case, it may pose a potential problem for reproducibility in animal research, especially since different animal facilities, and even separate rooms within the same facility, will differ in the relative positioning of cage racks and room lighting. Furthermore, the use of different light sources and cage types may also affect the spectral composition of the light source. A good example of this is provided by comparing fluorescence fixtures to white LEDs, with white LEDs providing relatively less short-wavelength light and thus an S-cone depleted light environment. Furthermore, the age of cages (with repeated cycles of washing) and the age of lighting fixtures may also affect the light conditions experienced by animals. Together these aspects of facility design mean that light levels experienced by laboratory mice may vary greatly between studies.

To try and reduce this potential source of variation, researchers should factor cage position into experimental design to account for differences in light intensity experienced between animals (Lucas et al., 2024). Ideally, researchers should also report the light levels experienced by animals within the cage, rather than just the room lighting. More detailed characterisation of the lighting is helpful, particularly SPDs, as these enable the effects of light on the different photoreceptors of the mouse retina to be determined (Lucas et al., 2014). However, in the absence of a spectrophotometer, reporting the type of lighting (and manufacturer) and photopic lux can be

helpful. Lux meters are cheap and widely available and can provide a simple measure of light intensity. Whilst lux is based on human perceived brightness and is not directly relevant to the visual system of mice, it provides an approximation of intensity. Furthermore, for any given light source, the ratio of melanopic to photopic lux (M/P ratio) can be determined and used to convert photopic lux measurements to melanopic irradiance. For example, the MP ratio of daylight is 1.0, but for a cool white fluorescent light source this may be 0.56. As such, 100 photopic lux from such a light will give 56 melanopic irradiance. In the future, technological developments may help standardisation in this area, for example, cage racks or cages with inbuilt lighting.

In conclusion, this study highlights how light can vary greatly across a single IVC rack, and the subsequent effects this can have on a range of circadian entrainment metrics such as activity levels and the timing of activity onset. Given the widespread effects of light on visual and circadian physiology and behaviour, such differences may reflect a source of uncharacterised variability in mouse studies and may be important for improving reproducibility.

2.6 Supplementary material

2.6.1 Supplementary figures

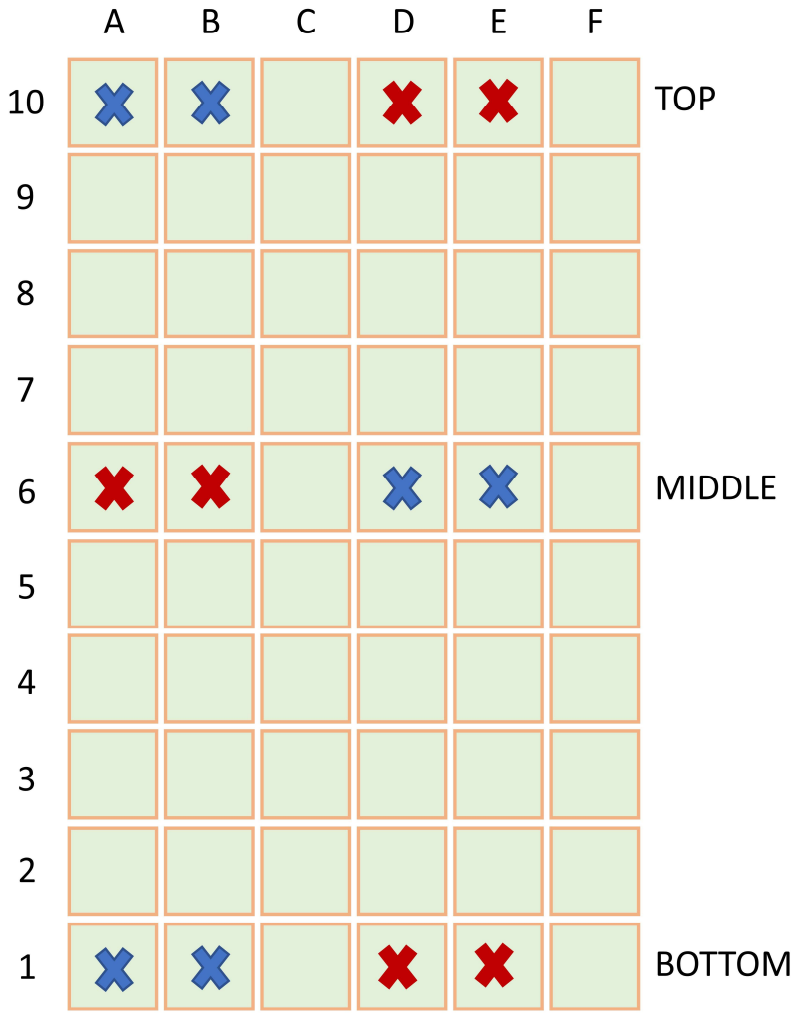

Figure S2.1 Experimental design schematic, showing the top, middle and bottom positions on the DVC rack for the standard cages (blue) and red cages (red).

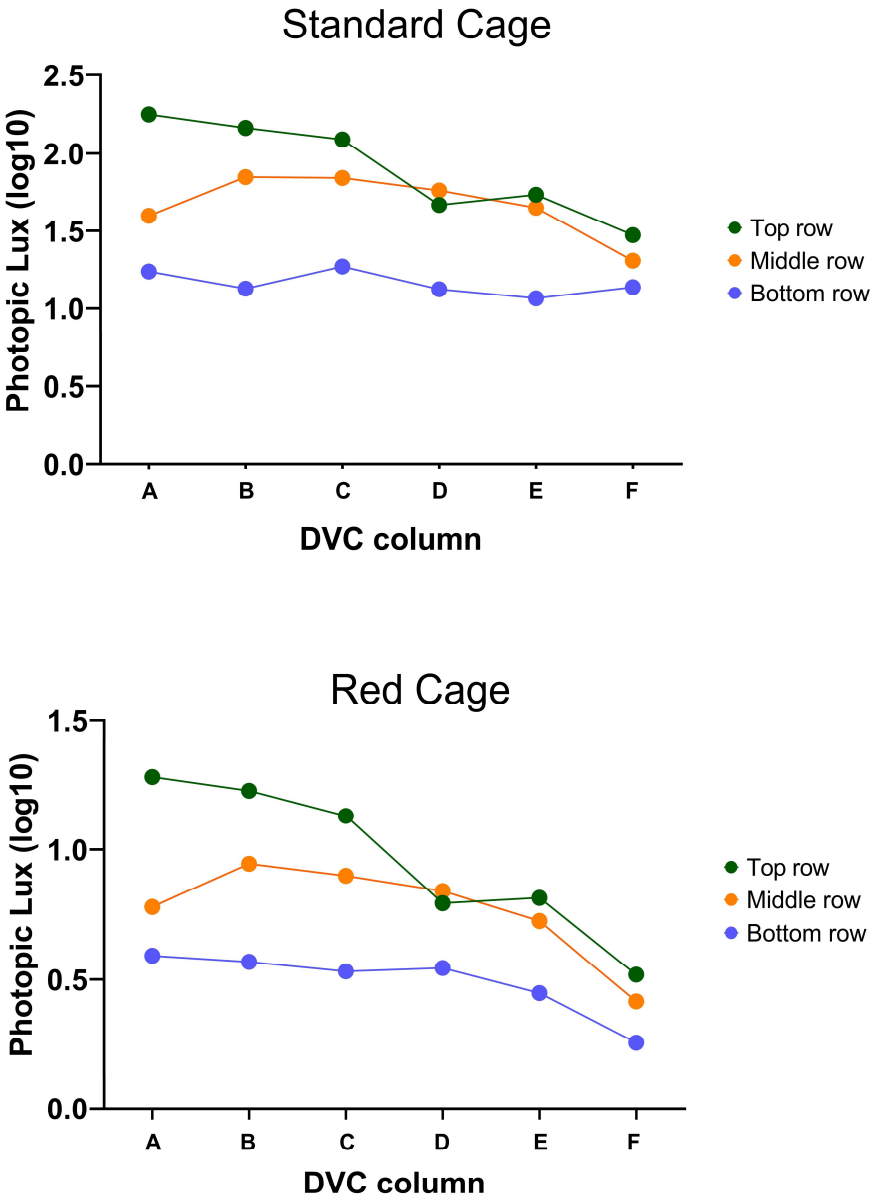

Figure S2.2 Change in light intensity (photopic lux (log10)) across the columns and rows of the DVC rack, within a standard cage and red cage.

2.6.2 Supplementary tables

DVC position	Front of Cage	Middle of Cage	Back of Cage
10A	482.9	25.0	24.6
10B	405.2	16.1	15.2
10C	339.1	17.4	12.1
10D	118.4	11.8	9.3
10E	139.6	10.3	12.5
10F	65.4	13.9	9.8
6A	88.1	22.5	8.3
6B	193.8	11.4	6.1
6C	194.5	9.3	5.1
6D	157.3	11.1	4.8
6E	118.8	10.6	4.3
6F	45.0	9.6	6.4
1A	33.7	8.2	10.1
1B	28.5	8.0	3.8
1C	30.6	21.5	3.6
1D	29.5	6.2	4.2
1E	19.4	11.7	3.6
1F	23.8	13.4	2.6

DVC position	Front of Cage	Middle of Cage	Back of Cage
10A	54.2	1.5	1.7
10B	47.9	1.4	1.5
10C	38.0	1.3	1.1
10D	16.6	1.3	0.6
10E	17.5	1.0	1.0
10F	7.5	1.3	1.1
6A	14.4	2.1	1.5
6B	24.2	1.9	0.4
6C	22.5	1.2	0.1
6D	19.7	0.7	0.3
6E	14.6	0.9	0.3
6F	6.3	1.1	0.4
1A	8.4	3.1	0.3
1B	7.8	2.9	0.3
1C	7.7	2.4	0.1
1D	7.1	3.1	0.2
1E	5.9	2.2	0.3
1F	3.4	1.6	0.3

Table S2.1 Within-cage light intensity measurements (photopic lux). Measurements taken at the front, middle and back of standard cages (top table) and red cages (bottom table), in each column across the top, middle and bottom rows of the DVC rack.

Lux	LPA	DPA	RA	Activity Onset
Photopic	R^2 = 0.2466 *p* = 0.0033	R^2 = 0.2466 *p* = 0.0033	R^2 = 0.2431 *p* = 0.0036	R^2 = 0.2764 *p* = 0.0017
Melanopic	R^2 = 0.2637 *p* = 0.0022	R^2 = 0.2637 *p* = 0.0022	R^2 = 0.2600 *p* = 0.0024	R^2 = 0.3215 *p* = 0.0006
S-cone	R2 = 0.2584 P = 0.0025	R2 = 0.2584 P = 0.0025	R2 = 0.2546 P = 0.0027	R2 = 0.3301 P = 0.0005
Rhodopic	R2 = 0.2619 P = 0.0023	R2 = 0.2619 P = 0.0023	R2 = 0.2582 P = 0.0025	R2 = 0.3155 P = 0.0007
M-cone	R2 = 0.2536 P = 0.0028	R2 = 0.2536 P = 0.0028	R2 = 0.2498 P = 0.0031	R2 = 0.3071 P = 0.0008

Table S2.2 Linear regression values for key circadian entrainment metrics and each α-opic irradiance (log10) values.

Chapter 3. Light sampling behaviour regulates circadian entrainment

The following chapter contains reproduced material from the following paper, accepted for publication at BMC Biology:

Steel et al, 2024 (accepted): Light sampling behaviour regulates circadian entrainment in mice.

3.1 Abstract

The natural light environment is far more complex than that experienced by animals under laboratory conditions. As a burrowing species, wild mice are able to self-modulate their light exposure, a concept known as light sampling behaviour. By contrast, under laboratory conditions mice have little opportunity to exhibit this behaviour. To address this issue, here we introduce a simple nestbox paradigm to allow mice to self-modulate their light environment. Dark nestboxes fitted with passive infrared sensors were used to monitor locomotor activity, circadian entrainment, decision making and light sampling behaviour. Under these conditions, mice significantly reduce their light exposure to an average of just 0.8hrs across a 24hr period. In addition, mice show a distinct pattern of light sampling behaviour, with peaks at dawn and dusk under a ramped light dark cycle. Furthermore, we show that the timing of light sampling behaviour depends upon endogenous circadian rhythms and is abolished in mice lacking a circadian clock, indicating a feedback loop between light, the circadian clock and behaviour. Our results highlight the important role of behaviour in modifying the light signals available for circadian entrainment under natural conditions.

3.2 Introduction

Much of our knowledge of photoentrainment comes from the study of rodent models under laboratory conditions (Foster et al., 2020; Tir et al., 2022). However, the laboratory light environment is highly simplified compared to the natural light environment in which the laboratory mouse (*Mus musculus*) and other mouse species live in the wild, and under which their circadian system evolved (Latham and Mason, 2004; Phifer-Rixey and Nachman, 2015). In nature, both the intensity and spectrum of light change predictably across the 24hr period as a function of solar

angle. Intensity can range from 0.001 photopic lux on a starlit night to over 100,000 photopic lux on a sunny day, and light at twilight (dawn and dusk) is short-wavelength enriched due to both atmospheric absorption and scatter (Foster and Helfrich-Förster, 2001; Spitschan et al., 2017, 2016). However, in the laboratory, mice are generally housed under 12hr:12hr light/dark (LD) cycles of broad spectrum white light sources, which may be a simple on/off square-wave or involve ramped light transitions (Peirson et al., 2018).

The way in which an animal interacts with the light environment is also more complex under natural conditions. In the wild, mice build underground burrows (Sutherland and Singleton, 2003) - a behaviour that has also been demonstrated under semi-natural (Schmid-Holmes et al., 2001) and laboratory environments (Adams and Boice, 1981; Bouchard and Lynch, 1989), and which allow animals to self-modulate their light exposure across the day. The motivation to move in and out of a burrow, or to the burrow entrance, is unlikely to solely be light. Rather, a balance of temperature considerations, food availability, predation risk and activity of conspecifics may drive this behaviour (Robbers et al., 2015; van der Vinne et al., 2015). However, light exposure is an important consequence, and this has been termed light sampling behaviour (DeCoursey, 1986; Decoursey and Menon, 1991; Roenneberg and Foster, 1997). In this way, behaviour is an important factor in determining the timing, intensity and spectrum of light available for photoentrainment (Häfker et al., 2022). Under laboratory conditions this is often overlooked, with mice typically having little opportunity to self-modulate their light exposure (Jud et al., 2005).

It has been clearly documented that circadian behaviour is very flexible (Riede et al., 2017). For example, mice show reliable nocturnal activity under laboratory conditions. However, when environmental conditions vary in a more naturalistic way, diurnal activity has been observed - such as under low night time temperatures (Daan et al., 2011; van der Vinne et al., 2014) and conditions of limited food availability (Hut et al., 2011; Northeast et al., 2019). This does not result from a change in the phase of the underlying SCN clock, but may reflect independent entrainment of peripheral clocks which facilitate flexibility (Van Der Veen et al., 2017). A strongly reductionist approach to experimental design has been suggested to result in local truths with little external validity (Calisi and Bentley, 2009; Gattermann et al., 2008; Richter et al., 2009; Tir et al., 2022; Van Der Veen et al., 2017; Würbel, 2001). As a result, a more naturalistic approach to research – studying physiology and behaviour under conditions in which species evolved - may benefit many fields, from neuroscience (Smith, 2023) to molecular biology (Heard, 2022).

Here we provide laboratory mice (*Mus musculus)* with dark nestboxes and therefore the opportunity to self-modulate their light exposure, allowing circadian entrainment to be studied under more

naturalistic conditions. It is possible that mice bred in the laboratory display behavioural differences to those living in the wild (Troxell-Smith et al., 2016), but they serve as a model. These behavioural aspects of photoentrainment have only been explored in a few studies previously - in mice (Refinetti, 2004), hamsters (Boulos et al., 1996) and flying squirrels (DeCoursey, 1986; Decoursey and Menon, 1991). Whilst it has been suggested that self-modulating light exposure does not have a significant effect on photoentrainment in mice (Refinetti, 2004), this has not been explored under more naturalistic conditions with gradual twilight transitions. Here we show that when given the choice, mice will significantly reduce their daily light exposure and exhibit a distinct pattern of light sampling behaviour, with peaks at twilight. Furthermore, the timing of this light sampling behaviour depends upon endogenous circadian rhythms and is abolished in mice lacking a circadian clock (*Cry1*$^{-/-}$,*Cry2*$^{-/-}$). These data illustrate the importance of light sampling behaviour in modulating photoentrainment.

3.3 Materials and Methods

3.3.1 Animals and housing conditions

For the first light sampling study, 12 C57BL/6J mice were used. They were tested in two cohorts of 6 animals, run at separate times. To examine the role of the circadian clock in regulating light sampling behaviour, 6 *Cry1*$^{-/-}$,*Cry2*$^{-/-}$ mice (lacking a circadian clock (van der Horst et al., 1999)) and 6 congenic C57BL/6J controls were used. All animals were aged ~10 weeks at the start of the control week and all groups were sex balanced. All animals were singly housed with *ad libitum* access to food and water, located in a food hopper and water bottle in the main cage (i.e. outside the nestbox) (Fig. 3.1C). The substrate of the cages were sawdust shavings (eco-pure aspen chips 4, Datesand; UK) and we observed no evidence of animals blocking the entrance of the nestbox. Sizzlenest was provided as a nesting material throughout the experiment (sizzlenest, Datesand; UK). It was placed in the main cage at the beginning of the experiment, and the majority of mice moved the sizzlenest into the nestbox.

Cages were placed within light-tight ventilated chambers (LTCs) equipped with multiple WiFi controlled cool-white (4500 CCT) light-emitting diodes (LEDs) (LIFX light-strip; LIFX, Cremorne, Australia), providing a light level of 200 photopic lux (5 S-cone opic lux, 170 melanopic lux, 169 rhodopic lux and 170 M-cone opic lux) throughout the light phase; calculated using the Rodent Toolbox (Lucas et al., 2014). The spectral power distribution of the cool-white LED consisted of a high, narrow peak at ~450nm and a lower, broader peak at ~560nm (Fig. S3.1; spectral power distribution (SPD) reported in supplementary materials), measured using a

calibrated Ocean Optics USB2000+ Spectrophotometer (Ocean Insight, Oxford, United Kingdom). The temperature of the animal holding room was maintained at 19-21°C. All experimental procedures were conducted at the University of Oxford, England, in accordance with the United Kingdom Animals (Scientific Procedures) Act 1986 under Project License PP0911346 and Personal License I82616702. All procedures were in accordance with the University of Oxford Policy on the Use of Animals in Scientific Research.

3.3.2 Experimental design

All animals, in all experiments, were exposed to the same initial sequence of conditions (Table 3.1). Prior to the onset of the experiment, all mice were habituated to a reverse square-wave 12hr:12hr LD cycle (lights on at 19:00 and lights off at 07:00) for 2 weeks. This LD cycle remained constant for weeks 1-6 of the experiment. Following habituation there was a control week of standard laboratory conditions, before a nestbox was added to each cage for 2 weeks (Fig. 3.1A). The first week was to allow habituation to the nestbox and only the second week of recordings were used in analysis. The nestbox remained in place for the remainder of the experiment. Throughout week 4, forage mix (LBS forage mix; LBS Biotechnology, UK) was added to the cage floor during daily welfare checks, in addition to standard food in the food hopper (Fig. 3.1C), to examine the effect of being able to take food back to the nestbox on activity and entrainment. In weeks 5 and 6, a 12:2:8:2hr cycle was used to explore the effect of a more naturalistic LD cycle. This was composed of a 12hr light phase (170 melanopic lux of cool-white LED) followed by a 2hr ramp of decreasing light intensity, an 8hr dark phase and a 2hr ramp of increasing light intensity. Both ramps followed an exponential pattern, with light intensity measuring 16 photopic lux at 1hr into the ramp. The timings of the 12:2:8:2hr ramped LD cycle were based on the length of daylight and twilight naturally occurring at the spring and vernal equinoxes in Oxford, UK (sourced from https://www.timeanddate.com/sun/uk/oxford). The equinox LD cycle was used since it is an intermediate LD cycle, with the length of the light phase being in-between those of the summer and winter solstices. The first week was to allow habituation to the ramped LD cycle and only the second week of recordings were used in analysis. All animals in the second experiment (*Cry1*$^{-/-}$*,Cry2*$^{-/-}$ vs. C57BL/6J controls) were exposed to an additional 2 weeks of constant dark (DD) at the end, to check for expected free-running locomotor activity patterns in C57BL/6J controls and arrhythmicity in *Cry1*$^{-/-}$*,Cry2*$^{-/-}$. The first week of DD was for habituation, and only the second week was used for analysis (data not shown).

Week	Lighting	Condition	Purpose
1	Reverse 12:12hr LD cycle	Standard	Control
2	Reverse 12:12hr LD cycle	Nestbox	Nestbox habituation
3	Reverse 12:12hr LD cycle	Nestbox	Nestbox data collection
4	Reverse 12:12hr LD cycle	Nestbox + forage mix	Nestbox + forage mix
5	Reverse 12:2:8:2hr LD cycle	Nestbox	Ramped LD habituation
6	Reverse 12:2:8:2hr LD cycle	Nestbox	Ramped LD data collection
7	Constant dark (DD)	Nestbox	DD habituation
8	Constant dark (DD)	Nestbox	DD data collection

Table 3.1 Experimental design timeline. All animals in all studies were exposed to week 1-6 conditions. The 12 animals in the second study ($Cry1^{-/-}$,$Cry2^{-/-}$ vs. C57Bl6/J) were exposed to an additional two weeks (weeks 7 and 8, shaded in grey).

3.3.3 Locomotor activity monitoring

From week 2 onwards, all cages were fitted with a nestbox. The nestbox was designed in Blender (v3.6.4 LTS, https://www.blender.org/), sliced in Ultimaker Cura (v5.4.0; files can be found in the supplementary material) and 3D printed (Ultimaker S3 printer) in black ABS plastic (Ultimaker 1621). The nestboxes (Fig. 3.1B) were comprised of two sections – a base and a top which were glued together, and all walls were 5mm thick. The base (90mm(H) x 100mm(W) x 140mm(D)) had two internal sections, a larger nesting section at the back (internal dimensions of 85mm(H) x 90mm(W) x 80mm(D)) and a smaller atrium section at the front (internal dimensions of 85mm(H) x 90mm(W) x 45mm(D)), a design influenced by Kallmyer (et al., 2019). Between the nesting section and the atrium, and the atrium and the main cage, there were staggered open archways measuring 30mm(H) x 40mm(W). This allowed free movement between compartments, and for light to be detected from the atrium entrance whilst ensuring a dark nesting section. As measured by an XL-500 BLE Spectroradiometer (dynamic range = 0.1 to 40,000 photopic lux; NanoLambda, Korea) the light level in the nesting section was <0.1 photopic lux and the atrium section ranged from <0.1 to 0.4 photopic lux, with distance from the entrance into the main cage (Fig. 3.1C). The top section of the nestbox was a 5mm thick wall (21mm(H) x 100mm(W) x 140mm(D)) and was glued on top of the nestbox base to ensure the structure was flush with the top of the cage. A passive infrared sensor (PIR) (Brown et al., 2017) was fitted into a 10mm diameter hole in the centre of each of the nesting and atrium compartments, and a third PIR sensor was fitted 22cm above each cage. Each PIR sensor records movement as a binary measurement every 10ms and combines this data across 1s bins, outputting a percentage activation of the sensor across every 1s epoch. This enabled quantification of locomotor activity circadian entrainment, decision making

and light sampling behaviour. Locomotor activity was defined as movement in the main cage, outside of the nestbox. Light sampling behaviour was defined as a movement within the nestbox - specifically from the dark nest to the atrium compartment, from which the animal is able to detect the external light environment, as at the burrow entrance. Under this definition, light sampling behaviour can occur across the 24hr period, including during the dark phase when there is no light to sample. For this reason, it is perhaps more accurate to describe it as 'light environment sampling' behaviour, where the light environment could be light or dark. For simplicity, these terms will be used interchangeably. This is to enable visualisation of light environment sampling behaviour across the 24hr period. Every 6 PIRs were connected to a 6-port Arduino (Arduino Uno R3). 3 Arduinos were subsequently connected to a Raspberry Pi (Raspberry Pi 3 B) and Node Red (v3.1.0) was used to collect and backup data on the Raspberry Pi. PIRs collected activity data every 1s, as the standard 10s data collection (Brown et al., 2017) did not provide a high enough temporal resolution to accurately track the animal as it moved between sensors. The light schedule of the LTCs was confirmed using a light-dependent resistor (LDR) connected to the PIR system.

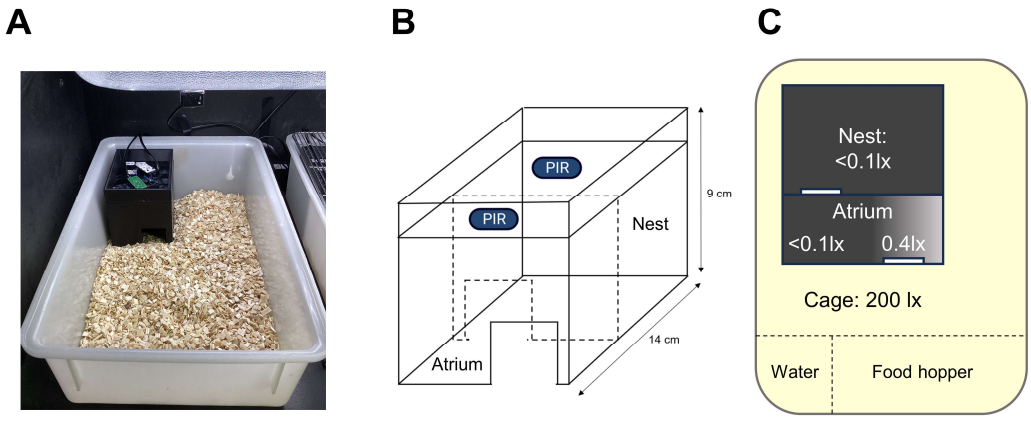

Figure 3.1 – Experimental setup. **(A)** Photo of nestbox in-situ, with passive-infrared sensor (PIR) above cage. **(B)** Schematic of nestbox design (not to scale), with PIRs. **(C)** Light levels across nestbox and cage, measured using an XL-500 BLE Spectroradiometer (NanoLambda, Korea), with location of water bottle and food hopper marked.

3.3.4 Data processing

Raw PIR activity and LDR data was processed in MATLAB (v.R2022b), ImageJ (v.1.53a, using the Actogram J plugin (Schmid et al., 2011)) and Excel (v.2310). No significant differences between

cohorts 1 and 2 of the first C57BL/6J light environment sampling study were found, so cohorts were processed and analysed together.

Locomotor activity profiles. Raw main cage PIR activity and LDR data starting at ZT0 for 7 consecutive days (ZT = zeitgeber time; ZT0 = lights on, ZT12 = lights off) was smoothed with a 30min moving average to generate daily activity profiles for each experimental condition.

Location and light exposure. A MATLAB function *(location_finder.m)* was written to calculate the location (cage, atrium or nest) of each mouse at each 1s time point. This function filled in the location of the mouse using the 3 PIR channels of activity data (cage, atrium, nest) to account for the mouse being present but immobile in a location. If all PIR channels were reading 0, then it moved back rows until it hit a value of >0 in one of the columns. A value of 1 was assigned to this channel. This produced a dataset for each mouse, where 1 equalled present and 0 equalled not present, across every second at all three locations (cage, atrium, nest). Using the location data, daily light exposure could subsequently be calculated. This was defined as the time spent (hrs) in the main cage during the light phase. For the control week this is automatically 12hrs, as there was no nestbox available.

Light environment sampling behaviour and decision making. Analysis of light environment sampling behaviour and decision making was also based on the location data. A MATLAB function *(simplify_columns.m)* was written which took the location data and generated a new matrix, to ensure that only one sensor was active at a time (if a mouse moved across the three PIR sensors within 1-3 seconds, then two or three sensors would show activity at each time point, due to sensor lag). If all three location columns equalled 0, three 0s were assigned to the new matrix. If all columns were 1, a 1 was assigned to the atrium column and a 0 to the nest and cage (since the mouse is moving from the cage to the nest, through the atrium, or vice versa). If two columns equalled 1, then it moved up rows until one of the rows equalled 0. A 0 was assigned to this column and a 1 to the other column. A MATLAB function *(transitions.m)* was written to then take the simplified data and create a new matrix identifying light environment sampling behaviour (defined as a nest to atrium transition, and assigned as '1' in the new matrix), followed by either entry to the cage (a "go" decision, assigned as '2') or a return to the nest (a "no-go" decision, assigned as '3') (Fig. 3.3C). The sum of the "go" and "no go" transitions equalled the total number of light environment sampling events.

Circadian entrainment metrics. Key circadian entrainment metrics were calculated as in (Brown et al., 2019), using activity data from the main cage PIR sensor. MATLAB was used to calculate

light phase activity, dark phase activity, relative amplitude, inter-daily stability and intra-daily variability. The chi-squared periodogram power (Qp) (Sokolove and Bushell, 1978) and activity onsets were calculated using inbuilt functions in Actogram J (Schmid et al., 2011; Sokolove and Bushell, 1978).

3.3.5 Statistical analysis

Statistical analysis and data visualisation were performed in MATLAB and Prism Graph-pad (v.9.5.0). All data is reported as mean across days and animals, +/- SEM, and $\alpha = 0.05$ was adopted in all analyses. All locomotor, light environment sampling and decision making daily profiles are visualised in 30 min bins. Any animals that did not routinely use the nestbox were removed from the analysis (2 C57BL/6J animals in the initial light environment sampling study, and 3 of the *Cry1*$^{-/-}$,*Cry2*$^{-/-}$ animals in the second experiment). The Greenhouse-Geisser correction was performed with all ANOVAs, unless otherwise stated. A post-hoc Tukey test was used when all pairwise comparisons were desired, and a Tukey-Kramer test where sample sizes were unequal; whilst a post-hoc Bonferroni test was used for a specific comparison between the control and experimental treatments. Further details on statistical tests used for each dataset are reported in the results section.

3.4 Results

3.4.1 Nestbox availability significantly reduces daily light exposure

10 out of 12 C57BL/6J animals routinely used the nestbox (Fig. S3.2), thereby reducing their daily light exposure. Daily light exposure was significantly different between the control and nestbox condition [$t(9) = 235.2$, $p<0.0001$], and between the control and nestbox + forage mix ('+forage mix') condition [$t(9) = 195.6$, $p<0.0001$; one-sample t-test against a control mean of 12.0hrs], with mice reducing their average daily light exposure to 0.8hrs under the nestbox condition, and to 0.6hrs under the nestbox and forage mix condition (Fig. 3.2A). The addition of forage mix in addition to a nestbox also significantly reduced light exposure, compared to the nestbox only condition [$t(9) = 4.8$, $p < 0.0009$; paired t-test]. This difference is likely to result from mice being able to take food back to the nestbox under the forage mix condition, rather than having to leave the nestbox to feed from the external food hopper (Fig. 3.1C) under the nestbox only condition.

3.4.2 Nestbox availability with forage mix significantly affects measures of circadian disruption

Based upon the main cage sensor, the addition of a nestbox in combination with forage mix resulted in significant differences in metrics of circadian rhythm disruption in C57BL/6J mice, compared to under the control or nestbox only conditions (Fig. 3.2B). Experimental condition (control, nestbox, nestbox + forage mix ('+ forage mix')) had a significant effect on light phase activity [$F(2.2, 20.1) = 11.3$, $p = 0.0004$], relative amplitude [$F(2.4, 21.6) = 6.8$, $p = 0.0034$], inter-daily stability [$F(2.2, 19.4) = 10.8$, $p = 0.0006$] and periodogram power [$F(1.9,16.7) = 11.4$, $p = 0.0009$], as tested by a one-way repeated-measures ANOVA. Further circadian metrics were calculated and are reported in the supplementary material (Fig. S3.3). Across all parameters, post-hoc Tukey tests demonstrated significantly more robust activity patterns under the nestbox + forage mix condition compared to the control or nestbox only conditions, as evidenced by decreased light phase activity (control vs nestbox + forage mix, $p = 0.0411$; nestbox vs nestbox + forage mix, $p = 0.01$), increased relative amplitude (nestbox vs nestbox + forage mix, $p = 0.0198$), inter-daily stability (control vs nestbox + forage mix, $p = 0.0335$; nestbox vs nestbox + forage mix, $p = 0.0089$) and periodogram power (control vs nestbox + forage mix, $p = 0.0241$; nestbox vs nestbox + forage mix, $p = 0.0055$) (Brown et al., 2019). These findings demonstrate how adding environmental enrichment can modify commonly calculated metrics of circadian behaviour.

3.4.3 Daily locomotor activity does not reflect daily light environment sampling behaviour

The daily locomotor activity profile of C57BL/6J mice (Fig. 3.2C) illustrates low activity levels across the light phase, followed by a peak in activity at the onset of the dark phase, with levels declining across the rest of the night. Daily light environment sampling events (Fig. 3.2D) (defined as movement from the nest to the atrium) also show a rhythmic pattern, with lower levels during the light phase and higher levels at night. However, it differs to locomotor activity with light environment sampling events remaining constant across the dark phase. This pattern is consistent across days, under all conditions (Fig. S3.4). Differences in the pattern of locomotor activity and light environment sampling behaviour are further demonstrated when sex differences are considered (Fig. S3.5). Females show significantly higher locomotor activity, under both a 12:12hr (Fig. S3.5,A) [$F(1,10) = 14.1$, $p = 0.0037$] and 12:2:8:2hr LD cycle (Fig. S3.5,C) [$F(1,10) = 6.1$, $p = 0.0332$]. However, there is no significant main effect of sex on light environment sampling behaviour, under either a 12:12hr (Fig. S3.5B) [$F(1,8) = 1.4$, $p = 0.2639$] or 12:2:8:2hr LD cycle (Fig. S3.5D) [$F(1,8) = 0.9$, $p = 0.3647$] (two-way repeated-measures ANOVA and post-hoc Bonferroni test).

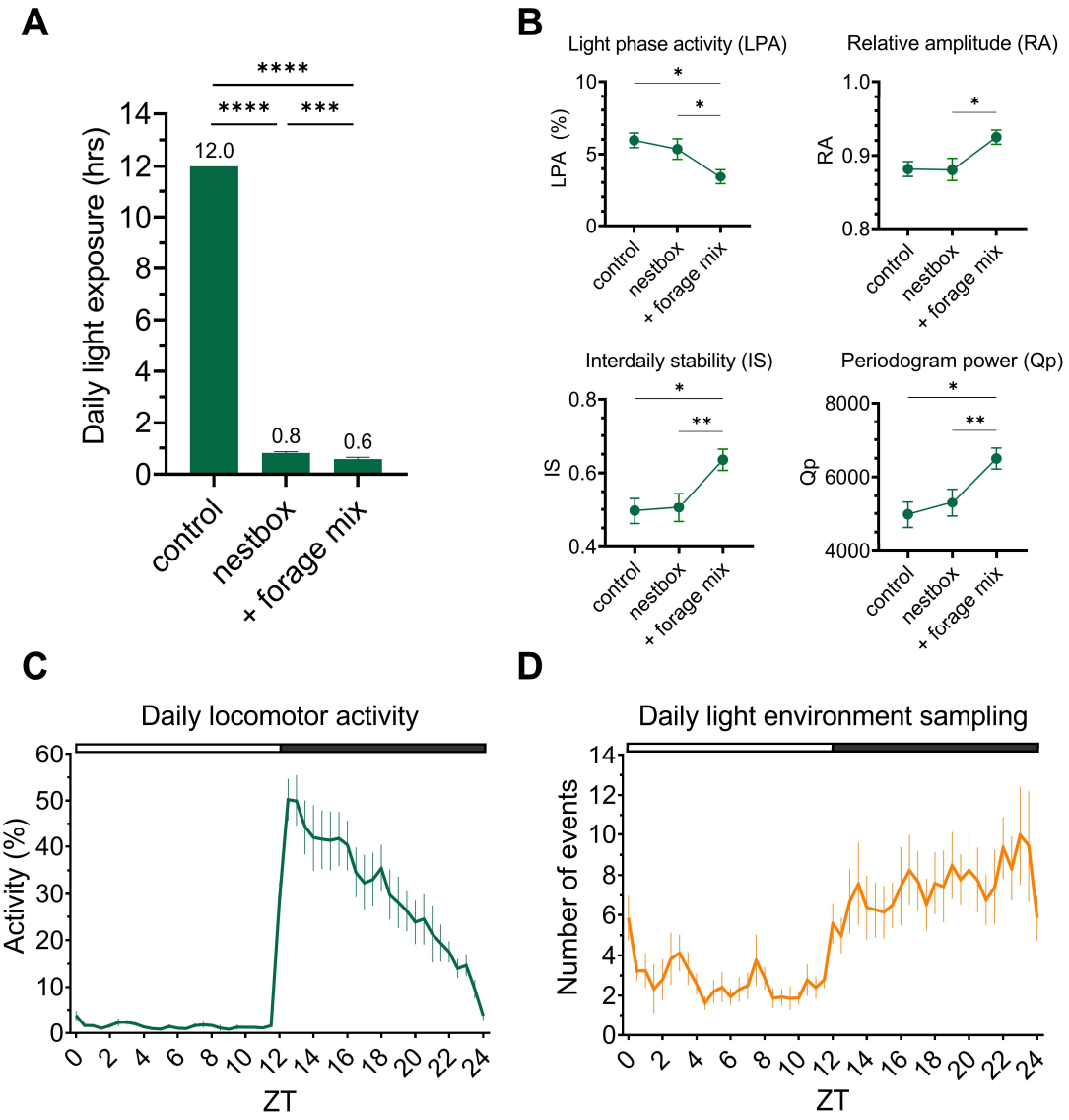

Figure 3.2 - Effects of nestbox availability on light exposure and behaviour. **(A)** Daily light exposure (hrs) of animals across experimental conditions. **(B)** Key circadian entrainment metrics across experimental conditions. (A,B) The combined nestbox and forage mix condition is referred to as '+ forage mix'. **(C)** Daily locomotor activity profile of animals housed with a nestbox, calculated using the main cage PIR. **(D)** Daily light environment sampling profile. White and black bar shows timing of light and dark, respectively (C,D). All results reported as mean across mice and days, +/- SEM. **** $p<0.001$, ** $p<0.01$, * $p<0.05$, between condition comparisons.

3.4.4 Under a ramped LD cycle mice show peaks in light environment sampling behaviour at twilight

Changing the LD cycle to a ramped 12:2:8:2hr LD cycle results in comparable locomotor activity patterns in C57BL/6J animals as under a square-wave 12:12hr LD cycle, in both sexes (Fig. S3.5A,C). However, a ramped LD cycle significantly alters the pattern of light environment sampling behaviour across time (Fig. 3.3A), with a significant main effect of light condition [$F(1,9) = 7.3$, $p = 0.0244$] and ZT [$F(3.5,31.7) = 14.0$, $p < 0.0001$] being observed, as well as a significant light condition x ZT interaction [$F(4.7,42.4) = 6.7$, $p = 0.0002$, two-way repeated measures ANOVA (Fig. 3.3A)]. A clear peak in light environment sampling events was seen at ZT22 under the ramped LD cycle compared to the square LD cycle ($p = 0.0023$, post-hoc Bonferroni test), immediately following the start of the light-on ramp (corresponding to 'dawn'). This pattern is consistent across sexes (Fig. S3.5D). To explore this difference further, the mean number of light environment sampling events occurring during dawn (ZT22-0), the day (ZT0-12) and dusk (ZT12-14) were calculated (Fig. 3.3B). Night time (ZT14-22) was not included since there is no light at this time to sample. A significant effect of time of day on number of events was observed [$F(2.0,17.8) = 16.4$, $p < 0.0001$, one-way repeated-measures ANOVA]. A post-hoc Tukey test demonstrated significantly higher levels of crepuscular activity shown by more light environment sampling events at twilight compared to the day [dawn vs. day ($p = 0.0014$), dusk vs. day ($p = 0.0005$)]. Interestingly, more light environment sampling was seen at dawn than dusk ($p = 0.0157$).

3.4.5 The nestbox paradigm allows for quantification of decision making behaviour, under a long-term home cage experiment

Following a light environment sampling event (movement from the nest to the atrium), an animal can either move into the cage (classified as a "go" decision) or return to the nest (classified as a "no-go" decision) (Fig. 3.3C). Categorising decision making following light environment sampling events under a ramped LD cycle (Fig. 3.3D) demonstrates that the peak in light environment sampling events at dawn can largely be explained by an increase in "no-go" decisions, with approximately twice as many "no-go" transitions as "go" decisions. Whilst no significant main effect of decision route was observed [$F(1,9) = 3.7$, $p = 0.0081$], there was a significant main effect of ZT [$F(4.4,39.8) = 14.0$, $p < 0.0001$] and a significant decision route x ZT interaction [$F(3.7,33.5) = 7.5$, $p = 0.0003$, two-way ANOVA and post-hoc Bonferroni test]; the latter demonstrating that, as expected in a generally nocturnal, photophobic species, the ratio of "no-go" to "go" decision routes changes across time, with "no-go" decisions being higher during the light phase (ZT22-14), and "go" decisions increasing at dark onset (ZT14-18).

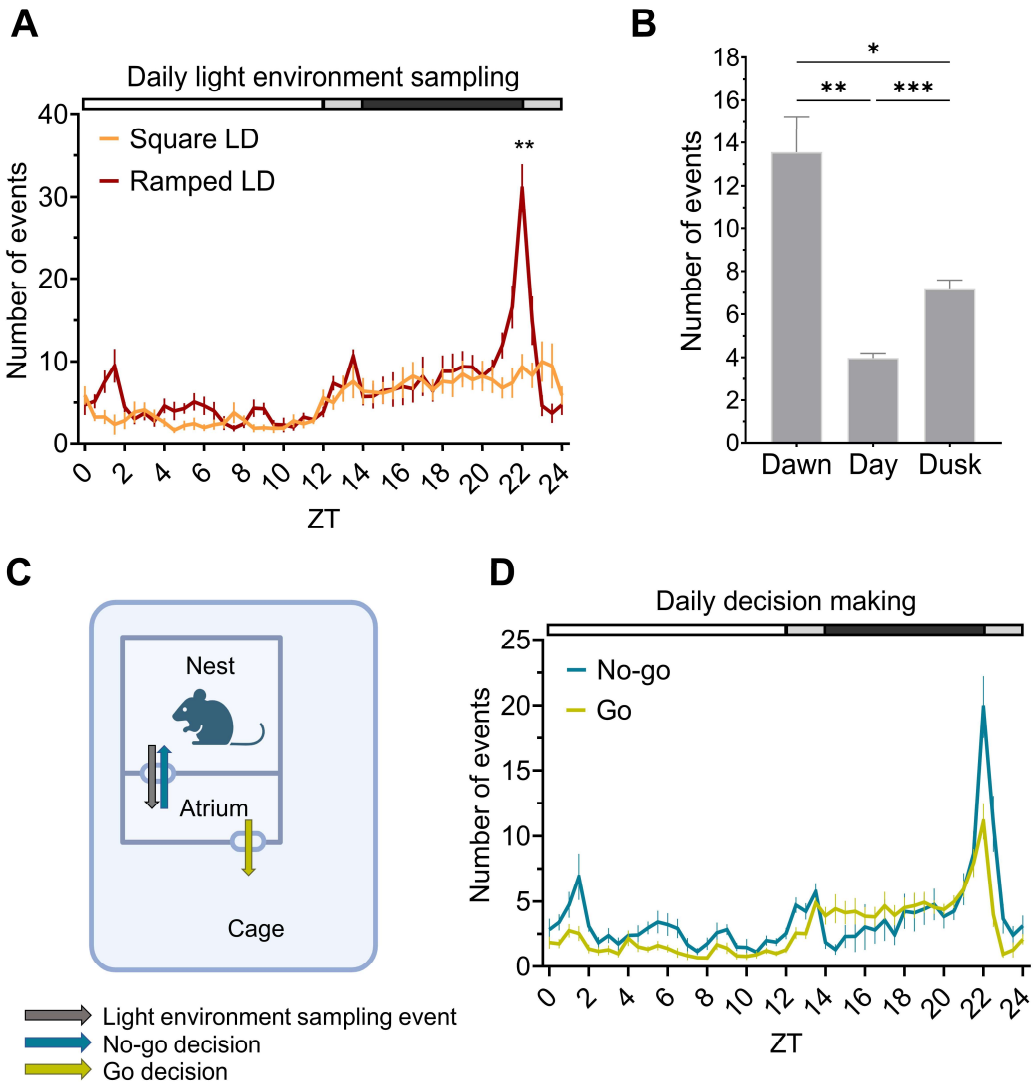

Figure 3.3 – Effects of a ramped LD cycle on light environment sampling behaviour. **(A)** Daily light environment sampling profile under a square 12:12hr LD cycle (green) and a ramped 12:2:8:2hr LD cycle (blue). **(B)** Number of light environment sampling events occurring during dawn (ZT22-0), the day (ZT0-12) and dusk (ZT12-14), under a ramped 12:2:8:2hr LD cycle. **(C)** Schematic demonstrating "no-go" or "go" decision making following light environment sampling behaviour. **(D)** Daily decision making profile showing "no-go" (red) and "go" (green) decisions under ramped 12:2:8:2hr LD cycle. White, grey and black bar shows timing of light, light ramp and dark, respectively (A,D). All results reported as mean across mice and days, +/- SEM. **** $p<0.001$, ** $p<0.01$, * $p<0.05$, between condition comparisons.

3.4.6 Mice lacking a circadian clock use the nestbox less than wildtype controls

To examine the role of circadian rhythms in determining the timing of light environment sampling behaviour, mice lacking a circadian clock (*Cry1*$^{-/-}$,*Cry2*$^{-/-}$) and congenic C57BL/6J controls were tested under the same paradigm as the first C57BL/6J light sampling experiment. Fewer *Cry1*$^{-/-}$,*Cry2*$^{-/-}$ mice (3 out of 6 animals) routinely used the nestbox compared to C57BL/6J WT counterparts (all 6 animals) (Fig. S3.7). This difference may relate to attenuated novelty-induced locomotor activity levels in *Cry1*$^{-/-}$,*Cry2*$^{-/-}$ (De Bundel et al., 2013) and altered photic sensitivity (Nakamura et al., 2011; Owens et al., 2012; Selby et al., 2000; Van Gelder et al., 2003); highlighting the sensitivity of our paradigm to demonstrate differences in behavioural and physiological phenotypes.

Of the mice that did use the nestbox, both *Cry1*$^{-/-}$,*Cry2*$^{-/-}$ mice and C57BL/6J WT counterparts reduced their daily light exposure when a nestbox was available (Fig. 3.4) [significant main effect of condition, $F(1.2,8.5) = 8$, $p<0.0001$, two-way repeated-measures ANOVA with Tukey-Kramer post-hoc test (C57BL/6J control vs. nestbox, $p<0.0001$; *Cry1*$^{-/-}$,*Cry2*$^{-/-}$ control vs. nestbox, $p = 0.0391$)]. However, *Cry1*$^{-/-}$,*Cry2*$^{-/-}$ mice reduced their daily light exposure less than the C57BL/6J WT counterparts (Fig. 3.4), to an average of 4.5hrs compared to 0.4hrs under the nestbox condition, respectively. This trend was reflected in a significant main effect of genotype on daily light exposure [$F(1,7) = 24.9$, $p = 0.0016$]. Forage mix in addition to a nestbox did not further significantly reduce daily light exposure in C57BL/6J mice, as in the previous C57BL/6J only study, remaining at 0.4hrs in both conditions (Fig. 3.4). This may result from a floor effect, since 0.4hrs is already lower than the 0.6hrs of daily light exposure exhibited by mice under the nestbox and forage mix condition in the C57BL/6J only study (Fig. 3.2A). However, in *Cry1*$^{-/-}$,*Cry2*$^{-/-}$ mice, forage mix availability reduced daily light exposure, resulting in a significant genotype x condition interaction [$F(2,14) = 27.1$, $p<0.0001$]. However, as defined by a post-hoc Tukey-Kramer test, this reduction was not significant.

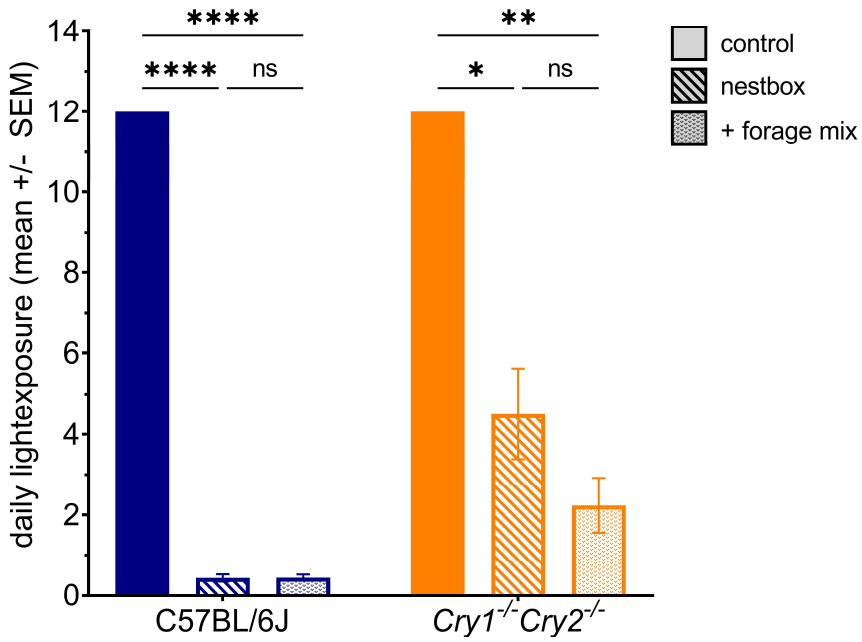

Figure 3.4 – Effects of nestbox availability on daily light exposure in C57BL/6J and Cry1$^{-/-}$Cry2$^{-/-}$ animals. Daily light exposure (hrs) perceived by C57BL/6J (blue) and Cry1$^{-/-}$Cry2$^{-/-}$ animals (orange) under different conditions. The combined nestbox and forage mix condition is referred to as '+ forage mix'. All results reported as mean across mice and days, +/- SEM. **** $p<0.001$, ** $p<0.01$, * $p<0.05$, between condition comparisons.

3.4.7 Mice lacking a circadian clock show rhythmic daily locomotor activity but arrhythmic daily light environment sampling behaviour

Both C57BL/6J (Fig. 3.5A, blue) and *Cry1*$^{-/-}$,*Cry2*$^{-/-}$ mice (Fig. 3.5A, orange) show rhythmic patterns in locomotor activity across time [significant main effect of ZT, $F(2.6,18.0) = 14.83$, $p<0.0001$, two-way repeated-measures ANOVA and post-hoc Bonferroni test]. This is to be expected, as although *Cry1*$^{-/-}$,*Cry2*$^{-/-}$ mice lack a circadian clock they are still able to show rhythmic locomotor activity patterns under an LD cycle (van der Horst et al., 1999) due to negative masking (Mrosovsky, 1999). Although locomotor activity rhythms in *Cry1*$^{-/-}$,*Cry2*$^{-/-}$ mice had a lower amplitude than in C57BL/6J control counterparts, they followed a similar pattern resulting in no significant main effect of genotype [$F(1,7) = 10.03$, $p=0.0158$]; but a significant ZT x genotype interaction [$F(48,336) = 6.4$, $p<0.0001$] since light phase activity was slightly higher in *Cry1*$^{-/-}$,*Cry2*$^{-/-}$ mice but lower than C57BL/6J mice during the dark phase.

However, despite daily locomotor activity being rhythmic in *Cry1*$^{-/-}$,*Cry2*$^{-/-}$ mice, light environment sampling behaviour is arrhythmic (Fig. 3.5B – orange), as confirmed by chi-squared periodogram analysis (data not shown). This is in contrast to the rhythmic pattern exhibited by the C57BL/6J mice (Fig. 3.5B – blue) (no significant main effect of ZT [$F(2.8,19.8) = 1.8$, $p = 0.1760$], but a

significant main effect of genotype [$F(1,7) = 14.6$, $p = 0.0065$] and genotype x ZT interaction [$F(48,336) = 1.73$, $p = 0.0030$], two-way repeated-measures ANOVA and post-hoc Bonferroni test). Together, this suggests that the circadian clock is important for determining the timing of light environment sampling behaviour. Moreover, these data show that arrhythmicity in mice lacking a circadian clock can be detected under a LD cycle, by measuring light environment sampling instead of locomotor activity.

3.4.8 Mice lacking a circadian clock do not show peaks in light environment sampling behaviour at twilight

The crepuscular peaks in light environment sampling behaviour seen in C57BL/6J mice under a ramped LD cycle are abolished in mice lacking a circadian clock (Fig. 3.5C). This difference in light environment sampling across time between genotypes is statistically significant (significant main effect of genotype [$F(1,7) = 29.7$, $p = 0.0010$] and ZT [$F(4.4,30.9) = 4.8$, $p = 0.0032$], as well as genotype x ZT interaction [$F(48,336) = 5.5$, $p<0.0001$]; two-way repeated-measures ANOVA and post-hoc Bonferroni test). The mean number of light environment sampling events occurring during dawn (ZT22-0), the day (ZT0-12) and dusk (ZT12-14) were calculated (Fig. 3.5D). Night time (ZT14-22) was not included since there is no light at this time to sample. A significant main effect of ZT [$F(1.3,12.6) = 9.2$, $p = 0.0071$] and genotype [$F(1,10) = 31.0$, $p = 0.0002$] were observed (two-way repeated-measures ANOVA and post-hoc Bonferroni test). There was also a significant ZT x genotype interaction [$F(2,20) = 12.2$, $p = 0.0003$], demonstrating that light environment sampling varies across twilight and the day differently between C57BL/6J and *Cry1*$^{-/-}$,*Cry2*$^{-/-}$ mice. A post-hoc Bonferroni test highlighted significantly higher levels of light environment sampling events at dawn ($p = 0.0069$) and dusk ($p = 0.0477$) compared to during the day, in C57BL/6J mice (Fig. 3.5D, left panel), but no significant differences in *Cry1*$^{-/-}$,*Cry2*$^{-/-}$ mice (Fig. 3.5D, right panel). This adds further support to the idea that the circadian clock is important for regulating the timing of light environment sampling behaviour, and therefore the amount and type of light available to an organism for photoentrainment.

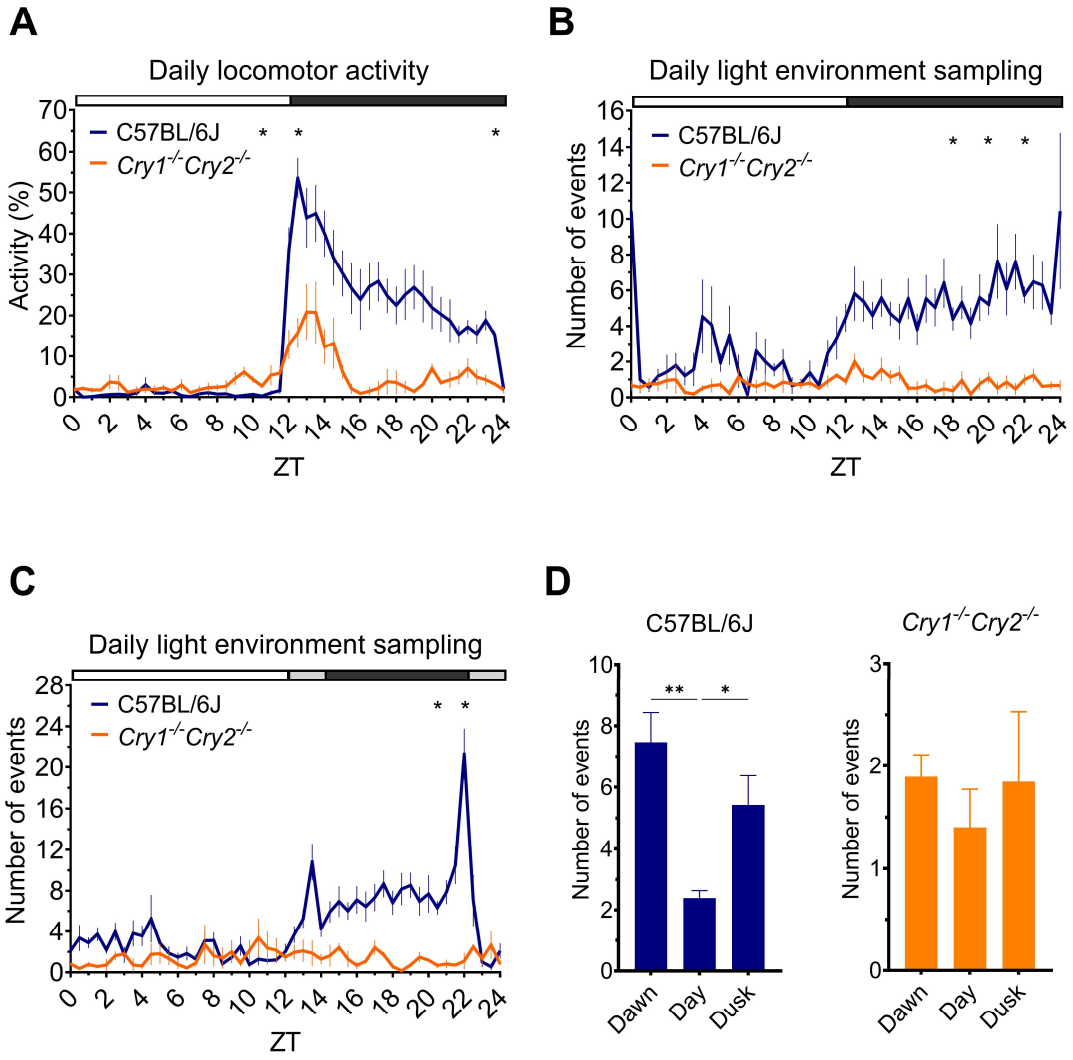

Figure 3.5 - The circadian clock is important for the timing of light environment sampling behaviour. In all subplots C57BL/6J animals are shown in blue and $Cry1^{-/-}Cry2^{-/-}$ animals shown in orange. **(A)** Daily locomotor activity profile of C57BL/6J and $Cry1^{-/-}Cry2^{-/-}$ animals housed with a nestbox under a 12:12hr LD cycle, calculated using the main cage PIR. **(B)** Daily light environment sampling profile of C57BL/6J and $Cry1^{-/-}Cry2^{-/-}$ animals under a 12:12hr LD cycle. **(C)** Daily light environment sampling profile of C57BL/6J and $Cry1^{-/-}Cry2^{-/-}$ animals under a 12:2:8:2hr LD cycle. (A-C) * $p < 0.05$, between genotype comparison. White, grey and black bar shows timing of light, light ramp and dark, respectively. **(D)** Number of light environment sampling events occurring during dawn (ZT22-0), the day (ZT0-12) and dusk (ZT12-14) by C57BL/6J and $Cry1^{-/-}Cry2^{-/-}$ animals (note different scales). **** $p<0.001$, ** $p<0.01$, * $p<0.05$, time of day comparisons. All results reported as mean across mice and days, +/- SEM.

3.5 Discussion

Here we take an ecologically guided approach to circadian entrainment by providing the opportunity for mice to self-modulate their light exposure. We demonstrate that under this paradigm C57BL/6J mice will significantly reduce their daily light exposure to less than an hour across the 24hr period. This reduction mirrors previous literature on nocturnal den-dwelling flying squirrels, where animals housed with simulated dens only exposed themselves to a few minutes of light each day (DeCoursey, 1986; Decoursey and Menon, 1991). DeCoursey observed that some flying squirrels spent the entire light phase in the dark nest, and free-ran for several days until their activity onset advanced into the light phase (DeCoursey, 1986; Decoursey and Menon, 1991). In the current study, all animals showed robust entrainment which is consistent with previous studies in mice (Refinetti, 2004). Refinetti (2004) represents the only previous study to investigate light sampling behaviour in mice and suggests no significant effect of being able to self-modulate light exposure on photoentrainment. However, in this study locomotor rhythms were primarily measured using wheel running behaviour, under square-wave LD cycles. Wheel running only provides a measure of voluntary activity and under some conditions is known to influence behaviour and entrainment (Deboer and Tobler, 2000; Edgar et al., 1991; Novak et al., 2012). Here we measure activity across the cage, atrium and nest at high resolution (1s) and show that it is only under more naturalistic ramped twilight conditions that crepuscular light sampling behaviour is observed.

Given the photophobic behaviour of mice (Bourin and Hascoët, 2003; Crawley et al., 1980) a reduction in light exposure when a nestbox is available is not surprising. However, the extent of the reduction is striking and illustrates a preference for light avoidance that is rarely accounted for in circadian studies and rodent husbandry. Light has potent effects on physiology and behaviour more widely, including on metabolism, hormone regulation and pain responses (Do, 2019). Our results therefore raise the question of whether enforced light exposure under standard laboratory conditions may result in behavioural and physiological effects that do not occur in the wild, and are largely unaccounted for in experimental design and analyses. A recent expert working group recommended that laboratory animals should have the opportunity to escape light by retreating to a shelter (Lucas et al., 2024). Although shelter enrichment such as red plastic or cardboard houses are often used, these reduce rather than abolish light exposure and are unlikely to reduce light exposure below the threshold for entrainment (Butler and Silver, 2011; Ebihara and Tsuji, 1980; Foster and Helfrich-Förster, 2001; Peirson et al., 2018).

The motivation for animals to use the nestbox may in part be light avoidance. However, the regular use of the nestbox during the dark phase (Fig. 3.2D) suggests that light avoidance alone cannot explain this. A nestbox may aid behavioural thermoregulation, since standard laboratory temperatures are ~8°C below the thermoneutral zone of 30°C in mice (Gaskill et al., 2011; Gordon, 2012). However, preliminary thermal imaging (FLIR one pro, Teledyne FLIR) of cages with a nestbox recently removed show a 0.3°C higher temperature in the location of the nestbox, compared to the main cage, when no animal has been nesting in the cage (Fig. S3.6A); and a 3.5°C increase when an animal has been recently using the nestbox (Fig. S3.6B). This is comparable to the 4.2°C increase in temperature in a nest built without a nestbox compared to the main cage (Fig. S3.6C), suggesting that building a nest within a nestbox does not dramatically influence thermoregulation. However, this could differ with the varying dimensions of mice (Chakraborty et al., 2017; https://www.dimensions.com/element/house-mouse) relative to the nestbox volume. Extending our paradigm to incorporate a transparent nestbox control, as well as temperature modulation (Gordon et al., 2017) and different nesting materials (Gaskill et al., 2013), could clarify how different motivations interact to regulate this behaviour (Davis et al., 2022). Thigmotaxis, an innate preference demonstrated by rodents to seek shelter or move in contact with walls instead of exposing themselves to an aversive open area (Barnett, 1963; Zhang et al., 2023) could also be another factor driving use of the nestbox.

In addition to simply using the nestbox, mice showed extensive light sampling behaviour (Fig. 3.2D) distinct from overall locomotor activity (Fig. 3.2C). Light sampling behaviour was defined as the movement from the nest to atrium section of the nestbox, since the external light environment could be detected from here (Fig. 3.1C), mirroring the movement to a burrow entrance. The further reduction in light exposure when forage mix was added (Fig. 3.2A) suggests that the need to feed may be a key motivator behind light sampling behaviour. In support of this hypothesis, Decoursey and Menon (1991) showed that 69% of time spent outside of the nestbox during the light phase by flying squirrels involved feeding and drinking.

Regardless of the motivation, our data demonstrates that behaviour can directly determine the timing of light exposure, with implications for photoentrainment. Under a natural light environment this would directly influence the intensity and spectral composition of light exposure, which vary across the 24hr cycle (Spitschan et al., 2016; Walmsley et al., 2015). Under a ramped LD cycle, the pattern of light exposure is consistent across days (Fig. S3.4), with clear peaks in light sampling behaviour at twilight in C57BL/6J mice (Fig. 3.3A,5C). This provides experimental evidence to support the hypothesis that nocturnal burrow-dwelling rodents sample their light environment more at twilight, thereby regulating the timing of activity with respect to the phase

response curve (PRC) (Roenneberg and Foster, 1997), as under the discrete entrainment model (Pittendrigh and Daan, 1976). However, evidence suggests that models of photoentrainment cannot always be generalised between species with different natural histories, and therefore different patterns of light exposure. For example, the European ground squirrel entrains without ever seeing twilight (Hut et al., 1999), and a subterranean rodent, the tuco-tuco, can entrain to a single 1hr light pulse delivered randomly within the day (Flôres et al., 2016).

Since all other conditions remained constant between the square-wave and ramped LD cycles, the dynamically changing light levels almost certainly provide a more salient stimulus for light sampling behaviour compared to abrupt square-wave changes in light exposure. This suggests that rods and cones may play an important role in regulating this behaviour since they have an increased temporal resolution compared with melanopsin (Foster et al., 2020). S-cones may be particularly important under natural twilights, which are short-wavelength enriched. Indeed, recent data has demonstrated the light-seeking and activity promoting effects of selective S-cone activation (Tamayo et al., 2023) which would align with increased light sampling behaviour. In addition, levels of S-cone opic lux have been shown to correlate most strongly with activity onset in mice under a ramped white fluorescent LD cycle compared to other photoreceptor α-opic lux (Steel et al., 2022). The increased light sampling at dawn compared with dusk is intriguing (Fig. 3.3A,5C). This could result from light levels increasing against a dark background at dawn - generating greater stimulus contrast against the dark-adapted retina compared to at dusk, where a light-adapted retina must detect decreasing light levels. Given these different photosensory tasks of detecting dawn and dusk the photoreceptors involved may even differ – with rods playing more of a role at dawn and cones more at dusk. Moreover, the presence of a nestbox may change the nature of this task, for example, by decreasing light adaptation at dusk. The detailed role of different photoreceptors in mediating light sampling behaviour remains to be fully explored (Mouland et al., 2019; van Diepen et al., 2013; van Oosterhout et al., 2012; Walmsley et al., 2015).

By understanding and recreating the natural light environments of model organisms we may be able to better account for the differences we see between laboratory and field studies in circadian neuroscience (Calisi and Bentley, 2009). Flôres (et al., 2016) tackled this issue by simulating the natural pattern of light exposure of the tuco-tuco in the laboratory. In our study this is taken further by giving animals the opportunity to self-modulate their pattern of light exposure; an approach which may yield greater mechanistic insights into photoentrainment under naturalistic conditions. However, comparisons between our data and house mouse activity patterns in the wild are limited by the small number of studies published on the latter, and methodological differences

(Chambers et al., 2000; Robbers et al., 2015; Sutherland and Singleton, 2003). Whilst our locomotor activity data mirrors wild studies, with activity peaking in the 2hrs following sunset and declining across the remainder of the night (Sutherland and Singleton, 2003), these studies do not characterise light exposure, or light sampling behaviour, which we know differs from overall locomotor activity (Fig. 3.1C,D). Conversely, our studies were performed under constant temperature conditions, food and water provided *ad libitum*, and with no risk of predation, which does not accurately recapitulate natural conditions (van der Vinne et al., 2015).

Here we also investigated the mechanistic basis of light sampling behaviour. We demonstrate for the first time that light sampling behaviour is arrhythmic in mice lacking a circadian clock (*Cry1*$^{-/-}$ *Cry2*$^{-/-}$) (Fig. 3.5B,C,D), even though locomotor activity remains rhythmic under a LD cycle due to masking (Fig. 3.5A) (Mrosovsky, 1999). Along with the regular pattern of daily light sampling behaviour shown by wildtype mice (Fig. S3.4), this suggests that the circadian clock plays an important role in providing a consistent pattern of light exposure for photoentrainment. This may help to optimise photoentrainment by preventing inappropriate phase shifts in activity that might arise if the timing of daily light exposure is highly variable (Van Der Veen et al., 2017). In this way, light sampling behaviour is a downstream output of the SCN that provides an important feedback to modulate light input to the SCN clock (Fig. 3.6B). This feedback loop between behaviour, light and the circadian clock (Fig. 3.6B) cannot occur under standard laboratory conditions (Fig. 3.6A), showing how the provision of a dark nestbox can enable the more complex features of photoentrainment to be studied.

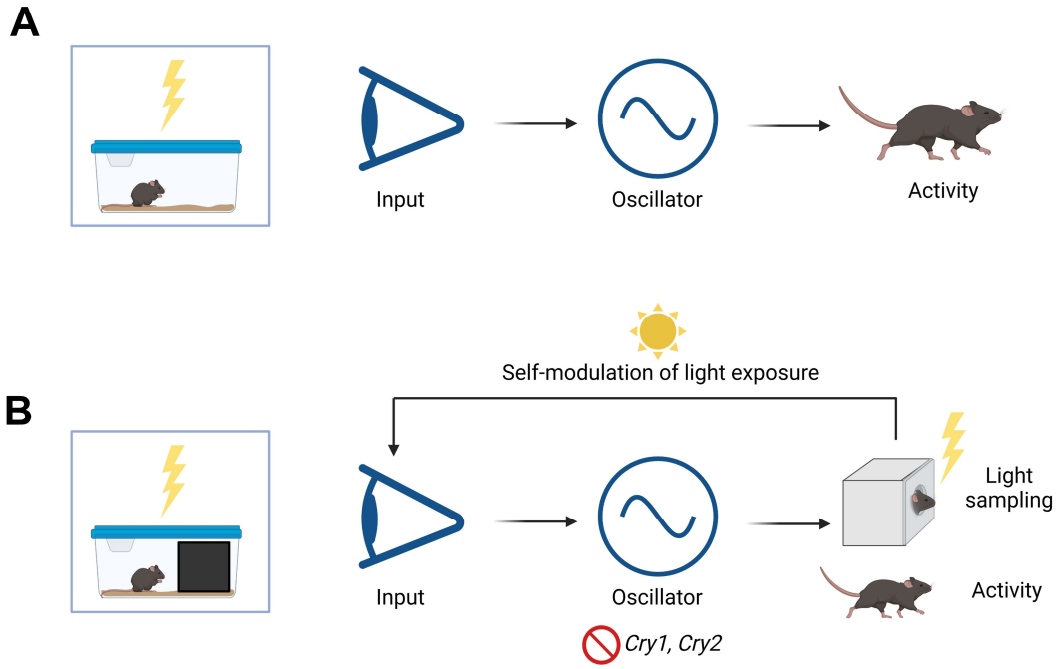

Figure 3.6 - Photoentrainment schematic under standard laboratory conditions **(A)** and with a dark nestbox **(B)**, illustrating the feedback loop between behaviour, light and the circadian clock when a nestbox is present.

The model proposed in Fig. 3.6 will undoubtedly be more complex, with several potential explanations as to why CRY-deficient mice show arrhythmic light sampling behaviour under an LD cycle. These may be both behavioural and physiological, and could include differences in locomotor activity and exploratory behaviour (De Bundel et al., 2013), sleep/wake changes (Wisor et al., 2002), metabolic changes (Barclay et al., 2013; Bur et al., 2009; Cretenet et al., 2010), time-place learning (Van der Zee et al., 2008), retinal gating to the SCN (Nakamura et al., 2011), and photic sensitivity (Cameron et al., 2008; Foster and Helfrich-Förster, 2001; Wong et al., 2018). These additional phenotypes influencing circadian physiology and behaviour could also be candidate zeitnehmers (meaning 'time taker') (Roenneberg and Merrow, 1999) since they are under circadian control but feedback to impact the entrainment process by influencing light sampling behaviour (Hughes and Piggins, 2012). Of these factors, direct alterations to photic sensitivity in CRY-deficient mice may be of particular relevance to light sampling behaviour. Retinal development can be altered in mice lacking core clock genes, as demonstrated by the lack of an S-cone opsin retinal gradient in mice lacking Bmal1 (Sawant et al., 2017) and since CRY1 is expressed in both mouse cone photoreceptors it is possible that the abolition of cryptochrome may alter cone development and sensitivity (Cameron et al., 2008; Wong et al., 2018). Therefore, arrhythmic

light sampling behaviour may occur in CRY-deficient mice due to direct alterations to photic sensitivity associated with this model, in addition to behavioural and physiological circadian defects.

Beyond enhancing our understanding of photoentrainment, the nestbox paradigm presented here may also have other potential applications. The decision making behaviour we describe in the "go" vs "no go" responses (Fig. 3. 3C,D) is likely to reflect an internal conflict between the need to explore and access food and water versus staying in the safety of the dark nestbox (Davis et al., 2022). A long-term home cage test with ethological relevance (Gerlai and Clayton, 1999) might provide a measure of anxiety and avoid issues such as handling that can alter behavioural measures (File, 1993). In addition, Wiedenmayer (1997) showed that a dark chamber with a tunnel entrance is sufficient to prevent stereotypic digging behaviour in gerbils, whilst simply providing digging substrate was not. These findings suggest that providing a dark nestbox may serve to reduce stereotypic locomotor behaviour in rodent models (Würbel, 2001). Further studies are required to explore the wider benefits of home cage nest boxes for laboratory mouse behaviour.

Finally, consideration of light exposure patterns is also of relevance to human circadian studies, as the light environment experienced by humans in modern societies is very different to natural light exposure, with low light intensity during the day and artificial light at night extending our light phase beyond sunset (Okudaira et al., 1983; Webler et al., 2019; Wright et al., 2013). Indeed, bright light exposure during the daytime can decrease the sensitivity of the circadian system to dim light in the evening (Rångtell et al., 2016). Understanding how behaviour modifies the timing, intensity and wavelength of light exposure may provide opportunities for modifying human behaviour and environments to promote the establishment of healthier lighting exposure patterns (Webler et al., 2019).

In conclusion, here we provide a simple experimental paradigm that enables mice to self-modulate their light exposure, thereby addressing a key difference between the natural and laboratory light environment of mice (Sutherland and Singleton, 2003). In parallel, this approach allows quantification of locomotor activity, circadian entrainment, light sampling behaviour and decision making within a long-term home cage environment. We show that when given the opportunity, mice will significantly reduce their light exposure and exhibit light sampling behaviour, with peaks at twilight under a ramped LD cycle. This highlights the important role of behaviour in modifying the signals available for photoentrainment under more naturalistic environments, that is often overlooked in laboratory studies. Moreover, we show that light sampling behaviour is arrhythmic in mice lacking a circadian clock, demonstrating an important role for the circadian system in

regulating the timing of light exposure, and therefore the intensity and wavelength of light perceived under natural conditions. Collectively, our data illustrate how under natural conditions light sampling behaviour forms an important feedback on circadian entrainment, rather than being a simple output of the circadian clock.

3.6 Supplementary figures

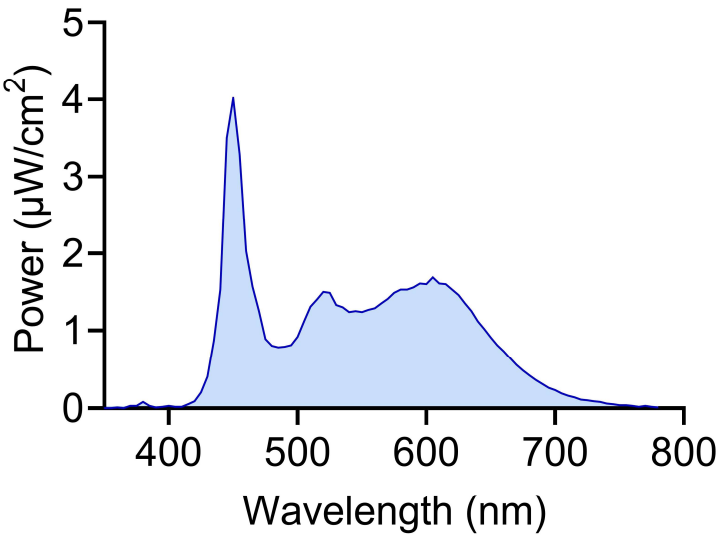

Figure S3.1 Spectral power distribution (SPD) of cool white LED (4500 CCT) used throughout the experiment (LIFX light-strip; LIFX, Cremorne, Australia). 200 photopic lux, 5 S-cone opic lux, 170 melanopic lux, 169 rhodopic lux, 170 M-cone opic lux, measured using a calibrated Ocean Optics USB2000+ Spectrophotometer (Ocean Insight, Oxford, United Kingdom).

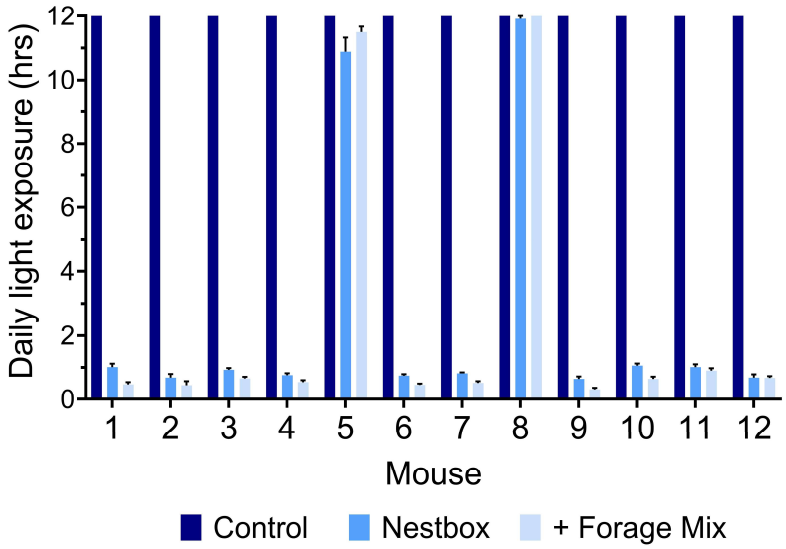

Figure S3.2 The majority of C57BL/6J mice routinely use the nestbox. Daily light exposure (hrs) (mean across days +/- SEM) of individual C57BL/6J mice across experimental conditions (control, nestbox, and nestbox + forage mix ('+forage mix')), in the C57BL/6J light sampling study.

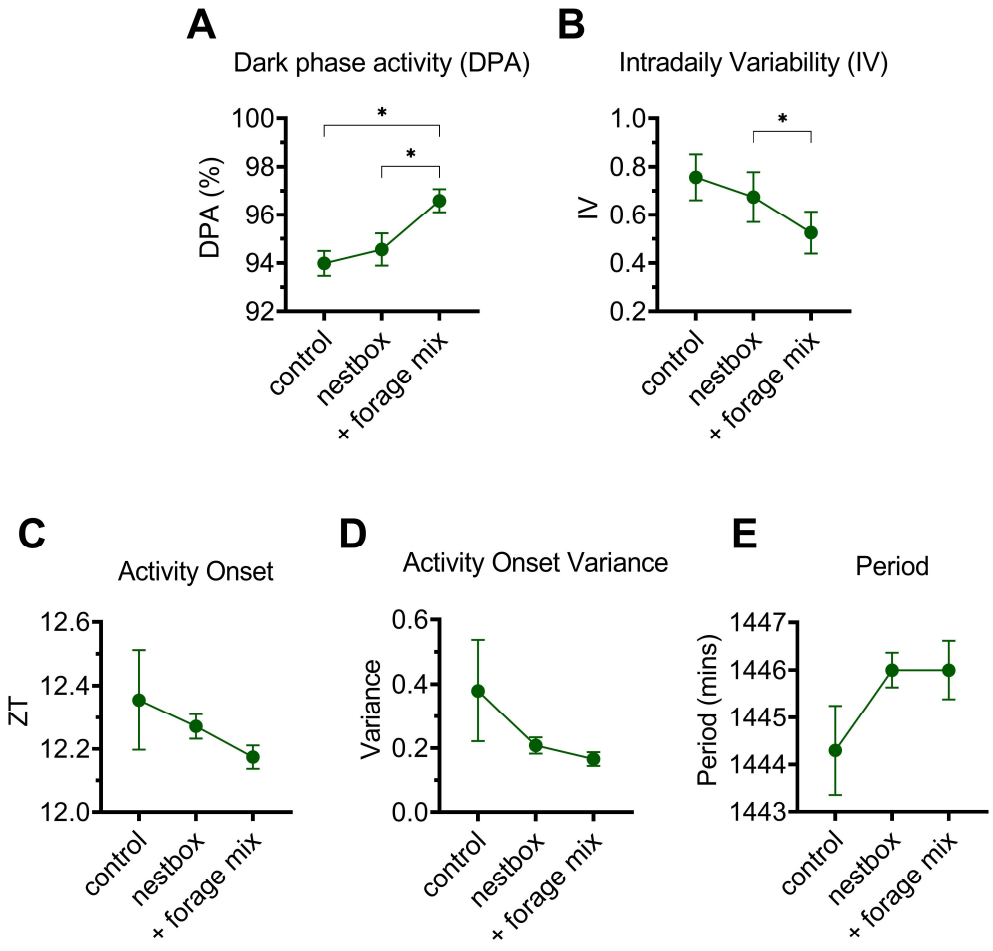

Figure S3.3 Other circadian entrainment metrics for C57BL/6J mice from the first light sampling study, across experimental conditions (control, nestbox, nestbox + forage mix ('+ forage mix'). Reported as mean +/- SEM. **(A)** Dark phase activity (%). **(B)** Intradaily variability. **(C)** Activity onset. **(D)** Activity onset variance (calculated as SD of activity onsets across days, across mice). **(E)** Circadian period. * $p<0.05$, between condition comparisons.

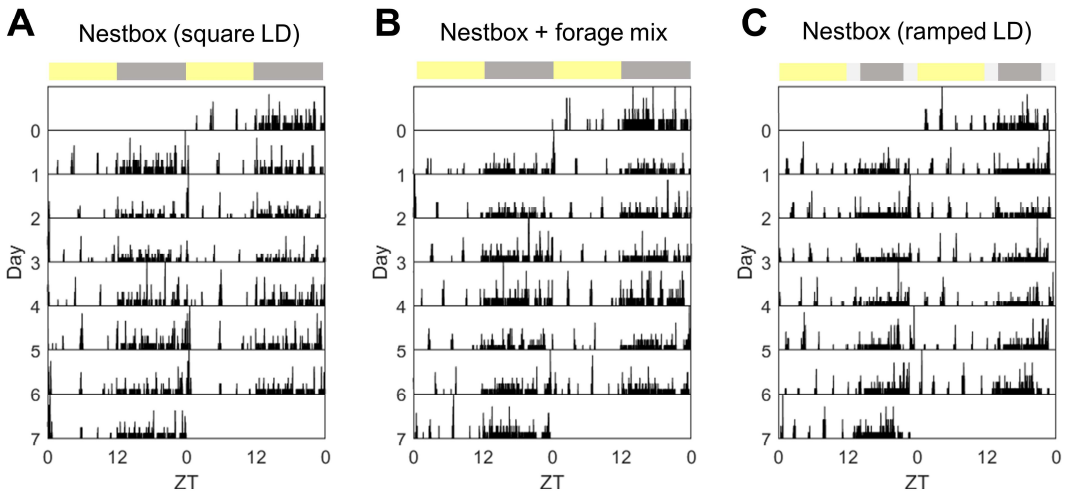

Figure S3.4 Light environment sampling behaviour shows consistent patterns across days. Double plotted actograms of light environment sampling events across a week of a representative C57BL/6J animal under experimental conditions. **(A)** Nestbox available, 12:12hr LD cycle. **(B)** Nestbox and forage mix available, 12:12hr LD cycle. **(C)** Nestbox available, 12:2:8:2hr LD cycle. Actograms produced using MATLAB code, adapted from https://github.com/abubnys/GA_actograms.git.

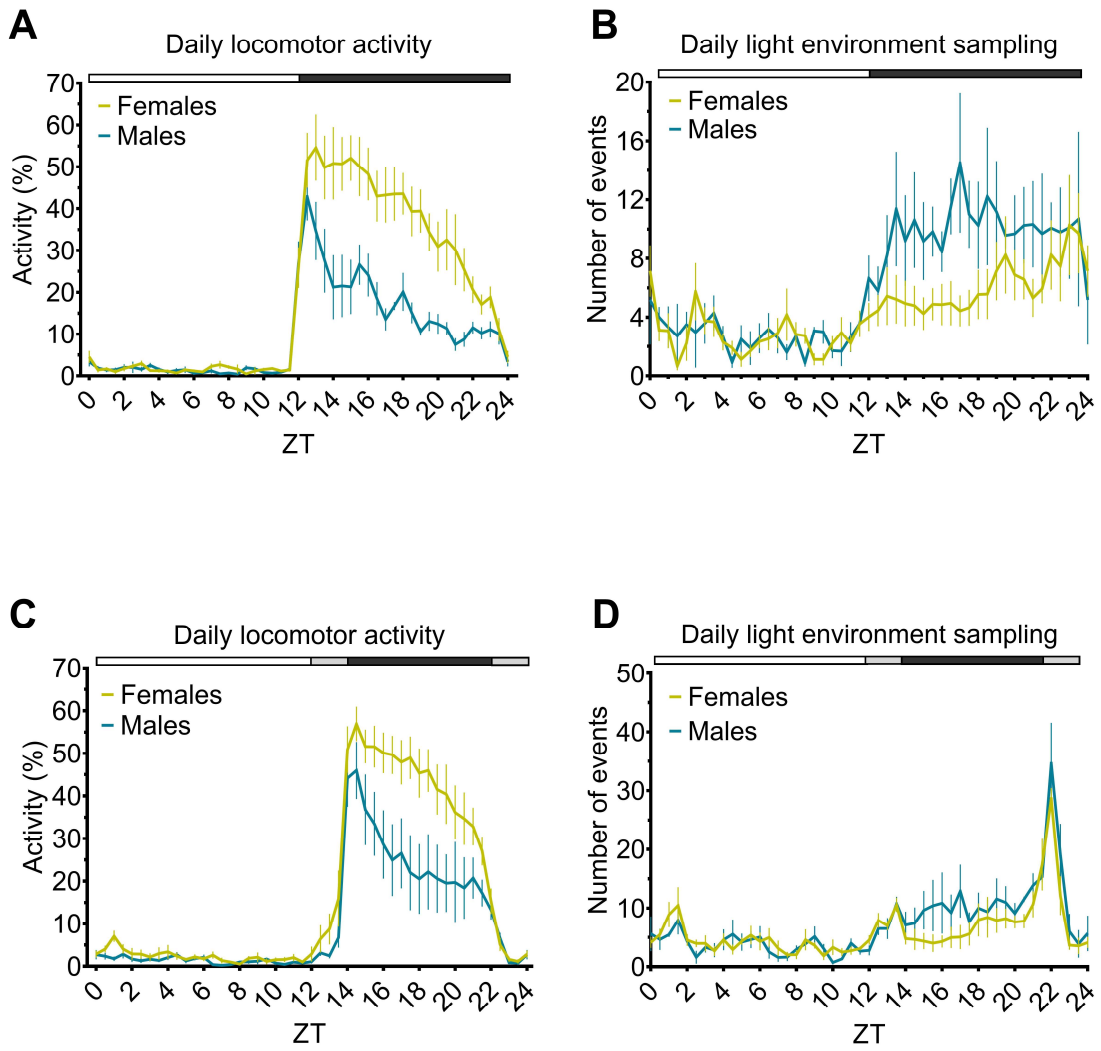

Figure S3.5 Males and females show differences in locomotor activity but not light environment sampling behaviour, under square and ramped LD cycles. **(A)** Daily locomotor activity profile of females (green) and males (blue) under 12:12hr LD cycle. **(B)** Daily light environment sampling profile of females (green) and males (blue) under 12:12hr LD cycle. **(C)** Daily locomotor activity profile of females (green) and males (blue) under 12:2:8:2hr LD cycle. **(D)** Daily light environment sampling profile of females (green) and males (blue) under 12:2:8:2hr LD cycle. All results reported as mean across days and animals, +/- SEM. * $p<0.05$, between sex comparisons. White, grey and black bar shows timing of light, light ramp and dark, respectively.

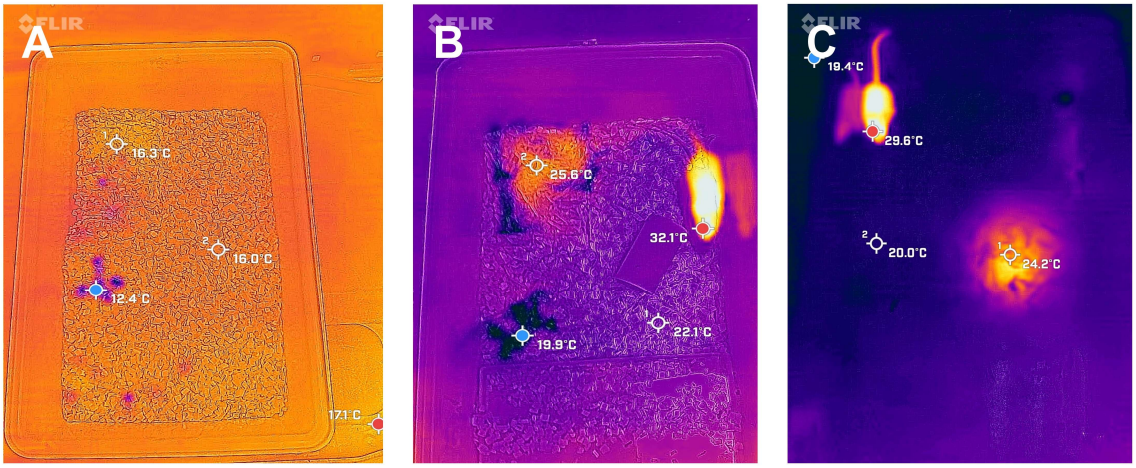

Figure S3.6 Thermal images of nests and nestboxes (FLIR one pro, Teledyne FLIR). **(A)** No nest or animal present. Imaged immediately after removal of uninhabited nestbox. Nestbox always positioned in top left corner of cage (A,B). **(B)** Nest built within nestbox. Imaged immediately after removal of nestbox and vacation of nest by animal. **(C)** Nest built with no nestbox present. Imaged immediately after vacation of nest by animal. In all photos, the blue dot refers to the lowest temperature spot and the red dot to the highest temperature spot. Spots 1 and 2 show the temperature of the zone of interest and a comparison to the main cage away from the nest and nestbox.

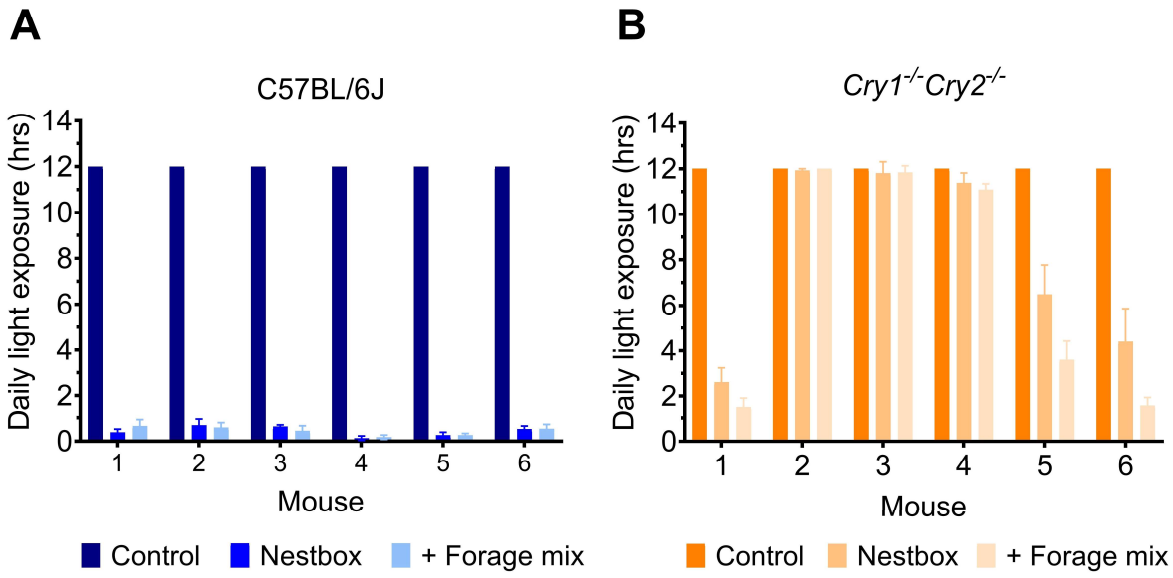

Figure S3.7 Fewer Cry1$^{-/-}$Cry2$^{-/-}$ mice use the nestbox than C57BL/6J mice. Daily light exposure (hrs) (mean +/- SEM) under experimental conditions (control, nestbox, nestbox + forage mix ('+ forage mix'). **(A)** C57BL/6J. **(B)** Cry1$^{-/-}$Cry2$^{-/-}$.

Chapter 4. The role of melanopsin and classical photoreceptors in regulating light sampling behaviour

4.1 Abstract

Here we use transgenic mouse strains to explore the role of different photoreceptors in regulating photoentrainment and light sampling behaviour; in particular, the peak in light sampling at twilight observed in C57BL/6J mice in Chapter 3. No significant between-genotype differences in light sampling were observed under a ramped LD cycle between *Opn4*$^{+/+}$ and *Opn4*$^{-/-}$ mice. However, it is possible that background strain differences may have limited the ability to detect the contribution of melanopsin to this behaviour. There was a significant effect of LD cycle condition (square-wave versus ramped) on light sampling behaviour in *Opn4*$^{+/+}$, but not *Opn4*$^{-/-}$ animals; with small peaks in sampling visible at twilight in *Opn4*$^{+/+}$ animals. The use of C3H-HeH mice (homozygous for the retinal degeneration allele *Pde6b*^{rd1}) suggest an important role for rods and cones in regulating light sampling behaviour at twilight; however, the lack of a sighted C3H control make firm conclusions difficult.

4.2 Introduction

In Chapter 3 of this thesis we demonstrated that C57BL/6J mice exhibit large peaks in light sampling behaviour at dawn and dusk under a ramped LD cycle. This behaviour is abolished in mice lacking a circadian clock, suggesting a feedback loop between light, the clock and behaviour. Equally, this behaviour was not shown by C57BL/6J mice under a square-wave LD cycle, highlighting that the gradual change in light intensity under the ramped LD cycle is an important cue in driving this behaviour. The obvious question arising from these observations is which photoreceptors are involved in providing input to the SCN to regulate this behaviour. Photoreceptor knockout mouse strains have commonly been used to investigate the role of rods, cones and melanopsin in regulating non-image forming responses to light (Altimus et al., 2008; Freedman et al., 1999; Hattar et al., 2003; Lucas et al., 2001, 1999; Lupi et al., 2008; Pilorz et al., 2016; Tam et al., 2016). Therefore, here we use mice lacking melanopsin (O*pn4*$^{-/-}$) (Lupi et al., 2008; Pilorz et al., 2016; Tam et al., 2016) and mice lacking rods and cones (C3H-HeH,

homozygous for the retinal degeneration allele *Pde6b*^{rd1}) (Ebihara and Tsuji, 1980; Lucas et al., 1999; Lupi et al., 2008; Pittler and Baehr, 1991; Tam et al., 2016), to probe the role of different photoreceptors in light sampling behaviour, and in particular, in driving the peak in light sampling behaviour observed at dawn and dusk.

It is difficult to separate the role of rods, cones and melanopsin in regulating photoentrainment and other light-driven behaviours, since ipRGCs - the primary conduit of retinal signals to the SCN - combine extrinsic and intrinsic retinal signals (Aggelopoulos and Meissl, 2000; Güler et al., 2008). However, rods, cones and melanopsin have very different response characteristics (Mouland and Brown, 2022). Therefore considering the photosensory nature of light sampling can help form predictions regarding photoreceptor involvement. Peaks in light sampling at dawn and dusk are likely to be driven by the detection of dynamically changing light levels – at dawn this will be at low light intensities against a dark-adapted background, whilst at dusk this will be at higher light intensities against a light-adapted background. Therefore, given the importance of rods in facilitating light detection and photoentrainment at low intensities (~7-11 log quanta, Altimus et al., 2010; Butler and Silver, 2011; Ebihara and Tsuji, 1980; Yoshimura et al., 1994) and the role of cones in integrating intermittent and rapidly changing light levels at higher intensities (~10-15 log quanta, Foster et al., 2020; Peirson et al., 2018) (Lall et al., 2010; van Diepen et al., 2021) we predict that rods and cones may be particularly important in driving light sampling behaviour at dawn and dusk, respectively.

In contrast, melanopsin is expressed at a far lower density than rods and cones (~1/1000) resulting in a lower sensitivity to light (Do, 2019; Do et al., 2009). To compensate, melanopsin has a far longer integration time than rods (20x longer) and cones (>100x longer) (Do, 2019; Do et al., 2009). This results in slower responses to light (Berson et al., 2002; Mouland and Brown, 2022), with the dark-adapted single-photon response of M1 ipRGCs lasting for ~8s, compared to ~200ms in rods and ~80ms in cones (Cao et al., 2014; Do, 2019; Do et al., 2009; Emanuel et al., 2017; Mendez et al., 2000). The lower sensitivity to light and slower response characteristics of melanopsin may make it less suited to detecting the changing light levels at twilight, which are likely required for driving the peaks in light sampling behaviour. However, melanopsin can still integrate light over a timescale of minutes (Do, 2019) and as such, its temporal sensitivity is likely to be sufficient to coarsely track twilight, which can last up to several hours. Therefore, the role of melanopsin is difficult to predict. In addition, melanopsin is also sensitive to light levels from ~11-15 log quanta (Dacey et al., 2005). This means it would be activated between -7 and -6 degrees of solar elevation during natural twilight, since 10.9 and 11.3 log quanta are available to melanopsin at these times, respectively (calculated using the Rodent Toolbox and raw data from Spitschan et

al., 2016). Therefore, whilst the features of melanopsin may initially appear to make it less suited to tracking twilight compared to rods and cones, it is possible it may still contribute to light sampling at dawn and dusk.

The circadian entrainment phenotype of *Opn4*$^{-/-}$ mice is relatively subtle, which is perhaps surprising given the differences in response characteristics that make melanopsin well-suited to circadian photoreception. *Opn4*$^{-/-}$ mice show some attenuated responses such as reduced phase delays to evening light pulses and negative masking (Panda et al., 2002b; Ruby et al., 2002), but they are able to entrain robustly to an LD cycle (Panda et al., 2002b; Ruby et al., 2002). This finding has always been attributed to the extrinsic rod/cone input to ipRGCs, but developmental reorganisation may also occur too. It is possible that under a more nuanced natural behavioural assessment of photoentrainment, differences in *Opn4*$^{-/-}$ mice may become more apparent.

4.3 Materials and Methods

4.3.1 Animals and housing conditions

To explore the role of melanopsin on light sampling behaviour, 6 melanopsin-knockout mice (*Opn4*$^{-/-}$) on a C57BL/6J x Sv129 background were used, with 6 WT (*Opn4*$^{+/+}$) littermates as controls. *Opn4*$^{-/-}$ and *Opn4*$^{+/+}$ mice were obtained from cross breeding heterozygous mice (*Opn4*$^{+/-}$). Both *Opn4* groups were sex and aged matched, with mice ranging from 8 to 16 weeks old at the onset of the control week. 12 rodless–coneless (*rd/rd cl*) mice on a C3H-HeH background were used to explore the role of rods and cones on light sampling behaviour. These animals have a complete loss of rod and cone photoreceptors after 80 days of age, therefore all mice were ~12.5 weeks old at the onset of the control week. C3H WT mice without the rd (*Pde6b*^{rd1}) mutation were not available to act as a control. C3H and *Opn4* groups were run as separate cohorts, but following the same experimental design.

All animals were singly housed in the same conditions as Chapter 3 - with *ad libitum* access to food and water, located in a food hopper and water bottle in the main cage (i.e. outside the nestbox). Sizzlenest was provided as a nesting material throughout the experiment (Sizzlenest, Datesand; UK). Cages were placed within light-tight ventilated chambers (LTCs) equipped with multiple WiFi controlled cool-white (4500 CCT) light-emitting diodes (LEDs) (LIFX light-strip; LIFX, Cremorne, Australia), providing a light level of 200 photopic lux (5 S-cone opic lux, 170 melanopic lux, 169 rhodopic lux and 170 M-cone opic lux) throughout the light phase; calculated using the Rodent Toolbox (Lucas et al., 2014). The spectral power distribution of the cool-white LED consisted of a high, narrow peak at ~450nm and a lower, broader peak at ~560nm; measured using

a calibrated Ocean Optics USB2000+ Spectrophotometer (Ocean Insight, Oxford, United Kingdom). The temperature of the animal holding room was maintained at 19-21°C. All experimental procedures were conducted at the University of Oxford, England, in accordance with the United Kingdom Animals (Scientific Procedures) Act 1986 under Project License PP0911346 and Personal License I82616702. All procedures were in accordance with the University of Oxford Policy on the Use of Animals in Scientific Research.

4.3.2 Experimental design

Prior to the onset of the experiment, all mice were habituated to a reverse square-wave 12hr:12hr LD cycle (lights on at 19:00 and lights off at 07:00) for 2 weeks. A reverse LD cycle was used throughout the experiment to minimise disruption caused by daily welfare checks. This LD cycle remained constant for weeks 1-6 of the experiment. Following habituation there was a control week of standard laboratory conditions, before a nestbox was added to each cage for 2 weeks. The first week was to allow habituation to the nestbox and only the second week of recordings were used in analysis. The nestbox remained in place for the remainder of the experiment. Throughout week 4, forage mix (LBS forage mix; LBS Biotechnology, UK) was added to the cage floor during daily welfare checks, in addition to standard food in the food hopper, to examine the effect of being able to take food back to the nestbox on activity and entrainment. In weeks 5 and 6, a reverse 12:2:8:2hr cycle was used to explore the effect of a more naturalistic LD cycle (the light phase remained at 170 melanopic lux of cool-white LED, and the intensity ramped exponentially across 2hrs, measuring 16 photopic lux at 1hr). The first week was to allow habituation to the ramped LD cycle and only the second week of recordings were used in analysis.

4.3.3 Locomotor activity monitoring (see section 3.3.3)

4.3.4 Data processing (see section 3.3.4)

4.3.5 Statistical analysis

Statistical analysis and data visualisation were performed in MATLAB and Graph-pad Prism (v.9.5.0 (730)). $\alpha = 0.05$ was adopted in all analyses. All locomotor, light environment sampling and decision making daily profiles are visualised in 30 min bins, unless otherwise stated. Any animals that did not routinely use the nestbox were removed from the analysis (mouse 1 in the *Opn4*$^{+/+}$group (Fig. S4.1A); mouse 5 in the *Opn4*$^{-/-}$ group (Fig. S4.1B); mouse 2 in the C3H group (Fig. S4.2A)). The Greenhouse-Geisser correction was performed with all ANOVAs, and corrected degrees of freedom reported, unless otherwise stated. A post-hoc Tukey test was used when all pairwise comparisons were desired, whilst a post-hoc Bonferroni test was used for a

specific comparison between the control and experimental treatments. Further details on statistical tests used for each dataset are reported in the results section.

4.4 Results

4.4.1 *Opn4*$^{-/-}$ vs *Opn4*$^{+/+}$ mice

There are no significant differences between *Opn4*$^{-/-}$ and *Opn4*$^{+/+}$ mice in daily light exposure (Fig. 4.1A; S4.1A,B), locomotor activity (Fig. 4.1B,C), light environment sampling (Fig. 4.1D,E; S4.1C,D), decision making (data not shown) or circadian entrainment metrics (Fig. 4.1F-I, S4.1E-I). However, a significant effect of LD cycle condition (square-wave vs. ramped) on the number of light environment sampling events was observed within *Opn4*$^{+/+}$ (Fig.S4.1C) but not within *Opn4*$^{-/-}$ animals (Fig.S4.1D). These results will be discussed in turn in more detail.

4.4.1.1 Daily light exposure

The majority (5/6) of both *Opn4*$^{-/-}$ and *Opn4*$^{+/+}$ mice regularly use the nestbox; extensively reducing their daily light exposure (Fig.S4.1A,B). Of the animals that do regularly use the nestbox, there was a significant reduction in daily light exposure across both genotypes in the presence of a nestbox, or nestbox and forage mix - to an average of 0.7hrs in *Opn4*$^{-/-}$ animals and 0.8hrs in *Opn4*$^{+/+}$ animals (Fig. 4.1A) [main effect of condition [$F(1.4,10.9) = 13704$, $p < 0.0001$; two-way ANOVA and post-hoc Tukey test]. Accordingly, there was no significant effect of genotype [$F(1,8) = 0.4$, $p = 0.5585$] or genotype x condition interaction [$F(2,16) = 0.35$, $p = 0.7132$].

4.4.1.2 Locomotor activity

Both *Opn4*$^{+/+}$ and *Opn4*$^{-/-}$ animals show robust photoentrainment, exhibiting rhythmic locomotor activity cycles in the presence of a nestbox under a square-wave 12:12hr LD cycle (Fig. 4.1B) [main effect of time, $F(2.0,19.6) = 20.0$, $p < 0.0001$] and ramped 12:2:8:2hr LD cycle (Fig. 4.1C) [main effect of time, $F(1.3,13.0) = 21.8$, $p = 0.0002$]. Accordingly, there was no significant effect of genotype on locomotor activity across either the square-wave LD cycle (Fig. 4.1B) [$F(1,10) = 0.1$, $p = 0.7683$] or ramped LD cycle (Fig. 4.1C) [$F(1,10) = 0.0$, $p = 0.8460$; two-way ANOVA]; or genotype x time interaction [square-wave LD cycle, Fig. 4.1B, $F(48,480) = 0.5$, $p=0.9994$; ramped LD cycle, Fig. 4.1C, $F(48,480) = 0.1$, $p>0.9999$]. The same pattern applies to locomotor activity across the control and nestbox + forage mix conditions (data not presented), and corroborates previous research that mice lacking melanopsin show robust entrainment of locomotor activity (Ruby et al., 2002).

4.4.1.3 Light environment sampling and decision making

Light environment sampling shows a rhythmic pattern across the 24hr period in both *Opn4*$^{+/+}$ and *Opn4*$^{-/-}$ animals (Fig. 4.1D) [$F(5.4,54.2) = 16.6$, $p < 0.0001$; two-way ANOVA with post-hoc Bonferroni test]. Although small peaks in light environment sampling at dawn and dusk under a ramped LD cycle can be seen in *Opn4*$^{+/+}$ animals, but not *Opn4*$^{-/-}$ animals (Fig. 4.1D), there was no significant effect of genotype [$F(1,10) = 0.5$, $p = 0.4883$], or genotype x time interaction [$F(48,480) = 1.1$, $p = 0.3243$] on light environment sampling under a ramped LD cycle (Fig. 4.1D). Similarly, when the data in Fig. 4.1D is averaged into light environment sampling events occurring during dawn (ZT22-24), the day (ZT0-12) and dusk (ZT12-14) (Fig. 4.1E), there was no significant effect of genotype [$F(1,10) = 4.0$, $p = 0.0736$; two-way ANOVA with post-hoc Bonferroni test]. However, there was a significant effect of time [$F(1.2,12.0) = 11.2$, $p = 0.0043$] and interestingly, a significant time x genotype interaction [$F(2,20) = 3.9$, $p = 0.0367$]. This latter result demonstrates that the pattern of light environment sampling across time does differ between genotypes. Higher sampling levels may occur at dawn in *Opn4*$^{+/+}$ animals compared to *Opn4*$^{-/-}$ animals (Fig. 4.1E); however, there were no significant post-hoc differences. This could be a result of a small effect size, requiring a larger sample size to resolve.

To explore this interaction further, within-genotype differences in light environment sampling across LD conditions (square-wave versus ramped LD cycles) were investigated (Fig.S4.1,C,D). As expected, since *Opn4*$^{+/+}$ animals have an intact retina, changing the LD cycle from a square-wave 12:12hr cycle to a ramped 12:2:8:2hr cycle had a significant effect on the pattern of light environment sampling (Fig.S4.1C), resulting in a main effect of condition [$F(1,5) = 6.9$, $p = 0.0470$; two-way ANOVA with post-hoc Bonferroni test]. A main effect of time was also present [$F(3.1, 15.5) = 8.2$, $p = 0.0016$]. This reflects the rhythmic pattern of light environment sampling across the 24hr period. Peaks at dawn and dusk were observed under the ramped LD cycle (Fig.S4.1C), as in C57BL/6J animals, but there were no significant post-hoc differences, or condition x time interaction [$F(3.0,14.8) = 2.5$, $p = 0.0961$]. This reflects the scale of the peaks, which were ~1.6x lower at dawn in *Opn4*$^{+/+}$ animals compared to C57BL/6J animals, and ~2.9x lower at dusk (data not presented; for C57BL/6J data see Chapter 3). These differences are likely to arise from background strain differences, and may limit the detection of significant effects of genotype between *Opn4*$^{+/+}$ and *Opn4*$^{-/-}$ animals (Fig. 4.1D,E). Interestingly, in *Opn4*$^{-/-}$ animals (Fig.S4.1D) there was no main effect of condition on light environment sampling behaviour between a square-wave and ramped LD cycle [$F(1,5) = 0.0$, $p = 0.9476$; two-way ANOVA with post-hoc Bonferroni test]; suggesting that rods and cones are not sufficient to drive changes in light environment sampling behaviour under a ramped LD cycle. The pattern of light environment sampling was still

rhythmic across the 24hr period in *Opn4*$^{-/-}$ animals (Fig.S4.1D), resulting in a main effect of time [$F(1.9,9.3) = 9.4$, $p = 0.0064$], but no significant condition x time interaction [$F(2.3,11.6) = 1.7$, $p = 0.2262$].

Finally, as expected from the lack of significant difference between *Opn4*$^{+/+}$ and *Opn4*$^{-/-}$ animals in locomotor activity (Fig. 4.1B,C) and light environment sampling (Fig. 4.1D), there was no significant effect of genotype on the decision making ratio (go:no-go) across any conditions (data not presented).

4.4.1.4 Circadian entrainment metrics

There was no significant effect of genotype on any circadian entrainment metric calculated, including light phase activity (Fig. 4.1F), relative amplitude (Fig. 4.1G), intra-daily variability (Fig. 4.1H) or activity onset (Fig. 4.1I) (remaining circadian metrics are presented in Fig.S4.1E-I).

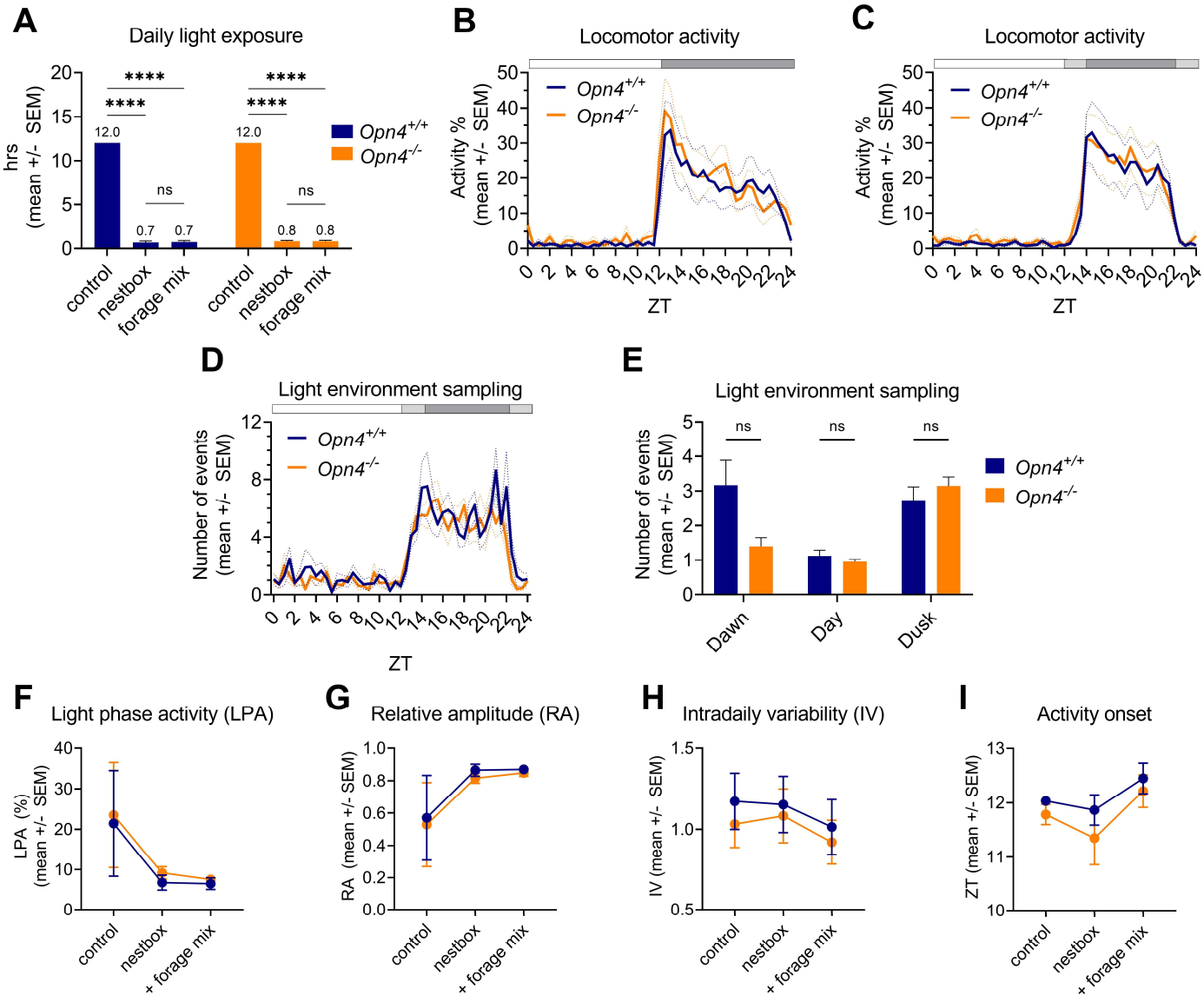

Figure 4.1 - Opn4$^{+/+}$ vs. Opn4$^{-/-}$ mice. (A) Daily light exposure (hrs) of Opn4$^{+/+}$ (blue) and Opn4$^{-/-}$ mice (orange) across experimental conditions (control, nestbox, and nestbox + forage mix ('+forage mix')). **(B)** Locomotor activity of Opn4$^{+/+}$ (blue) and Opn4$^{-/-}$ mice (orange) under a square-wave 12:12hr LD cycle. **(C)** Locomotor activity Opn4$^{+/+}$ (blue) and Opn4$^{-/-}$ mice (orange) under a ramped 12:2:8:2hr LD cycle. **(D)** Light environment sampling of Opn4$^{+/+}$ (blue) and Opn4$^{-/-}$ mice (orange) under a ramped LD cycle. **(E)** Light environment sampling of Opn4$^{+/+}$ (blue) and Opn4$^{-/-}$ mice (orange) under a ramped LD cycle averaged across dawn (ZT22-24), day (ZT0-12) and dusk (ZT12-14). **(F-I)** Circadian entrainment metrics across conditions (control, nestbox, and nestbox + forage mix ('+forage mix')) for OPN4$^{+/+}$ (blue) and OPN4$^{-/-}$ (orange) mice. **(F)** Light phase activity, **(G)** Relative amplitude, **(H)** Intradaily variability, **(I)** Activity onset. **(B-D)** White, grey and black bar shows timing of light, light ramp and dark, respectively. All results reported as mean across mice and days, +/- SEM. **** p<0.001, ** p<0.01, * p<0.05, between genotype and condition comparisons.

4.4.2 C3H mice

Sighted C3H mice, without the rd (*Pde6b^{rd1}*) mutation, were not available to act as a control. Therefore, this results section focuses on within-subject differences across LD cycle conditions in rodless-coneless (*rd/rd cl*) mice on a C3H background. Daily light exposure (Fig. 4.2A; S4.2A), locomotor activity (Fig. 4.2B,C), light environment sampling (Fig. 4.2D,E), decision making (Fig.S4.2B) and circadian entrainment metrics (Fig. 4.2F-H; S4.2C-H) are assessed.

4.4.2.1 Daily light exposure

The majority (11/12) of C3H animals routinely use the nestbox (Fig.S4.2A). Of these mice, their average daily light exposure is significantly reduced to 0.9hrs across the 24hr period (Fig. 4.2A) [$t(10) = 128.8$, $p < 0.0001$; one-sample t-test against a control mean of 12hrs]. The addition of forage mix to the nestbox paradigm does not further significantly reduce daily light exposure (Fig. 4.2A) [$t(10) = 0.1$, $p = 0.8856$; paired t-test].

4.4.2.2 Locomotor activity

All mice show robust photoentrainment under both square-wave 12:12hr LD cycles (Fig. 4.2B) [main effect of time, $F(2,22) = 156.7$, $p < 0.0001$; two-way ANOVA with post-hoc Tukey test (post-hoc differences not visualised)] and a 12:2:8:2hr ramped LD cycle (Fig. 4.2C) [main effect of time, $F(2,22) = 100.3$, $p < 0.0001$; two-way ANOVA with post-hoc Bonferroni test]. This demonstrates, as expected, that photoentrainment can still occur in the absence of rods and cones (Freedman et al., 1999). Interestingly, there is a small peak in activity prior to ZT12 under both a square-wave (Fig. 4.2B) and ramped LD cycle (Fig. 4.2C) – a phenotype which has been observed previously in C3H mice (Kopp, 2001; van Dorp et al., 2024). The addition of a nestbox, or a nestbox and forage mix, has no significant effect on the daily profile of locomotor activity shown by C3H mice (Fig. 4.2B) [no main effect of condition, $F(1.8,19.3) = 1.1$, $p = 0.3591$]. However, there is a significant time x condition interaction [$F(7,77) = 3.0$, $p = 0.0083$; two-way ANOVA] which is likely driven by the addition of forage mix causing lower light phase activity but higher dark phase activity levels (Fig. 4.2B). Under a 12:2:8:2hr ramped LD cycle (Fig. 4.2C), C3H mice still demonstrate a gradual onset of activity across the 2hr ramp compared to under the square-wave LD cycle. This suggests that melanopsin alone is sufficient to track gradual changes in light intensity. This results in a main effect of condition on locomotor activity (Fig. 4.2C) [$F(1,11) = 66.8$, $p < 0.0001$] and a significant time x condition interaction [$F(6.9,75.9) = 26.5$, $p < 0.0001$, with significant post-hoc differences at ZT12.5-14 and ZT22.5].

4.4.2.3 Light environment sampling and decision making

C3H mice show a rhythmic pattern of light environment sampling behaviour across time under both a square-wave 12:12hr LD cycle and ramped 12:2:8:2hr LD cycle (Fig. 4.2D) [main effect of time, $F(3.9,43.3) = 10.6$, $p < 0.0001$; two-way ANOVA with post-hoc Bonferroni test]. However, unlike in C57BL/6J mice (Chapter 3), there is no main effect of condition [$F(1,11) = 0.1$, $p = 0.7130$] or time x condition interaction [$F(2.5,27.2) = 1.7$, $p = 0.1901$]. This suggests that whilst light environment sampling in the absence of rods and cones is still significantly higher at dawn and dusk than during the day (Fig. 4.2E, [$F(1.4,15.1) = 13.5$, $p = 0.0011$], one-way ANOVA with post-hoc Tukey test), melanopsin alone is insufficient to generate the behavioural differences observed in retinally-intact mice (Chapter 3) on transition from a square-wave to ramped LD cycle (Fig. 4.2D). The lack of significant difference in light environment sampling between the square-wave and ramped LD cycle (Fig. 4.2D), but significant delay in locomotor activity onset (Fig. 4.2C), can be explained by a decrease in "go" decisions under the ramped LD cycle at ZT12-14 compared to the square-wave cycle (Fig.S4.2B). However, there is no main effect of condition [$F(1,11) = 0.1$, $p = 0.7325$; two-way ANOVA with post-hoc Bonferroni test] and the post-hoc differences at ZT13 did not quite reach significance [$p = 0.0573$, post-hoc Bonferroni test].

4.4.2.4 Circadian entrainment metrics

Finally, there are significant differences in multiple circadian entrainment metrics across conditions within C3H mice (Fig. 4.2F-H, Fig.S4.2C-E; one-way RM ANOVA with post-hoc Tukey test). Of particular interest are the significant differences between the nestbox and nestbox + forage mix conditions, since a nestbox is present in both conditions - thereby removing any methodological differences in metric calculation. Activity onset occurs significantly later (by 1.1hrs) when forage mix is added [$p < 0.0001$, post-hoc Tukey test], indicating that the ability to bring food back to the nestbox reduces the urgency to feed at the onset of the dark phase. Light phase activity (Fig. 4.2F), relative amplitude (Fig. 4.2G), and activity onset variance (Fig.S4.2E) all decrease when forage mix is added, whilst dark phase activity increases (Fig.S4.2C). These changes are all indicative of increased circadian entrainment robustness (Brown et al, 2016). This demonstrates how home cage enrichment can alter circadian entrainment metrics in C3H mice, in a similar way to C57BL/6J mice in Chapter 3.

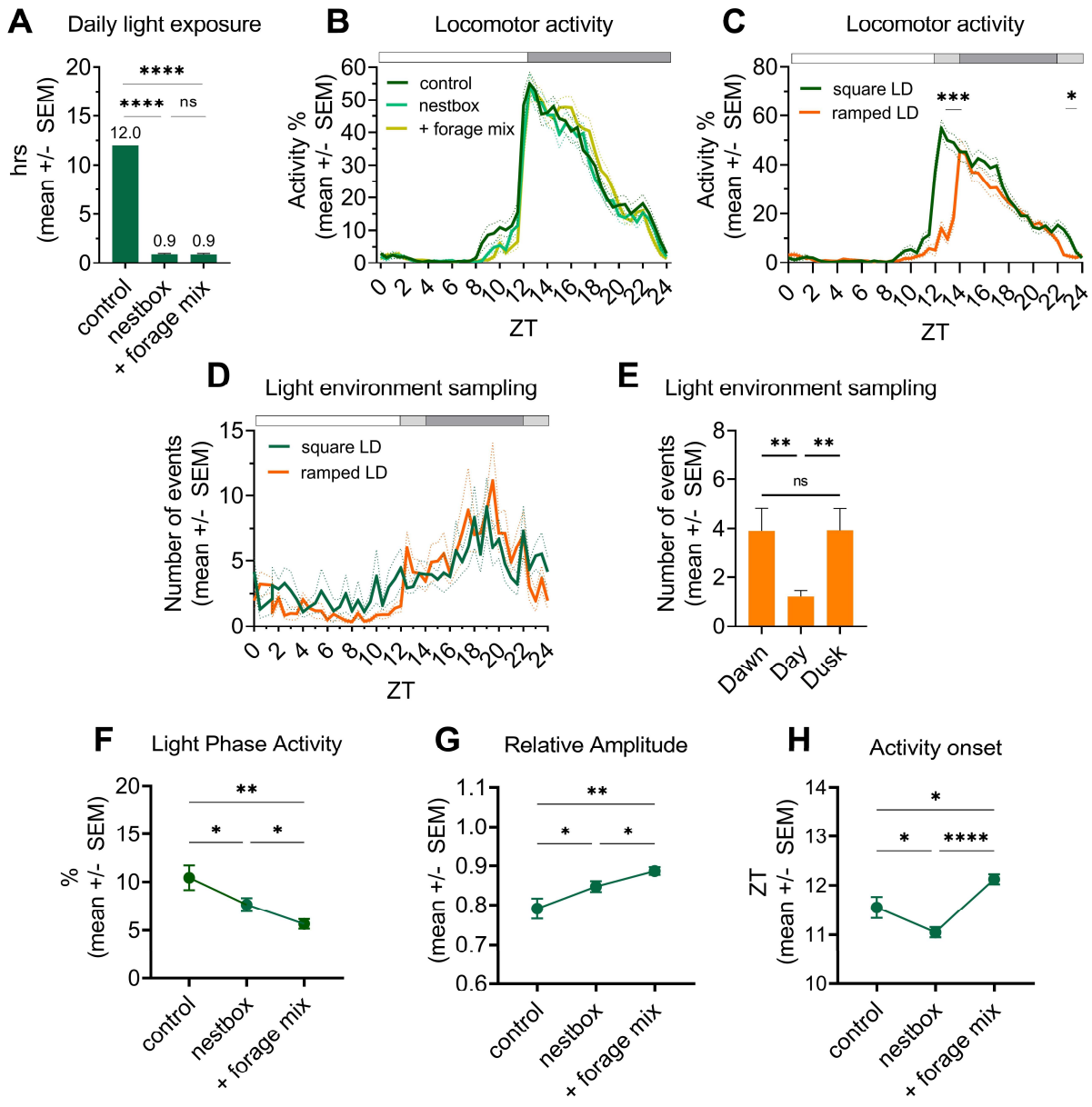

Figure 4.2 - C3H mice. (A) Daily light exposure (hrs) across experimental conditions (control, nestbox and nestbox + forage mix ('+forage mix')). **(B)** Locomotor activity under a square-wave LD cycle, across experimental conditions (control (dark green), nestbox (mid-green), and nestbox + forage mix ('+forage mix') (yellow)). Post-hoc differences not plotted. **(C)** Daily locomotor activity profile under a square-wave LD cycle (green) and a ramped LD cycle (orange). Nestbox is present in both conditions. **(D)** Light environment sampling under a square-wave LD cycle (green) and a ramped LD cycle (orange). **(E)** Light environment sampling under a ramped LD cycle, averaged into events during dawn (ZT22-24), day (ZT0-12) and dusk (ZT12-14). **(B-D)** White, grey and black bar shows timing of light, light ramp and dark, respectively. **(F-H)** Circadian entrainment metrics across conditions. **(F)** Light phase activity, **(G)** Relative amplitude, **(H)** Activity onset. All results reported as mean across mice and days, +/- SEM. **** $p<0.001$, ** $p<0.01$, * $p<0.05$, between condition comparisons.

4.5 Discussion

Here we use mice lacking melanopsin (*Opn4*$^{-/-}$) against wildtype controls (*Opn4*$^{+/+}$), and mice lacking rods and cones (C3H; homozygous for the *Pde6b*^{rd1} allele), to explore the role of melanopsin and classical photoreceptors in regulating light sampling behaviour. The role of photoreceptors in driving high levels of light sampling behaviour at twilight was of particular interest. As expected, all genotypes showed robust photoentrainment of locomotor activity (Fig. 4.1B,C; 2B,C) (Foster et al., 1991; Panda et al., 2002b; Ruby et al., 2002). Similarly, all genotypes extensively used the nestbox (Fig. 4.1A,2A) and exhibited light sampling behaviour (Fig. 4.1D;2D); corroborating previous research that light aversion in mice persists in the absence of classical photoreceptors or melanopsin (Semo et al., 2010). Regarding increased levels of light sampling at twilight, limitations regarding background strain differences and lack of a C3H sighted control prevented firm conclusions from being made. However, the data suggests that melanopsin may contribute in addition to rods and cones. These results will be discussed in turn.

No significant difference in light sampling levels were observed under a square-wave and ramped LD cycle in *Opn4*$^{-/-}$ animals (Fig.S4.1D). This data suggests that rods and cones are not sufficient to drive peaks in light sampling at dawn and dusk. It is therefore tempting to conclude that melanopsin could play a role. However, there was no significant effect of genotype (*Opn4*$^{+/+}$ versus *Opn4*$^{-/-}$) on light sampling levels under a ramped LD cycle (Fig. 4.1D), suggesting that the presence of melanopsin, in addition to rods and cones, does not have a significant impact. This is surprising since *Opn4*$^{+/+}$ animals have an intact retina, and therefore may be expected to respond to a ramped LD cycle in a similar way to C57BL/6J animals. Whilst small peaks in light sampling at twilight are visible in *Opn4*$^{+/+}$ mice (Fig. 4.1D, S4.1C), and there is a main within-genotype effect of LD cycle condition (square-wave versus ramped) on light sampling events (Fig.S4.1C) that is not present in *Opn4*$^{-/-}$ animals, there are no significant post-hoc differences in the number of light sampling events at twilight in *Opn4*$^{+/+}$ mice between a square-wave and ramped LD cycle (Fig.S4.1C).

Since both *Opn4*$^{+/+}$ mice and C57BL/6J mice have intact retinas, the smaller scale of peaks in light sampling by *Opn4*$^{+/+}$ mice (~1.6x lower than C57BL/6J animals at dawn, and ~2.9x lower at dusk) are likely to reflect variation between background strains. Background strain is often a problem when studying more complex behavioural phenotypes (Crusio, 2004). The *Opn4* colony was bred on a C57Bl6 x 129 background, and previous literature has shown 129 mice to have a higher anxiety phenotype than C57BL/6J, including for light-dark exploration (Bouwknecht and Paylor, 2002; Crawley, 2008), and lower locomotor activity levels (Hossain et al., 2004). Since light sampling behaviour reflects an approach avoidance conflict between the dark, sheltered nestbox

and the light, open cage, it is logical that mice with a 129 background show reduced light sampling at twilight. Therefore, background strain differences may be driving overall lower levels of light sampling in the *Opn4* groups, which may prevent detection of any significant between-genotype differences (*Opn4*$^{+/+}$ vs. *Opn4*$^{-/-}$) under a ramped LD cycle. Indeed, based upon the increasing light intensity, the threshold for melanopsin activation will be reached around 67s into our 2hr dawn ramp, so it would not be surprising if it was involved. These background strain differences makes it difficult to assess the extent of melanopsin's contribution. It would be helpful to repeat this experiment in melanopsin-deficient mice bred on a lower anxiety phenotype strain, such as C57BL/6J. In addition, ipRGC subtypes express different levels of melanopsin, and receive different levels of extrinsic input from rods and cones. Therefore, deletion of the *Opn4* gene may alter relative, or even remove opposing, contributions of different ipRGC subtypes to behaviour (Do, 2019). Furthermore, melanopsin is expressed outside of ipRGCs, in the cornea, iris (Xue et al., 2011) and blood vessels (Sikka et al., 2014), adding a further layer of complexity to interpreting results (Do, 2019).

Although data from *Opn4*$^{+/+}$ and *Opn4*$^{-/-}$ mice suggest that rods and cones are not sufficient to drive peaks in light sampling at twilight (Fig. 4.1E) in mice of a C57Bl6 x 129 background, results from *rd/rd cl* mice demonstrate that melanopsin alone is also not sufficient. Between-subject comparisons cannot be made due to the lack of a C3H sighted control and clear differences between mice of C3H and C57BL/6J backgrounds, including the ability to secrete melatonin and sleep architecture (Adamah-Biassi et al., 2013; Hoelter et al., 2008; Stehle et al., 2002; van Dorp et al., 2024). However, within-subject C3H comparisons are still valid. The most interesting of these comparisons is that changing from a square-wave to a ramped LD cycle had no significant effect on light sampling behaviour in C3H mice – with peaks at twilight absent under both conditions (Fig. 4.2D). As expected from the characteristics of rods and cones, this suggests that they are required for increased light sampling levels at twilight under a ramped LD cycle, and melanopsin is not sufficient for this behaviour. Photoreceptor activation threshold calculations confirm that rods will have been activated within the first 1s into our dawn ramp and M-cones by 7 seconds in, whilst S-cones will not have been activated until 22.5 minutes in, due to the low levels of short-wavelength light in white LEDs. The use of a sighted C3H control, in addition to more specific transgenic models where either rods or cones are removed would provide further insight into these results. Similarly, a more gradual twilight ramp – where the activation thresholds of photoreceptors are more spread out over time - could provide greater resolution to detect differences in behaviour, especially when activity levels are low during dawn and dusk.

It has traditionally been challenging to identify a role for cones in photoentrainment compared to rods and melanopsin, since the rapid adaption of cones under sustained light has been thought to limit their contribution to the first few seconds of a light response (Brown et al., 2011; Dobb et al., 2017; Lall et al., 2010; Mouland and Brown, 2022). Yet here we demonstrate that cones, along with rods and melanopsin, are likely to be important in increasing light sampling at twilight – thereby regulating photoentrainment with respect to the phase response curve. This adds to the growing evidence base for the role of cones in photoentrainment under more naturalistic conditions (Mouland et al., 2019; Walmsley et al., 2015). It is interesting to consider whether the addition of a dark nestbox may increase the role of cones. The use of a dark nestbox changes the pattern of retinal light exposure during the light phase - from constant (under which cones adapt rapidly; Brown et al., 2011; Dobb et al., 2017), to intermittent - thereby increasing temporal contrast, to which cones respond significantly (Lall et al., 2010; van Diepen et al., 2021). Therefore, it is possible that the addition of a nestbox, or use of burrows under natural conditions, may actually generate different relative contributions of rods, cones and melanopsin to photoentrainment, than under standard laboratory conditions. This hypothesis could be examined by performing multielectrode arrays (MEAs) on ex vivo wildtype mouse retinas with natural light exposure stimuli.

However, the functional significance of increased temporal contrast for circadian phase resetting may be limited. Dobb (et al., 2017) demonstrates that whilst the SCN can encode naturalistic temporal modulations in irradiance, this does not alter circadian phase resetting. Instead, the circadian system integrates temporal contrast in irradiance to assess average light intensity. Furthermore, the contribution of cone irradiance signals to SCN firing actually reduces as spatiotemporal contrast increases (Mouland et al., 2021). Therefore, even if cones respond more in the presence of a nestbox, it remains challenging to predict the functional significance of this. Since the SCN influences a range of processes e.g., the SCN connects to important neuroendocrine centres (Kriegsfeld and Silver, 2006), it has been tentatively suggested that temporal modulations in SCN firing could be utilised in processes beyond circadian entrainment (Dobb et al., 2017; Mouland and Brown, 2022).

To conclude, here we use transgenic mouse strains to investigate the role of melanopsin, rods and cone photoreceptors in regulating light sampling behaviour. We confirmed that mice lacking melanopsin, as well as those lacking rods and cones, still extensively utilise the dark nestbox (Fig. 4.1A, 2A) and exhibit light sampling behaviour (Fig. 4.1D, 2D). One of our key aims was to assess the contribution of different photoreceptors to increased levels of light sampling events at twilight observed in C57BL/6J mice in Chapter 3 of this thesis. In C3H mice, there was no increase in

light sampling at twilight under a ramped LD cycle (Fig. 4.2D). This may confirm our hypothesis that rods and cones are important for increased light sampling at twilight, likely driven by the detection of changing light levels. However, conclusions are limited by the lack of a sighted C3H control. Similarly, although the melanopsin study had an appropriate control, background strain variations between C57BL/6J x 129 (the Opn4 mice) and C57BL/6J (used in Chapter 3) made firm conclusions difficult. However, it is possible that melanopsin may also contribute to light sampling at twilight (Fig. 4.1D; S4.1C,D). Therefore, whilst previous literature found relatively normal photoentrainment in mice lacking melanopsin under standard laboratory conditions (12:12hr square-wave LD cycles; Panda et al., 2002b; Ruby et al., 2002) and indeed we see no significant differences between *Opn4*$^{+/+}$ and *Opn4*$^{-/-}$ mice in locomotor activity or circadian entrainment metrics under these conditions (Fig. 4.1B,C,F-I; Fig.S4.1F-J); the use of a more naturalistic ramped light environment and nuanced behavioural assessment may indicate an important, albeit subtle role for melanopsin in photoentrainment. That is, in contributing to the regulation of increased light sampling at twilight. However, as discussed, further studies are required to confirm this.

4.6 Supplementary figures

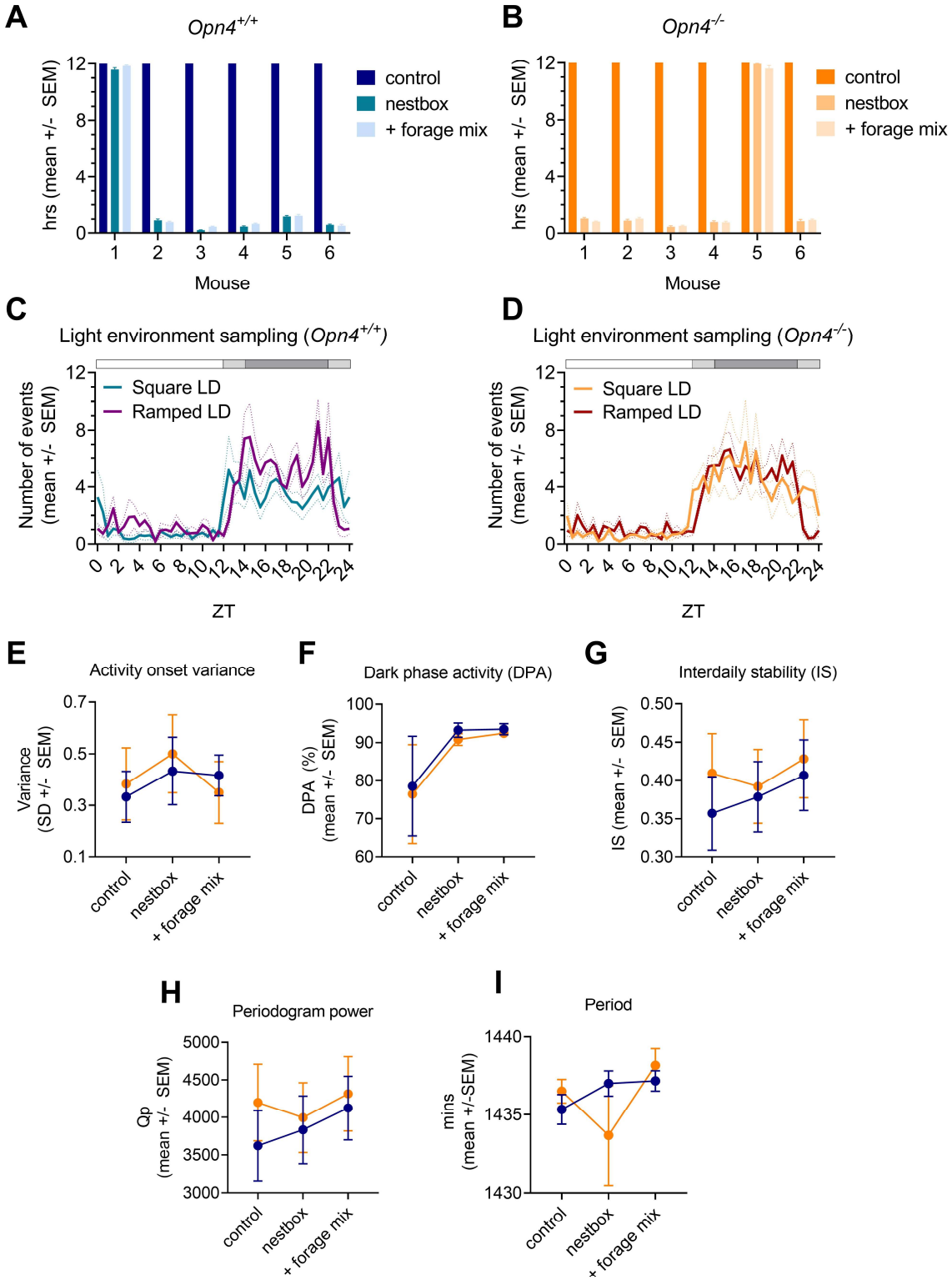

Figure S4.1 - Opn4$^{+/+}$ vs. Opn4$^{-/-}$ mice. Figure legend on the next page.

Figure S4.1 - Opn4$^{+/+}$ vs. Opn4$^{-/-}$ mice. Daily light exposure (hrs) of individual Opn4$^{+/+}$ mice **(A)** and Opn4$^{-/-}$ mice **(B)** across experimental conditions (control, nestbox, and nestbox + forage mix ('+forage mix')). **(C)** Light environment sampling under a square-wave (blue) and ramped (purple) LD cycle in Opn4$^{+/+}$ mice. **(D)** Light environment sampling under a square-wave (orange) and ramped (red) LD cycle in Opn4$^{-/-}$ mice. **(E – I)** Circadian entrainment metrics across conditions (control, nestbox, and nestbox + forage mix ('+forage mix')) for Opn4$^{+/+}$ (blue) and Opn4$^{-/-}$ (orange) mice. **(E)** Activity onset variance, **(F)** Dark phase activity, **(G)** Interdaily stability, **(H)** Period, **(I)** Periodogram power. White, grey and black bar shows timing of light, light ramp and dark, respectively **(C,D).** All results reported as mean across days **(A,B)** or across mice and days **(C-I)** +/- SEM. **** $p<0.001$, ** $p<0.01$, * $p<0.05$, between genotype and condition comparisons.

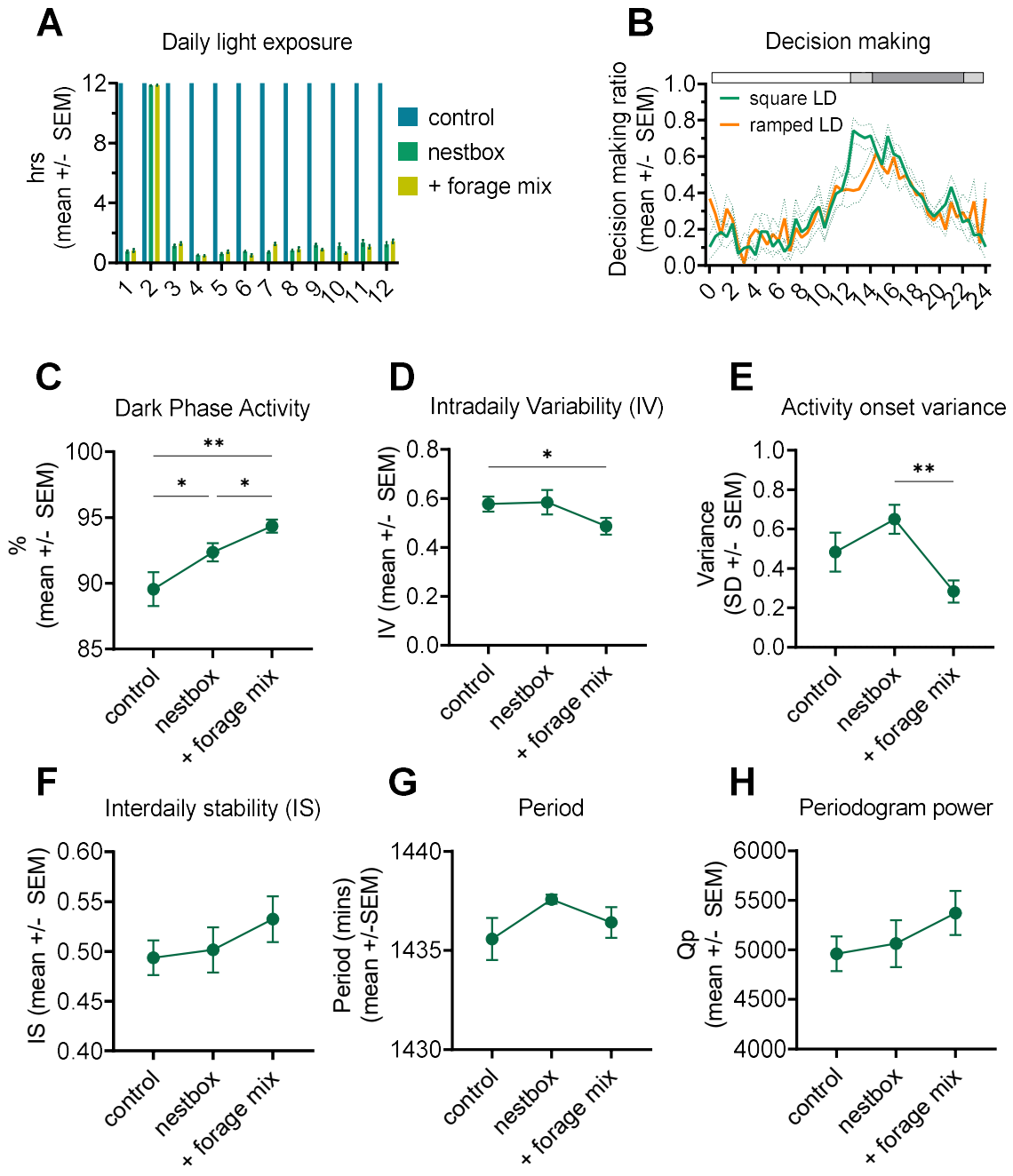

Figure S4.2 - C3H mice. (A) Daily light exposure (hrs) of individual mice across experimental conditions (control (blue), nestbox (green), and nestbox + forage mix ('+forage mix') (yellow)). **(B)** Decision making ratio (>0.5 = 'go'; <0.5 = 'no-go') under a square-wave 12:12hr LD cycle (green) and 12:2:8:2hr ramped LD cycle (orange). White, grey and black bar shows timing of light, light ramp and dark, respectively. **(C-H)** Circadian entrainment metrics across conditions. **(C)** Dark phase activity, **(D)** Intradaily variability, **(E)** Activity onset variance, **(F)** Interdaily stability, **(G)** Period, **(H)** Periodogram power. All results reported as mean across days **(A)** or across mice and days **(B-H)**, +/- SEM. **** p<0.001, ** p<0.01, * p<0.05, between condition comparisons.

Chapter 5. Effects of natural light spectra on light sampling behaviour and circadian entrainment

Many thanks to Kieran Foster (Physics Workshop, University of Oxford) who built the violet LEDs used in this Chapter.

5.1 Abstract

The spectrum of natural daylight differs greatly to that of artificial lighting utilised in standard laboratory animal housing. The natural light environment undergoes predictable daily changes in intensity and spectrum which do not occur in the laboratory, with enrichment of short-wavelength light at twilight. Therefore, building upon the data in Chapters 3 and 4, here we use different wavelength LEDs to simulate the experience of daylight and twilight on the mouse retina, in the presence of a dark nestbox to enable behavioural regulation of light exposure. We demonstrate that the introduction of spectral changes associated with civil twilight alters mouse behaviour at dusk compared to an intensity-only control ramp – advancing activity onset by 0.5hrs and light sampling behaviour by 1hr; which may support recent data that the circadian system is sensitive to colour. Interestingly, no significant differences in behaviour are observed at dawn, indicating that photoreceptor involvement in the detection of dawn and dusk may differ. However, our data also suggests that whilst spectral changes associated with twilight may modulate behaviour, it is the gradual ramping of light intensity at dawn and dusk which is the most significant feature of the natural light environment in influencing light sampling behaviour in mice.

5.2 Introduction

The light environment experienced by the burrow-dwelling mouse in the wild differs greatly to that in the laboratory. Firstly, as discussed in Chapter 3, mice cannot self-regulate their light exposure in the laboratory and secondly, the spectrum and intensity of light is very simplified compared to natural light. Due to the rotation of the Earth on its axis, the spectrum and intensity of light changes predictably across the 24hr period in natural environments (Spitschan et al., 2017,

2016). Intensity changes from 0.001 photopic lux on a starlit night to >100,000 photopic lux on a sunny day; with moonlight providing further variation in irradiance levels at night (Palmer and Johnsen, 2015; Spitschan et al., 2016). The greatest changes in both intensity and spectrum occur at twilight, which is separated into three phases defined by solar elevation (civil twilight, 0 to -6 degrees; nautical twilight, -6 to -12 degrees; and astronomical twilight, -12 to -18 degrees). The length of twilight varies with time of year and latitude, due to the changing angle of the setting or rising sun's path with respect to the horizon. For example, in the UK, twilight can last 7hrs 19mins on dates near the summer solstice (June 21st, Oxford, UK), with the sun never sinking further than 18 degrees below the horizon, resulting in no true night. In contrast, at the winter solstice (December 21st, Oxford, UK), twilight is reduced to 2hrs 5mins (October 10th) (https://www.timeanddate.com/sun/uk/oxford). Due to atmospheric absorption and scatter (Hulburt, 1953) twilight is short-wavelength enriched (< 500nm; peak power ~455nm) relative to daylight (Spitschan et al., 2016; Walmsley et al., 2015). Further complexity in the natural light environment arises by variation in intensity resulting from cloud cover and behavioural movements, as well as differential spectral reflectance of materials in the local environment (Morimoto et al., 2019; Shiwen et al., 2021). In contrast, laboratory studies are generally performed under 12hr:12hr light/dark (LD) cycles of broad spectrum white light sources, which have little short-wavelength light (Lucas et al., 2024). Although the use of ramped intensity LD cycles have become more common, spectral changes are still lacking.

The depleted short-wavelength components of white light sources used in the laboratory are of particular significance, since mice have a short-wavelength sensitive cone (λ max = 360nm) (Jacobs et al., 1991; Peirson et al., 2018) and UV light influences non-image forming (NIF) responses in mice (Allen et al., 2011; Van Oosterhout et al., 2012). Therefore it is likely that differences in behaviour will occur under standard laboratory and natural environments. Indeed, studies have demonstrated that mice will become partially diurnal when housed in semi-natural, outside environments (Daan et al., 2011); although differences could have been driven by multiple factors such as changes in food availability, temperature, predation and social structure. Natural light environments are important for many behaviours in a range of organisms, such as appropriate spawning timing in the bristle worm (Poehn et al., 2022) and hunting in kestrels (Viitala et al., 1995). More specifically, differences in the shape of the phase response curve (PRC) in rodents (Sharma et al., 1997) and bats (Joshi and Chandrashekaran, 1985) have been shown across different types of white light with varying levels of UV light, and daylight. Therefore, recent expert guidance has recommended that laboratory animals should be housed under light environments with alpha-opic lux values equivalent to daylight, for both welfare and scientific reproducibility; although

emphasises that more research on the effects of natural light environments on behaviour is needed (Lucas et al., 2024).

Whilst daylight may drive differences in behaviour, twilight is considered to be the key signal for photoentrainment; with temporal gating resulting in the circadian clock being most sensitive to light at dawn and dusk (Brown, 2016; Foster et al., 2020). In addition, skeletal photoperiods which deliver brief light exposure at twilight only, are sufficient for entrainment in rodents (Rosenwasser et al., 1983; Stephan, 1983) and can encode daylength in the SCN (Olde Engberink et al., 2020). There are several cues associated with natural twilights which could be used to tell the time of day - changes in intensity, spectrum and the position of the sun relative to the horizon (Brown, 2016; Foster and Helfrich-Förster, 2001; Roenneberg and Foster, 1997). As previously demonstrated in Chapter 3 gradual changes in intensity of a white LED at dawn and dusk were found to be important in driving significantly higher levels of light environment sampling behaviour (DeCoursey, 1986; Roenneberg and Foster, 1997). Here we extend this study to explore the effects of spectral changes at twilight, in addition to changes in intensity, on circadian entrainment and light environment sampling behaviour.

Using colour to track twilight has been suggested several times (Foster and Helfrich-Förster, 2001; Roenneberg and Foster, 1997; Solessio and Engbretson, 1993). Spectral opponency, whereby signals from two photoreceptors with different spectral sensitivities are compared, is required to detect colour (Jacobs, 2014; Svaetichin and MacNichol., 1958). This is due to photon wavelength dictating only the probability of absorption by a photoreceptor, but not the photoreceptor output – which is consistent regardless of wavelength. This concept is referred to as the principle of univariance (Rushton, 1972). More recent studies have demonstrated both theoretically (Spitschan et al., 2017; Woelders et al., 2018) and experimentally (Mouland et al., 2019; Walmsley et al., 2015) that spectral opponency could be used to track twilight. Furthermore, spectral opponency has been found in neurons of the mouse SCN and differences in entrainment, as quantified by body temperature, were observed under natural twilights (Walmsley et al., 2015). However, spectral changes alone are not sufficient for entrainment in mice (Mouland et al., 2019), with colour signals providing only a modulating effect. An advantage of using spectral opponency to track twilight is the elimination of shared noise (Buchsbaum et al., 1997; Spitschan et al., 2017) – which could allow for more accurate tracking of twilight when weather events such as cloud cover increase variability in intensity signals (Mouland et al., 2019; Woelders et al., 2018). Here we seek to extend our understanding of how entrainment at the behavioural level differs under natural light environments, by measuring other key outputs such as locomotor activity and light environment sampling behaviour.

Therefore, here we utilise the concept of alpha-opic lux (Lucas et al., 2024, 2014) to simulate the experience of daylight and twilight on the mouse retina. The use of alpha-opic lux (weighted to each of the mouse photoreceptors individually) is necessary to study the effects of colour and irradiance independently for mice. The traditional unit of light intensity, photopic lux, is based on human visual sensitivity (Lucas et al., 2024, 2014) and therefore lights differing in spectrum, but matched in brightness for a human observer, will appear differently to mice. Whilst photoreceptor transgenic lines are a useful tool to explore the role of different photoreceptors in regulating behaviour (Brown et al., 2010; Foster et al., 1991; Freedman et al., 1999; Lucas et al., 2001), they are associated with problems. These include background strain differences, as demonstrated in Chapter 4; or altered retinal organisation - since ipRGC activation is dependent upon both extrinsic input (rod and cone derived) and intrinsic (melanopsin derived) responses, the ablation of rods and cones can alter melanopsin responses compared to in an intact retina (Allen et al., 2011; Allen and Baño-Otálora, 2022). Therefore, using light stimuli which result in differential activation of photoreceptors in wildtype mice, is a useful method to further dissect the role of different photoreceptors in regulating behaviour and physiology (Estévez and Spekreijse, 1982; Mouland et al., 2021, 2019; Spitschan and Woelders, 2018; Walmsley et al., 2015).

5.3 Materials and Methods

5.3.1 Animals and housing conditions

This study used a cohort of 12 C57BL/6J mice (6 female and 6 male; Envigo, Blackthorn, UK, RRID: IMSR_ JAX:000664) aged ~8 weeks at the start of the control week. C57BL/6J mice were used to address how wildtype mice respond to light, in order to be of greatest relevance for animals used by the majority of researchers. All animals were singly housed with *ad libitum* access to food and water, and sizzlenest was present throughout the experiment. Cages were placed in light-tight ventilated chambers (LTC) equipped with multiple light-emitting diodes (LEDs) (details outlined in the visual stimuli section of the methods). Prior to the onset of the experiment, all animals were habituated to a reverse (to minimise the disruption from daily welfare checks) 12h:12h light dark cycle of 200 photopic lux (170 melanopic lux) of cool-white LED (Fig. 5.1A) throughout the light phase (lights on at 7pm, lights off at 7am), generated by WiFi controlled cool-white (4500 CCT) light-emitting diodes (LEDs) (LIFX light-strip; LIFX, Cremorne, Australia). The spectral power distribution of the cool-white LED consisted of a high, narrow peak at ~450nm and a lower, broader peak at ~560nm (Fig. 5.1A), measured using a calibrated Ocean Optics USB2000+ Spectrophotometer (Ocean Insight, Oxford, United Kingdom). The temperature of the animal

holding room was maintained at 19-21°C. All experimental procedures were conducted at the University of Oxford, England, in accordance with the United Kingdom Animals (Scientific Procedures) Act 1986 under Project License PP0911346 and Personal License I82616702. All procedures were in accordance with the University of Oxford Policy on the Use of Animals in Scientific Research.

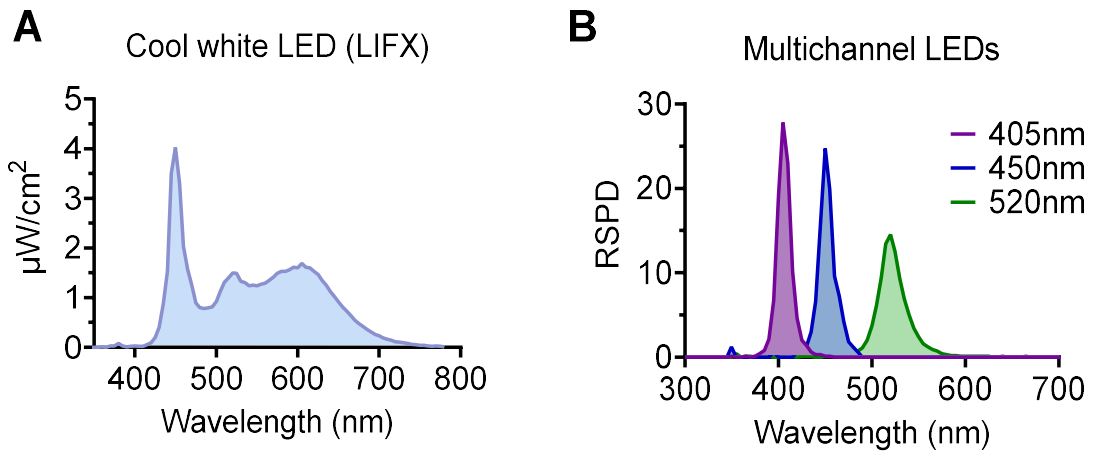

Figure 5.1 (A) SPD of cool white LED (LIFX) at 200 photopic lux (170 melanopic lux). **(B)** RSPDs of multichannel LEDs (λmax = 405nm (violet); λmax = 450nm (blue); λmax = 520nm (green)).

5.3.2 Experimental Design

All animals received the same series of conditions, in the same order (Table 5.1). Conditions 2 and 4 had three days of habituation at the beginning, to allow for habituation to the nestbox and a ramped light dark cycle, as previous data had showed that activity patterns stabilised after this period. Only the last week of recordings in these conditions were analysed.

Condition	Day	Purpose	Nestbox	Light environment	LD cycle
N/A	1-12	Habituation	No	169.7 mel lux white LED	Reverse 12h:12h
1	12-19	Control	No	169.7 mel lux white LED	Reverse 12h:12h
2	19-29	Experimental	Yes	169.7 mel lux white LED	Reverse 12h:12h
3	29-36	Experimental	Yes	169.7 mel lux simulated daylight	Reverse 12h:12h
4	36-46	Experimental	Yes	169.7 mel lux white LED, followed by intensity only ramp	Reverse 12h:2h:8h:2h
5	46-53	Experimental	Yes	169.7 mel lux simulated daylight, followed by intensity only ramp	Reverse 12h:2h:8h:2h
6	53-60	Experimental	Yes	169.7 mel lux simulated daylight, followed by a ramp with twilight intensity and spectral changes	Reverse 12h:2h:8h:2h

Table 5.1 Experimental design timeline. Blue shading indicates which variable changed from the previous condition. 'mel lux' refers to melanopic lux.

5.3.3 Locomotor activity monitoring

See section 3.3.3

5.3.4 Data processing

See section 3.3.4

5.3.5 Visual stimuli

5.3.5.1 Simulating daylight

Multichannel LEDs (Fig. 5.1B), comprised of a violet LED strip (λmax = 405nm; custom built by the Physics Workshop, Oxford University and controlled via a custom LabView script), blue LED strip (λmax = 450nm; WiFi controlled, LIFX) and green LED strip (λmax = 520nm; WiFi controlled, LIFX), were used to simulate the experience of daylight on the mouse retina. Daylight was defined as the light environment measured at 24.1 degrees above the horizon on 19/07/2014 at 18:08:44 (Table S5.2; Spitschan et al., 2016 – measured in Cherry Springs State Park, Pennsylvania, US; a certified International Dark Sky Park). This measurement was selected as it started at a shorter wavelength (340nm) than the other daylight measurements, which started at 360nm, and so matched the spectral ratio of the CIE D65 (i.e. equal α-opic lux) more closely. This daylight spectral power distribution (SPD) was converted to 5nm bins from 300-780nm by linear interpolation, and normalised to the summated total, to produce a relative SPD (RSPD) (Fig. 5.3A, 'daylight'). The Rodent Toolbox (supplementary tool 2) was used to calculate the α-opic lux (Fig. 5.3B, 'daylight') and log quanta (Table S5.1, 'daylight') available to each mouse photopigment, produced by 170 melanopic lux of the daylight RSPD – to match the 170 melanopic lux produced by 200 photopic lux of the cool-white LED used in the habituation and control conditions.

The RSPDs of the three LED strips (Fig. 5.1B) were measured using a calibrated Ocean Optics USB2000+ Spectrophotometer (Ocean Insight, Oxford, United Kingdom) and the sum used as the input for the Rodent Toolbox (supplementary tool 3). The solver optimisation function in Excel (v2309) was used to calculate the power (μW/cm^2/s) required by each LED strip to produce the equivalent α-opic lux values as the daylight measurement. All LEDs were set to initial values of 10 μW/cm^2/s before the solver function was used. The following LED powers were calculated: violet (43.2 μW/cm^2/s), blue (3.3 μW/cm^2/s) and green (22.3 μW/cm^2/s) (Fig. 5.3A); producing α-opic lux values all within 0.4% of the target values (1dp) (Fig. 5.3B), and log quanta values that matched target values to 1dp (Table S5.1). The multichannel LEDs were set to the corresponding power using a power metre (PM160 wireless power metre, Thor Labs). α-opic lux values were confirmed to be within 2% of the target values, and log quanta values matched target values to

1dp, as measured using a calibrated Ocean Optics USB2000+ Spectrophotometer and calculated using the Rodent Toolbox (supplementary tool 2).

Condition 3 and 5 both used this simulated daylight environment (Table 5.1). Condition 3 used a reverse 12h:12h LD cycle of 170 melanopic lux of simulated daylight, whilst condition 5 used a reverse 12h:2h:8h:2h LD cycle of 170 melanopic lux of simulated daylight during the light phase, and a series of step changes in light intensity across the ramp (Fig. 5.4A,B), but with spectral ratios remaining equal to that produced by daylight (Fig. 5.3B). The timings of the 12:2:8:2hr ramped LD cycle were based on the length of daylight and twilight naturally occurring at the spring and vernal equinoxes in Oxford, UK (sourced from https://www.timeanddate.com/sun/uk/oxford). The equinox LD cycle was used since it is an intermediate LD cycle, with the length of the light phase being in-between those of the summer and winter solstices. Validation measurements were taken at 0, 56 and 92 minutes into the 2hr ramp – alpha opic lux values were within 9% of target values and log quanta values within 1dp of target values (supplementary file 10). Steps were necessary due to the technical limitations of the violet LED strip which ramped in intensity via a set series of steps (supplementary file 9). The overall ramp was exponential, with light intensity at 1hr into the ramp measuring 46.8 photopic lux (68.4 S-opic, 74.9 melanopic, 74.8 rhodopic, 74.2 M-opic lux) (Fig. 5.4B). The white LED ramp in condition 4 (Table 5.1) followed the same overall step changes in light intensity, as quantified by melanopic lux (data not presented). The multichannel LEDs were set to the corresponding power for each step using a power metre (PM160 wireless power metre, Thor Labs).

5.3.5.2 Simulating twilight

Condition 6 (Table 5.1) used a reverse 12h:2h:8h:2h light dark cycle of 170 melanopic lux of simulated daylight during the light phase (Fig. 5.3A), and an exponential change in light intensity across the 2hr ramp via a series of steps (Fig. 5.5E) which matched the intensity changes in condition 5 (Fig. 5.4B), as quantified by melanopic lux. This change in intensity occurred in combination with spectral changes associated with civil twilight (0 to -6 degrees solar elevation). Civil twilight was selected as this is the stage of twilight where the largest spectral changes occur (Fig. 5.5A), with spectral changes stabilising in nautical (-6 to -12 degrees solar elevation) and the signal to noise ratio becoming too low across astronomical twilight (-12 to -18 degrees solar elevation) (Fig. S5.1). The SPDs for each 1 degree increment of solar elevation from 0 to -6 degrees, as measured on 30/06/2014 between 20:28:05 and 21:06:06 (S2; Spitschan et al., 2016), were converted into 5nm bins from 300-780nm, and normalised to the summated total to produce RSPDs (supplementary file 5). The Rodent Toolbox (supplementary tool 2) was used to calculate

the ratio of α-opic lux (relative to the maximum value) available to each mouse photopigment produced by the RSPD of each degree of solar elevation across civil twilight. This method enabled us to simplify the spectral changes observed across twilight (Fig. 5.5A) to relevant changes in α-opic lux experienced by the mouse retina across civil twilight (Fig. 5.5B).

0 and -1 degrees of solar elevation produced the same α-opic lux ratio (Fig. 5.5B). Therefore, 0 degrees was removed from the simulation and each α-opic lux ratio for the remaining degrees of solar elevation (-1 to -6 in 1 degree increments) were assigned to each of the ramp intensity steps (simulating the -1 degrees α-opic lux ratio at the brightest step, down to -6 degrees α-opic lux ratio for the dimmest step). The RSPDs for -1 to -6 degrees were input into the Rodent Toolbox and corrected to produce the appropriate melanopic lux to match each step change in intensity across the ramp in condition 5. The α-opic lux values produced were then used as target values in the solver optimisation function in Excel (v2309) to calculate the power ($\mu W/cm^2/s$) required by each LED (Fig. 5.5C). All LEDs were set to a starting power of 10 $\mu W/cm^2/s$ before the solver function was used. The α-opic values produced by each stage of the twilight ramp (Fig. 5.5D) were within 0.9% of the target values (Fig. 5.5B), and log quanta values were within 1dp of target values (Table S5.2). The overall ramp was exponential, with light intensity at 1hr into the ramp measuring 38.8 photopic lux (74.3 S-opic, 74.9 melanopic, 70.7 rhodopic, 68.2 M-opic lux) (Fig. 5.5E). The multichannel LEDs were set to the corresponding power for each step (Fig. 5.5C) using a power metre (wireless power metre, Thor Labs). Validation measurements were taken at minute 0, 56 and 92 into the 2hr ramp - α-opic lux values were confirmed to be within 10% of the target values, and log quanta values matched target values to 1dp, as measured using a calibrated Ocean Optics USB2000+ Spectrophotometer and calculated using the Rodent Toolbox (supplementary tool 2).

5.3.6 Statistical analysis

Statistical analysis and data visualisation were performed in MATLAB and Prism Graph-pad (v.9.5.0 (730)). $\alpha = 0.05$ was adopted in all analyses. All locomotor, light environment sampling and decision making daily profiles are visualised in 30 min bins, unless otherwise stated (Fig. 5.5H,I,L,M). Any animals that did not routinely use the nestbox were removed from the analysis (mouse 1 was excluded from light exposure analyses in Figs.2 and 3; and mouse 8 was excluded from light exposure analyses in Figs.4 and 5). The Greenhouse-Geisser correction was performed with all ANOVAs, and corrected degrees of freedom reported, unless otherwise stated. A post-hoc Tukey test was used when all pairwise comparisons were desired, whilst a post-hoc Bonferroni test was used for a specific comparison between the control and experimental treatments. Further details on statistical tests used for each dataset are reported in the results section. Activity and light

environment sampling onset for every 24hr period for each mouse was calculated using Actogram J's inbuilt function, which first smooths the data (using the standard deviation of a smoothing Gaussian distribution). Following this, activities are considered to be 'active' if they exceed the threshold of the median of all activity values, or all activity values excluding zero (best fit assessed visually to ensure no systematic bias) (Schmid et al, 2011).

5.4 Results

5.4.1 Nestbox use is consistent with previous studies (Fig. 5.2)

As expected from results in Chapter 3, the majority of mice (11/12) use the nestbox (Fig. S5.2A), reducing their daily light exposure to an average of 0.8hrs across the 24hr period (Fig. 5.2A). This is significantly lower than the control condition [$t(10) = 86.3$, $p < 0.0001$; one-sample t-test against a control mean of 12.0hrs]. Interestingly, daily light exposure is significantly lower in males compared to females (Fig. S5.2B) [$t(12) = 10.2$, $p < 0.0001$, unpaired t-test]. This matches the higher levels of main cage locomotor activity in females than males during the light phase in both the control and nestbox conditions under a square-wave white LED LD cycle [main effect of sex, $F(1,10) = 6.3$, $p = 0.0307$; but no significant condition x sex interaction; three-way ANOVA; data not visualised]. This could result from higher oestrogen levels in females, which promotes CNS arousal (Garey et al., 2003). Daily locomotor activity (Fig. 5.2B) and light environment sampling profiles (Fig. 5.2C) averaged across animals show similar patterns to those in Chapter 3, with peaks of light environment sampling at twilight under a ramped LD cycle compared to a square-wave LD cycle (Fig. 5.2C) [main effect of time, $F(6.2,67.9) = 12.7$, $p < 0.0001$; no main effect of condition, $F(1,11) = 1.4$, $p = 0.2576$; time x condition, $F(6.0,65.5) = 3.6$, $p = 0.0038$; two-way ANOVA]; the latter interaction demonstrating the difference in pattern of light environment sampling behaviour across time between conditions. Overall, nestbox use under a square-wave and ramped LD cycle of white LED in this study is comparable to Chapter 3 results under the equivalent conditions.

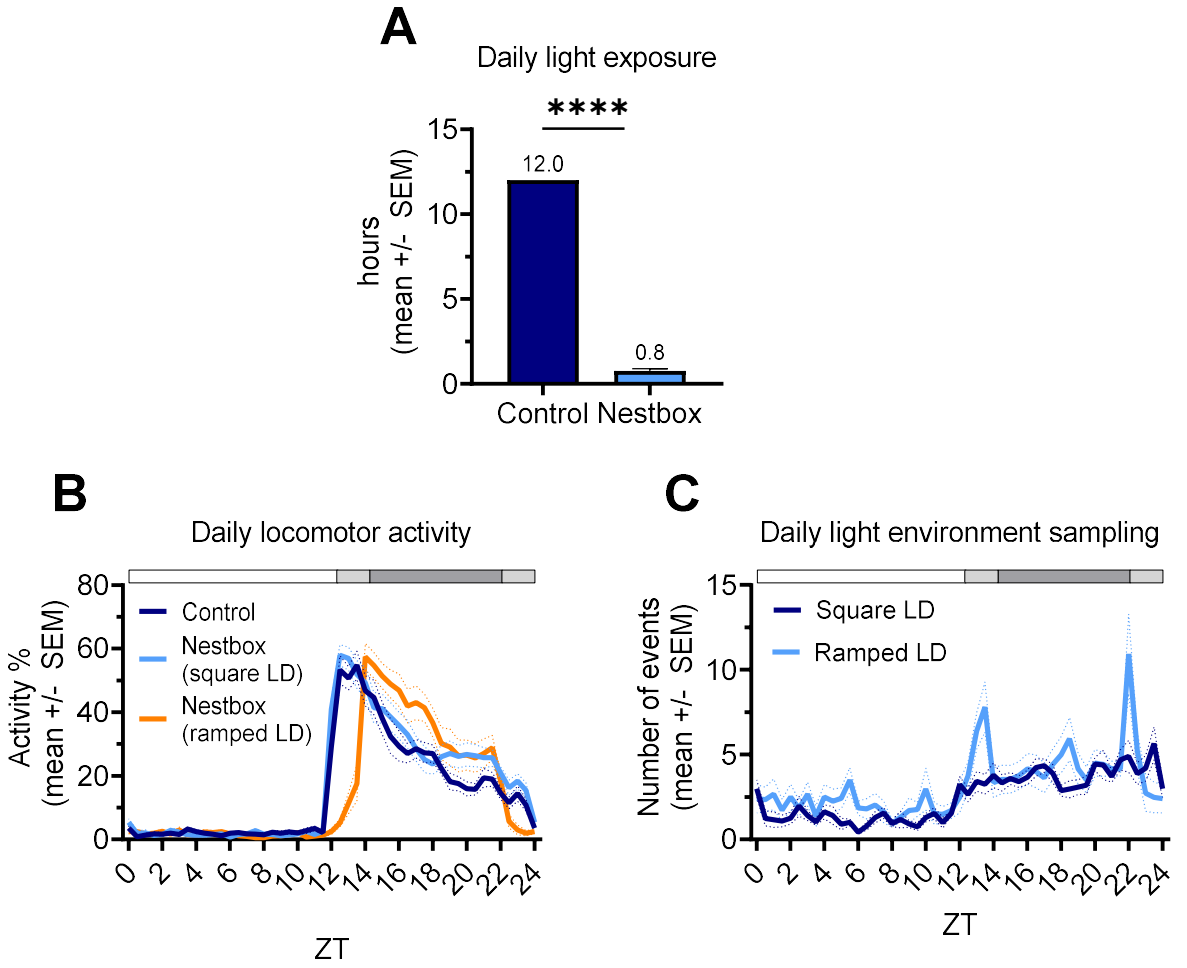

Figure 5.2 - (A) Daily light exposure (hrs) under control and nestbox conditions. **(B)** Main cage daily locomotor activity profile under the control (no nestbox) 12:12hr square-wave LD cycle (dark blue), nestbox with 12:12hr square-wave LD cycle (pale blue), and nestbox with ramped 12:2:8:2hr LD cycle (orange) conditions. **(C)** Daily light environment sampling profile under a square 12:12hr LD cycle (pale blue) and a ramped 12:2:8:2hr LD cycle (dark blue). White, grey and black bar shows timing of light, light ramp and dark, respectively **(B,C).** All results reported as mean across mice and days, +/- SEM. **** $p<0.001$ between condition comparisons.

5.4.2 The effect on behaviour of a square-wave LD cycle of daylight, compared to a white LED (Fig. 5.3)

Changing the square-wave LD cycle from a white LED to the equivalent melanopic lux of daylight only had modest effects on behaviour (Fig. 5.3A). It does not have a significant effect on the extent of nestbox use and subsequent light exposure (Fig. 5.3C) [$p = 0.7646$, Wilcoxon signed rank test]. Locomotor activity in the main cage is significantly lower under daylight than the white LED (Fig. 5.3D) [main effect of time, $F(3.0,32.7) = 65.6$, $p < 0.0001$; main effect of condition, $F(1,11) = 26.8$, $p = 0.0003$; time x condition, $F(4.8,52.8) = 4.8$, $p = 0.0013$; two-way ANOVA with post-hoc Bonferroni test]. However, this is only true for the dark phase [main effect of condition, $F(1,11) = 28.2$, $p = 0.0002$], not the light phase [no main effect of condition, $F(1,11) = 1.2$, $p = 0.3039$]. Furthermore, the effect of condition on locomotor activity is no longer significant when sex is incorporated into the model (data not visualised) [main effect of sex, $F(1,10) = 13.7$, $p = 0.0041$; no main effect of condition $F(0.1,0.8) = 25.7$, $p = 0.0616$]; although there is no condition x sex interaction [$F(1,10) = 0.6$, $p = 0.4624$] demonstrating that the effect of sex on locomotor activity is equivalent across conditions. There is also no main effect of condition on light environment sampling behaviour (Fig. 5.3E) [$F(1,11) = 0.1634$, $p = 0.6938$; two-way ANOVA]. However, as quantified by a post-hoc Bonferroni test, light sampling behaviour is significantly higher under daylight than white LED at ZT11.5 [$p = 0.0265$] suggesting that daylight may promote earlier anticipation of the dark phase by light sampling behaviour, perhaps reflecting increased exploration levels.

There is no effect of condition, or condition x time interaction, on the ratio of decision making across conditions (Fig. 5.3F). As expected from the lower dark phase locomotor activity under daylight than the white LED (Fig. 5.3D), light phase activity (%) (Fig. 5.3G) is significantly higher under daylight [$t(11) = 2.3$, $p = 0.0431$], whilst dark phase activity (%) (Fig. 5.3H) [$t(11) = 2.3$, $p = 0.0431$] and relative amplitude are both significantly lower (Fig. 5.3I) [$t(11) = 2.3$, $p = 0.0431$] (paired t-tests). In addition, intra-daily variability – a measure of sleep/wake fragmentation, is significantly higher under daylight than the white LED (Fig. 5.3J) [$t(11) = 3.1$, $p = 0.0094$; paired t-test]. These metrics indicate increased circadian entrainment disruption under daylight compared to the white LED (Brown et al, 2016). Other metrics of circadian disruption were calculated, but no significant differences were observed (data not presented). Overall, replacing a square-wave LD cycle of white LED with daylight increases some metrics of circadian disruption, but beyond this has little effect on the behavioural parameters measured.

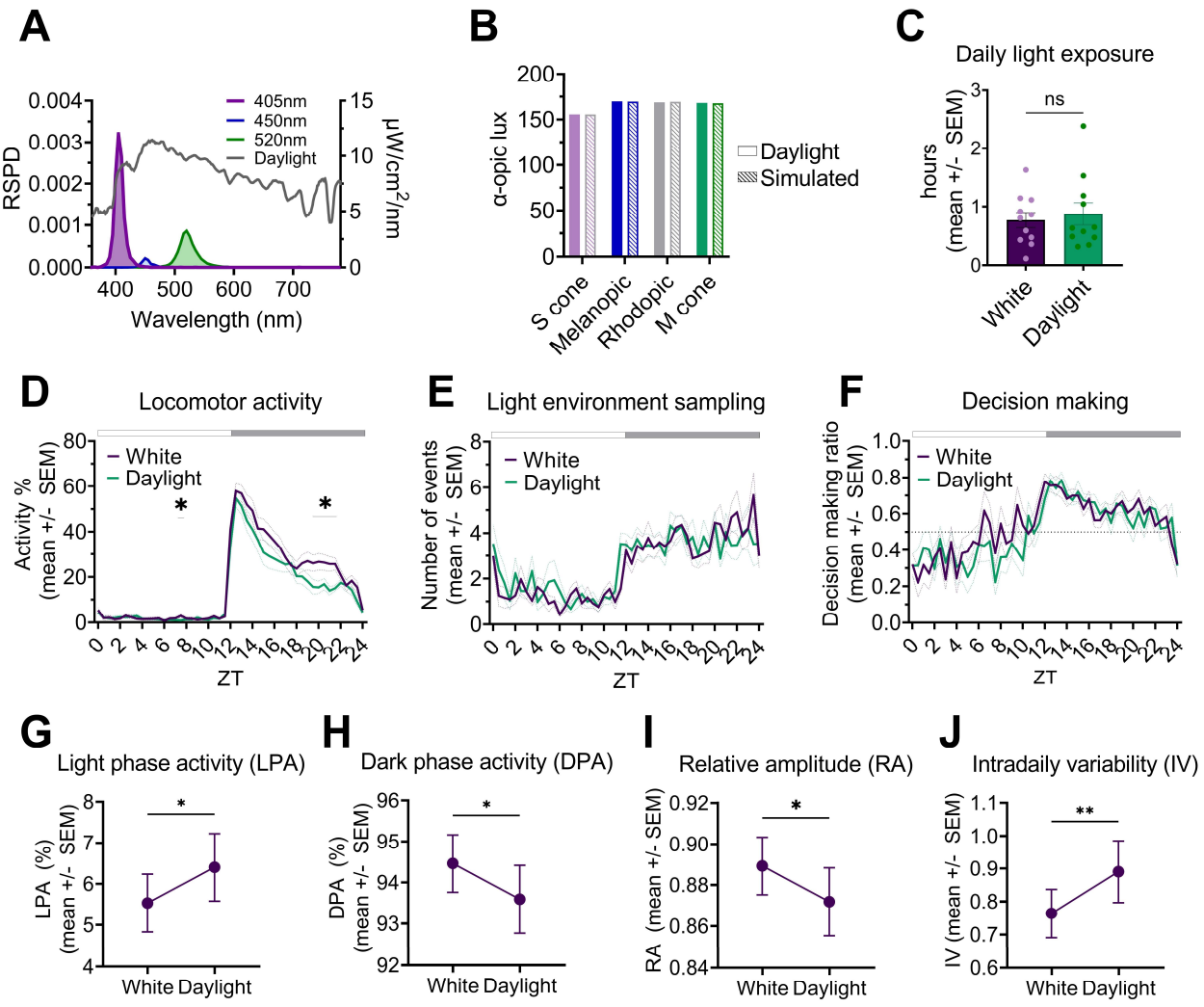

Figure 5.3 - Simulation of, and behaviour under, a 12:12hr square-wave LD cycle of cool white LED ('White') and a 12:12hr square-wave LD cycle of simulated daylight ('Daylight'). **(A)** RSPD of daylight (grey, data from Spitschan et al, 2016) on left y-axis. The power (μW/cm^2/nm) of each multichannel LED (λmax = 405nm (violet); λmax = 450nm (blue); λmax = 520nm (green)) required to simulate daylight (grey) on right y-axis. **(B)** α-opic lux produced by 200 photopic (170 melanopic lux) of daylight (data from Spitschan et al, 2016) and simulated daylight ('simulated') (produced by the LEDs in panel A). **(C)** Daily light exposure (hrs) with a nestbox present, under white and daylight conditions. **(D)** Main cage daily locomotor activity profile with a nestbox present, under white and daylight conditions. **(E)** Daily light environment sampling profile with a nestbox present, under white and daylight conditions. **(F)** Daily decision making profile with a nestbox present, under white and daylight conditions. Values >0.5 indicate more 'go' decisions. **(D,E,F)** White and black bar shows timing of light and dark, respectively. Significant post-hoc differences indicated with *. **(G-J)** Key circadian measures under white and daylight conditions. ** p<0.01, * p<0.05 between condition comparisons. **(G)** Light phase activity (%). **(H)** Dark phase activity (%). **(I)** Relative amplitude. **(J)** Intradaily variability. All results reported as mean across mice and days, +/- SEM.

5.4.3 The effect on behaviour of a ramped LD cycle of daylight, compared to a white LED (Fig. 5.4)

Under a 12:2:8:2hr ramped LD cycle of daylight (with changes in intensity-only across the ramp) mice expose themselves to significantly less light than under the same LD cycle of a white LED (Fig. 5.4C). Light exposure is reduced by an average of 0.8hrs across the 24hr, from 2.1hrs to 1.3hrs period (light phase is defined as the start of the ramp on, to lights fully off) (Fig. 5.4C) [$p = 0.0020$; Wilcoxon signed rank test]. Mice show similar changes in behaviour (locomotor activity, light sampling behaviour and decision making) when changing from a square-wave to a ramped LD cycle under both white and daylight conditions (data not presented), including clear peaks in light environment sampling at twilight under a ramped daylight LD cycle. However, when comparing the two ramped LD cycle conditions (daylight vs white LED) locomotor activity is significantly lower under daylight (Fig. 5.4D) [main effect of time, $F(1.7,18.4) = 54.5$, $p<0.0001$; main effect of condition, $F(1,11) = 6.4$, $p = 0.0284$; time x condition, $F(3.8,41.4) = 4.6$, $p = 0.0044$; two-way ANOVA with post-hoc Bonferroni test]. As under the square-wave LD cycle conditions(Fig. 5.3D), the effect of condition on locomotor activity is only significant during the dark phase [main effect of condition, $F(1,11) = 5.0$, $p = 0.0478$] not the light phase [no main effect of condition, $F(1,11) = 0.9$, $p = 0.3655$]. There is no significant effect of condition on light sampling behaviour (Fig. 5.4E) or decision making (Fig. 5.4F). Overall, changing the light environment from a white LED to daylight, under a 12:2:8:2hr ramped LD cycle, significantly reduces daily light exposure, but otherwise has modest effects on behaviour.

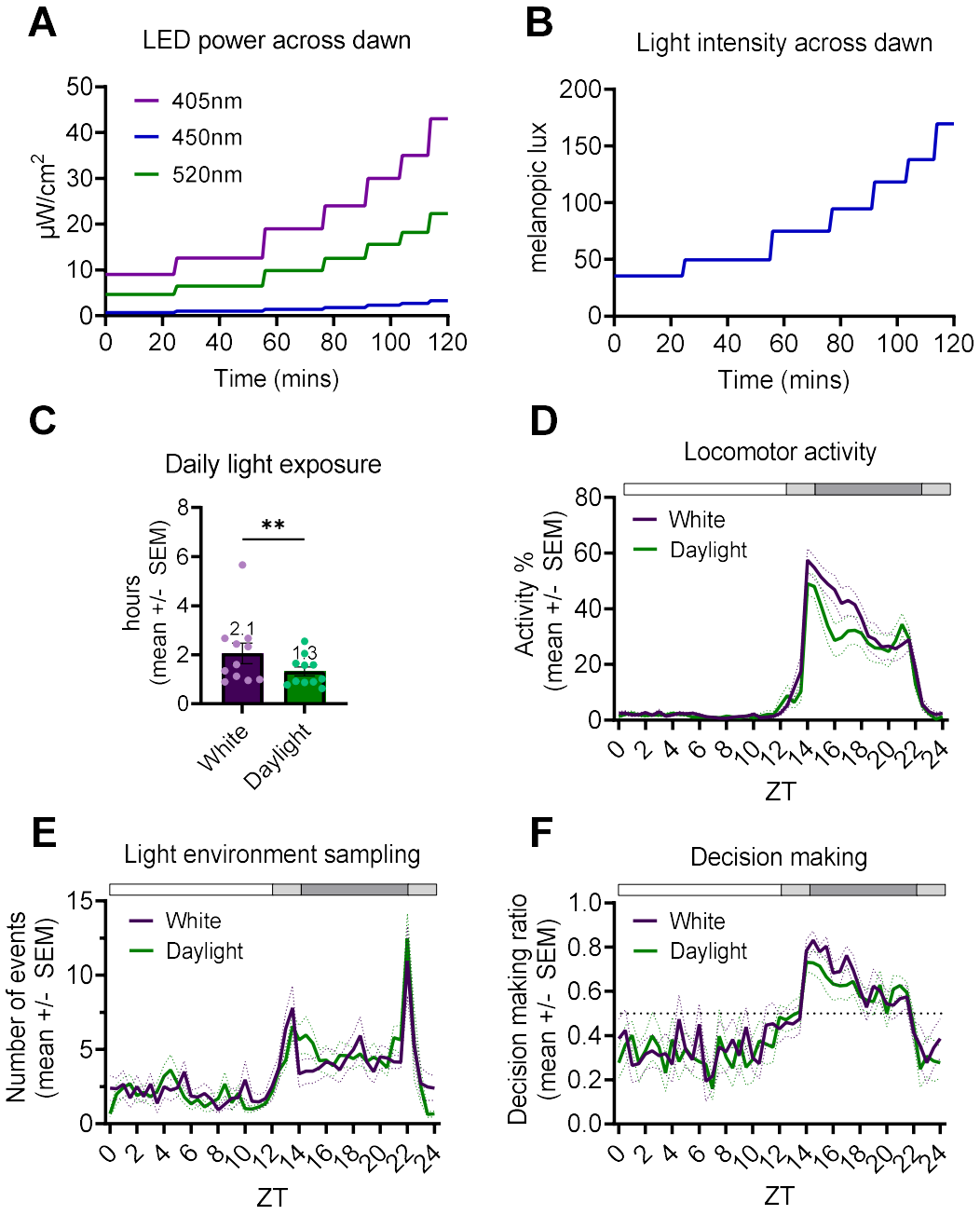

Figure 5.4 - Simulation of, and behaviour under, a 12:2:8:2hr LD cycle of a cool white LED ('White') and a 12:2:8:2hr LD cycle of simulated daylight ('Daylight') (intensity-only ramp). **(A)** Power (µW/cm^2/nm) of each multichannel LED (λmax = 405nm (violet); λmax = 450nm (blue); λmax = 520nm (green)) required to maintain a constant α-opic lux ratio, whilst changing intensity, across the 2hr dawn ramp of the 'Daylight' condition. **(B)** Changes in light intensity (melanopic lux) across the 2hr dawn ramp. **(C)** Daily light exposure (hrs) under the white and daylight ramped conditions. Light phase defined as the start of the ramp on to lights fully off. **(D)** Main cage daily locomotor activity profile with a nestbox present, under white and daylight ramped conditions. **(E)** Daily light environment sampling profile with a nestbox present, under white and daylight ramped conditions. **(F)** Daily decision making profile with a nestbox present, under white and daylight ramped conditions. Values >0.5 indicate more 'go' decisions. **(D,E,F)** White and black bar shows timing of light and dark, respectively. All results reported as mean across mice and days, +/- SEM. ** $p<0.01$ between condition comparisons.

5.4.4 The effect on behaviour of introducing twilight spectral changes, compared to a daylight intensity-only ramp (Fig. 5.5)

Introducing spectral changes associated with civil twilight across the 2hr dawn and dusk ramp, in addition to changes in intensity ('twilight' condition), resulted in significantly higher levels of daily light exposure compared to under the intensity-only daylight ramp, by an average of 0.5hrs (Fig. 5.5F) [$p = 0.0029$, Wilcoxon signed rank test]. This increase in daily light exposure is likely to result from the higher levels of locomotor activity observed at dusk under the twilight condition (Fig. 5.5H). Although there is no main effect of condition on the daily profile of main cage locomotor activity (Fig. 5.5G), [main effect of time, $F(1.7,19.1) = 35.0$, $p < 0.0001$; no main effect of condition, $F(1,11) = 2.2$, $p = 0.1630$; no time x condition interaction, $F(3.7, 40.6) = 2.1$, $p = 0.1078$; two-way ANOVA], when the dawn and dusk ramps are analysed at a higher level of temporal resolution, averaged across all three PIR sensors, a significant effect of condition on locomotor activity becomes apparent at dusk (Fig. 5.5H), but not dawn (Fig. 5.5I). Locomotor activity is significantly higher across dusk (ZT12-14) under the twilight condition compared to the daylight intensity-only ramp (Fig. 5.5H) [main effect of time, $F(2.7,29.6) = 18.5$, $p < 0.0001$; main effect of condition, $F(1,11) = 11.4$, $p = 0.0062$; time x condition, $F(1.9,21.3) = 4.1$, $p = 0.0314$; two-way ANOVA, with significant post-hoc differences at ZT13.2 and ZT13.3, post-hoc Bonferroni test]. However, there is no significant effect of condition on locomotor activity at dawn (Fig. 5.5I), [main effect of time, $F(2.9,31.2) = 52.0$, $p < 0.0001$; no main effect of condition, $F(1,11) = 0.9$, $p = 0.3669$; no time x condition interaction, $F(3.3,36.2) = 0.7$, $p = 0.5467$; two-way ANOVA]. Accordingly, activity onset is significantly earlier under twilight conditions than the daylight intensity-only ramp by 0.5hrs (Fig. 5.5J) [$p = 0.0156$, Wilcoxon signed rank test]. One animal free-ran under the twilight condition, and was removed from this analysis.

Similarly, there is no main effect of condition on the daily profile of light environment sampling behaviour (Fig. 5.5K) [main effect of time, $F(3.8,42.0) = 10.4$, $p < 0.0001$; no main effect of condition, $F(1,11) = 2.4$, $p = 0.1509$; no time x condition interaction, $F(5.4,59.2) = 1.8$, $p = 0.1263$; two-way ANOVA]. However, when the dusk ramp is explored at a higher level of temporal resolution (Fig. 5.5L), as expected there is a main effect of time [$F(3.6,39.5) = 13.7$, $p < 0.0001$]. In addition, although the effect of condition at dusk does not quite reach the threshold for significance [$F(1,11) = 4.0$, $p = 0.0723$], there is a significant time x condition interaction [$F(5.1,56.5) = 4.6$, $p = 0.0012$] and significant post-hoc differences at ZT13.2 and ZT13.8 (two-way ANOVA with post-hoc Bonferroni test) (Fig. 5.5L). This indicates a significant difference in the pattern of light environment sampling behaviour across dusk between conditions. Accordingly, the peak in light environment sampling at dusk, or light environment sampling 'onset', occurs

significantly earlier under twilight conditions than under the daylight intensity-only ramp, by 1.1hrs (Fig. 5.5N) [$t(10) = 4.6$, $p = 0.0010$; paired t-test]. However, at dawn there is no significant difference in the pattern of light sampling behaviour across time between conditions (Fig. 5.5M), [main effect of time, $F(3.8,41.9) = 8.5$, $p < 0.0001$; main effect of condition, $F(1,11) = 0.8$, $p = 0.3883$; time x condition, $F(2.9,32.1) = 1.9$, $p = 0.1470$]. Overall, locomotor activity and light environment sampling behaviour are significantly higher and start earlier at dusk, but not dawn, under a twilight ramp compared to an daylight intensity-only ramp.

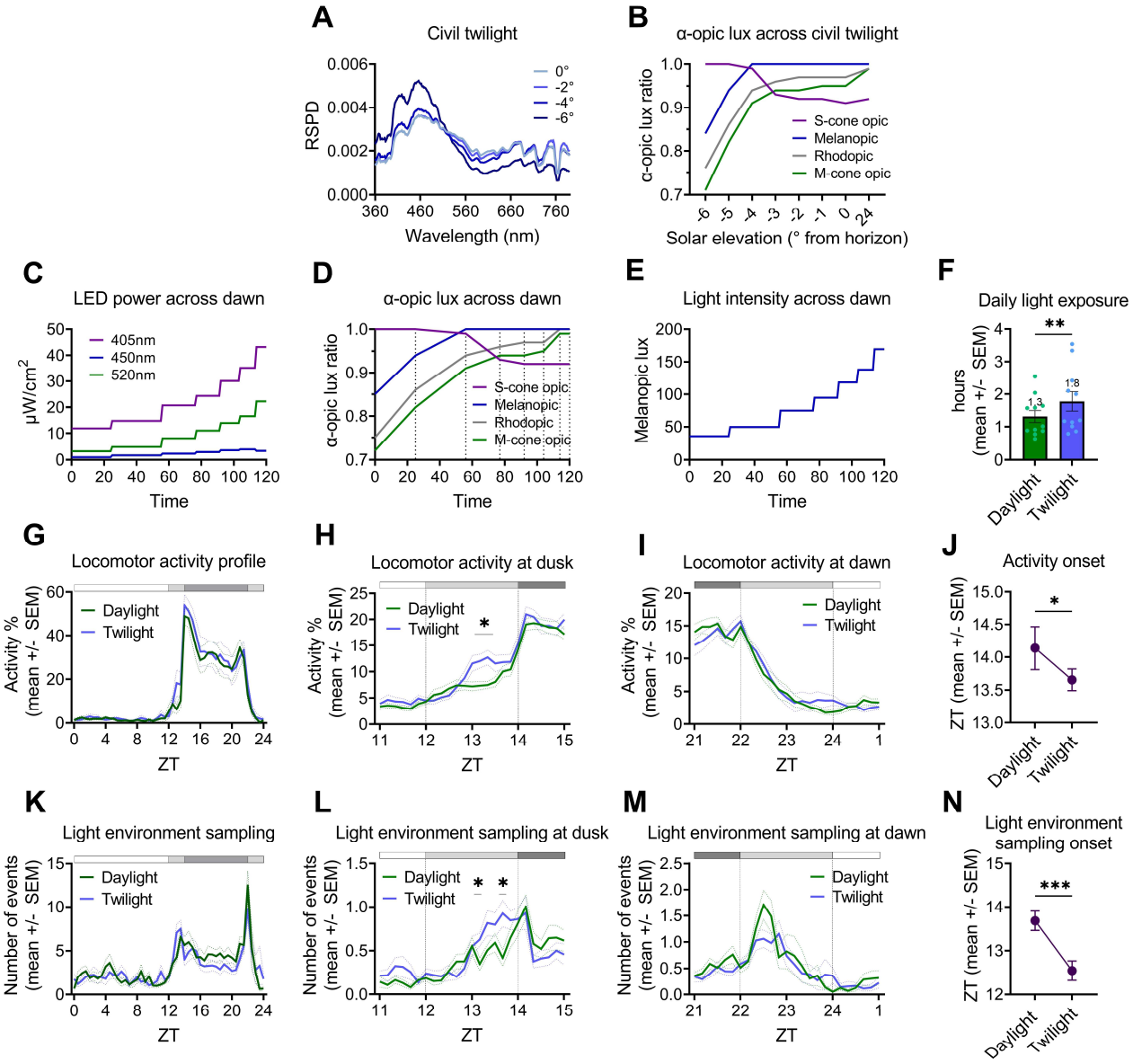

Figure 5.5 – Simulation of, and behaviour under, a 12:2:8:2hr LD cycle of simulated daylight ('Daylight') (intensity-only ramp) and a 12:2:8:2hr LD cycle of simulated twilight ('Twilight') (intensity and spectral ramp). **(A)** Spectral changes (RSPDs) across civil twilight in increments of 2 degrees of solar elevation, relative to the horizon (data from Spitschan et al, 2016). **(B)** α-opic lux ratio across civil twilight (relative to the maximum value). **(C)** Power (μW/cm^2/nm) of each multichannel LED (λmax = 405nm (violet); λmax = 450nm (blue); λmax = 520nm (green)) required to produce both spectral and intensity changes across the 2hr twilight dawn ramp). **(D)** α-opic lux ratio (relative to the maximum value) across 2hr dawn ramp, produced by LED powers in C. The ramp was achieved in a series of steps, indicated by dotted lines. **(E)** Light intensity (melanopic lux) across 2hr twilight ramp. **(F)** Daily light exposure (hrs) under daylight and twilight ramped conditions. Light phase is defined as the start of the ramp on, to lights fully off. **(G-I)** Locomotor activity profiles with a nestbox present, under daylight and twilight ramped conditions, **(G)** across 24hr period (30 min bins), main cage, **(H)** across dusk (dusk indicated by dotted lines), 10 min bins, average of all three PIR sensors **(I)** across dawn (dawn indicated by dotted lines), 10 min bins, average of all three PIR sensors. **(J)** Locomotor activity onset (ZT) under daylight and twilight ramped conditions. **Figure 5 legend continued on next page.**

Figure 5.5 legend continued. (K-M) Light environment sampling profiles under daylight and twilight ramped conditions, **(K)** across 24hr period (30 min bins), **(L)** across dusk (dusk indicated by dotted lines), 10 min bins. **(M))** across dawn (dawn indicated by dotted lines), 10 min bins. **(N)** Light environment sampling onset (ZT) under daylight and twilight ramped conditions. **(H,L)** Data is plotted for ZT11-15, but statistics performed on ZT12-14 only. **(L,M)** Data is plotted for ZT21-1, but statistics performed on ZT22-24 only. (**D-F,K-M)** White and black bar shows timing of light and dark, respectively. All results reported as mean across mice and days, +/- SEM. ***p<0.001, **p<0.01, *p<0.05 between condition comparisons.

5.5 Discussion

Here we use multichannel LEDs to simulate the experience of daylight and twilight on the mouse retina, in the presence of a dark nestbox to enable more naturalistic light avoidance behaviour. Whole cage locomotor activity monitoring enabled quantification of light sampling behaviour, decision making (via assessment of 'go' or 'no go' movements from the atrium) and circadian entrainment. We demonstrate that the introduction of spectral changes associated with natural civil twilight (Spitschan et al., 2016) alters mouse behaviour, compared to an intensity-only ramp; which could corroborate recent research that the mouse circadian system is sensitive to colour (Mouland et al., 2019; Walmsley et al., 2015). Interestingly, simply replacing the standard laboratory white LED with daylight, under either a square-wave 12:12hr or ramped 12:2:8:2hr LD cycle, had only subtle effects on behaviour (Fig. 5.3,4). It was the introduction of a ramped LD cycle, of any spectrum (white LED, daylight or twilight ramp) that generated the clearest behavioural differences – resulting in peaks in light sampling behaviour at dawn and dusk (Fig. 5.4E, 5.5K), as demonstrated previously (Chapter 3). These data indicate that the most significant feature of the natural light environment in influencing mouse behaviour is arguably the gradual ramping of light intensity; with twilight spectral changes across this ramp further modulating behaviour (Fig. 5.5).

However, although modest, our data does still indicate behavioural differences when a daylight spectrum is introduced instead of a white LED – for example, a slight advancement of the onset of light sampling behaviour at dusk (Fig. 5.3E). Differences are not necessarily surprising since white LEDs are short-wavelength depleted compared to daylight, resulting in lower activation of the S-cone (Lucas et al., 2024), and UV light has been shown to alter SCN population firing and induce phase shifts (Van Oosterhout et al., 2012) and promote exploration (Tamayo et al., 2023). In fact, all of the mouse photopigments can respond to short-wavelength light due to a β-band in the UV part of the spectrum (Mouland and Brown, 2022). Therefore, recent expert advice to house model organisms under light environments with similar alpha-opic lux ratios to natural light environments should be followed (Lucas et al., 2024); but our data emphasise that this should

occur in combination with the gradual ramping of intensity. Our study also demonstrates how alpha-opic lux can be used to model complex light environments (Lucas et al., 2024, 2014).

Introducing spectral changes associated with civil twilight resulted in significant differences in behaviour, compared to the daylight-intensity only ramp (Fig. 5.5). These two LD cycles had the same light phase condition (Fig. 5.3A) and the ramps were matched for changes in melanopic lux (Fig. 5.4B,5E). The only difference was that the ratio of alpha-opic lux changed dynamically across the twilight ramp (Fig. 5.5D), but remained constant in the daylight intensity-only ramp. Increased locomotor activity was observed at dusk under the twilight ramp compared to the daylight-intensity ramp, but not at dawn (Fig. 5.5H,I) resulting in an ~0.5hr earlier activity onset (Fig. 5.5J). Similarly, light environment sampling behaviour was elevated under twilight conditions at dusk, resulting in a ~1.5hr earlier quantification of the onset of light environment sampling behaviour (Fig. 5.5N). Whilst there was no significant effect of condition at dusk (Fig. 5.5L), there was a significant condition x time interaction at dusk (Fig. 5.5L) which did not occur at dawn (Fig. 5.5M). These data suggest two things, which will be discussed in turn: that the colour of light has a significant effect on behaviour, which could occur via the modulation of the circadian system or through acute changes; and secondly, that these changes in spectrum seem more relevant at dusk than dawn in mice.

Research has shown that a subset of mouse SCN neurons exhibit opponent responses to selective stimulation of S-cones and M-cones, with the majority demonstrating blueON:yellowOFF responses, enabling colour detection (Walmsley et al., 2015). Furthermore, introducing naturalistic diurnal variation in colour resulted in differences in circadian entrainment compared to irradiance only signals; as quantified by body temperature. Our data extends our understanding of the influence of colour on behaviour to locomotor activity and light environment sampling; although surprisingly we see an opposite effect on circadian phase – with colour changes at twilight delaying peak body temperature (Walmsley et al., 2015) but advancing activity and light sampling onset in our study. The effect of spectral cues at twilight on body temperature rhythms was abolished in mice lacking cones (Walmsley et al., 2015), indicating a role for cones in relaying colour information to the SCN; an idea developed by Mouland (et al., 2019). Traditionally, establishing a role for cones in photoentrainment has been difficult, with evidence suggesting that rods and melanopsin provide the major inputs and cones are not required for photoentrainment (Brown, 2016; Freedman et al., 1999; Lall et al., 2010). However, these data were collected under square 12:12hr LD cycles of white light. This demonstrates how using simplified, artificial light environments marginalises the normal role of cones in photoentrainment.

Although it is known that a subset of SCN neurons are sensitive to colour (Walmsley et al., 2015), it is not clear how this information reaches the SCN. Due to the principle of univariance discussed previously, spectral opponency is required to detect colour (Jacobs, 2014; Svaetichin and MacNichol., 1958). Although there is evidence for limited rod-cone opponency in mice, which can explain colour vision in the upper visual field despite the strong M-cone:S-cone dorsal:ventral retinal gradient (Joesch and Meister, 2016; Mouland et al., 2023; Qiu et al., 2021; Szatko et al., 2020); the majority of colour information in mammals originates from S-cone:M-cone opponency (Feord et al., 2023; Puller and Haverkamp, 2011). ipRGCs, specifically of the M1 subclass, are the primary conduit of both intrinsic and extrinsic signals to the SCN, via the RHT (Beier et al., 2021; Hattar et al., 2002). Therefore, M1 neurons were the obvious candidate for transmitting colour information from the retina to the SCN. However, although colour opponency has been detected in primate ipRGCs (Dacey et al., 2005), M1 cells do not appear to exhibit cone-mediated colour opponent responses (Mouland et al., 2023; Weng et al., 2013). Conversely, although M5 rodent cells have shown to receive cone opponent signals (Stabio et al., 2018), these are not thought to project to the SCN. Therefore, it remains an open question as to how the SCN receives colour input. It is possible that separate inhibitory (perhaps recently identified GABAergic ipRGCs projecting from M-cone dominated areas of the retina (Sonoda et al., 2020)) and excitatory ipRGCs (perhaps glutamatergic ipRGCs projecting from S-cone dominated areas of the retina) could provide convergent input (Chang et al., 2013; Feord et al., 2023; Mouland et al., 2023).

It is important to consider why circadian sensitivity to colour would be an evolutionary advantageous strategy. Mouland et al (2019) demonstrates that the mouse circadian system is less responsive to blue light than yellow light of equivalent brightness; suggesting that the short-wavelength enrichment of light in late twilight suppresses circadian responses to light. This differential sensitivity could allow for more accurate tracking of twilight and therefore more precise entrainment, by separating the early and late stages of twilight more clearly. Early twilight appears more yellow and is also brighter, resulting in a stronger circadian response, whilst later stages of twilight appear more blue and are dimmer, resulting in even weaker circadian responses. The constriction of the mouse pupil in response to S-cone activation would further exacerbate this difference (Allen et al., 2011). In addition, colour cues may provide a more robust signal for entrainment when stochastic variations in light levels (e.g. from cloud cover, or movement in and out of shade) make absolute irradiance a less reliable signal of time of day (Mouland et al., 2019; Woelders et al., 2018). Tracking twilight using colour may therefore not only help improve the accuracy of time of day detection, but also of time of year – since this is based on the detection of photoperiod (Woelders et al., 2018).

Although circadian sensitivity to colour has been demonstrated (Mouland et al., 2019; Walmsley et al., 2015) it is necessary to question whether the effects of colour on behaviour observed in our data originate from the modulation of the circadian system or from acute effects of light. It is well established that bright light directly suppresses activity in rodents (negative masking; Mrosovsky, 1999), with melanopsin being implicated as the major regulator of this behaviour (Mrosovsky and Hattar, 2003; Pilorz et al., 2016; Thompson et al., 2008) in addition to its involvement in light aversion (Matynia et al., 2012). However, the relative role of S-cone and M-cones, and therefore the role of colour in acute responses to light has only been investigated more recently, with Tamayo (et al., 2023) demonstrating that selective activation of S-cone irradiance (similar to that experienced at twilight) results in increased activity and light-seeking behaviour in mice. This phenomenon was found to be spectrally-opponent, with longer-wavelength cones resulting in the opposite effect (Tamayo et al., 2023). This aligns with the increased light environment sampling behaviour (Fig. 5.5L,N) and earlier activity onset (Fig. 5.5J) at dusk observed under blue-enriched twilight ramps in our data. Interestingly, the clear increase in locomotor activity under the twilight ramp occurs ~40mins into the dusk ramp (Fig. 5.5H), coinciding with the point at which the ratio of S-cone opic lux increases most steeply (Fig. 5.5D). At this time point, log quanta available to S-cones is 12.8 and to M-cones is 13.6 (supplementary file 12) – both within the ~10 to 15 log quanta sensitivity range of cones (Peirson et al., 2018). It would be interesting to repeat the experiment with an S-cone KO mouse strain, to examine if this response is abolished.

However, if the differences are solely driven by acute responses to short-wavelength light, we would expect to see increased activity under the daylight intensity-only ramp compared to the white ramp, but no such difference is observed (Fig. 5.4D,E). This suggests that the change in colour across the twilight ramp must also provide an important cue, rather than arising solely from elevated S-cone activation. Further experiments to separate the acute and circadian effects of light would be informative. For example, entraining wildtype mice to the daylight intensity-only ramp LD cycle, and then introducing twilight spectral changes to the ramp, before a constant dark condition. The ZT from which mice free run under constant dark would enable assessment of whether the behavioural changes under twilight are under acute or circadian control – if acute, mice would free run from activity onset under the daylight intensity-only ramp condition, but if circadian, mice would free run from the timing of activity onset under the twilight ramp.

It is interesting that colour cues appear to influence mouse behaviour more at dusk than dawn (Fig. 5.5H,I,L,M). It suggests that the photosensory task of tracking dawn and dusk differ, and may utilise different relative contributions and sequences of photoreceptors; further complicated by daily variations in photoreceptor function resulting from the retinal clock (Cameron et al., 2008;

Xue et al., 2015). Whilst dusk requires the detection of decreasing light levels against a light-adapted retina (more suited to cones; although nestbox use may reduce light-adaptation), dawn requires detecting low, increasing light levels against a dark adapted retina (more suited to rods). If cones play a comparatively larger role at dusk than dawn, and are also required for colour detection, this could explain why we see greater differences in behaviour at dusk than dawn under natural twilights. The monitoring of transgenic photoreceptor knockout models under these naturalistic twilights would provide further insight (Walmsley et al., 2015). In addition, the differences could be related to the differing sensitivity of the clock at these times – mice have fast clocks (<24hrs) and therefore their PRC shows a large delay at dusk and a small advance at dawn, since a daily phase delay is required to adjust their clock to 24hrs (Brown, 2016). It is possible that organisms with a slow clock (>24hrs) may show more significant differences in behaviour at dawn than dusk under natural twilights.

This idea assumes though that other species utilise colour to track twilight. In theory, this ability might be available to any organism capable of colour detection, and indeed, behavioural and physiological responses to colour are widespread across the phylogenetic tree - from prokaryotes (e.g. *Halobacterium salinarium;* Hildebrand and Schimz, 1986) and single-cell eukaryotes (e.g. the circadian period of the dinoflagellate *Gonyaulax polyedra* lengthens under pulses of red light, and shortens under blue light; Hastings and Sweeney, 1960; Roenneberg and Hastings, 1988); to higher order organisms including many birds, fish and reptiles and mammals. This suggests that the use of colour to modulate physiology and behaviour is evolutionarily conserved (for more detail see Spitschan et al., 2017). Although it is important to note that since photoreceptor sensitivity differs between species, colour changes across twilight will appear more or less extreme, rendering tracking twilight either more or less useful. It is unclear how far these findings may extend to humans. However, the presence of colour opponency in primate ipRGCs (Dacey et al., 2005) and the regulation of the human pupillary light reflex (PLR) (controlled by an S-cone opponent circuit; Spitschan et al., 2014) indicates that colour could have a modulatory effect on human circadian sensitivity. This raises important issues with regard to lighting design, although further research on circadian responses to colour in humans is required.

Overall, this study demonstrates that the spectrum of natural daylight and twilight modulates mouse behaviour; in addition to illustrating how alpha-opic lux can be used to model complex light environments. However, this study only simulated natural light during the light phase. Given that our data has also demonstrated that mice spend the majority of the light phase in a dark nestbox, it raises the interesting question of whether simulating natural light at night (moonlight

and starlight) would also influence mouse behaviour; as has been demonstrated in other organisms (Poehn et al., 2022).

5.6 Supplementary materials

5.6.1 Supplementary figures

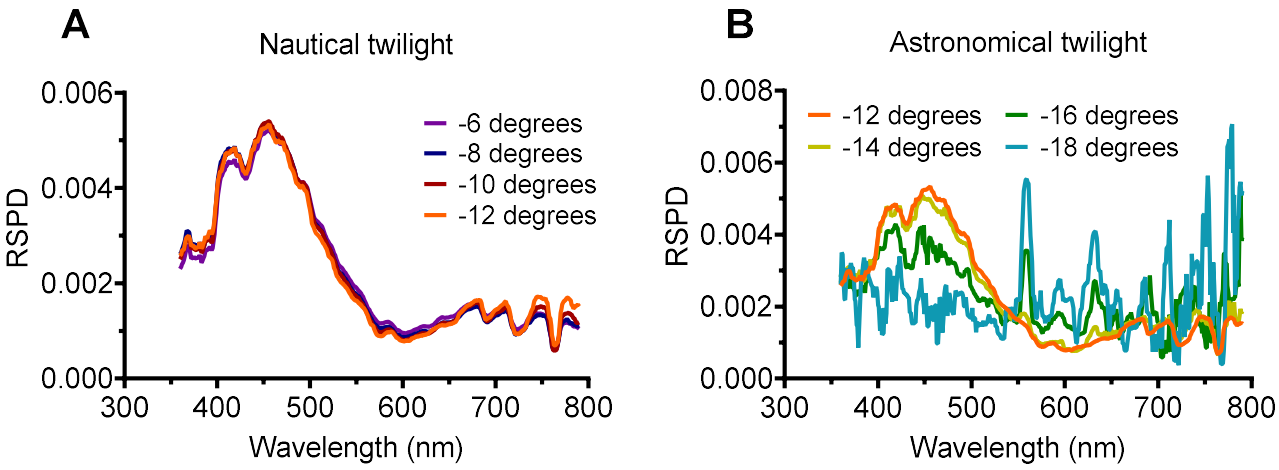

Figure S5.1 - Spectral changes (RSPDs) across nautical **(A)** and astronomical **(B)** twilight in increments of 2 degrees of solar elevation, relative to the horizon (data from Spitschan et al, 2016).

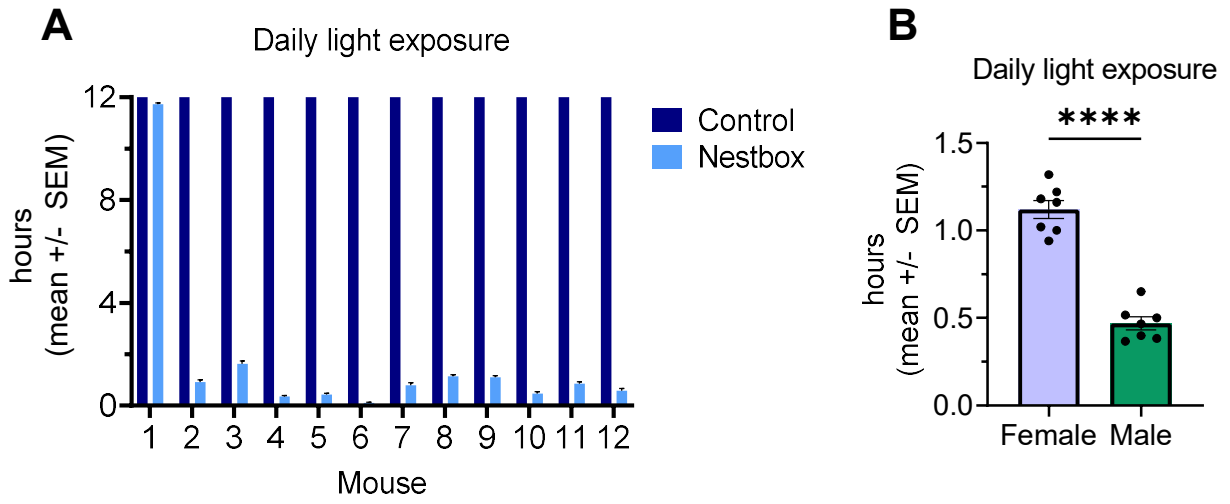

Figure S5.2 - (A) Daily light exposure (hrs) across individuals under the control (dark blue – automatically 12hrs) and nestbox conditions, under a square-wave 12:12hr white LED LD cycle. **(B)** Daily light exposure (hrs) under the nestbox condition (square-wave 12:12hr white LED LD cycle) averaged across individuals, by sex. All data reported as mean +/- SEM. **** $p<0.0001$.

5.6.2 Supplementary tables

	Daylight	Simulated daylight
S-cone	13.1	13.1
Melanopsin	13.8	13.8
Rods	13.8	13.8
M-cone	13.8	13.8

Table S5.1 - log quanta (1dp) available to each photoreceptor under daylight and simulated daylight.

Civil twilight						
Solar elevation (degrees)	-6	-5	-4	-3	-2	-1
S-cone	12.5	12.6	12.7	12.8	12.9	13.0
Melanopsin	13.1	13.3	13.4	13.5	13.6	13.7
Rods	13.1	13.3	13.4	13.6	13.7	13.7
M-cone	13.1	13.2	13.4	13.6	13.7	13.7
Simulated civil twilight						
Solar elevation (degrees)	-6	-5	-4	-3	-2	-1
S-cone	12.5	12.6	12.8	12.8	12.9	13.0
Melanopsin	13.1	13.2	13.4	13.5	13.6	13.7
Rods	13.1	13.2	13.4	13.6	13.6	13.7
M-cone	13.1	13.2	13.4	13.6	13.7	13.7

Table S5.2 - log quanta (1dp) available to each photoreceptor across civil twilight (corrected for changes in melanopic lux occurring across the daylight intensity-only ramp – condition 5) and simulated twilight condition.

5.6.3 Supplementary files

Supplementary files and tools listed below can be accessed here: https://drive.google.com/drive/folders/1uhJY_YRlIMJHJMOe8pZ9o-ytN5BWtN7z?usp=sharing)

1. Multichannel LED RSPDs (violet, blue, green, cool white) in 5nm bins, 300-780nm.
2. Supplementary data figure captions from Spitschan et al, 2016. Caption for Table S5.2 describes the raw data used in this study.
3. Wavelength spacing for raw data in Table S5.2 (Spitschan et al, 2016).
4. Raw daylight and twilight light measurement data (Table S5.2, Spitschan et al, 2016).
5. Selected SPDs taken from Spitschan et al, 2016. Single daylight measurement and civil twilight measurements.
6. Daylight measurement (from Spitschan et al, 2016) corrected for 169.7 melanopic lux.
7. SPD of 169.7 melanopic lux of simulated daylight, produced by multichannel LEDs.
8. Validation daylight measurement - SPD of 169.7 melanopic lux of simulated daylight.
9. Daylight intensity-only ramp (condition 5) working.
10. Validation daylight intensity-only ramp measurements.
11. Twilight ramp (condition 6) working.
12. Validation twilight ramp measurements.

5.6.4 Supplementary tools

1. 'Conversion of raw data to 300-780nm scale.csv' – converts SPD into 5nm bins from 300-780nm.
2. 'Rodent Toolbox v2.csv' – Rodent toolbox, used to calculate alpha-opic lux and log quanta from an SPD.
3. 'Rodent Toolbox v2 METAMERS.csv' – Rodent toolbox amended so that the input is the sum of the multichannel LEDs RSPDs. Used to calculate the power of each LED required to achieve target alpha-opic lux.

Chapter 6. Characterising the light environment of a natural woodland using hyperspectral imaging

Disclaimer

The data collection and analysis pipeline methods in this chapter have been published in the following paper: Shiwen et al., 2021. Hyperspectral characterisation of natural illumination in woodland and forest environments. Proceedings Volume 11815, Novel Optical Systems, Methods, and Applications XXIV. DOI: 10.1117/12.2595301.

Shiwen Li and Laura Steel are co-first authors of Shiwen et al., 2021. Project conceptualisation was led by Manuel Spitschan, Hannah Smithson and Stuart Peirson. Data collection was performed by Laura Steel and Shiwen Li. The hyperspectral lightprobe analysis pipeline was created by Takuma Morimoto. This pipeline was run by Laura Steel, with assistance from Takuma Morimoto.

Further spectral analysis of the hyperspectral lightprobes presented in this chapter was performed by Laura Steel, and has not been published.

6.1 Abstract

The natural light environment is complex and dynamic; varying in intensity and spectrum across space, direction and time. Here we present a hyperspectral imaging system and post-processing pipeline to characterise a light environment in a highly spectrally, spatially and directionally resolved way. Further analysis of the resulting hyperspectral lightprobes demonstrate that the spectrum of light in a natural woodland changes across the year, and is dependent upon transmission and reflection of light by vegetation. In addition, there is considerable directional variation in spectrum within a scene. Clustering of the hyperspectral lightprobes into key spectral components suggests that changes in the extent of vegetation are primarily driving this seasonal and directional spectral variation. The relative alpha-opic lux produced by these light environments are also quantified and discussed in relation to non-image forming (NIF) responses to light in humans, since the relevance of directional and seasonal variation in light on circadian behaviour is not well understood.

6.2 Introduction

Light is a significant driver of many non-image forming (NIF) visual functions in mammals (Peirson et al., 2018). This includes circadian photoentrainment (Hattar et al., 2003), sleep (Lupi et al., 2008), melatonin suppression (Lucas et al., 1999), the pupillary light reflex (Lucas et al., 2001), and cognition and mood (Legates et al., 2012). Therefore, characterising the properties of natural light environments is of considerable importance (Morimoto, 2022). The spectrum of daylight has been well characterised – initially by Judd et al (1964) in which a set of 622 daylight spectral power distributions were analysed, with the majority of variance shown to be explained by a linear combination of three functions. This work was incorporated into the CIE standard illuminant D65 (CIE, 2022).

However, the light environment experienced by an organism is far more complex than the D65 SPD. At the organismal level, lens transmission (where relevant) and photoreceptor complement provide physiological determinants on the wavelength and intensity of light detected. In addition, as discussed in Chapters 3 and 5, an organism's behaviour can directly influence the timing of light exposure, and therefore the intensity and spectrum. At a broader level, the rotation of the earth on its axis results in changes in the intensity and spectrum of illumination across the 24hr period, whilst atmospheric absorption and scattering result in short-wavelength enrichment of light at twilight (Hulburt, 1953; Spitschan et al., 2016; Walmsley et al., 2015; discussed in Chapter 5). In contrast, starlight and moonlight is long-wavelength enriched relative to daylight (Lawrence et al., 2003; Palmer and Johnsen, 2015). Furthermore, light can then be modified by the differential absorbance, transmission and reflectance of materials; since most materials do not exhibit Lambertian properties (reflecting light equally in all directions) (Fontana, 2023; Morimoto et al., 2019; Shiwen et al., 2021; Webler et al., 2019). Absorbance, transmission and reflectance can all vary across space, direction and time - generating further complexity (Webster et al., 2007); which is the focus of this chapter. All these features alter the type and pattern of light perceived by an organism, generating what has been referred to as a unique "spectral diet" (Webler et al., 2019). Since the original measurements of daylight which D65 was based upon were taken in open environments e.g. roof tops (Henderson and Hodgkiss, 1963; Judd et al., 1964), they have not incorporated these additional complexities. As a result, the CIE standard illuminant D65 model does not fully reflect the natural light environment. For example, Spitschan et al (2016) demonstrated the inability of the model to describe spectral changes at twilight.

In order to fully characterise the complex light environment that organisms experience, the spectral, spatial, directional and temporal dimensions of light should be considered (Shiwen et al.,

2021). Whilst many natural light environment datasets have been collected, they often focus on a single dimension of this complexity. For example, many use conventional multispectral cameras, which may have good spatial resolution (defined by pixel resolution), but bin light into three channels – red, green and blue ('RGB') corresponding to human colour vision (Fig. 6.1B) (Nilsson and Smolka, 2021). This makes recovering the full spectra from the data difficult, since different spectral environments may result in similar camera responses (Shiwen et al., 2021). In contrast, hyperspectral cameras bin light into many wavelength channels (Fig. 6.1C), generating flexibility to study the physiological responses of animals with different photoreceptor complements (Shiwen et al., 2021). Meanwhile, other datasets have used hyperspectral techniques, but only at one time point and therefore lack temporal variation (Juola et al., 2022; Nascimento et al., 2016). Finally, many light environments have been characterised using spectrophotometers (Palmer and Johnsen, 2015; Spitschan et al., 2016). Whilst still valuable, spectrophotometers average incoming light to a single point from a wide range of angles and therefore do not provide spatial resolution (Fig. 6.1A) (Morimoto, 2022). Thus, combining multiple features of complexity is challenging.

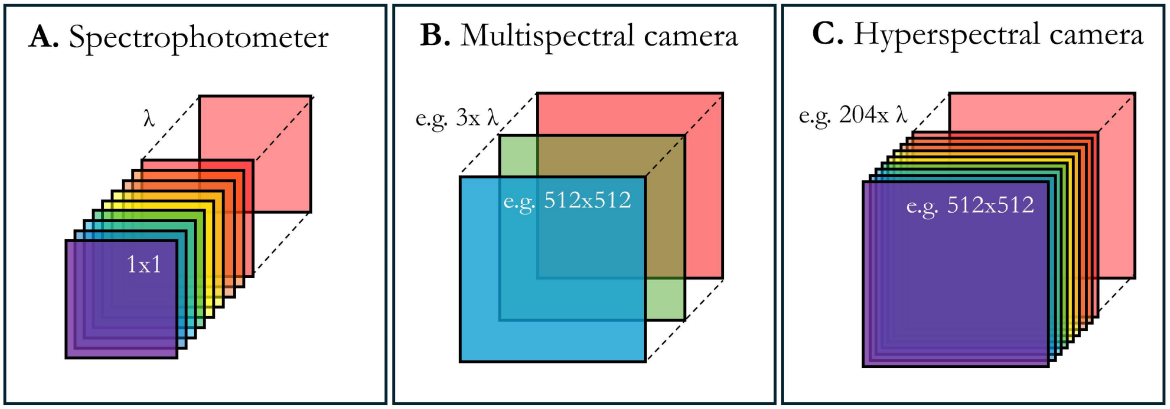

Figure 6.1 – Schematic to compare the spectral and spatial resolution of spectrophotometers **(A)**, multispectral cameras (in this example, an RGB camera) **(B)**, and hyperspectral cameras **(C)**. Dimensions on the front square refer to pixel resolution. Dimensions on the side refer to the number of wavelength channels (λ) – defining spectral resolution.

Here we present a portable method for characterising a natural light environment in a spectrally, spatially, directionally and temporally resolved way, by using a hyperspectral camera to image a chrome sphere (Shiwen et al., 2021). This extends the method developed in Morimoto (et al., 2019) to the complexities of a natural environment. Spectral and spatial resolution is provided by a hyperspectral camera, which samples light from 400-1000nm across 204 spectral channels at a 512 x 512 pixel resolution. Directional resolution is achieved by imaging a mirrored chrome sphere which reflects light equally in all directions, in order to capture variation in light arriving from

different angles. This method was validated in the natural environment of Wytham Woods, Oxfordshire and data was collected across a year to capture temporal variation, as well as across two different locations. Both locations were part of a separate research project investigating the impacts of the fungal pathogen *Hymenoscyphyus fraxineus* on European Ash (*Fraxinus excelsior*) mortality, known as ash dieback (Dahlsjö et al., 2024). Each location represented woodland at different stages of ash dieback progression, and further details on the site differences will be provided in the methods section.

Hyperspectral lightprobes can be generated from raw hyperspectral images. These are two-dimensional hyperspectral illumination maps, in which every pixel contains information about the incident light reaching a single point from a particular direction (Morimoto, 2022). An SPD can therefore be extracted for each pixel in the hyperspectral lightprobe. Shiwen et al (2021) presented an analysis pipeline to generate hyperspectral lightprobes. This method was based on Morimoto et al (2019), which itself built on the method developed for RGB images by Debevec (2005). In this chapter, the data and analysis pipeline reported in Shiwen et al (2021) is used to generate hyperspectral lightprobes. Further analysis is then performed on the hyperspectral lightprobes to characterise how the spectrum and intensity of light, and resulting alpha-opic values (Lucas et al., 2024; Schlangen and Price, 2021) change within a scene, between locations and across seasons. This follows a similar concept to the 'spectral diet' but for a natural environment (Webler et al., 2019). As with the majority of hyperspectral cameras, the system used in this study only samples light down to 400nm. Therefore, this chapter focuses on human responses to light, as the lack of short-wavelength light sampled means it is impossible to make inferences to mice, which possess a UV-sensitive cone.

It is known that natural light environments and schedules result in differences in human behaviour compared to those of electric light (Stothard et al., 2017). Whilst a large portion of this effect is likely to be driven by differences in relative intensities between night and day (Brown et al., 2022), research in rodents has also demonstrated differences in circadian entrainment under natural spectra (De Oliveira et al., 2019; Walmsley et al., 2015). Similarly, Chapter 5 reports differences in circadian entrainment at dusk when a twilight ramp incorporates changes in spectrum in addition to intensity. Therefore, the scale of spectral changes at civil twilight simulated in Chapter 5 can be used as a coarse comparison to assess whether variation in the natural light environment arising from reflectance is likely to be biologically relevant to circadian entrainment, and other non-image forming visual functions in mammals. This relevance could either be as a useful cue or as spectral noise that the circadian and visual system has to cope with. The human circadian research community has emphasised the need to understand which features of the natural light environment

are important for optimising physiology, and specifically mention the role of spectral composition (Münch et al., 2020; Rea et al., 2002; van Bommel and van den Beld, 2004). Filling these knowledge gaps may enable healthier built environments with regard to non-image forming effects of light (Khademagha et al., 2016).

6.3 Materials and Methods

6.3.1 Data collection (Shiwen et al., 2021)

The hyperspectral imaging system (Fig. 6.2A) was comprised of a SpecimIQ push-broom broom hyperspectral imaging spectrometer (Specim; Oulu, Finland, 512 × 512 px resolution, 400-1000 nm, 204 spectral channels; 31 × 31 ° FOV) used to image a 76.2 mm diameter chrome sphere, which reflects light equally in all directions and has an etched equator (AISI 52100 chrome steel ball, Simply Bearings Ltd, Lancashire, UK). The hyperspectral camera was placed at one end of a bespoke rotating arm (800 mm in length), and imaged the chrome sphere, positioned in the centre of the arm on a stationary stand (50 mm in height) (Fig. 6.2A). The rotating arm increased the speed of data acquisition, to minimise changes in the light environment across the data acquisition period. The chrome sphere was imaged against a white card to facilitate sphere extraction in post-processing analysis, and weights were positioned to counterbalance the camera. The system was mounted on a tripod (Manfrotto, UK) (Fig. 6.2A). Since each acquisition only captured light reflected from one side of the sphere, it was necessary to image the sphere from 6 equally spaced angles. This also allowed us to fill in pixels lost from the reflection of the imaging system in the sphere, via the stitching together of these images in post-processing (Fig. S6.1). Furthermore, due to the high dynamic range of the natural light environment, two rounds of data acquisition with different integration times were required to prioritise the sky and ground pixels respectively. Therefore, each data acquisition comprised of 12 images.

This imaging system was validated in two sites, approximately 100m apart, (named by Wytham Woods as Sites B and C) within the temperate broadleaved woodland of Wytham Woods, Oxfordshire, Britain. The most common tree species in the woodland are sycamore, beech, ash and hazel (Dahlsjö et al., 2024). Both sites were part of a research project investigating the impacts of the fungal pathogen *Hymenoscyphyus fraxineus* on European Ash (*Fraxinus excelsior*) mortality, known as ash dieback. Site B is ash-dominated, whereas Site C has been experimentally manipulated to accelerate ash dieback; resulting in less than 20% ash tree abundance. Therefore Site C represents the woodland a few decades after the ash trees have disappeared and have been

replaced by other species, such as oak and hazel (see Fig.1, Dahlsjö et al., 2024). This results in Site C having a denser canopy than Site B. Both sites were sampled on six separate visits between April and December 2021, between 10am-12pm. This resulted in a total of 144 images (6 angles x 2 integration times x 2 sites x 6 days).

6.3.2 Post-processing pipeline: generating hyperspectral lightprobes (Shiwen et al., 2021)

For each data acquisition (6 angles x 2 integration times x 1 site x 1 day) the 12 images were unwrapped and stitched together in post processing (Fig. S6.1) to generate a full illumination map of the environment, known as a hyperspectral lightprobe. The post processing pipeline built on methods developed in Morimoto et al (2019), and dealt with three main problems which arose due to the complexities of collecting data in the field. Firstly, the loss of pixels due to the reflectance of the imaging system in the sphere, secondly, the integration of the two rounds of data acquisition and thirdly, how to deal with misalignment of the imaging system (Fig. S6.1). The post-processing pipeline was developed by Takuma Morimoto and further details can be found in Shiwen et al (2021). The pipeline resulted in 12 lightprobes, each measuring ~250 x ~490 pixels, across 204 spectral channels.

6.3.3 Analysis of hyperspectral lightprobes

All analysis was carried out in MATLAB (R2024a). All data visualisation was performed in MATLAB and GraphPad Prism (v. 9.5.0).

6.3.3.1 Extraction of spectra

Lightprobes were imported into MATLAB using the *hypercube* function from the MATLAB Hyperspectral Image Processing Toolbox. The SPD of each pixel in radiance ($W/cm^2/sr$) could be directly extracted from the lightprobe, and were subsequently resampled from 400-720nm in 5nm bins. RSPDs were calculated by normalising each value of an SPD to the total sum of the SPD, whilst mean SPDs and RSPDs of lightprobe regions were calculated by averaging across pixels.

6.3.3.2 Calculation of alpha-opic lux

SPDs for each lightprobe pixel or region were in radiance ($W/cm^2/sr$). Due to the geometric complexities of the lightprobes, a radiance to irradiance conversion was not performed. Radiance values were used as an estimate of irradiance and input into the Irradiance Toolbox (Lucas et al., 2013) to calculate alpha-opic lux values for the human photopigments. As such, to prevent misinterpretation of results, only relative alpha-opic lux values were used (expressed as a %).

6.3.3.3 Clustering of key spectral components

To cluster the hyperspectral lightprobes into key spectral components, linear spectral unmixing analysis was used to identify the abundance of different types of material within a hyperspectral scene. Linear spectral unmixing analysis selects a set of 'pure' spectral signatures, known as endmembers, which represent a single material in a scene (Kale et al., 2017). Each remaining pixel in the hyperspectral image can then be modelled using a linear combination of two or more endmember spectrums, and the proportion of each endmember present in the spectra of each pixel is calculated. Abundance mapping can then be used to visualise the relative abundance of materials in an hyperspectral lightprobe, by assigning each pixel to the endmember class which forms the highest fraction of that pixel.

Multiple methods have been developed for extracting endmembers from hyperspectral images, each with their own challenges (Kale et al., 2019; Somers et al., 2011). Pre-developed endmember libraries are often used, but if based on a different type of environment to your hyperspectral image, they are not always appropriate. Therefore, direct selection of endmembers from an image is an accepted methodology (Chen et al., 2021; Plaza et al., 2002; Somers et al., 2011; Tao et al., 2023). In our analysis we followed this latter methodology. To determine the appropriate number of endmembers to select, principle component analysis (PCA) was performed using the *hyperca* function of the MATLAB hyperspectral Image Processing Toolbox (Fig. 6.4A) (Tao et al., 2023). For all lightprobes, PCA demonstrated the occurrence of two key spectral clusters – with PC1 and PC2 cumulatively explaining >96.8% of variance (Fig. 6.4A). Visual assessment of two key pixel types in the lightprobes (sky and vegetation) further supported the selection of two endmember classes. Endmembers were selected directly from the lightprobes using the *roipoly* function in the Image Processing and Computer Vision Toolbox in MATLAB, which selects regions of interest (ROIs) (Fig. 6.4D.2).

Due to differences in weather conditions and season, sky and vegetation pixels differed greatly in colour and brightness between lightprobes. Therefore, sky and vegetation endmembers were selected individually for each lightprobe. Two sky ROIs were selected within each lightprobe (to allow for selection of a blue and grey sky region) and three vegetation ROIs were selected for each lightprobe (to allow for selection of leaves, bark and ground regions). This process was used to generate an endmember library which was used for subsequent spectral unmixing and abundance mapping - performed using the *estimateAbundanceLS* function in the Hyperspectral Image Processing Toolbox in MATLAB, which uses the least-squares method to calculate the proportion of each endmember present in the spectra of each pixel (Fig. 6.4D.3). All pixels assigned to either of the sky endmember classes were grouped together into a sky category, whilst all pixels assigned

to any of the three vegetation endmember classes were grouped together into a vegetation category. The percentage of pixels in the overall sky and vegetation categories were calculated in order to track changes across the seasons (Fig. 6.4B,C). The mean spectra (Fig. 6.4D.4) and alpha-opic lux (Fig. 6.4D.5) of each pixel category (sky and vegetation) could then be extracted.

6.3.3.4 Vertical segmentation of lightprobes

In order to assess the directional spectral variation within each lightprobe (Morimoto et al., 2019), a column of nine 20x20 pixel squares were extracted from each lightprobe, at the same coordinates across lightprobes (Fig. 6.6A). Spectrum was observed to be consistent horizontally within each lightprobe (data not presented), so only vertical segmentation was explored in the final analysis. The SPD, RSPD and alpha-opic lux values of each pixel square were calculated, as above (3.2.1 and 3.2.2). An estimate of overall radiance levels in each pixel square were calculated by summing the radiance values across wavelengths (400-720nm) of the mean SPD for the corresponding pixel square. Since photons of short-wavelengths are more energetic than long-wavelengths, this method may overestimate intensity values of lightprobe regions with a more short-wavelength enriched SPD.

6.4 Results

6.4.1 Development of a portable, hyperspectral imaging method (Fig. 6.2)

Here we validate a new portable method to characterise light environments using off-the-shelf components, including in natural environments where data collection is often more challenging (Fig. 6.2A). Our images are highly spectrally resolved (400-1000nm; 204 spectral channels), spatially resolved (512 x 512 pixel resolution, compared to single summary measurements recorded using spectrophotometers), directionally resolved (due to imaging a chrome sphere, which reflects light equally in all directions and therefore captures light coming from different angles) and temporally resolved (from sampling across time, capturing variation arising from weather and seasons). We present a post-processing pipeline (Fig. S6.1) for the generation of hyperspectral lightprobes (Fig. 6.2B), which extends that of Morimoto et al (2019) by successfully resolving issues arising from data collection in the field – namely, combining ground and sky images and correcting the misalignment of the imaging system. The hyperspectral lightprobes can be further analysed to characterise light environments.

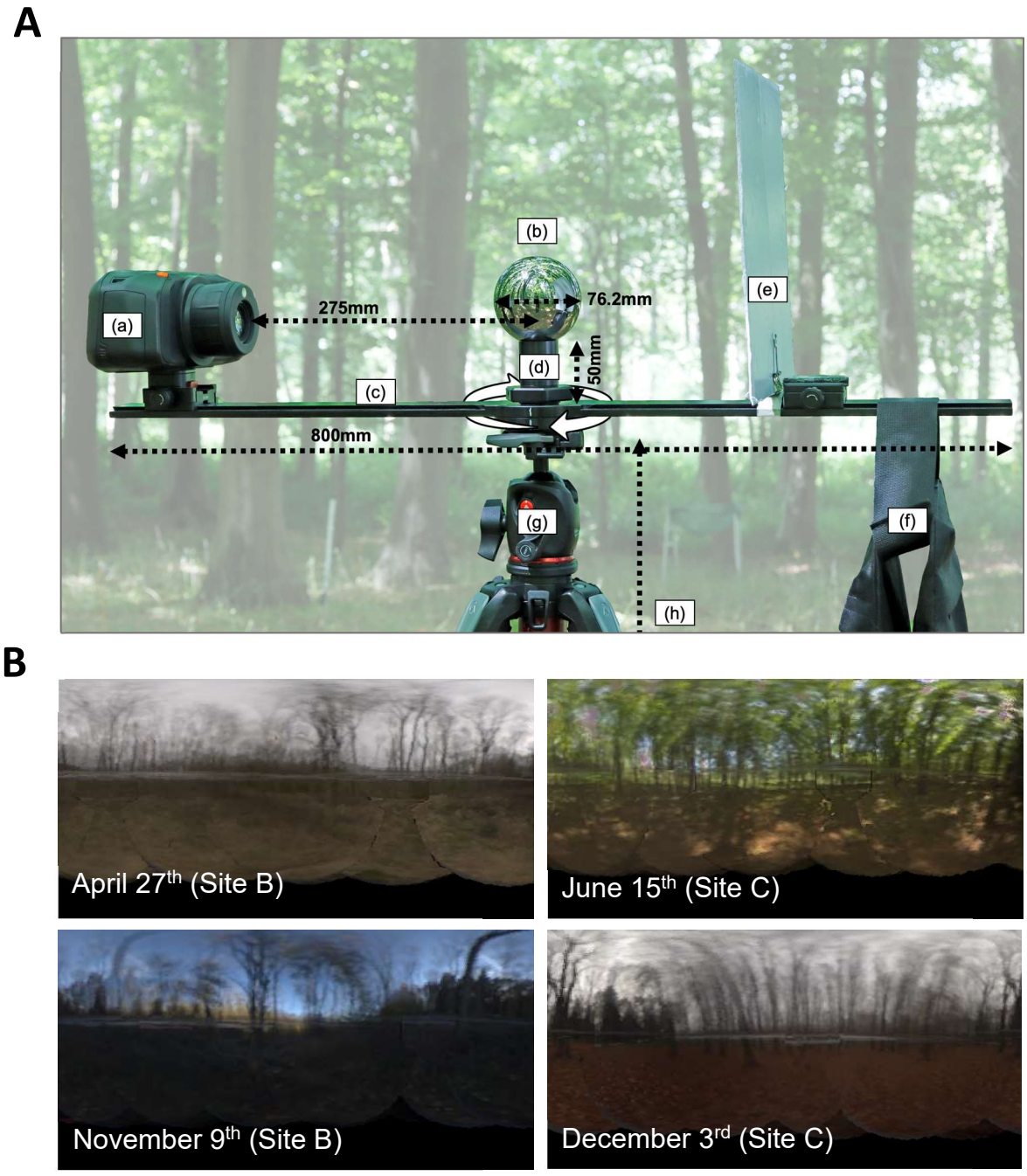

Figure 6.2 - Data collection and generation of hyperspectral lightprobes. **(A)** Bespoke imaging system setup: **(a)** SPECIM IQ hyperspectral camera, **(b)** chrome sphere, **(c)** rotating arm, **(d)** stationary stand, **(e)** white card, **(f)** counterweight, **(g)** tripod, **(h)** distance between ground and the tripod's head, ~1360mm. Distance between **(a)** and **(b)** is measured from the lens to the centre of the chrome sphere. **(B)** RGB representation of a sample of generated hyperspectral lightprobes, across different months and sites (B or C). Panel A and corresponding figure legend taken from Shiwen et al (2021).

6.4.2 The overall spectrum of light in a natural woodland change considerably across seasons, and may be linked to vegetation type and cover. The resulting changes in relative alpha-opic lux values may be biologically relevant for NIF functions (Fig. 6.3).

As shown in both Fig. 6.3A (Site B) and Fig. 6.3B (Site C), the shape of the RSPDs from the overall lightprobe change strikingly across the seasons in a natural woodland. Whilst the measurements in both sites for April and December, as well as for May in Site B are comparable to D65, the spectra collected in Summer and Autumn months differ clearly to the CIE standard. These differences are quantified via a Spearman's rank correlation matrix Fig. 6.2C and 2D – for example, in Site C the RSPD for June has a -0.24 correlation with D65 and November has a 0.00 correlation, emphasising that D65 is unlikely to effectively model natural woodland spectra in Summer and Autumn months.

The nature of these differences vary with location. In Site B, the RSPDs become relatively short-wavelength (<450nm) enriched in October and November. This could be due to the larger canopy gaps present in Site B than C, and perhaps low foliage cover in Autumn and Winter months, resulting in greater transmittance of short-wavelength sunlight (Hovi and Rautiainen, 2020). In contrast, from May to November in Site C, the RSPDs show a peak at ~550nm and ~720nm, whilst this peak is only present in June in Site B. Evidence from the literature suggests that these peaks are characteristic of vegetation (Noda et al., 2021; Ollinger, 2011). The reflectance peak in the near-infrared region is caused by a lack of any strongly absorbing compounds in plants, resulting in the reflectance or transmission of ~90% of light in this region (Jacquemoud and Ustin, 2019; Ustin and Jacquemoud, 2020). Similarly, photosynthetic photopigments in plant tissues (chlorophyll *a,* chlorophyll *b* and *β*-carotene) all have low absorption of light across 500-600nm, resulting in the distinctive reflectance peak at 550nm (Ustin and Jacquemoud, 2020). This can be demonstrated in Fig. 6.4, in which the SPD for D65 (Fig. 6.4A) has been corrected for the absorption of light by the three main photosynthetic photopigments (Fig. 6.4B), to produce a characteristic peak in the 500-600nm range (Fig. 6.4C). In theory, the SPD of any light environment could be corrected by the absorption coefficients of photosynthetic photopigments, to explore the influence of vegetation on the spectrum of light.

The timing of leaf-fall by different tree species may therefore explain the differences in spectrum observed between Site B and C. Site B is ash dominated, a species which can start dropping leaves as early as July, with all leaves having fallen by October. In contrast, Site C is dominated by oak and hazel – which have leaves that usually remain entirely green until October and even retain some leaves until Spring (Otto and Nilsson, 1981). Therefore it is likely that differences in

spectrum between sites may arise due to variation in vegetation type and cover – this hypothesis will be explored in Fig. 6.5.

Whether these spectral changes are likely to be biologically relevant for NIF functions in humans is explored in Fig. 6.3E and 6.3F. Fig. 6.3E shows the percentage of activation of each human photopigment, expressed in relative alpha-opic lux, produced by the entire lightprobe for each site across the seasons. The changes can be compared to those in Fig. 6.3F, which show the equivalent changes across civil twilight for human photopigments, which are known to produce differences in locomotor activity and light sampling behaviour in mice (Chapter 5). Whilst the changes in relative alpha-opic lux are more modest in Site C, the difference between the relative alpha-opic lux values calculated from Site B in October and April are of the same scale as the differences between daylight (using data measured at 24 degrees of solar elevation) and -5 degrees of solar elevation in the civil twilight data (Fig. 6.3F). In both comparisons, S-cone activation increases ~6%, whilst L-cone activation drops by approximately the same amount (Fig. 6.3E,F). This suggests that changes in alpha-opic lux observed across seasons may be relevant for NIF functions in mammals. In the natural woodland reflectance data (Fig. 6.3E) when the alpha-opic lux ratio does deviates from that of D65, the direction of change differs between sites. In Site B there is greater relative activation of S-cones and melanopsin, whilst in Site C there is greater relative activation of M and L-cones. As discussed, this can be explained by the presence of the 550nm and 720nm peak in Site C RSPDs (Fig. 6.3B), compared to the depletion of long-wavelength light in Site B (Fig. 6.3A). We predict that these site differences arise from variation in the extent and timing of vegetation cover between sites, and will be explored further in Fig. 6.5.

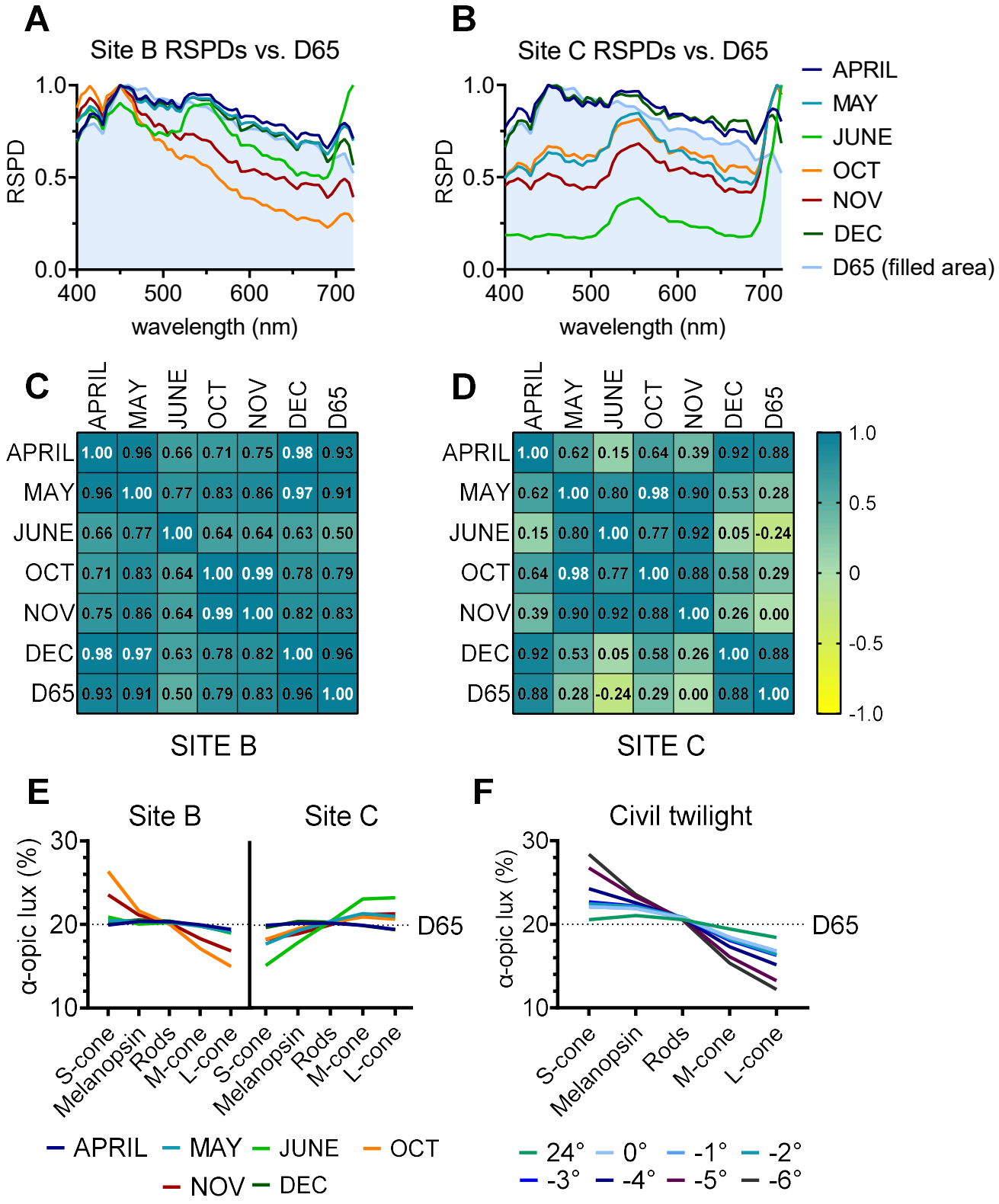

Figure 6.3 - Spectral characteristics of entire lightprobes across seasons and sites, and compared to D65. **(A-B)** Relative spectral power distribution (RSPD) of entire lightprobes collected in Site B **(A)** and Site C **(B)** and D65 (filled area), from 400-720nm in 5nm bins. **(C-D)** Spearman's rank correlation matrix for RSPDs of entire lightprobes and D65 in Site B **(C)** and C **(D),** from 400-720nm in 5nm bins. **(E-G)** Relative alpha-opic lux (%) for human photoreceptors across entire lightprobes collected in Site B **(E)** and Site C **(F)**, and across civil twilight (0 to -6 degrees of solar elevation; 24 degrees represents daylight. Calculated using data from Spitschan et al., 2016) **(G).**

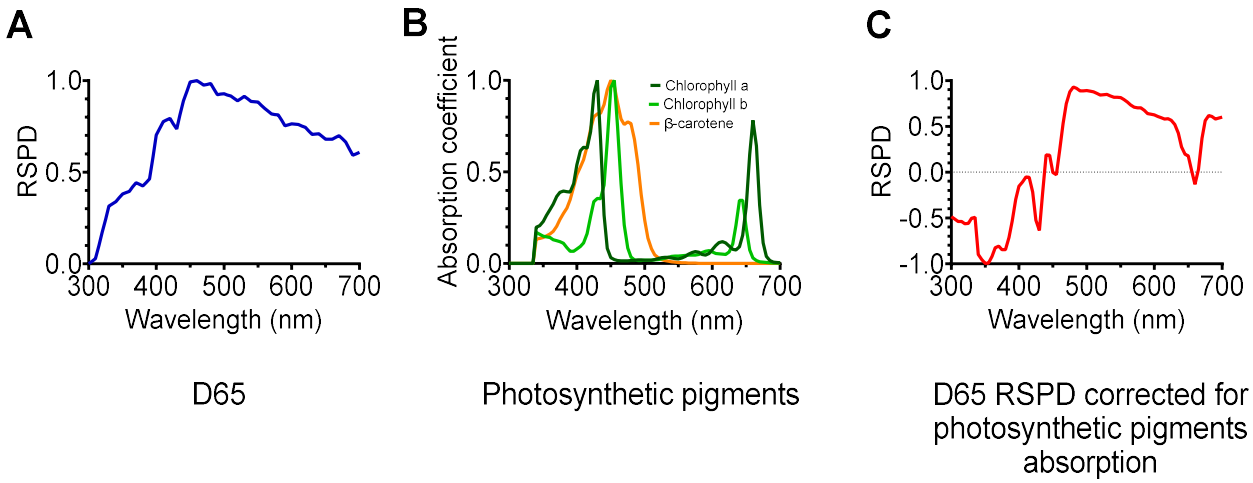

Figure 6.4 – (A) RSPD of CIE D65 (CIE, 2022)**. (B)** Absorption of common photosynthetic pigments (chlorophyll a (dark green), chlorophyll b (light green), β-carotene (orange)). **(C)** D65 RSPD corrected for the absorption of light by the photosynthetic pigments in **(B).** Data for (B) from Serge Helfrich (File:Chlorophyll Absorption Spectrum.svg - Wikimedia Commons).

6.4.3 PCA and spectral unmixing analysis identifies two key spectral components of the natural woodland light environment (Fig. 6.5).

To explore the features underlying the observed changes in spectra across sites and seasons presented in Fig. 6.3, spectral unmixing analysis was performed. This identifies the abundance of different materials in each scene, as defined by their spectral signature. PCA identified two key spectral components in each lightprobe, with PC1 and PC2 explaining a cumulative variance of >96.8% in all lightprobes (Fig. 6.5A). PC3 explained a mean variance of 0.6% across lightprobes, so is likely to reflect noise (Fig. 6.5A). From a visual assessment, abundance mapping (Fig. 6.5D,3) successfully allocated pixels to appropriate endmember classes, suggesting effective endmember selection (Fig. 6.5D,2). Our results clearly demonstrate that the natural woodland light environment clusters into two key components – identified to be consistent with spectra reported in the literature for sky (CIE, 2022; Judd et al., 1964; Spitschan et al., 2016) and vegetation (Noda et al., 2021; Ollinger, 2011).

Fig. 6.5B and Fig. 6.5C report the proportion of sky and vegetation pixels across seasons, for Site B and C, respectively. Differences in the proportion of vegetation pixels between sites and across seasons, supports our hypothesis that both the extent and type of vegetation cover is important for determining the overall spectrum of light. Firstly, as expected for a deciduous woodland, vegetation cover peaks in June in both sites. However, peak cover is over 10% higher in Site C (97.8%) than Site B (86.9%). This supports our observations that the canopy in Site C is denser. Secondly, vegetation cover remains high in Site C across Summer and Autumn – still being at

98.6% in October, before falling to 76.3% in December. In contrast, vegetation cover in October in Site B has already fallen to 73.4% and remains similar in December (70.1%). This supports our hypothesis that the timing of leaf fall in tree species most abundant in Sites B (ash) and C (oak and hazel) is an important driver of seasonal patterns in spectrum – since leaf fall in ash occurs earlier than oak and hazel, which often retain some leaves throughout winter. The extent of vegetation cover also has a direct effect on the relative activation of photoreceptors (Fig.6.5D.5). Interestingly, both sky and vegetation pixels generate the same relative activation of rods, but sky pixels show reduced L-cone activation, whilst vegetation generates low S-cone activation and high M-cone and L-cone activation, due to the characteristic reflectance peaks at 550nm and 720nm.

Although it is clear that vegetation cover has a significant effect on the light environment, it may also be relevant to consider the seasonal changes in the spectrum of sky pixels. Due to the earth having an elliptical, rather than circular orbit around the sun, the sun appears higher in the sky during the Summer than Winter. As a result, sunlight has a longer path through the atmosphere in Winter than in Summer. In a similar way to twilight, sunlight in Winter can therefore be more short-wavelength enriched than in Summer, due to an increase in the Chappius effect (the stronger absorption of longer wavelength light by ozone). However, this effect will be more extreme at high latitudes (Fosbury and Jeffery, 2022; Hazlerigg et al., 2023) and may not be relevant at lower latitudes such as ours (Woelders et al., 2018).

To investigate this we explored seasonal changes in the RSPD of sky pixel endmembers (Fig. S6.2). Sky pixels from June and November show greater short-wavelength enrichment than the remaining months, in both sites (Fig. S6.2). However, differences in cloud cover between sampling days make interpretation challenging. When the spectra were correlated with the weather conditions recorded for each sampling day (data not presented), June and November were the only days with sunny and clear skies, rather than overcast. Clouds are thought to reflect light equally in all directions (Mie scattering). This is because the diameter of water droplets in clouds are approximately the same size or larger than the wavelength of light (Lockwood, 2016). Therefore on clear days, Mie scattering is reduced and instead Rayleigh scattering is more prevalent. Rayleigh scattering is when short-wavelength light is scattered more strongly than long-wavelength light, by atmospheric particles much smaller than the wavelength of light (Lockwood, 2016). As such, clear and sunny conditions such as those on the June and November data collection days, will have a greater proportion of short-wavelength light. As such, due to differences in weather conditions between sampling days, and therefore types of scattering, it is hard to assess the contribution of seasonal changes in sun position on the spectrum of sky pixels. Further data collection across clear and overcast days each month would be required to investigate this.

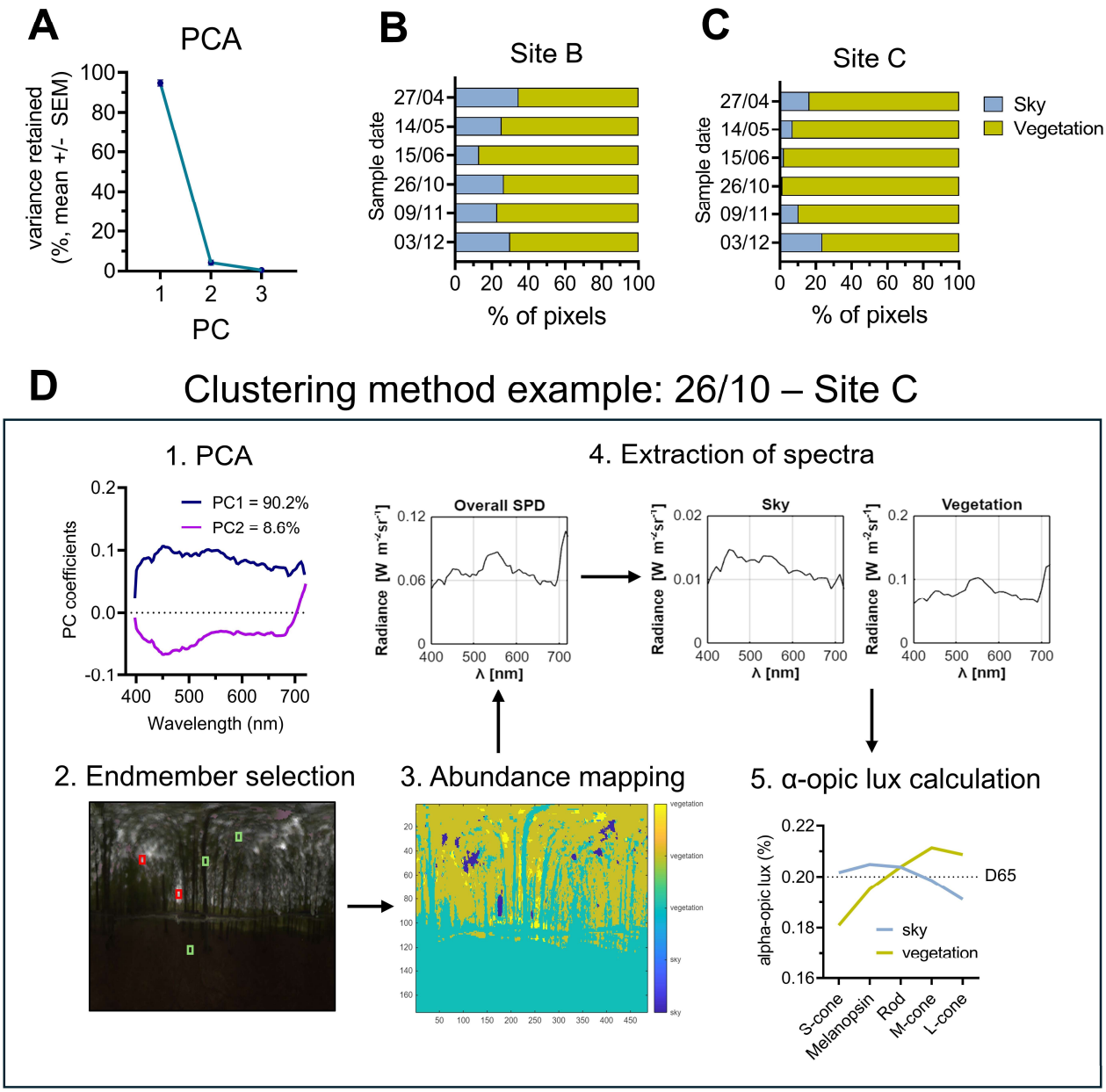

Figure 6.5 - Key spectral components of lightprobes, across seasons and sites. **(A)** PCA results: variance retained by PC1-3, reported as mean +/- SEM across lightprobes. In all lightprobes, PC1+2 explained >96% of variance. **(B-C)** Clustering analysis results – % of pixels clustered into 'sky' or 'vegetation' in each lightprobe, across seasons in site B **(B)** and site C **(C). (D)** Example of lightprobe clustering method (collected on 26/10 in Site C) using PCA and spectral unmixing. **1.** PC1+2 explain 98.8% of all variance. **2.** Endmember selection (red = sky endmembers; green = vegetation endmembers). **3.** Abundance mapping using endmember library generated by endmember selection (sky pixels in navy; vegetation pixels in teal, orange and yellow). All pixels in either of the sky groups were combined into a "sky" category, and all pixels in any of the three vegetation groups were combined into a "vegetation" category. **4.** Extraction of mean SPD for overall lightprobe, sky category and vegetation category. **5.** Relative α-opic lux (%) produced by mean sky and vegetation SPD. Ratio produced by D65 marked by dashed line.

6.4.4 Vertical segmentation of lightprobes demonstrates directional variation in spectrum and intensity, with subsequent changes to relative alpha-opic lux (Fig. 6.6).

Vertical segmentation analysis of lightprobes, similar to in Morimoto et al (2019), demonstrates that incident angle has a clear effect on spectrum and intensity. Each rectangle in each column of Fig. 6.6B,C shows the mean RSPD of the corresponding rectangle in the segmented lightprobe presented in Fig. 6.6A, for Site B (Fig. 6.6B) and Site C (Fig. 6.6C). Each rectangle in each column of Fig. 6.6D or 6E then shows the relative alpha-opic lux of the RSPD in the corresponding rectangle presented in Fig. 6.6B or 6C, respectively. Each column in Fig. 6.6B-E show the results for each lightprobe sampled across the seasons, whilst the background colour reflects log radiance levels.

These data visualisations demonstrate a clear directional effect of light, which differs across season and site. Site B shows a fairly consistent vertical pattern across seasons, with more short-wavelength enrichment in the upper hemisphere. A peak at 550nm and 720nm gradually develops across the lower hemisphere, as vegetation cover increases and therefore the rate of secondary reflections increase (Fig. 6.6B). Presumably as a result of these secondary reflections, light intensity decreases from the upper to lower hemisphere by 1 log (or 2 log in November) (Fig. 6.6B). In contrast, Site C shows a spectral signature in the upper hemisphere consistent with leaf cover across May to November (Noda et al., 2021; Ollinger, 2011) (Fig. 6.6C), which matches the later leaf-fall time of oak and hazel present in Site C . Across the lower hemisphere, the peak at 550nm becomes more blunted, producing a spectral signature similar to that of bark (Juola et al., 2022; Otto and Nilsson, 1981) or soil (Ollinger, 2011) reported in the literature (Fig. 6.6C). The upper hemisphere from May to November in Site C has a lower light intensity than Site B, likely as a result of increased vegetation cover during these months – highlighted by the clustering analysis in Fig. 6.5B,C.

These data emphasise that there is large directional variation in intensity and spectrum in natural woodland environments, which will not be captured using summary spectrophotometer measurements. Directional variation in light was previously considered to be less importance to human vision – in particular, for the perception of 3D shapes, due to the 'light-from-above prior'. The light-from-above-prior is an assumption thought to be made by the human visual system that light comes from overhead when extracting information on 3D shapes from shadows. However, research has emphasised that light from above plays a more limited role than previously thought and that secondary reflections in the lower hemisphere are likely to be important to human visual perception of 3D structures (Adams et al., 2004; Morgenstern et al., 2011; Morimoto et al., 2019). Therefore, directional variation is important to characterise for elements of visual perception, as

well as potentially for NIF functions - since they have subsequent effects on patterns of relative alpha-opic lux (Fig. 6.5D,E). Some of the changes in relative alpha-opic lux are subtle (e.g. December Site B, Fig. 6.5D) and therefore unlikely to be of biological relevance. However, others are of a larger scale, such as in June in Site B (Fig. 6.5D) where relative S-cone opic lux changes from ~25% at the top of the lightprobe to ~12% at the bottom of the lightprobe. This change in relative alpha-opic lux is greater than that occurring at civil twilight (Fig. 6.3F), which is known to induce behavioural changes in mice (Chapter 5). Therefore, directional variation in relative photoreceptor activation arising from reflectance may be of biological relevance to NIF functions.

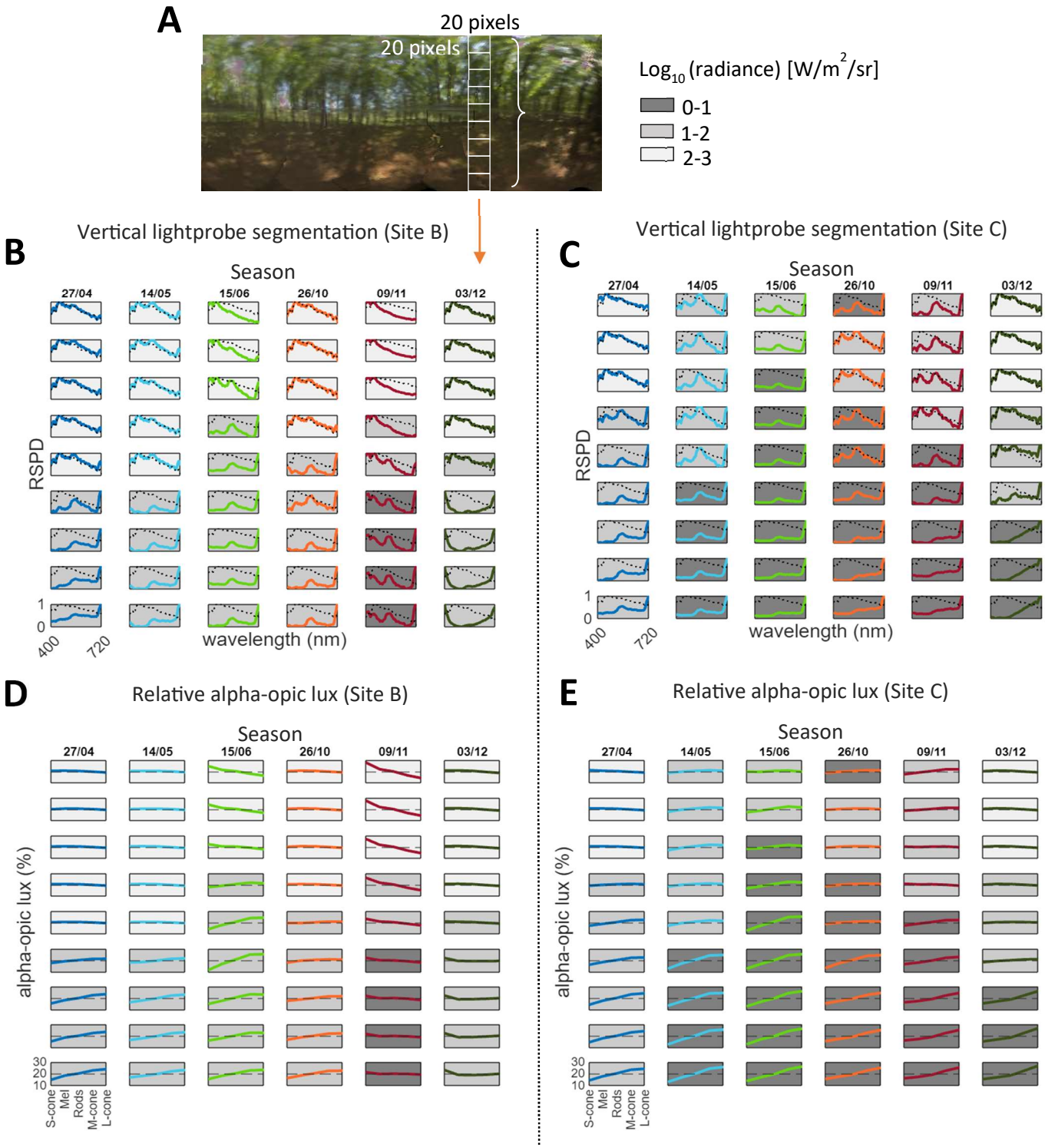

Figure 6.6 - Directional spectral variation of lightprobes, across seasons and sites. **(A)** Schematic of example lightprobe indicating the location of the nine 20x20 pixel grids, from which the mean spectra and alpha-opic lux were extracted in panels. **(B-C)** Mean RSPD (400-720nm) of each pixel grid - each lightprobe forms one column of the panel, and D65 RSPD is marked by the dotted black line. Background colour represents the log radiance level of the pixel grid. Reported for Site B **(B)** and Site C **(C). (D-E)** Alpha-opic lux, expressed as a %, for each pixel grid. Each lightprobe forms one column of the panel, and D65 RSPD is marked by the dotted black line. Background colour represents the log radiance level of the pixel grid. Reported for Site B **(D)** and Site C **(E).**

6.5 Discussion

Here we present a method to characterise a complex natural light environment, along spectral, spatial, directional and temporal axes. Further analysis is performed to assess how spectrum in a natural woodland environment changes within a scene, between locations and across seasons, and whether these changes are likely to be relevant for NIF functions in humans. Since the evolution of sensory systems are driven in part by the environment in which an organism lives, it is expected that they will be adapted to the statistical properties of the signals to which they are exposed (Baden et al., 2020; Geisler, 2008; Simoncelli and Olshausen, 2001). Therefore, whilst more casual inferences about the tasks required of a sensory system can be useful for informing hypotheses, determining statistical regularities and patterns in natural environments can result in novel questions which are more directly related to the environment's key components (Geisler, 2008; Webler et al., 2019). Here we will discuss questions arising from the seasonal and directional changes observed in our dataset for NIF functions, following a consideration of the limitations of our data collection and analysis methods.

Methodological limitations

As with the majority of hyperspectral cameras, our imaging system only sampled down to 400nm. Therefore it failed to detect UV light, which is of great relevance to mouse behaviour (Tamayo et al., 2023; Van Oosterhout et al., 2012) due to their UV-sensitive cone (λmax ~360nm) (Jacobs et al., 1991). Therefore, inferences were only made to humans, which have a much lower sensitivity to light below 400nm. It would be interesting to repeat data collection with a hyperspectral camera sensitive to wavelengths of light below 400nm, such as that built by Nevala and Baden (2019) or the Resonon Pika UV hyperspectral camera (Stern, 2021). This would enable the calculation of absolute alpha-opic lux values for mice, to extend the field's understanding beyond visual processing (Qiu et al., 2021) to NIF functions of light in natural environments. In addition, although sampling time was reduced by the bespoke rotating arm, sampling of one site could still take up to 90 mins. This was sufficient time for changes in illumination resulting from cloud cover to occur (Shiwen et al., 2021).

Methodological limitations extended to the analysis of the hyperspectral lightprobes. Spectral unmixing presented in Fig. 6.5 is a form of dimensionality reduction for hyperspectral data, which is possible due to spectral redundancy generated by the many narrow spectral sampling bands (Signoroni et al., 2019). Finding an appropriate method for spectral unmixing is not a trivial task and is the topic of discussion in the literature (Cavalli, 2023; Kale et al., 2019). Whilst supervised selection of endmembers resulted in visibly accurate spectral unmixing and abundance mapping in

our analysis (Fig. 6.5) and was justified by using PCA to identify two key spectral components, an unsupervised endmember detection method such as fast iterative pixel purity index, or an unsupervised clustering approach like scene segmentation, may have been preferable to avoid potential subjective bias. However, these methods were piloted and failed to accurately cluster pixels into relevant materials. This was likely due to the disparate spatial structure of sky and vegetation pixels, and the large continuous variation in spectra found in forest environments (Cronin et al., 2014). Similarly, the changes in weather conditions between sampling days meant that segmentation in RGB colour space failed to consistently identify sky and vegetation pixels across lightprobes.

Seasonal changes in spectrum

One of our key findings is that the spectra of a natural woodland environment can deviate substantially across the seasons from D65 (Fig. 6.3). This suggests that, in addition to the CIE D65 model not successfully modelling twilight (Spitschan et al., 2016), it may poorly reflect seasonal spectral changes that are observed under natural environments with high levels of secondary reflection. Spectral unmixing and abundance mapping of the hyperspectral lightprobes (Fig. 6.5) suggest that changes in the extent of vegetation, likely driven by an increase in leaf cover, underly the seasonal changes in overall spectrum observed in both sites (Fig. 6.5A,B). The contribution of seasonal changes in the spectrum of sky pixels was also explored (Fig. S6.2). However, differences in weather conditions between sampling days, and subsequent levels of Rayleigh and Mie scatter, made interpretation difficult. Whilst in theory it is possible that seasonal changes in the sunlight spectrum may be contributing to the overall differences we observe, previous measurements made in the Netherlands (latitude: 53.24°) at a similar latitude to our study site (latitude: 51°) found little variation in spectrum across the four seasons (Woelders et al., 2018); suggesting that its contribution to our dataset will also be small. However, at higher latitudes such as in the Arctic (latitude: +69.5°), seasonal variation in the sunlight spectrum is more extreme. The longer path length of sunlight through stratospheric ozone in Winter results in a short-wavelength enriched spectrum, similar to that of twilight, for 8-11hrs of the day between September and April (Dominy and Harris, 2022; Fosbury and Jeffery, 2022; Hazlerigg et al., 2023). This has resulted in remarkable phenotypic plasticity in the Artic reindeer, in which the wavelength of peak reflection by its tapetum lucidum shifts from 541nm in Summer to 444nm in Winter; mediated by an alteration to collagen spacing (Dominy and Harris, 2022; Fosbury and Jeffery, 2022; Stokkan et al., 2013).

It therefore seems most likely that the spectral changes we observe in our dataset across seasons (Fig. 6.3) are primarily driven by changes in the extent of vegetation (Fig. 6.5). However, whether these seasonal spectral changes are of biological relevance to NIF functions in mammals is more

difficult to predict; although alpha-opic lux are useful in assessing this question. Whilst not all spectral changes resulted in changes to alpha-opic lux, relative S-cone and L-cone opic lux across Spring to Winter in Site B changed to the same extent as daylight to -5 degrees of solar elevation at civil twilight (Fig. 6.3E,F; Fig. 6.7B). A change in alpha-opic lux from daylight to -6 degrees of solar elevation has been shown to result in behavioural differences in mouse locomotor activity and light sampling (Chapter 5) and body temperature (Walmsley et al., 2015). Therefore, it is possible that seasonal spectral changes could be sufficient to generate differences in behaviour. However, the differences in temporal scale of these changes do make these extrapolations more tenuous – civil twilight occurs across minutes and hours, whereas seasonal changes occur across weeks and months. Furthermore, spectral changes at twilight occur at a time when the circadian clock is most sensitive to light (Foster et al., 2020). Consequently, it is likely that for seasonal spectral changes to be biologically relevant, their scale may need to be greater.

Furthermore, could seasonal variation in spectrum actually be a useful cue to organisms, and if so, for what? Perhaps seasonal spectral changes could be used in combination with photoperiod to detect time of year – in a similar way to how spectral changes at twilight improve the reliability of time of day detection (Mouland et al., 2019; Walmsley et al., 2015; Woelders et al., 2018). Afterall, many animals have circannual rhythms in physiology and behaviour which enable them to exploit seasonal changes in environmental conditions (Monecke et al., 2013; Paul et al., 2007), and it is known that photoperiod can alter melatonin secretion in humans (Wehr, 1991). Alternatively, is seasonal variation in spectrum more likely to be a source of spectral noise that the circadian and visual system have to cope with? For example, having to detect important spectral changes at twilight under different seasonal conditions.

The likelihood of seasonal variation in spectrum being a useful cue, as opposed to noise, depends on the reliability of seasonal spectral changes. As discussed, seasonal differences in spectra are likely to arise from a combination of changes in reflection from vegetation and changes in the sunlight spectrum, due to variation in the path length of sunlight through the atmosphere. The relative contribution of these two factors will be influenced by various elements, including the structure of the local environment (with more enclosed habitats such as woodlands having higher levels of secondary reflections than open environments), the plant species present (evergreen woodlands may have spectra associated with vegetation across the entire year) and latitude (with higher latitudes experiencing more seasonal variation in sunlight spectrum). Seasonal changes in spectrum arising from changes in reflectance from vegetation are unlikely to be a reliable marker of time of year due to other factors influencing leaf cover – such as predation rates, logging, and disease. In addition, the effect of reflectance would change with the movement of an organism

through an environment. Therefore, it is more likely to be spectral noise, than a useful cue. In contrast, seasonal changes in sunlight spectrum could in theory provide a reliable time of year cue at sufficiently high latitudes in open environments (Fosbury and Jeffery, 2022), and this possibility has not been explored in the literature.

Overall, our dataset outlines how the spectrum of a natural light environment, and subsequent alpha-opic lux available for humans, can vary greatly across the year and be very different to that of the CIE D65 spectrum (Fig. 6.3; 7A). Within our dataset, due to the deciduous woodland environment and low latitude, these changes are likely to be driven by changes in the extent of vegetation (Fig. 6.5; 7C), rather than changes in the spectrum of sunlight.

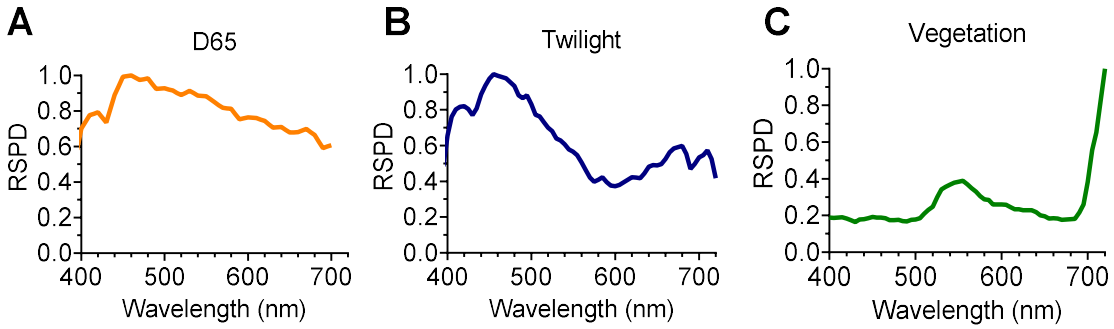

Figure 6.7 – Summary schematic of the spectral variation in the natural light environment. **(A)** The CIE D65 RSPD (CIE, 2022). **(B)** Twilight RSPD (measured at -5 degrees of solar elevation; Spitschan et al., 2016). **(C)** The RSPD of a vegetation pixel from the hyperspectral dataset presented in Shiwen et al (2021) and in this chapter.

Directional variation in the light environment

Segmentation analysis demonstrates clear directional variation in intensity and spectrum within our woodland scenes (Fig. 6.6). Interestingly, this variation was mainly observed vertically and not horizontally (data not presented). This is consistent with patterns found by Nilsson and Smolka (2021) in which elevation angle was a key driver of variation. The resulting pattern and extent of relative alpha-opic lux change varied with season and site – for example, whilst relative S-cone opic lux changes only by ~ 3% from top to bottom of the Site B lightprobe in December, it changes by 13% in June at the same location. This is 1.7 times larger than the change in S-cone opic lux across civil twilight (7.8%) (Fig. 6.3F) which we know to be relevant for NIF functions of light.

Directional variation is known to be relevant for visual processing (Adams et al., 2004; Morgenstern et al., 2011). An interesting question arising from our data and other characterisations of directional variation in lighting (Morimoto et al., 2019), is whether directional variation may be relevant for NIF responses to light. Indeed, the role of light distribution across the visual field was identified as a knowledge gap by an expert working group exploring the effect of daylight on humans (Münch et al., 2020). A limited number of studies suggest that direction, at least of electric light, is important for melatonin suppression – although relatively coarse directional variation in stimuli was used. Illumination of the inferior (Glickman et al., 2003; Lasko et al., 1999) and nasal (Rüger et al., 2005; Visser et al., 1999) portions of the retina were found to result in significantly more melatonin suppression than the equivalent illumination of the superior or temporal retina, respectively. However, extending this effect to other NIF forming resulted in less clear results. For example, Rüger et al (2005) found no effect of nasal versus temporal retinal illumination on absolute values of, or rhythms in, core body temperature.

These observations in melatonin suppression in humans could be explained by the sensitivity of the majority of SCN neurons to spatial patterns (Mouland et al., 2017), since photic information is relayed from the SCN to the pineal gland in which melatonin is synthesised. Mouland et al (2017) demonstrated that the receptive fields of the majority of SCN neurons in mice had small excitatory centres with large inhibitory surrounds, rendering them sensitive to spatial patterns, rather than global levels in illumination. Overall, a limited number of studies suggest that directional variation in lighting could influence the magnitude of NIF effects of light, making it important to characterise this variation. It would be interesting to repeat our study in urban and indoor environments, to assess how modern environments may alter natural directional variation in light and resulting alpha-opic lux. Recent evidence suggests that indoor scenes have reduced directional variation in light (Morimoto et al., 2019) and therefore this could be incorporated as a factor in the "daylighting design" of buildings (Khademagha et al., 2016; Münch et al., 2020) and human centric lighting more widely (Jalali et al., 2024).

Future directions

Several interesting future questions have arisen from the results and limitations of the exploratory dataset presented in this chapter. As previously mentioned, to make the results directly applicable to the visual system of animals with a UV-sensitive photoreceptor such as mice, it would be necessary to re-collect this data using a hyperspectral camera sensitive to light from 300-800nm (Stern, 2021). Using this updated dataset, the experience of daylight enriched with reflectance from vegetation (e.g. Fig. 6.7C) could be re-created in the laboratory and compared to the CIE standard of daylight (D65, Fig. 6.7A), to assess the impact of secondary reflections in a natural environment

on circadian behaviour. This could be achieved using relative alpha-opic lux, as in Chapter 5 of this thesis. This could be combined with a study assessing the importance of directional variation in lighting on behaviour, informed by the vertical segmentation analysis in Fig. 6.6. For example, D65 (Fig. 6.7A) could be simulated in the upper visual hemisphere, and daylight enriched by reflectance from vegetation (Fig. 6.7C) simulated in the lower visual hemisphere. Or more complex directional stimuli could be generated using a miniature projection system (Kautzky et al., 2024). This is of particular interest in the mouse, since the mouse retina has a ventral-dorsal gradient in photoreceptor expression, with UVS opsin and MWS opsin expressed most highly in the ventral and dorsal retina, respectively. This opsin gradient is likely to have been shaped by statistic regularities in the natural light environment (Qiu et al., 2021). Finally, it would be interesting to test whether seasonal changes in sunlight spectrum observed at higher latitudes (Hazlerigg et al., 2023) may contribute to the detection of time of year in seasonal breeders such as the arctic ground squirrel (Drescher, 1967; Williams et al., 2017). This could be explored by re-producing the relative alpha-opic lux generated by sunlight across the four seasons, presented as stimuli over a series of weeks. These spectral changes could then be titrated against changes in photoperiod to assess their relative importance in the detection of time of year.

To conclude, here we present a method to characterise light environments in a highly spectrally, spatially, and directionally resolved way, and validated the method in a natural woodland environment. We demonstrate that the spectrum of natural light can vary greatly across time and direction, thereby generating multiple interesting future questions regarding the role of these features of the natural light environment in NIF responses to light in mammals.

6.6 Supplementary material

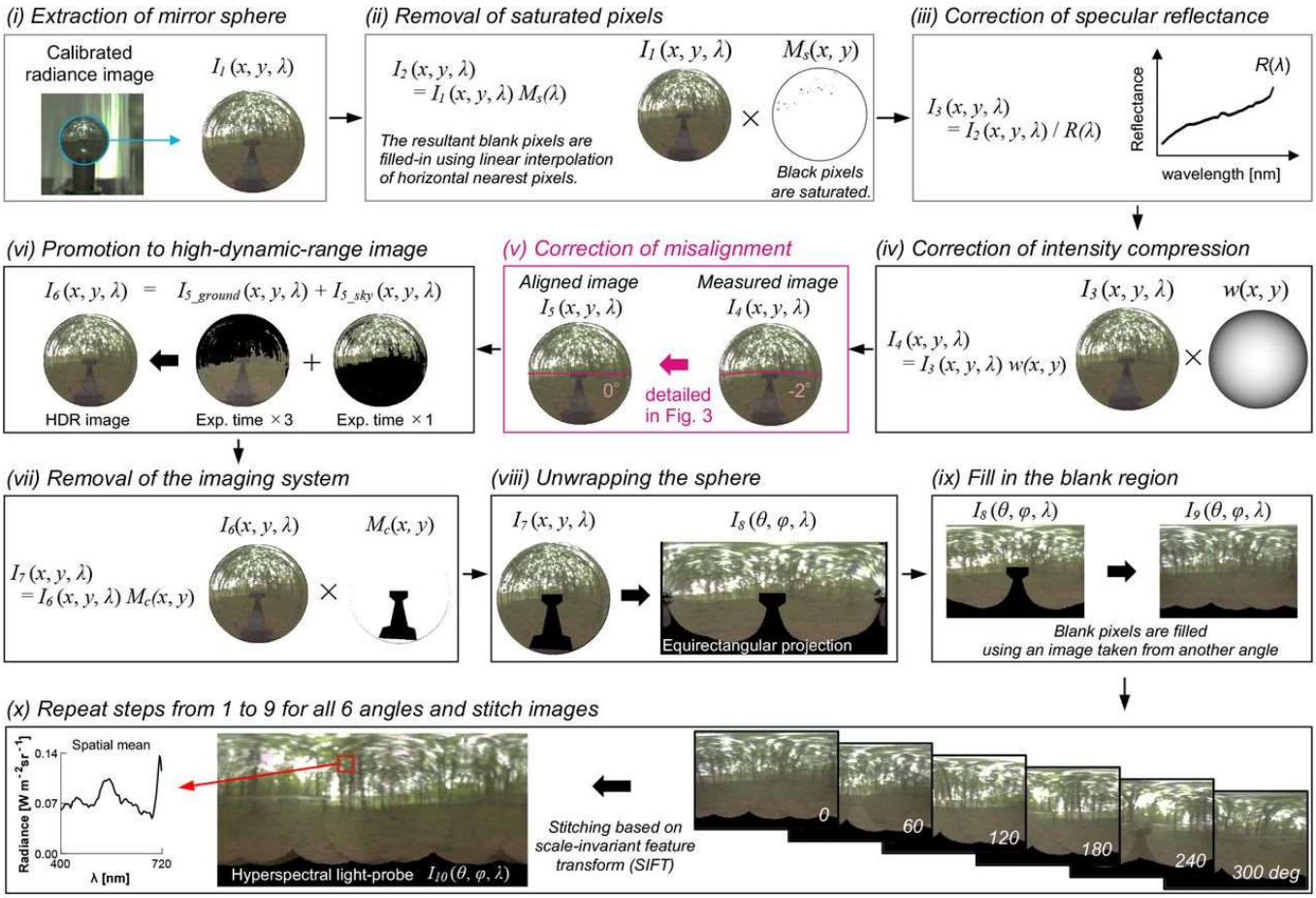

Figure S6.1 - The image-processing pipeline to generate a hyperspectral light probe. **(i)** A sphere image was extracted from the raw image using a custom-built automatic sphere detection algorithm. **(ii)** Any saturated pixels were removed. **(iii)** Reflectance of the sphere was not flat over wavelength and therefore it was corrected. **(iv)** We corrected the compression of intensity across the sphere. **(v)** We estimated the degree of misalignment and applied the correction. **(vi)** Two images taken at different integration times were combined. **(vii)** The reflection of the imaging system was erased. **(viii)** The image was transformed from spherical coordinates to the equirectangular projection "unwrapping". **(ix)** The blank region resulting from erasing the imaging system was filled with information from neighbouring images. **(x)** Finally, images were stitched using an automatic feature-detection algorithm to create a full-panorama hyperspectral environmental illumination map. Figure and legend details taken from Shiwen et al., 2021.

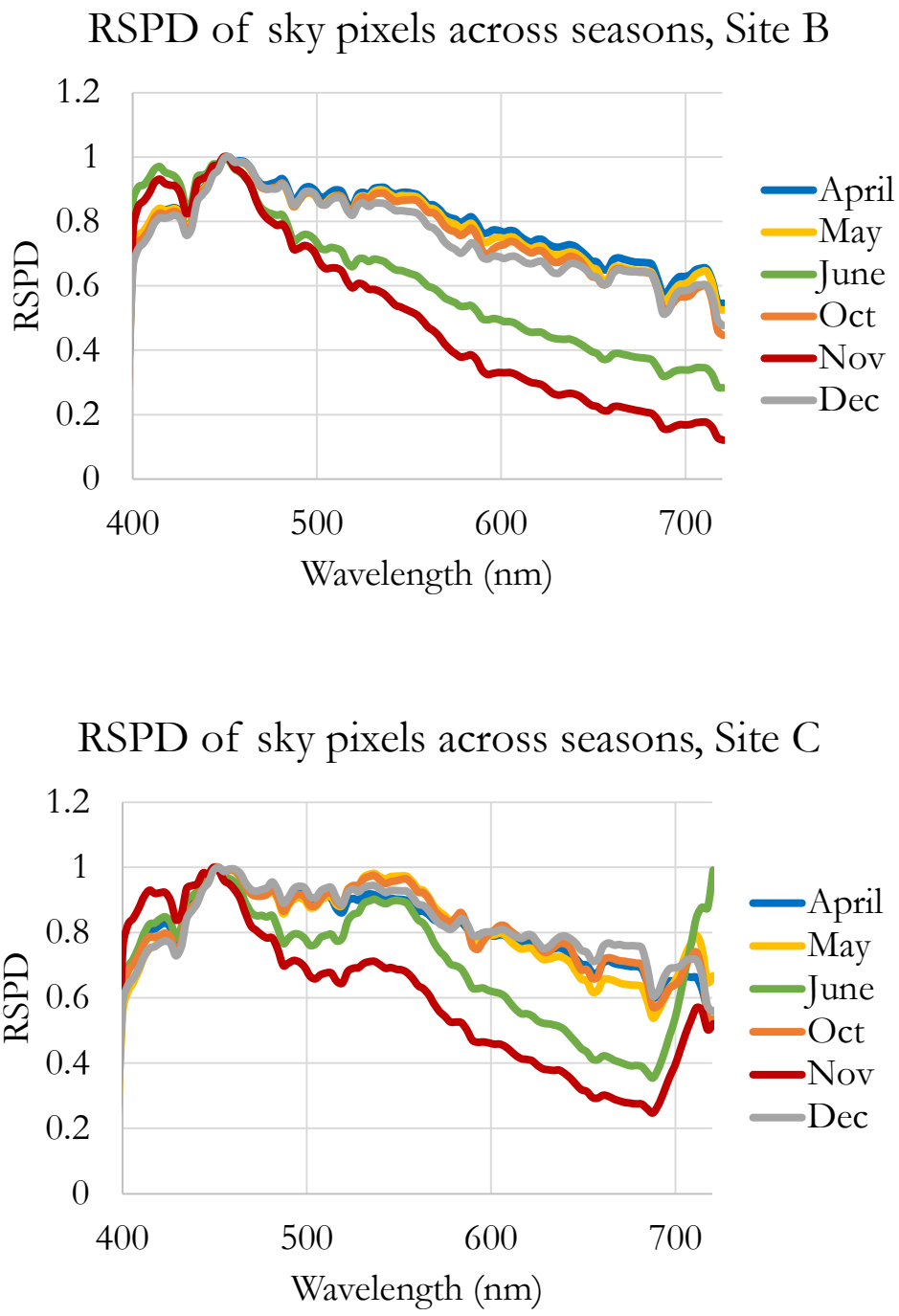

Figure S6.2 – The RSPD (400-720nm) of sky pixel endmembers (selected during the process of spectral unmixing in Fig. 6.3) across seasons in Site B (top panel) and Site C (bottom panel).

Chapter 7. General Discussion

The overall objective of this thesis was to further our understanding of circadian photoentrainment under naturalistic light environments. The disparity between the natural light environment (DeCoursey, 1986; Judd et al., 1964; Shiwen et al., 2021; Spitschan et al., 2016) and that of standard laboratory conditions (Lucas et al., 2024; Peirson et al., 2018), in combination with the plasticity of circadian rhythms (Calisi and Bentley, 2009; Daan et al., 2011; Van Der Veen et al., 2017; van der Vinne et al., 2014) make this objective critical to the field. In order to achieve this objective, four aims were established (section 1.6). This Chapter will discuss to what extent these aims have been achieved and how they have contributed to the field. Future directions will then be considered, before discussing whether an ecological approach to Neuroscience research is constructive.

7.1 Key findings

Aim 1: Characterise how mice are exposed to light under standard laboratory conditions.

The first aim was to characterise how mice are exposed to light under standard laboratory conditions, and assess the implications of this for our understanding of circadian photoentrainment. It was well established that both acute and circadian effects of light on locomotor activity are dose dependent (Contreras et al., 2021; Foster et al., 1991; Hattar et al., 2003) and that light levels can vary across standard mouse cage racks (Clough, 1982; Weihe et al., 1969). However, no study had systematically evaluated the effects of cage position, or material, on home cage light intensity and subsequent circadian entrainment. We demonstrated a 15-fold difference between highest and lowest light intensities across an IVC rack in clear cages, and a 10-fold difference in red cages. As predicted, there was a significant positive relationship between light intensity and strength of circadian entrainment (Steel et al., 2022). We concluded that the home cage light environment should be incorporated into experimental design and should be fully characterised to account for variation (Steel et al., 2022).

Aim 2: Design a paradigm to investigate the role of behaviour in regulating circadian photoentrainment.

Although the importance of behaviour was first investigated empirically in the 1950s (John W Twente, 1955), only sporadic studies since then have investigated the effect of an animal's ability

to self-select light exposure (light sampling) on circadian entrainment (Boulos et al., 1996; DeCoursey, 1986; Decoursey and Menon, 1991; Flôres et al., 2016; Hut et al., 1999; Kenagy, 1976; Lockard and Owings, 1974; Refinetti, 2004; Voûte et al., 1974). Prior to this thesis, Refinetti (2004) was the only study examining this in mice and argued that the ability to self-select light exposure had no significant effect on circadian photoentrainment. This is in contrast to Decoursey and Menon (1991) who suggested light sampling behaviour to be of great importance to circadian photoentrainment in flying squirrels. Refinetti (2004) primarily used wheel running as a measure of activity; providing a measure of voluntary activity only and potentially altering behaviour (Deboer and Tobler, 2000). Furthermore, in many of these previous studies only square-wave light:dark (LD) cycles were used (DeCoursey, 1986; Decoursey and Menon, 1991; Refinetti, 2004). Therefore, a more highly resolved characterisation of light sampling behaviour was required, including under more naturalistic ramped LD cycles.

In Chapter 3 we designed nestboxes consisting of a dark nest, and a lighter atrium - from which mice could sample the external light environment, as at the burrow entrance (Fig.3.1). We measured locomotor activity across the nestbox and main cage at a high temporal resolution (1s), to quantify light sampling behaviour, decision making ('go : no go') and circadian entrainment metrics. Using this paradigm we observed that C57BL/6J mice extensively used the nestbox, significantly reducing their daily light exposure to an average of 0.8hrs of light per 24hrs (Fig.3.2A). Light has a significant influence on physiology and behaviour (Do, 2019). Therefore our results bring into question whether the inability of laboratory rodents to avoid light under standard laboratory conditions may be influencing experimental read-outs. This is a potential issue for animal research more widely, and a recent expert working group for animal welfare and data reproducibility has recommended that laboratory animals should be able to escape the light (Lucas et al., 2024).

The introduction of a ramped LD cycle into our experimental design generated a distinct pattern of light sampling behaviour in wildtype mice – with striking peaks at dawn and dusk (Fig.3.3A, 3.5C). Our data identifies a previously unquantified role for behaviour in regulating light exposure at twilight – a period which has long been considered critical for the setting of the circadian clock (Boulos et al., 1996; Boulos and Macchi, 2005; Helfrich-Förster et al., 2020; Pittendrigh and Minis, 1964; Roenneberg and Foster, 1997). These results demonstrate that the natural light environment as experienced by burrow-dwelling species, varies not only in intensity and spectrum (Spitschan et al., 2016), but temporally. These findings generated a range of novel questions – including regarding the mechanisms regulating light sampling behaviour at twilight.

Aim 3: Investigate the mechanisms regulating light sampling behaviour and circadian photoentrainment.

Consequently, the third aim was to investigate the role of the circadian clock (Aim 3.1) and photoreceptors (Aim 3.2) in regulating the timing of light sampling behaviour, and circadian entrainment more broadly. These two questions were assessed across Chapters 3 and 4 using three transgenic mouse strains - one lacking a functional circadian clock, one lacking classical photoreceptors and one lacking melanopsin. Many previous knock-out studies have investigated the role of the molecular clock (Bunger et al., 2000; van der Horst et al., 1999) and photoreceptors (Altimus et al., 2010; Freedman et al., 1999; Mouland et al., 2019; Walmsley et al., 2015) in circadian entrainment. However, this has not been investigated under a paradigm where light sampling is possible, which for example, could alter the pattern of retinal light exposure.

Aim 3.1: The peaks in light sampling behaviour at twilight were abolished in mice lacking a circadian clock (Fig.3.5C). This identified a previously uncharacterised role for the circadian clock in ensuring appropriate timing of light exposure for photoentrainment. This suggests the presence of a feedback loop between light, the circadian clock and behaviour which cannot occur under standard laboratory conditions (Fig.3.6). The arrhythmicity of light sampling behaviour in mice lacking a circadian clock was in contrast to rhythmic locomotor activity (which was expected due to masking). As such, we show that by measuring light sampling behaviour instead of locomotor activity, arrhythmicity in *Cry1*$^{-/-}$,*Cry2*$^{-/-}$ mice can be detected under an LD cycle rather than having to use DD. Although, it is possible that the arrhythmicity of light sampling could arise from non-circadian factors such as reduced light sensitivity in *Cry1*$^{-/-}$,*Cry2*$^{-/-}$.

Aims 3.2: The results from transgenic strains were less conclusive in identifying the contributions of classical photoreceptors and melanopsin to the timing of light sampling behaviour. Preliminary results suggest that rods and cones may be particularly important, but that melanopsin may also contribute. However, background differences between C57 and 129 strains in light-dark exploration and locomotor activity levels made interpretation of behaviour in melanopsin knockout mice challenging (Bouwknecht and Paylor, 2002; Crawley, 2008; Hossain et al., 2004). In addition, there are well established issues with photoreceptor knockout models (Allen and Baño-Otálora, 2022; Lucas et al., 2020). Of particular significance is that ipRGCs combine both intrinsic signals from melanopsin, and extrinsic information from rods and cones (Lucas et al., 2012). Therefore, the contributions of each photoreceptor class in an intact retina may differ from the sum of their parts observed in isolation. Furthermore, retinal remodelling could inflate or deflate the relative importance of melanopsin in rodless-coneless mice, or rods and cones in melanopsin knockout strains. This may be particularly relevant in melanopsin knockout models,

since melanopsin is important in retinal development (Rao et al., 2013; Schmidt et al., 2008; Sekaran et al., 2005). Therefore, whilst transgenic models are powerful tools to investigate the role of photoreceptors in behaviour, they should be used in parallel with in vivo methods which preserve an intact retina, such as chemogenetic control of photoreceptors (Milosavljevic et al., 2016) or photoreceptor specific stimuli (Spitschan and Woelders, 2018). Allen and Baño-Otálora (2022) provide a useful summary of these methods. Finally, ex vivo tools, such as multi-electrode array (MEA) (Eleftheriou et al., 2020) may offer complementary methods to investigate the role of photoreceptors in light sampling behaviour. This possibility will be discussed in the 'Future directions' section.

Aim 4: Characterise and investigate the effects of naturally-occurring spectral changes in the light environment on light sampling behaviour and circadian entrainment.

Aim 4.1: In addition to the opportunity for light sampling behaviour, one of the key features of the natural light environment not present in circadian laboratory studies are naturally-occurring spectral changes. However, in contrast to the sporadic literature surrounding light sampling behaviour, this topic has a more developed and contemporary literature. Changes in spectrum across daylight and twilight have been well characterised (Spitschan et al., 2016), as well as the ability of the circadian system to use these spectral cues for circadian photoentrainment (Mouland et al., 2019; Walmsley et al., 2015; Woelders et al., 2018). Walmsley et al (2015) demonstrated that introducing spectral changes at twilight altered the phase of entrainment compared to an intensity-only ramp, using body temperature as a readout of circadian entrainment. Therefore, in Chapter 5 we extended Walmsley et al (2015) to behavioural proxies of entrainment, by using our nestbox paradigm to measure locomotor activity and light sampling behaviour under spectral changes associated with civil twilight.

Results from Chapter 5 corroborate results from Chapters 3 and 4 in emphasising that it is the *ramping* of a light stimulus (of any spectrum) that generates peaks in light sampling behaviour at dawn and dusk. Peaks in light sampling behaviour occurred under a ramped white LED (Fig.5.2C), an intensity-only daylight ramp (Fig.5.4E) and a ramp simulating spectral changes at civil-twilight (Fig.5.5K), but not under any of the square-wave LD cycle conditions (Fig.5.2C, 5.3E). However, significant differences in light sampling behaviour between the intensity-only daylight ramp and the civil twilight ramp (Fig.5.5K-N) imply that spectral changes modulate the timing of light sampling behaviour – with the onset of light sampling occurring 1.5hrs earlier at dusk when spectral changes were incorporated into the ramp (Fig.5.5N). Similarly, locomotor activity onset also occurred 0.5hrs earlier under the civil twilight ramp (Fig.5.5.G-J). The clear increase in locomotor activity under the civil twilight ramp (Fig.5.5H) coincides with the point at which the

ratio of S-cone opic lux increases most steeply (Fig.5.5D), linking to analysis in Chapter 2 where S-cone opic lux correlated most strongly with activity onset out of all the mouse alpha-opic metrics. This suggests that S-cone activation may be important in regulating the timing of activity onset (Tamayo et al., 2023; Van Oosterhout et al., 2012). As a result, the timing of activity onset under white LED laboratory lights may be especially different to under natural light environments, since white LEDs are short-wavelength depleted (Lucas et al., 2024). Collectively, our data contributes to a growing body of research indicating that the spectrum of light at twilight has a significant effect on mouse behaviour. However, it does not confirm whether this occurs via the modulation of the circadian system (Walmsley et al., 2015; Woelders et al., 2018) or acute responses to light (Tamayo et al., 2023). This could be assessed relatively simply in future experiments, as outlined in section 5.5.

Aim 4.2: Whilst the overall spectrum of natural daylight and twilight have been sufficiently characterised to simulate in the laboratory (Spitschan et al., 2016), these were generally measured using spectrophotometers which provide poor directional resolution. As such, these measurements tell us little about how reflections from materials influence spectrum – which is known to be significant in urban environments (Morimoto et al., 2019) and of relevance to NIF responses to light in humans (Webler et al., 2019). However, similar measurements have not been performed in a natural environment. Nilsson and Smolka (2021) performed directionally resolved measures of natural light environments, however the use of a multispectral RGB camera mean results can only be applied to human visual responses. Therefore, a highly spectrally and directionally resolved assessment of a natural environment was lacking in the literature.

In Chapter 6 we used a hyperspectral camera to measure the light environment of a woodland across a year in a spectrally, spatially and directionally resolved way. Analysis of the subsequent hyperspectral lightprobes demonstrated that the overall spectrum of light changes substantially across the year in a woodland, and is not always equivalent to the CIE D65 illuminant (CIE, 2022) – which is commonly used as a daylight standard (Fig.6.3). In addition, there was considerable directional variation in spectrum within a scene (Fig.6.6) – which has not been widely considered in circadian photobiology (Webler et al., 2019). Further analysis indicated that the majority of seasonal and directional variation in spectrum arose from changes in the extent of vegetation (Fig.6.5).

These descriptive results were accompanied by a quantification of the relative alpha-opic lux produced by each spectrum, to explore whether spectral variation arising from reflection may be sufficient to influence NIF responses to light (Webler et al., 2019). This was challenging to assess.

However, our exploratory analysis demonstrated the change in relative alpha-opic lux across seasons due to spectral reflectance to be equivalent to changes in relative alpha-opic lux between 0° and -5° of solar elevation at civil twilight – which we had shown to generate differences in behaviour in mice. This suggests, but by no means confirms, that reflectance could be relevant for NIF responses to light in mammals – perhaps most likely as a source of spectral noise which the circadian system has to cope with. However, due to the hyperspectral camera only sampling down to 400nm, inferences could not be made to mice (since they possess a UVS cone) and therefore only human alpha-opic lux and NIF responses were considered. This is useful in itself for the human circadian research community, and in fact has been identified as a knowledge gap (Münch et al., 2020). However, it would have been preferable to compare the relative alpha-opic lux changes at civil twilight (Chapter 5) to that generated by spectral reflectance (Chapter 6) within the same species. In addition, more frequent data collection across the year would have been helpful in increasing temporal resolution of the dataset, in order to control for the effect of weather when investigating seasonal changes. Therefore, whilst it was challenging to make firm conclusions about the effect of spectral reflectance in a natural environment on NIF responses from our dataset, our method successfully characterised the light environment in a highly spectrally, spatially and directionally resolved way.

Overall, the aims laid out in the Introduction were successfully achieved – perhaps with the exception of Aim 3.2 which sought to examine the role of classical photoreceptors and melanopsin in regulating light sampling behaviour. Due to the limitations of transgenic models and experimental design discussed above, interpretation of results was difficult. In the future, alternative methods may be useful for investigating this question and these will be discussed in the following section.

7.2 Future directions

Investigating the role of photoreceptors in light sampling behaviour

Throughout Chapters 3 to 5, there were several consistent differences between the peak in light sampling behaviour at dawn and dusk; suggesting differences in photoreceptor involvement. Specifically, the immediacy of the peak following the start of the light ramp, the scale of the peak, and whether spectral cues had a significant influence on the peak's characteristics. At dawn, the peak in light sampling events occurred almost immediately after the onset of the ramp, whereas at dusk the peak occurred later on (Fig.3.5C, 5.4E). In addition, the peaks in light sampling events were consistently larger at dawn than dusk (Fig.3.3A, 3.5C, 5.4E). Finally, spectral cues had a

significant effect on the timing and scale of peaks at dusk, but not dawn (Fig.5.5K-N). Examining these differences is a useful starting point for generating hypotheses relating to photoreceptor involvement in light sampling behaviour, on which to base future experiments.

These differences between light sampling at dawn and dusk may be driven by the different photosensory tasks of detecting dawn and dusk. Detecting dawn requires sensing increasing light levels against a dark-adapted retina, whereas at dusk decreasing light levels must be detected against a light-adapted retina. At least, this is true for non-burrowing, diurnal species or mice housed under standard laboratory conditions. If a nestbox or burrow is present the mouse retina may be dark-adapted at dusk – however, dawn and dusk will still differ, since the relative contrast of the stimuli will be higher at the onset of dawn than dusk. As such, the sequence of photoreceptor activation is likely to be different. Rods will be activated first at dawn, then cones followed closely by melanopsin; whilst at dusk the opposite would be true (Fig. 7.1). It is therefore tempting to hypothesis that rods are more important for driving peaks in light sampling at dawn, whilst cones and melanopsin are more important at dusk. Methods to directly test this hypothesis will be discussed at the end of this section. However, firstly, we will examine how data collected throughout Chapters 3 to 5 lend support to this hypothesis.

The delay of the peak in light sampling events at dusk could arise from an increased role of melanopsin (with slower kinetics) compared to at dawn, when rods (with faster kinetics) are likely to respond first. However, data from rodless-coneless mice (Chapter 4) indicate that melanopsin alone is not sufficient to drive light sampling peaks at dusk (Fig.4.2D), suggesting a role for rods and cones. This idea is corroborated by spectral cues having a significant modulatory effect on the peak in light sampling behaviour at dusk – a response likely to be dominated by opponent signals from S-cones and M-cones. Finally, the lack of response to spectral cues at dawn fits with a rod-dominated response to low light intensities of a dark-adapted retina. It is important to note that the changes in light intensity used in this thesis are not as extreme as those occurring in nature (Fig.7.1). Therefore, the exact timing of photoreceptor activation under the laboratory ramps would differ to those under fully natural conditions (Fig. 7.1). However, the sequence of activation and relative contribution may be similar, and are therefore are useful for generating hypotheses.

In addition, we hypothesise that the relative contributions of classical photoreceptors and melanopsin to circadian photoentrainment would actually differ in the presence of a nestbox (or a burrow), compared to under standard laboratory conditions. Due to light sampling, photoreceptors will be exposed to a stochastic pattern of light pulses of increasing light intensity at dawn (Fig. 7.2B), and decreasing light intensity at dusk – compared to a constant change in

intensity if a nestbox was not present (Fig. 7.2A). As such, light sampling may promote a role for cones compared to standard laboratory conditions, by increasing the temporal contrast of light stimuli (Lall et al., 2010).

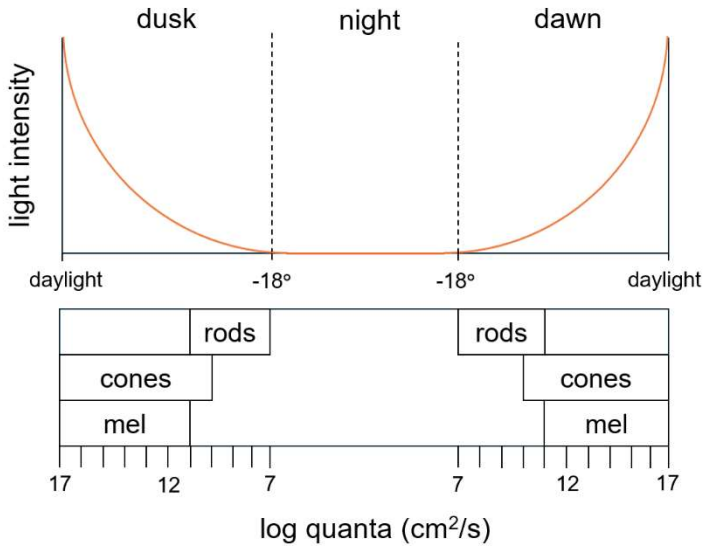

Figure 7.1 – Schematic demonstrating the different sequence of photoreceptor activation at dawn and dusk. -18° refers to degree of solar elevation, with -18° being the lower limit of astronomical twilight. Photoreceptor activation thresholds taken from Peirson et al (2018). Log quanta value of 100,000 photopic lux of 'daylight' calculated using the Rodent Toolbox. Log quanta value of -18° degrees of solar elevation calculated from raw data (Spitschan et al, 2016) using the Rodent Toolbox.

Comparing ex vivo retinal responses using multielectrode arrays (MEA) to a series of natural light stimuli of increasing complexity, would be one way to investigate both these hypotheses – firstly, that rods are more important in driving the peak in light sampling at dawn, whilst cones and melanopsin are more important at dusk; and secondly, that light sampling behaviour promotes a role for cones in photoentrainment. More broadly, it would further our understanding of how rods, cones and melanopsin drive behaviour under real-world light environments. Initially an array of natural spectra, for example, D65, daylight, twilight (at an intermediate solar elevation e.g. -5°) and vegetation, could be used at a range of constant intensities. The hyperspectral imaging in Chapter 6 could be repeated using a camera which samples below 400nm (Nevala and Baden, 2019) to generate spectra (Fig.6.5D) appropriate for the mouse retina. As in our behavioural studies in Chapter 5, a series of ramped light stimuli could then be introduced – a white LED, an intensity only daylight ramp, and an equivalent intensity ramp but with spectral changes associated with twilight. Two versions of each ramp could be used – firstly, a constant exposure to the ramped

LD cycle (Fig. 7.2A), and secondly, a stochastic pattern of light exposure arising from light sampling (Fig. 7.2B), generated from data in Chapter 3. This could be performed as a dawn ramp against a dark-adapted retina, and a dusk ramp against a light or dark-adapted retina. Finally, having considered the intensity, spectrum and temporal features of the natural light environment on retinal responses, the directional variation in lighting characterised in Chapter 6 could be explored. For example, with an updated hyperspectral dataset sampling below 400nm, the overall spectrum of the upper versus lower hemisphere could be projected onto the ex vivo retina on an MEA, using a miniature projection system. This has been done in recent studies to achieve complex visual stimuli (Kautzky et al., 2024). Throughout these experiments, the action of classical photoreceptors (Gamlin et al., 2007) and melanopsin (Jones et al., 2013) could be pharmacologically blocked e.g. using opsinamides in the case of melanopsin, to selectively examine the contribution of classical photoreceptors and melanopsin.

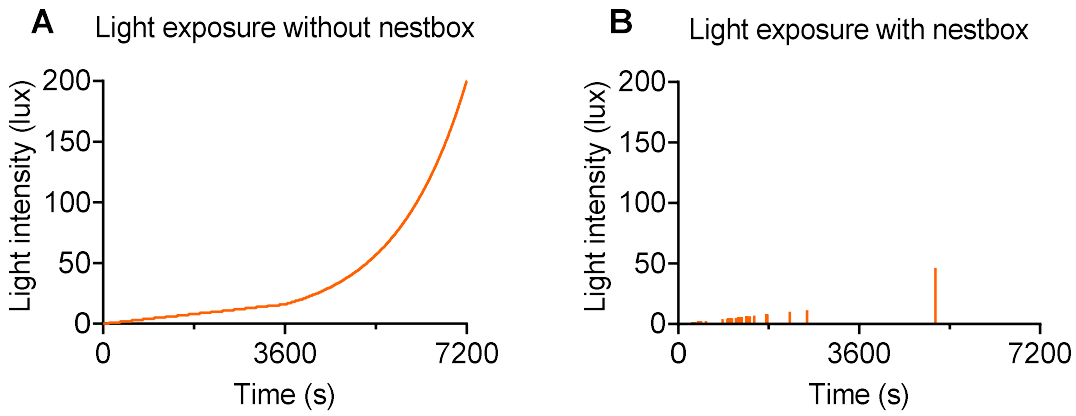

Figure 7.2 – Pattern of light exposure at dawn under a ramped LD cycle, without a dark nestbox present **(A)** and with a nestbox present **(B).** Data in (B) generated from a C57BL/6J mouse from Fig. 3.3A. This demonstrates how light sampling behaviour generates a stochastic pattern of light exposure. These light exposure patterns could be used as stimuli for multi-electrode array recordings.

7.3 An ecological approach to Neuroscience

7.3.1 Definitions

In this thesis, we took an ecological approach to the study of circadian photoentrainment, by bringing key features of the natural light environment into the laboratory. The concept of ecologically relevant experimental designs is referred to in the literature using multiple phrases, including "naturalistic" (Datta et al., 2019), "representative design" (Dhami et al., 2004) and

"ecological validity" (Chang et al., 2022; Keidser et al., 2020; Schmuckler, 2001; Stangl et al., 2023). However, it is worth clarifying the differences between these terms – especially the latter two, which have specific definitions.

Ecological validity is a measure of how representative results obtained in artificial laboratory conditions are of the specific real-world situation(s) in question (Keidser et al., 2022). As such, it can be considered a subtype of external validity – that is, the extent to which results obtained in one context can be generalised to another context (Beechey, 2022). In contrast, representative design is a *method* by which to increase the ecological (and external) validity of results, by sampling "stimuli, tasks and situations which are representative of a specific target ecology" (Brunswik, 1955; Holleman et al., 2020; Keidser et al., 2020; Matusz et al., 2019; Shamay-Tsoory and Mendelsohn, 2019). It is important to note that ecological validity was first used in the 1950s by the psychologist Egon Brunswick to describe something different – "the correlation between cues received at the peripheral nervous system and the identity of distant objects or events in the environment" (Brunswik, 1949; Keidser et al., 2022).

Representative design is in contrast to systematic design (Brunswik, 1955), which follows the reductionist approach of isolating variables of interest from all other influencing factors (Hammond, 1954). This reductionist approach, although extremely valuable, has been criticised for generating results lacking external validity (Krakauer et al., 2017). As an aside, over-standardisation of conditions has also been proposed to decrease external validity, and it has been suggested that systematic heterogeneity should be incorporated into experimental design (Voelkl et al., 2020; Würbel, 2001). This links to Chapter 2, in which because variation in light intensity was fully characterised, it could be leveraged to obtain interesting results – such as S-cone opic lux correlating most strongly with activity onset (Steel et al., 2022).

7.3.2 How can ecological validity be measured?

One of the biggest problems with ecological validity, and external validity more broadly, is how to measure it. Frameworks have been developed across various disciplines (Hoc, 2001; Keidser et al., 2020; Schmuckler, 2001) which assess components of experimental design, such as stimuli or task, on a continuum of artificiality-naturality and simplicity-complexity. However, the aspects of experimental design under consideration vary between disciplines (Chang et al., 2022; Hoc, 2001; Keidser et al., 2020; Schmuckler, 2001). Furthermore, the assessment of the artificiality or naturality, simplicity or complexity of an experimental design variable is highly subjective (Holleman et al., 2020). There have been attempts to make these continuums categorical to combat this subjectivity, with Matusz (et al., 2019) separating experimental design into three categories –

classical laboratory research, naturalistic laboratory research and fully-naturalistic real-world laboratory research. This was accompanied by a tool to quantify which category an experimental design correlated with most strongly. However, this was assessed via a series of questions in which the researcher themselves decided which category most closely represented their research (Naumann et al., 2022); rendering the tool, although perhaps useful, still vulnerable to subjectivity. It is also important to emphasise that complexity and naturality should be viewed from the subject's perspective. Seemingly simple experimental designs, such as our nestbox, provide great complexity and naturality in the pattern of light exposure for mice. Equally, experiments which are simple from the subject's perspective can still have ecological validity if the nature of the question being explored in the real world is also simple (Naumann et al., 2022). As such, whilst the importance of ecological validity is increasingly being recognised (Datta et al., 2019; Krakauer et al., 2017), objectively assessing the ecological validity of studies remains a challenging task (Holleman et al., 2020).

7.3.3 Does increasing ecological validity further understanding?

Whilst the concept of ecological validity is not new, it has gained traction within Neuroscience over the last decade. For example, PubMed results for "ecological validity neuroscience" produced 30 hits in 2014, 144 hits in 2023 and 98 hits for 2024 so far. Funding for projects linked to increasing ecological validity has increased in parallel – for example, the National Institute of Health BRAIN initiative has made $20 million available over the next two years to develop methods to quantify behaviour in more complex environments (Smith, 2023). Given the increase in studies and funding focusing on ecological validity, it is important to consider whether we are learning more with this approach.

One way in which ecological validity may be beneficial is by increasing the translatability of animal model results to humans. For example, the commonly used painkiller meloxicam works well when tested in a standard pain assay, but when mice are allowed to behave spontaneously (Turner et al., 2019) abnormal locomotor behaviour was detected, suggesting that meloxicam was not as effective as previously believed (Bohic et al., 2023). Standard non-ethological assays such as these could in part explain the 40-50% of human clinical trial failures that occur due to lack of clinical efficacy (when the drug doesn't produce its intended effect in humans), out of the overall failure of 90% of clinical trials (Sun et al., 2022). As such, some pharmaceuticals are thinking of adopting more naturalistic assays in drug discovery (Smith, 2023). On this topic, it is possible that the "go: no go" metric from our nestbox paradigm could be used as a more accurate measure of anxiety than conventional assessments; although this is yet to be tested. The nestbox assay would avoid handling issues, and the choice to leave or stay in a burrow (or nestbox) may be more salient to a

mouse, than, for example, the open or closed arms of an elevated plus maze. However, the use of naturalistic experimental design in drug discovery is still in its infancy, so arguably the effectiveness is yet to be evaluated.

In addition to improving the translatability of animal models, ecological validity can increase our understanding of how the brain responds to cues which drive behaviour – which is arguably a key goal of neuroscience (Datta et al., 2019). For example, insight into the neural circuitry of escape decisions has been achieved by using overhead expanding spots to mimic aerial predators (Evans et al., 2018). However, whilst increasing ecological validity can certainly promote understanding and translatability of results, it clearly does not render traditional laboratory studies unnecessary. All three of Matusz's (et al., 2019) experimental design categories (classical laboratory research, naturalistic laboratory research and fully-naturalistic real-world laboratory research) have complementary strengths and therefore should be used together.

7.4 Conclusions - do our results have ecological and external validity?

The overall objective of this thesis was to further our understanding of circadian photoentrainment under naturalistic light environments. We achieved this by incorporating features of the natural light environment, as experienced by a mouse, into our experimental design; thereby increasing ecological validity. In doing so we identified features of photoentrainment that are likely to be important under real-world conditions that had not previously been detected in laboratory studies. Our nestbox design demonstrated that behaviour is critical in regulating the timing of light exposure in mice, thereby directly determining the intensity and spectrum of light signals available for circadian photoentrainment in natural environments. Under a ramped LD cycle, wildtype mice exhibited striking peaks in light sampling behaviour at dawn and dusk, and we identified a novel role for the circadian clock in regulating the timing of these peaks. These data provide experimental evidence to support the hypothesis that burrow-dwelling species sample their light environment more at twilight, consequently regulating the timing of activity with respect to the phase response curve (Roenneberg and Foster, 1997). Furthermore, we demonstrated that the spectral cues associated with civil twilight alter the timing of mouse behaviour – extending recent work which showed spectral changes cause differences in entrainment of body temperature, and potentially corroborating their conclusions that the mouse circadian system is sensitive to colour (Walmsley et al., 2015).

It is also relevant to consider whether our approach increased the external validity of our results. In other words, are our results more representative of photoentrainment in other species and environments, than if we had obtained them under standard laboratory conditions? This is perhaps

more difficult to assess. Firstly, let us consider the role of behaviour in regulating light signals available for photoentrainment. Whilst this may be more extreme in burrow-dwelling, generally-photophobic organisms such as mice, it is still highly relevant in other species, including humans (Didikoglu et al., 2023; Siraji et al., 2023; Webler et al., 2019). This is especially true following the advent of electric lighting which has resulted in behaviour, rather than the solar cycle, being the primary determinant of light exposure in humans. This has been demonstrated by self-reported light exposure studies (Siraji et al., 2023) and those utilising wearable light sensor devices (Didikoglu et al., 2023; Okudaira et al., 1983; Webler et al., 2019). Although the pattern of retinal light exposure driven by mouse behaviour in the presence of a nestbox will not be the same as human light exposure in the real world, both will be stochastic. Therefore, our experimental design should increase the external validity of results. As discussed, ex vivo retinal electrophysiology studies with natural stimuli would further our understanding of how this behaviourally-driven temporal variation in light exposure impacts retinal responses. Secondly, our results show that spectral changes associated with civil twilight can alter mouse behaviour. These are likely to be relevant for any species capable of spectral opponency between short-wavelength and medium/long-wavelength light (Walmsley et al., 2015), which is widespread across the animal kingdom (Amann et al., 2014; Baden and Osorio, 2019; Jacobs, 1993; van der Kooi et al., 2021). Regarding directional variation in spectrum driven by reflectance explored in Chapter 6, these may actually be *more* relevant to diurnal, non-burrowing species such as humans, compared to mice (Webler et al., 2019) – since they are exposed to more light during the day. Therefore, it is possible to argue that our methods have increased not only the ecological validity but external validity of our results.

So, should all the elements of the natural light environment investigated in this thesis be integrated into standard circadian neuroscience laboratory studies? Providing a nestbox and using a ramped LD cycle (of any spectrum) arguably had the most significant effects on promoting naturalistic behaviour in mice (Chapters 3 to 5), whilst spectrum modulated the timing of light sampling behaviour (Chapter 5). Compared to the technical challenges of re-creating the spectral characteristics of daylight and twilight in the laboratory, adding a dark shelter and ramping the LD cycle are relatively simple interventions. Although, violet pumped LEDs could easily be used to provide higher levels of S-cone activation, even if natural spectral changes are not modelled (Lucas et al., 2024). These results are relevant for laboratory rodent research more widely. For example, the effect of simplified LD cycles has been raised as a concern in immunology (Graham, 2021) – since many features of the mammalian immune system are under circadian control (Hopwood et al., 2018; Onishi et al., 2020). Since experimental complexity must be traded off with feasibility,

the data in this thesis presents a convincing case for recommending the provision of a dark shelter and a ramped LD cycle in rodent circadian neuroscience studies, as well as in rodent research more widely (Lucas et al., 2024).

To conclude, by taking a naturalistic approach to the study of photoentrainment, we have furthered our understanding of circadian responses under natural conditions. This thesis demonstrates an important role for behaviour in regulating the timing of light exposure for photoentrainment, and the significance of spectral cues at twilight for the timing of activity onset. In addition, we identify that natural light environments have considerable directional variation, which raise interesting future questions regarding the relevance of this to circadian behaviour. Therefore, collectively, our data emphasise that the light signals available for photoentrainment in natural environments vary not only in intensity and spectrum, but along temporal and directional axes.

Appendix. The effect of nestbox availability on behavioural anxiety levels

1. Introduction

As demonstrated in Chapter 3 of this thesis, C57BL/6J mice will extensively reduce their daily light exposure to less than an hour across the 24hr period, when provided with a dark nestbox. Light is a very powerful stimulus for many aspects of physiology and behaviour, including learning and memory, mood, and sleep and arousal (Do, 2019). Therefore, our results raise the question of whether the inability to self-select light exposure under standard laboratory conditions may be influencing other behaviours and physiological processes, such as anxiety levels, that go largely unaccounted for in experimental designs. Adult mice show an increase in anxiety and depressive-like behaviours when exposed to constant light (LL) (Fonken et al., 2009) or altered light regimes as adults (Bouwknecht et al., 2007), or to dim light at night during early development (Borniger et al., 2014). The provision of an opaque, but not clear, tube reverses the increase in depressive-like behaviour seen on the forced swim test under LL (Fonken et al., 2009). We therefore hypothesised that providing the opportunity for mice to self-select their light regimen via the provision of a dark nestbox, would reduce levels of anxiety-like behaviour in mice, with important implications for animal welfare (Swetter et al., 2011).

Anxiety is a form of defensive behaviour; a set of highly conserved and adaptive responses to dangerous situations (Blanchard and Blanchard, 2008). More specifically, anxiety is a response to a *potential* danger, which is associated with uncertainty as to how to react most appropriately (Collins, 2023; Lezak et al., 2017). In contrast, fear is a response to an imminent threat, driving active avoidance if escape is possible, or freezing behaviour if not (Blanchard and Blanchard, 2008; Penninx et al., 2021). Finally, panic is evoked by immediate and unavoidable danger (Blanchard et al., 2001; Deakin and Graeff, 1991) - with depression developing in response to chronic exposure to an unavoidable threat, resulting in learned helplessness and behavioural despair (Collins, 2023; Wang et al., 2017). Although anxiety and fear can result in some similar physiological and behavioural responses, including elevated heart rate, increased arousal and vigilance, hypoactivity and suppressed food consumption (Lezak et al., 2017), they are associated with different brain regions - with the amygdala mediating fear-like behaviour and the bed nucleus of the stria

terminalis (BNST) (Walker et al., 2003) and ventral hippocampus (Forro et al., 2022) regulating anxiety-like behaviour.

Whilst anxiety, fear and panic are adaptive responses, if generated excessively or in inappropriate contexts, it can be maladaptive and be considered a disorder (Penninx et al., 2021). These can be categorised into generalised anxiety disorder, panic disorder and specific phobias (File et al., 1998; Judd et al., 1985). These different disorders were discovered in part from the varying efficacy of anxiolytic drugs, such as benzodiazepines, in treating them. Benzodiazepines are most effective at treating generalised anxiety, but becomes less effective against panic disorder, for which anti-depressants are more appropriate, and finally are ineffective against specific phobias where exposure therapy is required (File et al., 1998).

In this study, a battery of behavioural tests were selected to quantify anxiety levels – the elevated plus maze (EPM), open field (OF) test and light-dark box (LDB) test (Chen et al., 2024). Whilst these are all tests of unconditioned anxiety, using multiple tests reduces the likelihood that any phenotype is due to another aspect of sensorimotor or motivational performance, as well as providing a range of anxiogenic conditions which may help avoid ceiling or floor effects. The EPM, OF and LDB tests exploit the approach-avoidance conflict – the conflict between potential threats and rewards associated with exploration of a novel and potentially exposed environment. Mice have a natural desire to explore novel environments and objects (Barnett and Cowan, 1976; Hughes, 1997). However, they are simultaneously photophobic (Bourin and Hascoët, 2003; Crawley et al., 1980) and are fearful of novel or exposed places, and exhibit thigmotaxis – the innate desire to seek shelter (Barnett, 1963; Zhang et al., 2023). Therefore, conflict is generated in these tests by the option of exploring the EPM open arms or the safer, closed arms (File et al., 1998); the OF's brighter and more open central zone or the more sheltered outer zone (Võikar and Stanford, 2023); and the light or dark compartment of the LDB test (Campos-Cardoso et al., 2023; Crawley et al., 1980).

2. Materials and Methods

2.1 Animals and housing

This study used 24 C57BL/6J mice (12 males and 12 females), aged 10 weeks at the start of the experiment. Animals were group housed for an initial habituation week, before being singly housed for the remainder of the experiment, at 20-24°C and 45-65% ± 10% humidity, with *ad libitum* access to food (Envigo 2916) and water. Cages were placed within light-tight ventilated chambers (LTC) equipped with multiple cool-white light-emitting diodes (LEDs) (Luxeon Star LEDs;

Quadica Developments) set at 200 photopic lux (130 melanopic lux) on a 12h:12h square-wave light dark cycle. The spectral power distribution of the cool-white LED consisted of a high, narrow peak at ~450nm and a lower, broader peak at ~560nm. All mice were culled by Schedule 1 at the end of the experiment. All experimental procedures were conducted at the University of Oxford, England, in accordance with the United Kingdom Animals (Scientific Procedures) Act 1986 under Project License PP0911346 and Personal License I82616702.

2.2 Experimental design

The cohort was randomly split into two equal and sex-balanced groups (group A and group B). Both groups were habituated to new light dark (LD) cycles for one week: group A (lights on at 04:10, lights off at 16:10) and group B (lights on at 06:10, lights off at 18:10) so that both groups could be tested at the same zeitgeber time (ZT). Following habituation, all mice were singly housed for two weeks – group A under standard laboratory conditions described above, and group B with a dark nestbox in each cage. For details of the nestbox, please see section 3.3.3.

Following two weeks of different housing regimens, all mice in both groups were tested once on each of the following behavioural anxiety tests: EPM, OF and LDB test; with two days between each test. This series of tests is referred to as 'Trial 1'. Mice were tested in a counterbalanced order, considering group, sex, order of test type and starting compartment of the light-dark box test (i.e. either the light box or dark box; Deacon and Rawlins, 2005) (Table 1). Both groups of mice were tested at the equivalent ZT period - group A mice were tested between 09:30 and 11:00 (ZT5.3 – ZT6.8) and group B mice were tested between 11:30 and 13:00 (ZT5.3 and ZT6.8). All mice were then singly housed for a further two weeks but with the housing conditions reversed – group A with nestboxes, and group B without (control). All mice were then tested again (Trial 2) on the behavioural anxiety tests, following the same schedule as Trial 1.

Group	Sex	Day 1	Day 2	Day 3	Day 4	Day 5	Day 6	Day 7	Day 8
A	F	LDB			EPM			OF	
A	F	OF			LDB			EPM	
A	F	EPM			OF			LDB	
A	F		LDB			EPM			OF
A	F		OF			LDB			EPM
A	F		EPM			OF			LDB
A	M	LDB			EPM			OF	
A	M	OF			LDB			EPM	
A	M	EPM			OF			LDB	
A	M		LDB			EPM			OF
A	M		OF			LDB			EPM
A	M		EPM			OF			LDB
B	F	LDB			EPM			OF	
B	F	OF			LDB			EPM	
B	F	EPM			OF			LDB	
B	F		LDB			EPM			OF
B	F		OF			LDB			EPM
B	F		EPM			OF			LDB
B	M	LDB			EPM			OF	
B	M	OF			LDB			EPM	
B	M	EPM			OF			LDB	
B	M		LDB			EPM			OF
B	M		OF			LDB			EPM
B	M		EPM			OF			LDB

Table 1. Behavioural anxiety testing schedule, for each trial. EPM (elevated plus maze test), OF (open field test), LDB (light-dark box test). Yellow LDB denotes the animal starting in the light compartment, grey LDB denotes the animal starting in the dark compartment.

2.3 Behavioural anxiety testing

All tests were carried out in the room adjacent to the housing room, and mice were transported in dark, light-tight cages prior to testing. Each test ran for 10 minutes and was carried out under a cool white LED, at 200 photopic lux (130 melanopic lux) - as measured on the floor of the elevated plus maze, open field test box and light box (of the light-dark box), to match the light in the home cage environment. Automated tracking of behaviour was conducted using a USB video camera linked to ANY-maze software (Stoelting; RRID:SCR_014289), and entry into a zone was determined using the centre of the animal for all tests. All apparatuses were cleaned with 70% ethanol spray between each test.

2.3.1 Elevated plus maze (EPM) test

The EPM consisted of a cross-shaped maze with two closed arms (30 x 5cm with 20cm walls) opposite each other, two perpendicular open arms (30 x 5cm) and a central region (5 x 5cm), all elevated 50cm above the ground. The base of the maze was made of wood, painted black, whilst the walls of the closed arms were made of transparent perspex. Mice were put into the central

region of the maze facing the closed arms, and tracked for 10 minutes. The following behavioural parameters were extracted from ANY-maze: time in open arm (as a % of time in open and closed arms), open arm entries (as a % of open and closed arm entries) and open arm distance (as a % of total distance travelled), with higher levels indicating lower anxiety levels (Pellow et al., 1985). In addition, total distance travelled was extracted as a measure of overall locomotor activity.

2.3.2 Open field (OF) test

The OF consisted of a 25 x 25cm square chamber, with 25cm high walls. Two zones were created using the ANY-maze software – an 'outer zone' measuring 5cm in width around the perimeter of the chamber, and a 'central zone' measuring 15 x 15cm in the middle of the chamber. A third 'corner zone' was generated within the 'outer zone', consisting of 5 x 5cm square in each of the chamber corners. Mice were placed in the centre of the chamber and tracked for 10 minutes. The following behavioural parameters were extracted from ANY-maze: time in outer zone (as a % of total time), time in corner zones (as a % of total time) and total distance travelled (m). Lower levels of these first two parameters are considered to be indicative of lower anxiety levels (Prut and Belzung, 2003), whilst total distance travelled is a measure of overall locomotor activity.

2.3.3 Light-dark box (LDB) test

The LDB test consists of two adjacent compartments, each measuring 20 x 20cm, with 40cm high walls and a lid. The compartments are joined by a small open archway. One compartment is constructed from black plastic, is dark and the lid fitted with an IR USB camera ('dark compartment'). The other compartment is constructed from white plastic, and the lid is fitted with a cool white LED (Luxeon Star LEDs; Quadica Developments) set at 200 photopic lux (130 melanopic lux) and a USB camera ('light compartment'). Mice were placed into either of the compartments at the start of the test (the starting compartment was counterbalanced across groups and sex) and tracked for 10 minutes. The cameras were connected to ANY-maze tracking software and the following behavioural parameters were extracted: time spent in dark box (as a % of total time) and total number of transitions between compartments. Less time spent in the dark box indicates reduced anxiety, whilst total number of transitions is a measure of overall locomotor activity (Crawley et al., 1980).

2.4 Data processing and statistical analysis

Data were extracted from ANY-maze for each test into Excel (v.2310) in 1 minute bins across minutes 1 to 5 of the test, as is common practice in this field's literature (Bailey and Crawley, 2009; Collins, 2023; Glover et al., 2017). Prism Graph-pad (v.9.5.0 (730)) was used for data visualisation and statistical analysis, and SPSS (v.29.0.2.0(20)) was used for additional statistical analysis.

Normality was assessed using the Kolmogorov-Smirnov test (Prism Graph-pad). The following datasets were established to be parametric following a sqrt-transform: Fig.1C, Fig.2A,C; Fig.4D and Fig.5C. Although the following datasets were found to be non-parametric, and a sqrt-transform failed to correct this, a 3-way or 4-way ANOVA was still performed due to a lack of a non-parametric alternative: Fig.3A,B; Fig.4A,B,C; Fig.5A,B; Fig.6A,B.

There was a significant effect of repeat testing (trial 1 vs trial 2) on all tests, so trial 1 data were analysed independently (Fig.1-3) using 3-way repeated measures (RM) ANOVAs to explore the effect of housing condition, sex and test minute on anxiety and activity parameters. A mixed-effects model was used for trial 1 LDB total transitions since data values were missing due to an ANYmaze recording error. The order in which animals received different anxiety tests (EPM, OF, LDB) was also incorporated as a between-subjects factor in preliminary analysis, but had no significant main effect or interactions so was removed from the final analysis. To assess the effect of starting box (light or dark box) in the LDB test on anxiety and activity parameters, a 3-way ANOVA (condition, sex, starting box) was also used. There was no main effect of starting box on time spent in dark box or total number of transitions (data not presented). 4-way RM ANOVAs were used to explore the effect of group, sex, trial (trial 1 vs trial 2) and test minute on anxiety and activity parameters across trials 1 and 2 (Fig.4-6). There was only a significant main effect of sex on total distance travelled in the EPM (Fig.4D), so this factor was not visualised.

In all cases, Mauchly's test was used to check for sphericity, and a Greenhouse-Geisser correction applied where the assumption of sphericity was violated. Greenhouse-Geisser corrected degrees of freedom were reported in the following figures: Fig.1C, Fig.3A, Fig.4A, Fig.4B, Fig.5B, Fig.6B. Where a significant main effect or interaction was observed, a post-hoc test with Bonferroni correction for multiple comparisons was performed. All data are reported as mean +/- SEM and $\alpha = 0.05$ was adopted in all analyses. All ANOVA results for trial 1 are reported in supplementary table 1, and trial 1 versus 2 in supplementary table 2.

3. Results

3.1 Trial 1 (Fig.1-3)

3.1.1 No significant effect of nestbox availability on anxiety measures was observed in trial 1, across the EPM (Fig.1), OF (Fig.2) or LDB (Fig.3) test.

Measures of anxiety can be confounded by levels of overall activity (File, 2001, 1985). Therefore, a measure of overall activity was explored for each test in addition to anxiety parameters. In the

EPM, there was no significant effect of condition on total distance travelled (Fig.1A) [$F(1,20) = 1.7$, $p = 0.203$], allowing for comparison of anxiety parameters. Although there was a slight trend towards decreased anxiety under the nestbox condition as measured by time spent (Fig.1B) and distance travelled (Fig.1C) in the open arms of the EPM, this did not reach the threshold for significance in either parameter [open arm time, $F(1,20) = 1.9$, $p = 0.188$; open arm distance, $F(1,20) = 2.2$, $p = 0.152$]. In the OF, there was no significant effect of nestbox condition on total distance travelled (Fig.2A) [$F(1,20) = 0.1$, $p = 0.729$], as well as no significant effect of condition on either anxiety parameter - time in outer zone (Fig.2B) [$F(1,20) = 0.3$, $p = 0.608$] and corner zones (Fig.2C) [$F(1,20) = 0.0$, $p = 0.912$]. In the LDB, there was no significant effect of nestbox condition on total transition number, a measure indicative of overall activity (Fig.3A) [$F(1,19) = 2.0$, $p = 0.171$]; or on the anxiety measure - time spent in the dark box (Fig.3B) [$F(1,20) = 1.2$, $p = 0.285$].

3.1.2 Effect of test minute on anxiety measures across trial 1 in the EPM (Fig.1), OF (Fig.2) and LDB (Fig.3) test.

A trend of increasing anxiety across time in trial 1 in the EPM was observed across the first 5 minutes of the test, as measured by open arm distance (Fig.1C) [$F(3.0,60.3) = 2.9$, $p = 0.043$]. This trend is particularly clear in the control condition, however, there is no significant condition by test minute interaction. However, total distance travelled also significantly decreases with test minute (Fig.1A), suggesting that the increased anxiety observed across time, as measured by open arm distance, could result from an overall decrease in exploration due to habituation, rather than a genuine increase in anxiety. Conversely, in the LDB, time spent in the dark box decreases significantly across test minute main effect of test minute on dark box time suggesting reduced anxiety levels [$F(4,80) = 3.1$, $p = 0.021$]; but similarly, a main effect of test minute on total transitions [$F(2.0,37.5) = 3.8$, $p = 0.031$] indicates that apparent changes in anxiety levels may result from changes in overall exploration. Interestingly, however, in the OF test the time spent in the outer zone (FIg.2B) decreases significantly across the test [$F(4,80) = 3.0$, $p = 0.025$] but is not accompanied by a significant effect of test minute on total distance travelled (Fig.2A) [$F(4,80) = 1.6$, $p = 0.173$], suggesting it is more likely that the decrease in anxiety is a genuine effect (Fig.1B).

In summary, there was no significant effect of housing mice with a nestbox for two weeks on anxiety or overall activity levels across trial 1 of the EPM, OF and LDB test, suggesting that the ability to self-select light exposure does not have a significant effect on anxiety levels in mice.

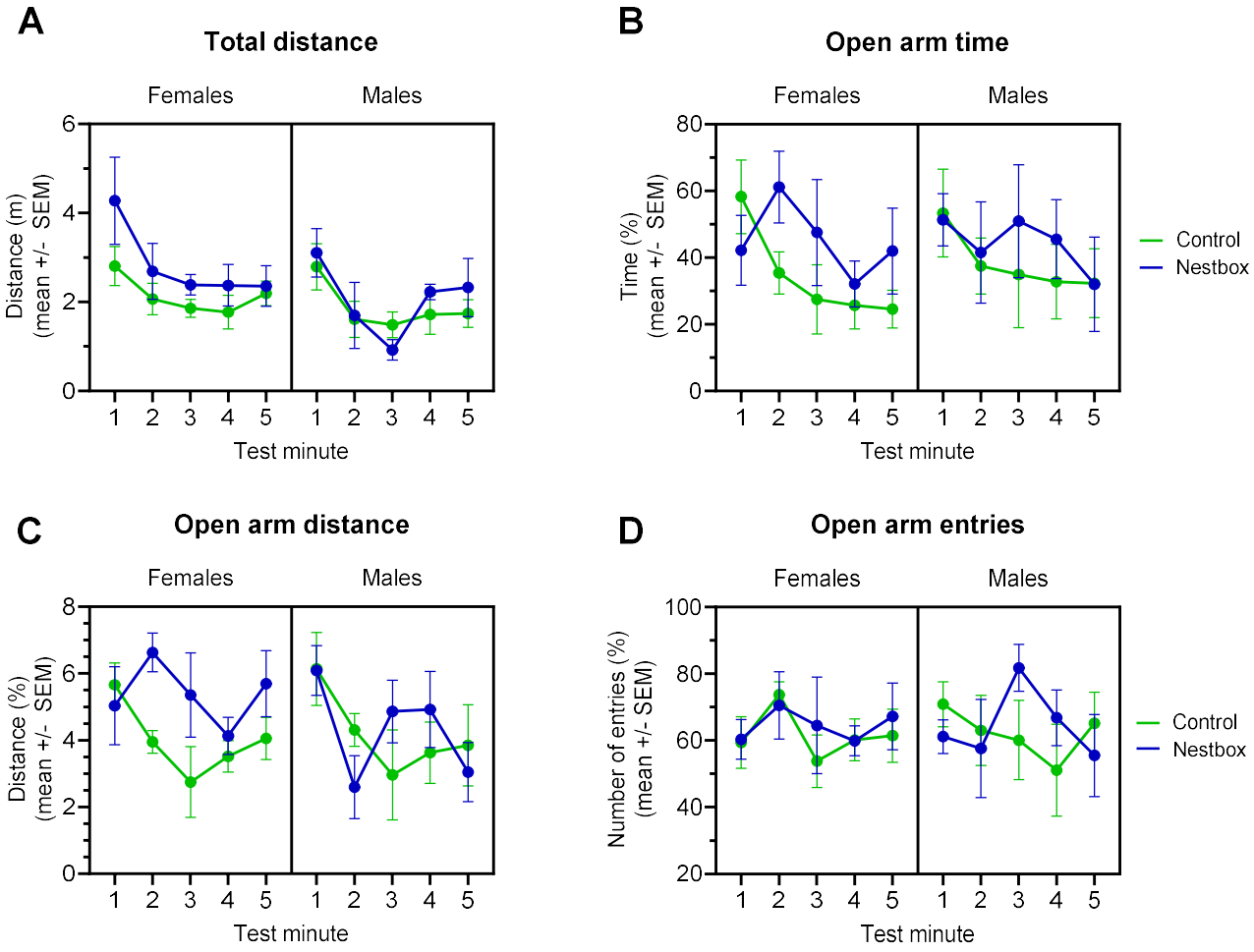

Figure 1 - Elevated plus maze, trial 1 (min 1-5). **(A)** Total distance travelled (m). **(B)** Open arm time (as a % of open + closed arm time). **(C)** Open arm distance (as a % total distance). **(D)** Open arm entries (as a % of open + closed arm entries). All parameters reported across conditions (control – green, nestbox – blue), sex (females – left panel, males – right panel) and test minute 1-5. All data reported as mean +/- SEM. Data in panel C has been sqrt-transformed. 3-way repeated measures ANOVA, with post-hoc Bonferroni test (*$p < 0.05$, **$p < 0.01$, ***$p < 0.001$).

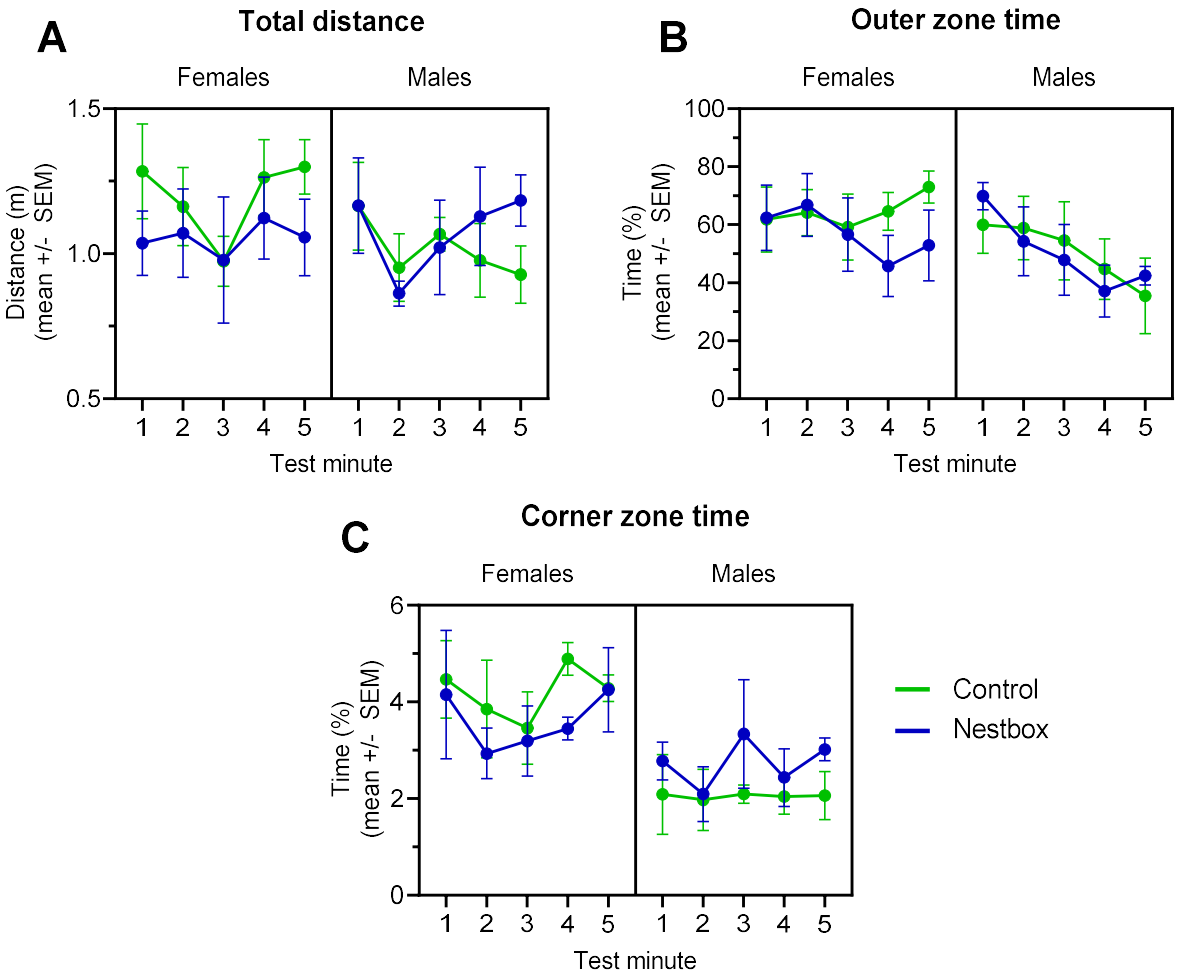

Figure.2 - Open field test, trial 1 (min 1-5). **(A)** Total distance travelled (m). **(B)** Time spent in outer zone (as a % of total time). **(C)** Time in corner zone (as a % of total time). All parameters reported across conditions (control – green, nestbox – blue), sex (females – left panel, males – right panel) and test minute 1-5. All data reported as mean +/- SEM. Data in panel B and C have been sqrt-transformed. 3-way repeated measures ANOVA, with post-hoc Bonferroni test (*$p < 0.05$, **$p < 0.01$, ***$p < 0.001$).

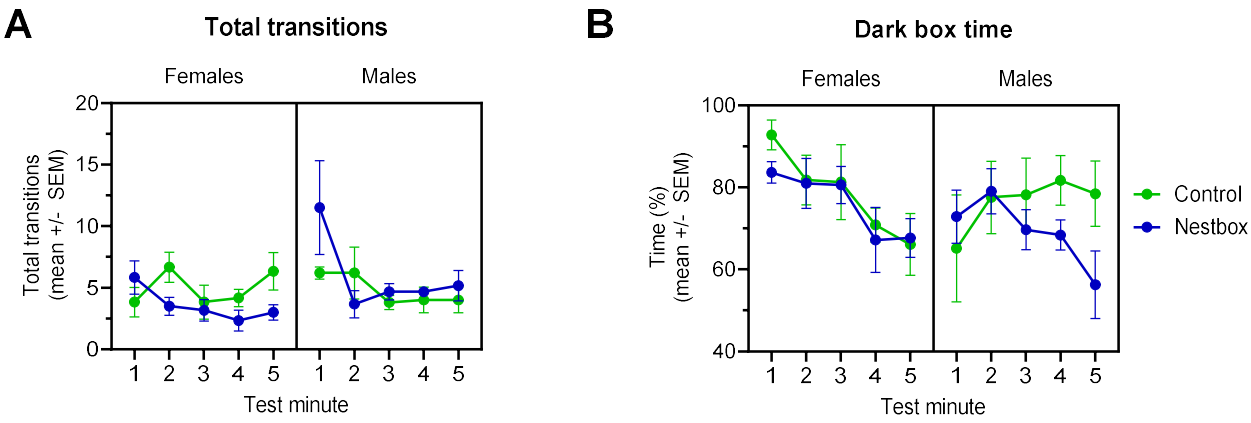

Figure 3 - Light dark box test, trial 1 (min 1-5). **(A)** Total number of transitions between boxes. **(B)** Time spent in dark box (as % of total time). All parameters reported across conditions (control – green, nestbox – blue), sex (females – left panel, males – right panel) and test minute 1-5. All data reported as mean +/- SEM. 3-way repeated measures ANOVA, with post-hoc Bonferroni test (*$p < 0.05$, **$p < 0.01$, ***$p < 0.001$).

3.2 Trial 1 and 2 data combined (Fig. 4-6)

3.2.1 A significant increase in anxiety measures was observed in EPM and OF in trial 2 compared to trial 1.

To explore whether there would be significant within-subject differences between control and nestbox conditions, a second trial of behavioural tests was performed a minimum of 2 weeks later. However, these results were confounded by a significant increase in measures of anxiety on trial 2 compared to trial 1 in the EPM (Fig.4) and OF (Fig.5) test, regardless of condition (EPM: open arm time Fig.4A) [$F(1,20) = 21.8$, $p < 0.001$]; open am entries (Fig.4B) [$F(1,20) = 22.2$, $p < 0.001$]; open arm distance (Fig.4C) [$F(1,20) = 69.7$, $p < 0.001$]. OF test: time in outer zone (Fig.5A) [$F(1,20) = 4.4$, $p = 0.050$]; time in corner zone (Fig.5B) [$F(1,20) = 4.8$, $p = 0.040$]). However, these increased levels of anxiety measures in trial 2 compared to trial 1 could result from habituation to the testing paradigm causing lower levels of exploration, rather than reflecting a genuine increase in anxiety, since measures of overall activity decrease significantly in trial 2 compared to trial 1. This is observed across all test types [EPM total distance (Fig.4D), main effect of trial, [$F(1,20) = 29.1$, $p < 0.001$]; OF total distance (Fig.5C), main effect of trial, [$F(1,20) = 15.9$, $p < 0.001$]; LDB total transitions (Fig.6B), main effect of condition, $F(1,19) = 4.4$, $p = 0.049$].

3.2.2 Effect of test minute and group on anxiety measures within and across trials in the EPM (Fig.4), OF (Fig.5) and LDB (Fig.6).

There was a significant main effect of test minute for both open arm time (Fig.4A) [$F(2.4, 47.3) = 2.8$, $p = 0.023$] and open arm distance (Fig.4C) [$F(4,80) = 4.5$, $p = 0.002$] in the EPM, with measures of anxiety increasing within and across both trials. This effect has been observed frequently with the EPM (File, 1993, 1990; File et al., 1998) and may be indicative of a specific phobia of the open arms being learnt early in trial 1, resulting in the testing of a different emotional state in trial 2 compared to trial 1. Group A mice were housed in the control condition prior to trial 1 and the nestbox condition prior to trial 2, whilst the order was reversed in group B mice. For all EPM anxiety parameters, group A mice showed lower levels of anxiety in minute 1 of trial 1, but higher levels of anxiety across the rest of trial 1 and trial 2 compared to group B mice; however, the effect of group did not reach significance in any parameter [open arm time, $F(1,20) = 3.9$; $p = 0.063$; open arm entries, $F(1,20) = 1.9$; $p = 0.182$; open arm distance, $F(1,20) = 3.2$, $p = 0.088$] and there was no significant group by trial interaction. These data are difficult to interpret. However, the trend could suggest that being housed with a nestbox on trial 1 (group B) may slow the acquisition of the specific phobia of open arms across trial 1, resulting in higher levels of open arm time, entries and distance at the start of trial 2. Although this difference between groups in minute 1 of trial 2 only reaches significance in open arm entries. To explore this further, minute 1 of each trial was compared across groups for the EPM parameters (Fig.7) and a significant increase in anxiety was observed between trials 1 and 2 in all parameters following the post-hoc Bonferroni test for group A (open arm time, $p = 0.0125$; open arm entries, $p = 0.0248$; open arm distance, $p = 0.0042$), but not group B.

In the OF (Fig.5), as previously discussed there was a significant increase in anxiety measures in trial 2 across all parameters. There was also a significant effect of test minute on time in the outer zone (Fig.5A) [$F(4,80) = 6.3$, $p < 0.001$]. This differed between groups, resulting in a significant test minute by group interaction [$F(4,80) = 2.6$, $p = 0.044$] – group A showed consistent levels of time in the outer zone within trials, whilst group B showed clear decreases. Similarly, in the LDB test (Fig.6) there was a significant effect of test minute on time in dark box (Fig.6A) [$F(4,80) = 3.4$, $p = 0.013$] and test minute by group interaction [$F(4,80) = 2.9$, $p = 0.028$]; with group B mice showing significantly higher levels of anxiety in minute 1 of trial 2 than group A mice. It is not clear what is driving these differences, but it is possible that mice in group B habituated less to the LDB in trial 1 and therefore showed greater anxiety at the start of trial 2 than group A mice.

In summary, there was no significant effect of housing mice with a nestbox for two weeks on anxiety levels across trial 1 of the EPM, OF and LDB test. In trial 2, a significant increase in

measures of anxiety, regardless of nestbox condition, was observed across all behavioural tests; confounding any within-subject comparisons of nestbox condition. A significant decrease in overall activity across all test types in trial 2 compared to trial 1, regardless of condition, suggests that an increase in anxiety measures may result from habituation to the testing paradigm. In some parameters, the order in which mice received each condition (group A vs B) appeared to have an effect; e.g. perhaps on the rate of acquisition of a specific phobia of the open arms (Fig.4A,C) although this was not significant, or the levels of habituation to the LDB test during trial 1 (Fig.6A). However, these results are difficult to interpret and further experiments would be required to come to firm conclusions.

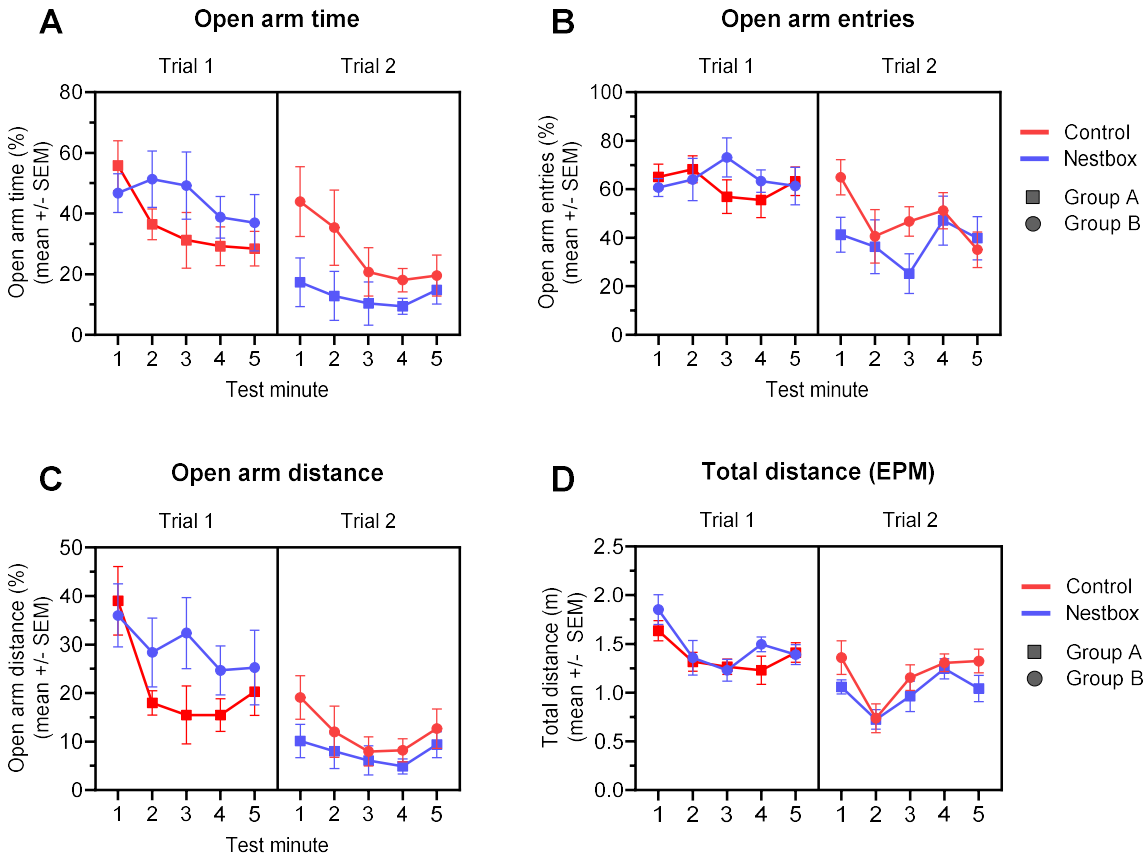

Figure 4 - Elevated plus maze, trial 1 vs trial 2 (min 1-5). **(A)** Open arm time (as a % of open + closed arm time). **(B)** Open arm entries (as a % of open + closed arm entries). **(C)** Open arm distance (as a % total distance). **(D)** Total distance travelled (m). In all parameters reported across trials (trial 1 – left panels, trial 2 – right panels), condition (control – red, nestbox – blue), group (group A – square, group B – circle) and test minute 1-5. Data in panel D has been sqrt-transformed. All data reported as mean +/- SEM. 4-way repeated measures ANOVA (between-subjects factor of sex not visualised), with post-hoc Bonferroni test (*$p < 0.05$, **$p < 0.01$, ***$p < 0.001$).

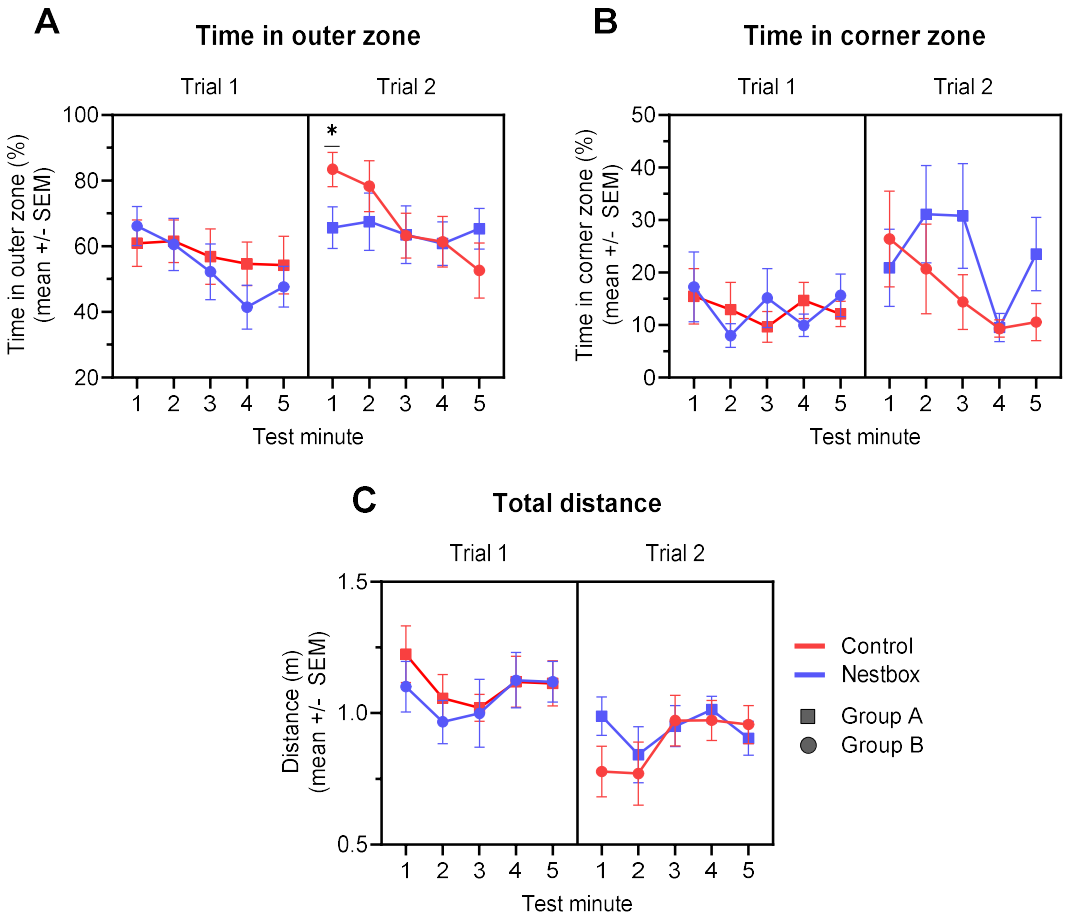

Figure 5 - Open field test, trial 1 vs trial 2 (min 1-5). **(A)** Time spent in outer zone (as a % of total time). **(B)** Time in corner zone (as a % of total time). **(C)** Total distance travelled (m). In all parameters reported across trials (trial 1 – left panels, trial 2 – right panels), condition (control – red, nestbox – blue), group (group A – square, group B – circle) and test minute 1-5. Data in panel C has been sqrt-transformed. All data reported as mean +/- SEM. 4-way repeated measures ANOVA (between-subjects factor of sex not visualised), with post-hoc Bonferroni test (*$p < 0.05$, **$p < 0.01$, ***$p < 0.001$).

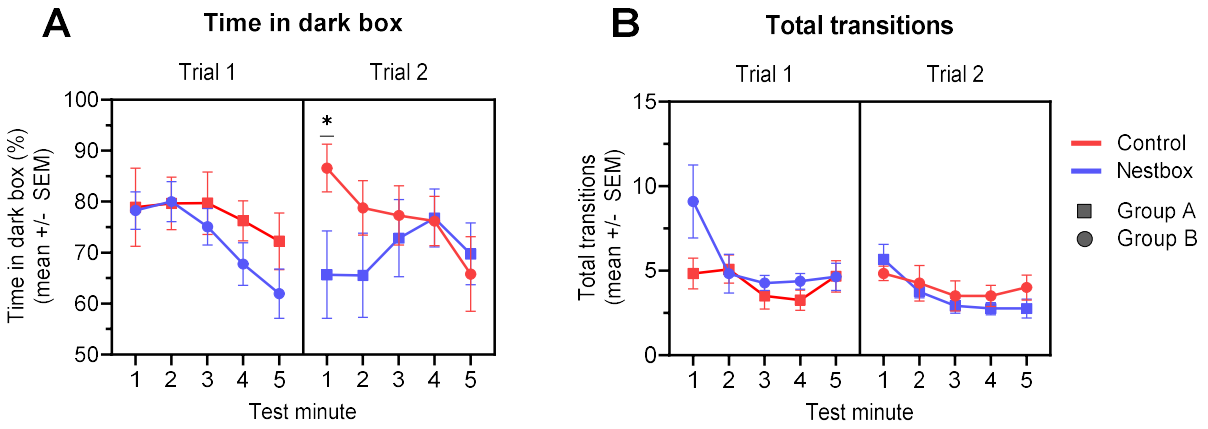

Figure 6 - Light dark box test, trial 1 vs trial 2 (min 1-5). **(A)** Time spent in dark box (as % of total time). **(B)** Total number of transitions between boxes. Both parameters reported across trials (trial 1 – left panels, trial 2 – right panels), condition (control – red, nestbox – blue), group (group A – square, group B – circle) and test minute 1-5. All data reported as mean +/- SEM. 4-way repeated measures ANOVA (between-subjects factor of sex not visualised), with post-hoc Bonferroni test (*$p < 0.05$, **$p < 0.01$, ***$p < 0.001$).

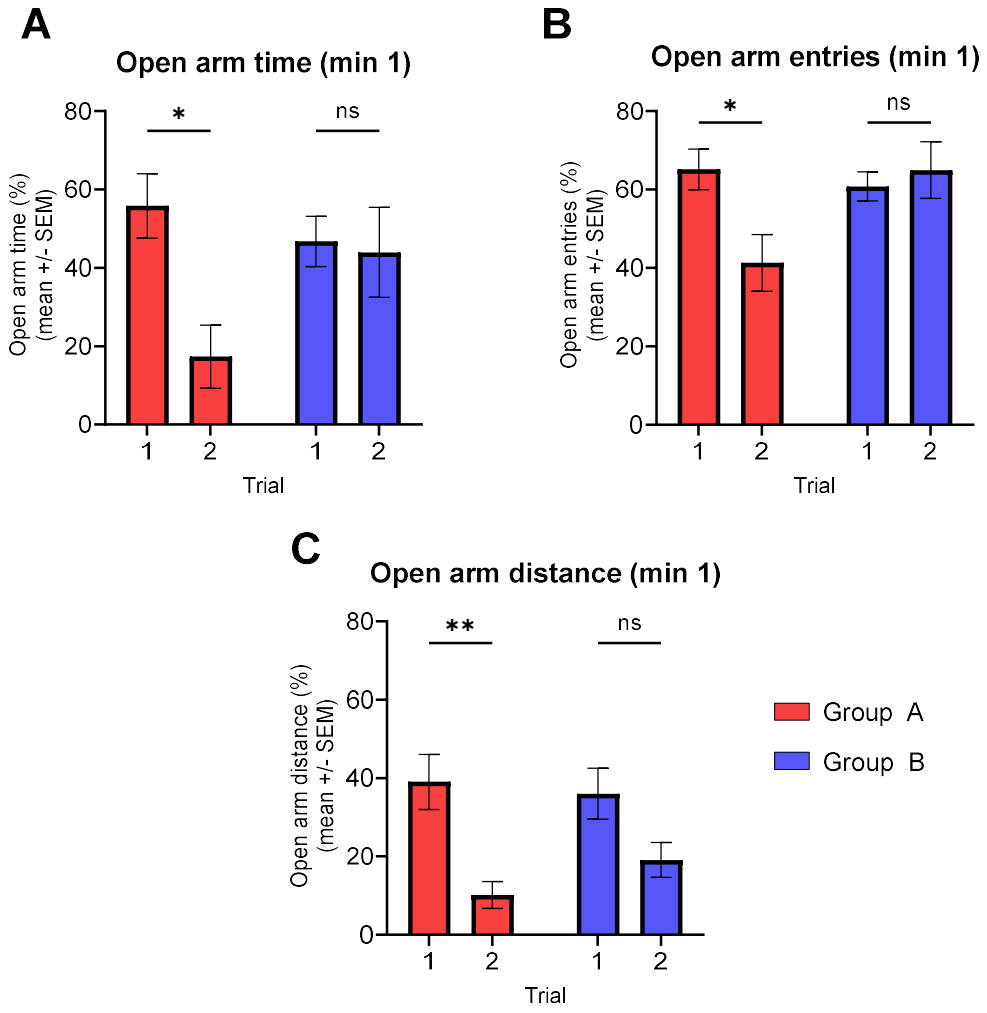

Figure 7 - Elevated plus maze, trial 1 vs trial 2 (min 1). **(A)** Open arm time (as a % of open + closed arm time). **(B)** Open arm entries (as a % of open + closed arm entries). **(C)** Open arm distance (as a % total distance). All parameters reported across trials and group (group A – red, group B – blue). All data reported as mean +/- SEM. 2-way ANOVA, with post-hoc Bonferroni test (*$p < 0.05$, **$p < 0.01$, ***$p < 0.001$).

4. Discussion

This study investigated whether long-term housing with a dark nestbox, and therefore the opportunity for mice to self-select their light exposure, would decrease anxiety-like behaviour as quantified by the EPM, OF and LDB tests. Each animal received two trials of each test type, with trial 1 preceded by two weeks of housing under the control (no nestbox) or nestbox condition, and trial 2 preceded by two weeks of housing under the alternate condition (control/nestbox), to allow for within-subject analyses. However, regardless of condition, a significant increase in measures of anxiety on trial 2 across the EPM and OF was observed. This observation likely arises from habituation to the testing paradigm, as demonstrated by a significant decrease in overall activity in trial 2 compared to trial 1, across all tests. Therefore, to assess the key question of interest – the effect of nestbox availability on anxiety levels, data from trial 1 only was used. However, in contrast to our predictions, we found no significant effect of nestbox availability on anxiety levels across the EPM (Fig.1), OF (Fig.2) or LDB test (Fig.3). This could reflect a genuine lack of effect of nestbox availability on anxiety levels. Indeed, no significant effect of providing an opaque tube under LD conditions for 3 weeks was observed in the EPM or OF test in male Swiss-Webster mice (Fonken et al., 2009). However, since within-subject comparisons were not possible, the between-subject comparisons could have subsequently been underpowered and unable to detect differences against high levels of intraspecific variation.

In addition, other factors may have confounded the results. Mice housed without a nestbox are likely to be more habituated to higher light levels and open spaces than mice housed with nestboxes. In parallel, light has a direct role in generating anxiogenic conditions in the LDB, OF (outer zone is dimmer) and EPM (closed arms may be dimmer), whilst open space generates anxiogenic conditions in the EPM and OF. Therefore, it is possible that these tests are inappropriate for testing subtle effects of a condition (nestbox availability) that may alter anxiety via modifying light exposure or habituation to enclosed spaces. To explore this idea, the daily light exposure of animals in the nestbox condition (reflecting extent of nestbox use) was correlated with anxiety parameters from the EPM, OF and LDB tests to assess if mice with lower daily light exposure levels showed reduced anxiety levels. However, no significant correlation was observed against any anxiety parameter (data not presented). To combat this potential limitation, other tests of anxiety, where light levels or open space are not associated with anxiety parameters could be used instead, such as ambiguous cue fear conditioning (Glover et al., 2017). The OF test has also received criticism, questioning whether reduced time in the central zone is actually indicative of anxiety-like behaviour, since only 56% of published studies reported an increase in central zone

activity following treatment with an established anxiolytic drug (Prut and Belzung, 2003; Võikar and Stanford, 2023).

There was a significant effect of trial on measures of anxiety across tests (Fig.4,5,6), with higher levels of anxiety measures in trial 2 regardless of condition. Issues with repeat testing have been commonly observed in the EPM (e.g. File et al., 1998), whilst prior exposure to an EPM can also limit the efficacy of benzodiazepines on LDB test results (Rodgers et al., 1992). Therefore, it is important to consider what the parameters that are indicative of anxiety in trial 1, are actually reflecting in trial 2. All these tests rely partly on novelty, and therefore repeat testing may result in habituation – a decrease in an innate response to a repeated stimulus (Çevik, 2014). In this context, habituation would lessen the approach-avoidance conflict since animals may have already explored the EPM open arms, OF test central zone and LDB light compartment (Bloch and Belzung, 2023; Võikar and Stanford, 2023). As demonstrated by the significant decreases in overall activity across all test types in this study, it is likely that the apparent increase in anxiety is actually a decrease in exploration.

The literature also demonstrates that the nature of emotional response generated in the EPM can change across trial 1 to trial 2, from unconditioned anxiety to a learnt specific phobia of the open arms, perhaps related to height. It is this latter state which is then tested in trial 2. This is referred to as the one trial tolerance phenomenon – since anxiolytic drugs are effective on trial 1, but not trial 2 (File, 1990; File et al., 1998). Rats with basolateral amygdala lesions immediately following trial 1 responded successfully to benzodiazepines in trial 2, suggesting a key role of this region in forming specific phobias (File et al., 1998). Our experimental design aimed to limit the generation of one trial tolerance by using 10 min trials, shown to extinguish the specific phobia of open arms due to extended exposure (File, 1993). In addition, we used a 2 week inter-trial interval - since an inter-trial interval of up to 2 weeks is known to result in one trial tolerance (File, 1990); although an interval beyond 2 weeks has not been tested (File, 1990). Despite these precautions, our data show a significant increase in anxiety-like behaviour in the EPM across trials in group A, but not group B (Fig.7) – perhaps reflecting a difference in acquisition rate of the learnt specific phobia between groups. Could the availability of a nestbox prior to trial 1 in group B lead to a reduced acquisition of the specific phobia compared to the control condition experienced by group A? The literature raises several interesting, and potentially conflicting suggestions. Stress influences different types of learning in differing ways (Sandi and Pinelo-Nava, 2007) - there is a linear-asymptotic relationship between stress and fear learning, but an inverted U-shape relationship with higher order learning such as spatial learning (Sandi et al., 1997). It is possible that control mice prior to trial 1 are more stressed since they have not been housed with a nestbox, which provides

shelter and darkness, and therefore show better fear acquisition; or that nestbox animals are more stressed than controls, due to being less habituated to light and open spaces, and therefore are less able to learn spatial components of the EPM e.g. open arm avoidance.

However, it is not possible to infer anything conclusive from these data. Further experiments would be required to explore the effect of nestbox availability on stress levels, e.g., plasma corticosteroid levels, and the subsequent effects on fear learning and spatial learning on the EPM, in relation to repeat testing. An alternative between-subjects experimental design, with half the cohort housed exclusively under control conditions and the other half with a nestbox, and all mice receiving one trial of the EPM after 2 weeks, and a second trial after 4 weeks, would be useful to tease apart the effects of nestbox condition on repeat testing in the EPM.

5. Supplementary tables

Trial 1	Total distance	Open arm entries	Open arm distance	Open arm time	Outer zone time	Corner zone time	Total distance	Dark box time	Total transitions
Main effect of condition	[F(1,20) = 1.7, p = 0.203]	[F(1,20) = 0.4, p = 0.522]	[F(1,20) = 2.2, p = 0.152]	[F(1,20) = 1.9, p = 0.188]	[F(1,20) = 0.3, p = 0.608]	[F(1,20) = 0.0, p = 0.912]	[F(1,20) = 0.1, p = 0.729]	[F(1,20) = 1.2, p = 0.285]	[F(1,19) = 2.0, p = 0.171]
Main effect of sex	[F(1,20) = 2.5, p = 0.132]	[F(1,20) = 0.0, p = 0.959]	[F(1,20) = 0.8, p = 0.3967]	[F(1,20) = 0.1, p = 0.800]	[F(1,20) = 1.7, p = 0.201]	**[F(1,20) = 15.0, p = 0.001]**	[F(1,20) = 0.8, p = 0.393]	[F(1,20) = 1.1, p = 0.304]	[F(1,19) = 0.0, p = 0.848]
Main effect of test minute	**[F(4,80) = 9.5, p < 0.0001]**	[F(4,80) = 0.3, p = 0.881]	**[F(3.0, 60.3) = 2.9, p = 0.043]**	[F(4,80) = 1.9, p = 0.117]	**[F(4,80) = 3.0, p = 0.025]**	[F(4,80) = 0.8, p = 0.528]	[F(4,80) = 1.6, p = 0.173]	**[F(4,80) = 3.1, p = 0.021]**	**[F(2.0,37.5) = 3.8, p = 0.031]**
Condition x sex	[F(1,20) = 0.6, p = 0.463]	[F(1,20) = 0.0, p = 0.974]	[F(1,20) = 1.5, p = 0.230]	[F(1,20) = 0.1, p = 0.711]	[F(1,20) = 0.2, p = 0.642]	[F(1,20) = 2.7, p = 0.115]	[F(1,20) = 1.2, p = 0.288]	[F(1,20) = 0.3, p = 0.615]	[F(1,19) = 2.5, p = 0.130]
Condition x test minute	[F(4,80) = 0.7, p = 0.583]	[F(4,80) = 0.9, p = 0.470]	[F(4,80) = 1.3, p = 0.296]	[F(4,80) = 0.9, p = 0.460]	[F(4,80) = 0.8, p = 0.528]	[F(4,80) = 0.6, p = 0.688]	[F(4,80) = 0.3, p = 0.881]	[F(4,80) = 0.6, p = 0.671]	[F(4,76) = 1.8, p = 0.135]
Sex x test minute	[F(4,80) = 0.7, p = 0.562]	[F(4,80) = 0.9, p = 0.463]	[F(4,80) = 1.8, p = 0.138]	[F(4,80) = 0.4, p = 0.791]	[F(4,80) = 1.7, p = 0.165]	[F(4,80) = 0.7, p = 0.570]	[F(4,80) = 1.1, p = 0.371]	[F(4,80) = 2.4, p = 0.053]	**[F(4,76) = 3.6, p = 0.010]**
Condition x sex x test minute	[F(4,80) = 0.7, p = 0.571]	[F(4,80) =0.5, p = 0.735]	[F(4,80) = 1.6, p = 0.185]	[F(4,80) = 0.5, p = 0.750]	[F(4,80) = 0.8, p = 0.523]	[F(4,80) = 0.1, p = 0.985]	[F(4,80) = 1.1, p = 0.381]	[F(4,80) = 1.5, p = 0.197]	[F(4,76) = 0.4, p = 0.840]

Supplementary Table 1 – summary of three-way repeated measures ANOVA results for trial 1 (Fig.1-3). Columns 1-4 refer to EPM, columns 5-7 refer to OF test and columns 8 and 9 refer to the LDB test. Significant results ($p \leq 0.05$) are indicated in bold. A mixed effects model was used for total transitions data, due to missing values. Greenhouse-Geisser corrected degrees of freedom are reported for open arm distance and total transitions. A sqrt-transform was applied to open arm distance, corner zone time and total distance (OF).

Trial 1 vs 2	Open arm time	Open arm entries	Open arm distance	Total distance	Outer zone time	Corner zone time	Total distance	Dark box time	Total transitions
Main effect of group	[F(1,20) = 3.9; p = 0.063]	[F(1,20) = 1.9; p = 0.182]	[F(1,20) = 3.2, p = 0.088]	[F(1,20) = 1.5, p = 0.242]	[F(1,20) = 0.0, p = 0.948]	[F(1,20) = 0.7, p = 0.416]	[F(1,20) = 0.4, p = 0.521]	F(1,20) = 0.0, p = 0.841]	[F(1,19) = 2.4, p = 0.137]
Main effect of sex	[F(1,20) = 0.9, p = 0.364]	[F(1,20) = 0.9, p = 0.367]	[F(1,20) = 0.0, p = 0.928]	**[F(1,20) = 5.5, p = 0.030]**	[F(1,20) = 2.3, p = 0.142]	[F(1,20) = 3.8, p = 0.066]	[F(1,20) = 0.6, p = 0.458]	[F(1,20) = 0.1, p = 0.707]	[F(1,19) = 0.5, p = 0.469]
Main effect of trial	**[F(1,20) = 21.8, p < 0.001]**	**[F(1,20) = 22.2, p <0.001]**	**[F(1,20) = 69.7, p < 0.001]**	**[F(1,20) = 29.1, p < 0.001]**	**[F(1,20) = 4.4, p = 0.050]**	**F(1,20) = 4.8, p = 0.040]**	**[F(1,20) = 15.9, p < 0.001]**	[F(1,20) = 0.2, p = 0.644]	**[F(1,19) = 4.4, p = 0.049]**
Main effect of test minute	**[F(2.4, 47.3) = 2.8, p = 0.023]**	[F(2.6, 52.3) = 0.9, p = 0.435]	**[F(4,80) = 4.5, p = 0.002]**	**[F(4,80) = 15.2 p < 0.001]**	**[F(4,80) = 6.3, p < 0.001]**	[F(2.8,56.3) = 1.7, p = 0.184]	[F(4,80) = 2.1, p = 0.094]	**[F(4,80) = 3.4, p = 0.013]**	**[F(2.1,40.6) = 8.6, p < 0.001]**
Group x sex	[F(1,20) = 0.0, p = 0.977]	[F(1,20) = 0.1, p = 0.795]	[F(1,20) = 1.0, p = 0.318]	[F(1,20) = 1.3, p = 0.261]	[F(1,20) = 0.3, p = 0.574]	[F(1,20) = 0.6, p = 0.443]	[F(1,20) = 0.4, p = 0.541]	[F(1,20) = 1.5, p = 0.236]	[F(1,19) = 2.8, p = 0.112]
Group x trial	[F(1,20) = 0.5, p = 0.484]	[F(1,20) = 0.7, p = 0.421]	[F(1,20) = 0.8, p = 0.376]	[F(1,20) = 0.4, p = 0.541]	[F(1,20) = 0.5, p = 0.480]	[F(1,20) = 1.4, p = 0.253]	[F(1,20) = 0.0, p = 0.948]	[F(1,20) = 3.5, p = 0.077]	[F(1,19) = 0.3, p = 0.575]
Group x test minute	[F(2.4, 47.3) = 0.5, p = 0.670]	[F(2.6, 52.3) = 1.6, p = 0.212]	[F(4,80) = 0.3, p = 0.876]	[F(4,80) = 1.0, p = 0.398]	**[F(4,80) =2.6, p = 0.044]**	[F(2.8,56.3) =0.6, p = 0.581]	[F(4,80) = 1.0, p = 0.423]	**[F(4,80) = 2.9, p = 0.028]**	[F(2.1,40.6) = 0.6, p = 0.575]
Sex x trial	[F(1,20) = 0.8, p = 0.387]	[F(1,20) = 0.8, p = 0.373]	[F(1,20) = 1.0, p = 0.322]	[F(1,20) = 0.6, p = 0.463]	[F(1,20) = 0.0, p = 0.844]	[F(1,20) = 0.9, p = 0.357]	[F(1,20) = 0.3, p = 0.578]	[F(1,20) = 0.7, p = 0.407]	[F(1,19) = 0.3, p = 0.580]
Sex x test minute	[F(2.4, 47.3) = 0.3, p = 0.777]	[F(2.6, 52.3) = 0.7, p = 0.553]	[F(4,80) = 1.7, p = 0.151]	[F(4,80) = 1.6, p =0.181]	[F(4,80) = 1.0, p = 0.403]	[F(2.8,56.3) = 0.6, p = 0.578]	[F(4,80) = 0.2, p = 0.918]	[F(4,80) = 2.3, p = 0.067]	**[F(2.1,40.6) = 3.6, p = 0.034]**
Trial x test minute	[F(3.2, 63.3) = 0.2, p = 0.876]	[F(3.8, 75.1) = 1.6, p = 0.183]	[F(4,80) = 1.1, p = 0.374]	**[F(4,80) = 6.9, p <0.001]**	[F(4,80) = 0.1, p = 0.963]	[F(3.2,63.9) = 2.4, p = 0.072]	[F(4,80) = 1.3, p = 0.275]	[F(4,80) = 1.1, p = 0.386]	[F(2.6,49.6) = 0.3, p = 0.828]

Supplementary table 2 – summary of four-way repeated measures ANOVA results for trial 1 v 2 (Fig.4,6,7). Columns 1-4 refer to EPM, columns 5-7 refer to OF test and columns 8 and 9 refer to the LDB test. All main effects and two-way interactions reported. Significant results ($p \leq 0.05$) are indicated in bold. Greenhouse-Geisser corrected degrees of freedom are reported for open arm time, open arm entries, corner zone time and total transitions. A sqrt-transform was applied to total distance (EPM) and total distance (OF).

References

Abe, M., Herzog, E.D., Yamazaki, S., Straume, M., Tei, H., Sakaki, Y., Menaker, M., Block, G.D., 2002. Circadian Rhythms in Isolated Brain Regions. J Neurosci 22, 350–356. https://doi.org/10.1523/JNEUROSCI.22-01-00350.2002

Adamah-Biassi, E.B., Stepien, I., Hudson, R.L., Dubocovich, M.L., 2013. Automated video analysis system reveals distinct diurnal behaviors in C57BL/6 and C3H/HeN mice. Behavioural Brain Research 243, 306–312. https://doi.org/10.1016/j.bbr.2013.01.003

Adams, N., Boice, R., 1981. Mouse (Mus) burrows: Effects of age, strain, and domestication. Animal Learning & Behavior 9, 140–144. https://doi.org/10.3758/BF03212036

Adams, W.J., Graf, E.W., Ernst, M.O., 2004. Experience can change the "light-from-above" prior. Nat Neurosci 7, 1057–1058. https://doi.org/10.1038/nn1312

Aggelopoulos, N.C., Meissl, H., 2000. Responses of neurones of the rat suprachiasmatic nucleus to retinal illumination under photopic and scotopic conditions. J Physiol 523 Pt 1, 211–222. https://doi.org/10.1111/j.1469-7793.2000.t01-1-00211.x

Al Enezi, J., Revell, V., Brown, T., Wynne, J., Schlangen, L., Lucas, R., 2011. A "melanopic" spectral efficiency function predicts the sensitivity of melanopsin photoreceptors to polychromatic lights. Journal of Biological Rhythms 26, 314–323. https://doi.org/10.1177/0748730411409719

Albrecht, U., Foster, R.G., 2002. Placing ocular mutants into a functional context: a chronobiological approach. Methods (San Diego, Calif.) 28, 465–477. https://doi.org/10.1016/S1046-2023(02)00266-9

Allen, A.E., Baño-Otálora, B., 2022. Slow vision: Measuring melanopsin-mediated light effects in animal models, in: Progress in Brain Research. Elsevier B.V., pp. 117–143. https://doi.org/10.1016/bs.pbr.2022.04.009

Allen, A.E., Brown, T.M., Lucas, R.J., 2011. A Distinct Contribution of Short-Wavelength-Sensitive Cones to Light-Evoked Activity in the Mouse Pretectal Olivary Nucleus. J. Neurosci. 31, 16833–16843. https://doi.org/10.1523/JNEUROSCI.2505-11.2011

Altimus, C.M., Güler, A.D., Alam, N.M., Arman, A.C., Prusky, G.T., Sampath, A.P., Hattar, S., 2010. Rod photoreceptors drive circadian photoentrainment across a wide range of light intensities. Nat Neurosci 13, 1107–1112. https://doi.org/10.1038/nn.2617

Altimus, C.M., Güler, A.D., Villa, K.L., McNeill, D.S., LeGates, T.A., Hattar, S., 2008. Rods-cones and melanopsin detect light and dark to modulate sleep independent of image formation. Proceedings of the National Academy of Sciences of the United States of America 105, 19998–20003. https://doi.org/10.1073/pnas.0808312105

Amann, B., Hirmer, S., Hauck, S.M., Kremmer, E., Ueffing, M., Deeg, C.A., 2014. True blue: S-opsin is widely expressed in different animal species. J Anim Physiol Anim Nutr (Berl) 98, 32–42. https://doi.org/10.1111/jpn.12016

Angerer, M., Pichler, G., Angerer, B., Scarpatetti, M., Schabus, M., Blume, C., 2022. From dawn to dusk—mimicking natural daylight exposure improves circadian rhythm entrainment in patients with severe brain injury. Sleep 45, zsac065. https://doi.org/10.1093/sleep/zsac065

Aranda, M.L., Schmidt, T.M., 2021. Diversity of intrinsically photosensitive retinal ganglion cells: circuits and functions. Cell Mol Life Sci 78, 889–907. https://doi.org/10.1007/s00018-020-03641-5

Aschoff, J., 1979. Circadian rhythms: influences of internal and external factors on the period measured in constant conditions. Z Tierpsychol 49, 225–249. https://doi.org/10.1111/j.1439-0310.1979.tb00290.x

Aschoff, J., Wever, R., 1965. Circadian rhythms of finches in light-dark cycles with interposed twilights. Comparative Biochemistry and Physiology 16, 507–514. https://doi.org/10.1016/0010-406X(65)90314-2

Aulsebrook, A.E., Jones, T.M., Rattenborg, N.C., Ii, T.C.R., Lesku, J.A., 2016. Sleep Ecophysiology: Integrating Neuroscience and Ecology. 590 Trends in Ecology & Evolution 31. https://doi.org/10.1016/j.tree.2016.05.004

Baden, T., Euler, T., Berens, P., 2020. Understanding the retinal basis of vision across species. Nat Rev Neurosci 21, 5–20. https://doi.org/10.1038/s41583-019-0242-1

Baden, T., Osorio, D., 2019. The Retinal Basis of Vertebrate Color Vision. Annu. Rev. Vis. Sci 5, 177–200. https://doi.org/10.1146/annurev-vision-091718

Baden, T., Schubert, T., Berens, P., Euler, T., 2018. The Functional Organization of Vertebrate Retinal Circuits for Vision, in: Oxford Research Encyclopedia of Neuroscience. https://doi.org/10.1093/acrefore/9780190264086.013.68

Bailes, H.J., Lucas, R.J., 2013. Human melanopsin forms a pigment maximally sensitive to blue light (λmax ≈ 479 nm) supporting activation of G(q/11) and G(i/o) signalling cascades. Proc Biol Sci 280, 20122987. https://doi.org/10.1098/rspb.2012.2987

Bailey, K.R., Crawley, J.N., 2009. Anxiety-Related Behaviors in Mice, in: Buccafusco, J.J. (Ed.), Methods of Behavior Analysis in Neuroscience, Frontiers in Neuroscience. CRC Press/Taylor & Francis, Boca Raton (FL).

Balsalobre, A., Damiola, F., Schibler, U., 1998. A serum shock induces circadian gene expression in mammalian tissue culture cells. Cell 93, 929–937. https://doi.org/10.1016/s0092-8674(00)81199-x

Barclay, J.L., Shostak, A., Leliavski, A., Tsang, A.H., Jöhren, O., Müller-Fielitz, H., Landgraf, D., Naujokat, N., van der Horst, G.T.J., Oster, H., 2013. High-fat diet-induced hyperinsulinemia and tissue-specific insulin resistance in Cry-deficient mice. Am J Physiol Endocrinol Metab 304, E1053-1063. https://doi.org/10.1152/ajpendo.00512.2012

Barnett, S.A., Cowan, P., 1976. Activity, Exploration, Curiosity and Fear: An Ethological Study. Interdisciplinary Science Reviews. 1. 43-62. 10.1179/030801876789768534.

Barnett, S.A., 1963. The rat: A study in behaviour. Aldine, Oxford, England.

Beale, A., Guibal, C., Tamai, T.K., Klotz, L., Cowen, S., Peyric, E., Reynoso, V.H., Yamamoto, Y., Whitmore, D., 2013. Circadian rhythms in Mexican blind cavefish Astyanax mexicanus in the lab and in the field. Nat Commun 4, 2769. https://doi.org/10.1038/ncomms3769

Beale, A.D., Whitmore, D., Moran, D., 2016. Life in a dark biosphere: a review of circadian physiology in "arrhythmic" environments. Journal of Comparative Physiology B: Biochemical, Systemic, and Environmental Physiology 186, 947–968. https://doi.org/10.1007/s00360-016-1000-6

Bechtold, D.A., 2008. Energy-responsive timekeeping. J Genet 87, 447–458. https://doi.org/10.1007/s12041-008-0067-6

Beechey, T., 2022. Ecological Validity, External Validity, and Mundane Realism in Hearing Science. Ear Hear 43, 1395–1401. https://doi.org/10.1097/AUD.0000000000001202

Beersma, D.G.M., Daan, S., Hut, R.A., 1999. Accuracy of Circadian Entrainment under Fluctuating Light Conditions: Contributions of Phase and Period Responses. J Biol Rhythms 14, 320–329. https://doi.org/10.1177/074873099129000740

Beersma, D.G.M., Gordijn, M.C.M., 2007. Circadian control of the sleep–wake cycle. Physiology & Behavior, Includes a Special Section on Chronobiology Aspects of the Sleep--Wake Cycle and Thermoreregulation 90, 190–195. https://doi.org/10.1016/j.physbeh.2006.09.010

Beier, C., Zhang, Z., Yurgel, M., Hattar, S., 2021. Projections of ipRGCs and conventional RGCs to retinorecipient brain nuclei. J Comp Neurol 529, 1863–1875. https://doi.org/10.1002/cne.25061

Bell-Pedersen, D., Cassone, V.M., Earnest, D.J., Golden, S.S., Hardin, P.E., Thomas, T.L., Zoran, M.J., 2005. Circadian rhythms from multiple oscillators: lessons from diverse organisms. Nat Rev Genet 6, 544–556. https://doi.org/10.1038/nrg1633

Berson, D.M., Dunn, F.A., Takao, M., 2002. Phototransduction by retinal ganglion cells that set the circadian clock. Science (New York, N.Y.) 295, 1070–1073. https://doi.org/10.1126/SCIENCE.1067262

Biller, A.M., Balakrishnan, P., Spitschan, M., 2024. Behavioural determinants of physiologically-relevant light exposure. Commun Psychol 2, 1–11. https://doi.org/10.1038/s44271-024-00159-5

Blanchard, D.C., Blanchard, R.J., 2008. Chapter 2.4 Defensive behaviors, fear, and anxiety, in: Blanchard, R.J., Blanchard, D.C., Griebel, G., Nutt, D. (Eds.), Handbook of Behavioral Neuroscience, Handbook of Anxiety and Fear. Elsevier, pp. 63–79. https://doi.org/10.1016/S1569-7339(07)00005-7

Blanchard, D.C., Griebel, G., Blanchard, R.J., 2001. Mouse defensive behaviors: pharmacological and behavioral assays for anxiety and panic. Neuroscience & Biobehavioral Reviews 25, 205–218. https://doi.org/10.1016/S0149-7634(01)00009-4

Bloch, S., Belzung, C., 2023. The Light–Dark Box Test in the Mouse, in: Harro, J. (Ed.), Psychiatric Vulnerability, Mood, and Anxiety Disorders: Tests and Models in Mice and Rats. Springer US, New York, NY, pp. 31–41. https://doi.org/10.1007/978-1-0716-2748-8_3

Bohic, M., Pattison, L.A., Jhumka, Z.A., Rossi, H., Thackray, J.K., Ricci, M., Mossazghi, N., Foster, W., Ogundare, S., Twomey, C.R., Hilton, H., Arnold, J., Tischfield, M.A., Yttri, E.A., St. John Smith, E., Abdus-Saboor, I., Abraira, V.E., 2023. Mapping the neuroethological signatures of pain, analgesia, and recovery in mice. Neuron 111, 2811-2830.e8. https://doi.org/10.1016/j.neuron.2023.06.008

Borniger, J.C., McHenry, Z.D., Abi Salloum, B.A., Nelson, R.J., 2014. Exposure to dim light at night during early development increases adult anxiety-like responses. Physiol Behav 133, 99–106. https://doi.org/10.1016/j.physbeh.2014.05.012

Bouchard, P.R., Lynch, C.B., 1989. Burrowing behavior in wild house mice: variation within and between populations. Behav Genet 19, 447–456. https://doi.org/10.1007/BF01066170

Boulos, Z., Macchi, M., Houpt, T.A., Terman, M., 1996. Photic Entrainment in Hamsters: Effects of Simulated Twilights and Nest Box Availability. J Biol Rhythms 11, 216–233. https://doi.org/10.1177/074873049601100304

Boulos, Z., Macchi, M.M., 2005. Season- and latitude-dependent effects of simulated twilights on circadian entrainment. Journal of Biological Rhythms 20, 132–144. https://doi.org/10.1177/0748730404272907

Boulos, Z., Macchi, M.M., Terman, M., 2002. Twilights Widen the Range of Photic Entrainment in Hamsters. Journal of biological rhythms. 17. 353-63. 10.1177/074873002129002654.

Bourin, M., Hascoët, M., 2003. The mouse light/dark box test. European Journal of Pharmacology 463, 55–65. https://doi.org/10.1016/S0014-2999(03)01274-3

Bouwknecht, J.A., Paylor, R., 2002. Behavioral and physiological mouse assays for anxiety: a survey in nine mouse strains. Behav Brain Res 136, 489–501. https://doi.org/10.1016/s0166-4328(02)00200-0

Bouwknecht, J.A., Spiga, F., Staub, D.R., Hale, M.W., Shekhar, A., Lowry, C.A., 2007. Differential effects of exposure to low-light or high-light open-field on anxiety-related behaviors: relationship to c-Fos expression in serotonergic and non-serotonergic neurons in the dorsal raphe nucleus. Brain Res Bull 72, 32–43. https://doi.org/10.1016/j.brainresbull.2006.12.009

Bowmaker, J.K., Dartnall, H.J., 1980. Visual pigments of rods and cones in a human retina. The Journal of Physiology 298, 501–511. https://doi.org/10.1113/jphysiol.1980.sp013097

Brainard, G.C., Richardson, B.A., King, T.S., Reiter, R.J., 1984. The influence of different light spectra on the suppression of pineal melatonin content in the syrian hamster. Brain Research 294, 333–339. https://doi.org/10.1016/0006-8993(84)91045-X

Brandstetter, H., Scheer, M., Heinekamp, C., Gippner-Steppert, C., Loge, O., Ruprecht, L., Thull, B., Wagner, R., Wilhelm, R., Scheuber, H.P., 2005. Performance evaluation of IVC systems. Laboratory animals 39, 40–44. https://doi.org/10.1258/0023677052886475

Brinkhof, M.W.G., Daan, S., Strubbe, J.H., 1998. Forced dissociation of food- and light-entrainable circadian rhythms of rats in a skeleton photoperiod. Physiology & Behavior 65, 225–231. https://doi.org/10.1016/S0031-9384(98)00051-1

Brown, L.A., Fisk, A.S., Pothecary, C.A., Peirson, S.N., 2019. Telling the time with a broken clock: Quantifying circadian disruption in animal models. Biology 8. https://doi.org/10.3390/biology8010018

Brown, L.A., Hasan, S., Foster, R.G., Peirson, S.N., 2017. COMPASS: Continuous Open Mouse Phenotyping of Activity and Sleep Status. Wellcome Open Res 1, 2. https://doi.org/10.12688/wellcomeopenres.9892.2

Brown, S.A., Zumbrunn, G., Fleury-Olela, F., Preitner, N., Schibler, U., 2002. Rhythms of Mammalian Body Temperature Can Sustain Peripheral Circadian Clocks. Current Biology 12, 1574–1583. https://doi.org/10.1016/S0960-9822(02)01145-4

Brown, T.M., 2016. Using light to tell the time of day: sensory coding in the mammalian circadian visual network.The Journal of experimental biology, 219(Pt 12), 1779–1792. https://doi.org/10.1242/jeb.132167

Brown, T.M., Allen, A.E., Al-Enezi, J., Wynne, J., Schlangen, L., Hommes, V., Lucas, R.J., 2013. The melanopic sensitivity function accounts for melanopsin-driven responses in mice under diverse lighting conditions. PLoS ONE 8, 1–8. https://doi.org/10.1371/journal.pone.0053583

Brown, T.M., Brainard, G.C., Cajochen, C., Czeisler, C.A., Hanifin, J.P., Lockley, S.W., Lucas, R.J., Münch, M., O'Hagan, J.B., Peirson, S.N., Price, L.L.A., Roenneberg, T., Schlangen, L.J.M., Skene, D.J., Spitschan, M., Vetter, C., Zee, P.C., Jr, K.P.W., 2022. Recommendations for daytime, evening, and nighttime indoor light exposure to best support physiology, sleep, and wakefulness in healthy adults. PLOS Biology 20, e3001571. https://doi.org/10.1371/journal.pbio.3001571

Brown, T.M., Gias, C., Hatori, M., Keding, S.R., Semo, M., Coffey, P.J., Gigg, J., Piggins, H.D., Panda, S., Lucas, R.J., 2010. Melanopsin Contributions to Irradiance Coding in the Thalamo-Cortical Visual System. PLOS Biology 8, e1000558. https://doi.org/10.1371/journal.pbio.1000558

Brown, T.M., Wynne, J., Piggins, H.D., Lucas, R.J., 2011. Multiple hypothalamic cell populations encoding distinct visual information. J Physiol 589, 1173–1194. https://doi.org/10.1113/jphysiol.2010.199877

Brunswik, E., 1955. Representative design and probabilistic theory in a functional psychology. Psychol Rev 62, 193–217. https://doi.org/10.1037/h0047470

Brunswik, E., 1949. Discussion: remarks on functionalism in perception. Journal of Personality, 18, 56–65. https://doi.org/10.1111/j.1467-6494.1949.tb01233.x

Buchsbaum, G., Gottschalk, A., Barlow, H.B., 1997. Trichromacy, opponent colours coding and optimum colour information transmission in the retina. Proceedings of the Royal Society of London. Series B. Biological Sciences 220, 89–113. https://doi.org/10.1098/rspb.1983.0090

Buhr, E.D., Takahashi, J.S., 2013. Molecular Components of the Mammalian Circadian Clock, in: Kramer, A., Merrow, M. (Eds.), Circadian Clocks, Handbook of Experimental Pharmacology. Springer, Berlin, Heidelberg, pp. 3–27. https://doi.org/10.1007/978-3-642-25950-0_1

Bunger, M.K., Wilsbacher, L.D., Moran, S.M., Clendenin, C., Radcliffe, L.A., Hogenesch, J.B., Simon, M.C., Takahashi, J.S., Bradfield, C.A., 2000. Mop3 is an essential component of the master circadian pacemaker in mammals. Cell 103, 1009–1017. https://doi.org/10.1016/s0092-8674(00)00205-1

Bur, I.M., Cohen-Solal, A.M., Carmignac, D., Abecassis, P.-Y., Chauvet, N., Martin, A.O., van der Horst, G.T.J., Robinson, I.C.A.F., Maurel, P., Mollard, P., Bonnefont, X., 2009. The circadian clock components CRY1 and CRY2 are necessary to sustain sex dimorphism in mouse liver metabolism. J Biol Chem 284, 9066–9073. https://doi.org/10.1074/jbc.M808360200

Butler, M.P., Silver, R., 2011. Divergent photic thresholds in the non-image-forming visual system: entrainment, masking and pupillary light reflex. Proceedings. Biological sciences 278, 745–750. https://doi.org/10.1098/RSPB.2010.1509

Calisi, R.M., Bentley, G.E., 2009. Lab and field experiments: Are they the same animal? Hormones and Behavior, 56(1), 1–10. https://doi.org/10.1016/j.yhbeh.2009.02.010

Callaway, E., Ledford, H., 2017. Medicine Nobel awarded for work on circadian clocks. Nature 550, 18–18. https://doi.org/10.1038/nature.2017.22736

Cameron, M.A., Barnard, A.R., Hut, R.A., Bonnefont, X., van der Horst, G.T.J., Hankins, M.W., Lucas, R.J., 2008. Electroretinography of wild-type and Cry mutant mice reveals circadian tuning of photopic and mesopic retinal responses. J Biol Rhythms 23, 489–501. https://doi.org/10.1177/0748730408325874

Campos-Cardoso, R., Godoy, L.D., Lazarini-Lopes, W., Novaes, L.S., dos Santos, N.B., Perfetti, J.G., Garcia-Cairasco, N., Munhoz, C.D., Padovan, C.M., 2023. Exploring the light/dark box test: Protocols and implications for neuroscience research. Journal of Neuroscience Methods 384, 109748. https://doi.org/10.1016/j.jneumeth.2022.109748

Cao, L.-H., Luo, D.-G., Yau, K.-W., 2014. Light responses of primate and other mammalian cones. Proc Natl Acad Sci U S A 111, 2752–2757. https://doi.org/10.1073/pnas.1400268111

Carter-Dawson, L.D., Lavail, M.M., 1979. Rods and cones in the mouse retina. I. Structural analysis using light and electron microscopy. Journal of Comparative Neurology 188, 245–262. https://doi.org/10.1002/cne.901880204

Carter-Dawson, L.D., LaVail, M.M., Sidman, R.L., 1978. Differential effect of the rd mutation on rods and cones in the mouse retina. Invest Ophthalmol Vis Sci 17, 489–498.

Cavalli, R.M., 2023. Spatial Validation of Spectral Unmixing Results: A Systematic Review. Remote Sensing 15, 2822. https://doi.org/10.3390/rs15112822

Çevik, M.Ö., 2014. Habituation, sensitization, and Pavlovian conditioning. Front Integr Neurosci 8, 13. https://doi.org/10.3389/fnint.2014.00013

Chakraborty, R., Park, H. na, Tan, C.C., Weiss, P., Prunt, M.C., Pardue, M.T., 2017. Association of Body Length with Ocular Parameters in Mice. Optom Vis Sci 94, 387–394. https://doi.org/10.1097/OPX.0000000000001036

Chambers, L.K., Singleton, G.R., Krebs, C.J., 2000. Movements and Social Organization of Wild House Mice (Mus Domesticus) in the Wheatlands of Northwestern Victoria, Australia. Journal of Mammalogy 81, 59–69. https://doi.org/10.1644/1545-1542(2000)081<0059:MASOOW>2.0.CO;2

Chang, L., Breuninger, T., Euler, T., 2013. Chromatic coding from cone-type unselective circuits in the mouse retina. Neuron 77, 559–571. https://doi.org/10.1016/j.neuron.2012.12.012

Chang, M., Büchel, D., Reinecke, K., Lehmann, T., Baumeister, J., 2022. Ecological validity in exercise neuroscience research: A systematic investigation. Eur J Neurosci 55, 487–509. https://doi.org/10.1111/ejn.15595

Chen, L., Lu, Y., Hua, X., Zhang, H., Sun, S., Han, C., 2024. Three methods of behavioural testing to measure anxiety – A review. Behavioural Processes 215, 104997. https://doi.org/10.1016/j.beproc.2024.104997

Chen, S., Woodcock, C.E., Bullock, E.L., Arévalo, P., Torchinava, P., Peng, S., Olofsson, P., 2021. Monitoring temperate forest degradation on Google Earth Engine using Landsat time series analysis. Remote Sensing of Environment 265, 112648. https://doi.org/10.1016/j.rse.2021.112648

CIE 2022. CIE standard illuminant D65, International Commission on Illumination (CIE), Vienna, Austria. https://doi.org/_10.25039/CIE.DS.hjfjmt59

Clough, G., 1982. Environmental effects on animals used in biomedical research. Biological Reviews 57, 487–523. https://doi.org/10.1111/j.1469-185X.1982.tb00705.x

Clough, G., Wallace, J., Gamble, M.R., Merryweather, E.R., Bailey, E., 1995. A positive, individually ventilated caging system: a local barrier system to protect both animals and personnel. Laboratory animals 29, 139–151. https://doi.org/10.1258/002367795780740221

Collins, H.M., 2023. Investigation of the behavioural and neurobiological effects of SSRI discontinuation in mice. [PhD thesis]. University of Oxford.

Colwell, C.S., 2011. Linking neural activity and molecular oscillations in the SCN. Nat Rev Neurosci 12, 553–569. https://doi.org/10.1038/nrn3086

Comas, M., Hut, R.A., 2009. Twilight and photoperiod affect behavioral entrainment in the house mouse (Mus musculus). Journal of Biological Rhythms 24, 403–412. https://doi.org/10.1177/0748730409343873

Contreras, E.O., Dearing, C.G., Ashinhurst, C.A., Fish, B.A., Hossain, S.N., Rey, A.M., Silva, P.D., Thompson, S., 2021. Pupillary reflex and behavioral masking responses to light as functional measures of retinal degeneration in mice. PloS one 16. https://doi.org/10.1371/JOURNAL.PONE.0244702

Crawley, Jacqueline, Goodwin, Frederick K, Crawley, J, Goodwin, F K, 1980. Preliminary Report of a Simple Animal Behavior Model for the Anxiolytic Effects of Benzodiazepines. Pharmacology Biochemistry & Behavior 13, 167–170.

Crawley, J.N., 2008. Behavioral phenotyping strategies for mutant mice. Neuron 57, 809–818. https://doi.org/10.1016/j.neuron.2008.03.001

Cretenet, G., Le Clech, M., Gachon, F., 2010. Circadian clock-coordinated 12 Hr period rhythmic activation of the IRE1alpha pathway controls lipid metabolism in mouse liver. Cell Metab 11, 47–57. https://doi.org/10.1016/j.cmet.2009.11.002

Cronin, T.W., Johnsen, S., Marshall, N.J., Warrant, E.J., 2014. Visual Pigments and Photoreceptors. Visual Ecology. https://doi.org/10.23943/princeton/9780691151847.003.0003

Crusio, W.E., 2004. Flanking gene and genetic background problems in genetically manipulated mice. Biol Psychiatry 56, 381–385. https://doi.org/10.1016/j.biopsych.2003.12.026

Daan, S., 2000. Colin Pittendrigh, Jürgen Aschoff, and the Natural Entrainment of Circadian Systems. J Biol Rhythms 15, 195–207. https://doi.org/10.1177/074873040001500301

Daan, S., Spoelstra, K., Albrecht, U., Schmutz, I., Daan, M., Daan, B., Rienks, F., Poletaeva, I., Dell'omo, G., Vyssotski, A., Lipp, H.-P., 2011. Lab Mice in the Field: Unorthodox Daily Activity and Effects of a Dysfunctional Circadian Clock Allele. JOURNAL OF BIOLOGICAL RHYTHMS 26, 118–129. https://doi.org/10.1177/0748730410397645

Dacey, D.M., Liao, H.-W., Peterson, B.B., Robinson, F.R., Smith, V.C., Pokorny, J., Yau, K.-W., Gamlin, P.D., 2005. Melanopsin-expressing ganglion cells in primate retina signal colour and irradiance and project to the LGN. Nature 433, 749–754. https://doi.org/10.1038/nature03387

Dahlsjö, C.A.L., Atkins, T., Malhi, Y., 2024. Large invertebrate decomposers contribute to faster leaf litter decomposition in Fraxinus excelsior-dominated habitats: Implications of ash dieback. Heliyon 10. https://doi.org/10.1016/j.heliyon.2024.e27228

Damiola, F., Le Minh, N., Preitner, N., Kornmann, B., Fleury-Olela, F., Schibler, U., 2000. Restricted feeding uncouples circadian oscillators in peripheral tissues from the central pacemaker in the suprachiasmatic nucleus. Genes Dev 14, 2950–2961. https://doi.org/10.1101/gad.183500

Dartnall, H.J.A., 1953. The interpretation of spectral sensitivity curves. Br Med Bull 9, 24–30. https://doi.org/10.1093/oxfordjournals.bmb.a074302

Datta, S.R., Anderson, D.J., Branson, K., Perona, P., Leifer, A., 2019. Computational Neuroethology: A Call to Action. Neuron 104, 11–24. https://doi.org/10.1016/j.neuron.2019.09.038

Dauchy, R.T., Wren, M.A., Dauchy, E.M., Hanifin, J.P., Jablonski, M.R., Warfield, B., Brainard, G.C., Hill, S.M., Mao, L., Dupepe, L.M., Ooms, T.G., Blask, D.E., 2013. Effect of Spectral Transmittance through Red-Tinted Rodent Cages on Circadian Metabolism and Physiology in Nude Rats, Journal of the American Association for Laboratory Animal Science.

Davis, H.J., Barabas, A.J., Gaskill, B.N., 2022. Titrating the preferences of altered lighting against temperature in female CD-1 laboratory mice, *Mus musculus*. Applied Animal Behaviour Science 246, 105541. https://doi.org/10.1016/j.applanim.2021.105541

De Bundel, D., Gangarossa, G., Biever, A., Bonnefont, X., Valjent, E., 2013. Cognitive dysfunction, elevated anxiety, and reduced cocaine response in circadian clock-deficient cryptochrome knockout mice. Frontiers in behavioral neuroscience, 7, 152. https://doi.org/10.3389/fnbeh.2013.00152.

De Oliveira, M.A.B., Scop, M., Abreu, A.C.O., Sanches, P.R.S., Rossi, A.C., Díez-Noguera, A., Calcagnotto, M.E., Hidalgo, M.P., 2019. Entraining effects of variations in light spectral composition on the rest-activity rhythm of a nocturnal rodent. Chronobiology International 36, 934–944. https://doi.org/10.1080/07420528.2019.1599008

Deacon, R.M.J., Rawlins, J.N.P., 2005. Hippocampal lesions, species-typical behaviours and anxiety in mice. Behavioural Brain Research 156, 241–249. https://doi.org/10.1016/j.bbr.2004.05.027

Deakin, J.F.W., Graeff, F.G., 1991. 5-HT and mechanisms of defence. J Psychopharmacol 5, 305–315. https://doi.org/10.1177/026988119100500414

Debevec, P., 2005. Image-based lighting, in: ACM SIGGRAPH 2005 Courses, SIGGRAPH '05. Association for Computing Machinery, New York, NY, USA, pp. 3-es. https://doi.org/10.1145/1198555.1198709

Deboer, T., Tobler, I., 2000. Running wheel size influences circadian rhythm period and its phase shift in mice. J Comp Physiol A 186, 969–973. https://doi.org/10.1007/s003590000150

DeCoursey, G., DeCoursey, P.J., 1964. Adaptive aspects of Activity Rhythms in Bats. Biological Bulletin 126, 14–27. https://doi.org/10.2307/1539413

DeCoursey, P.J., 1986. Light-sampling behavior in photoentrainment of a rodent circadian rhythm. J Comp Physiol A 159, 161–169. https://doi.org/10.1007/BF00612299

DeCoursey, P.J., 1972. LD ratios and the entrainment of circadian activity in a nocturnal and a diurnal rodent. J. Comp. Physiol. 78, 221–235. https://doi.org/10.1007/BF00697656

DeCoursey, P.J., 1960. Daily Light Sensitivity Rhythm in a Rodent. Science (New York, N.Y.), 131(3392), 33–35. https://doi.org/10.1126/science.131.3392.33

Decoursey, P.J., Menon, S.A., 1991. Circadian photo-entrainment in a noctural rodent: quantitative measurement of light-sampling activity. Animal Behaviour 41, 781–785. https://doi.org/10.1016/S0003-3472(05)80344-6

DeCoursey, P.J., Walker, J.K., Smith, S.A., 2000. A circadian pacemaker in free-living chipmunks: Essential for survival? Journal of Comparative Physiology - A Sensory, Neural, and Behavioral Physiology 186, 169–180. https://doi.org/10.1007/s003590050017

Demb, J.B., Singer, J.H., 2015. Functional Circuitry of the Retina. Annual Review of Vision Science 1, 263–289. https://doi.org/10.1146/annurev-vision-082114-035334

Dhami, M.K., Hertwig, R., Hoffrage, U., 2004. The role of representative design in an ecological approach to cognition. Psychol Bull 130, 959–988. https://doi.org/10.1037/0033-2909.130.6.959

Dhande, O.S., Huberman, A.D., 2014. Retinal ganglion cell maps in the brain: implications for visual processing. Curr Opin Neurobiol 24, 133–142. https://doi.org/10.1016/j.conb.2013.08.006

Dibner, C., Schibler, U., Albrecht, U., 2010. The mammalian circadian timing system: organization and coordination of central and peripheral clocks. Annual review of physiology 72, 517–549. https://doi.org/10.1146/ANNUREV-PHYSIOL-021909-135821

Didikoglu, A., Mohammadian, N., Johnson, S., van Tongeren, M., Wright, P., Casson, A.J., Brown, T.M., Lucas, R.J., 2023. Associations between light exposure and sleep timing and sleepiness while awake in a sample of UK adults in everyday life. Proceedings of the National Academy of Sciences 120, e2301608120. https://doi.org/10.1073/pnas.2301608120

Do, M.T.H., 2019. Melanopsin and the Intrinsically Photosensitive Retinal Ganglion Cells: Biophysics to Behavior. Neuron 104, 205–226. https://doi.org/10.1016/j.neuron.2019.07.016

Do, M.T.H., Kang, S.H., Xue, T., Zhong, H., Liao, H.-W., Bergles, D.E., Yau, K.-W., 2009. Photon capture and signalling by melanopsin retinal ganglion cells. Nature 457, 281–287. https://doi.org/10.1038/nature07682

Dobb, R., Martial, F., Elijah, D., Storchi, R., Brown, T.M., Lucas, R.J., 2017. The impact of temporal modulations in irradiance under light adapted conditions on the mouse suprachiasmatic nuclei (SCN). Sci Rep 7, 10582. https://doi.org/10.1038/s41598-017-11184-2

Dodd, A.N., Salathia, N., Hall, A., Kévei, E., Tóth, R., Nagy, F., Hibberd, J.M., Millar, A.J., Webb, A.A.R., 2005. Plant circadian clocks increase photosynthesis, growth, survival, and competitive advantage. Science 309, 630–633. https://doi.org/10.1126/science.1115581

Dominy, N.J., Harris, J.M., 2022. Adaptive optics in the Arctic? A commentary on Fosbury and Jeffery. Proceedings of the Royal Society B: Biological Sciences 289, 20221528. https://doi.org/10.1098/rspb.2022.1528

Douglas, R.H., Jeffery, G., 2014. The spectral transmission of ocular media suggests ultraviolet sensitivity is widespread among mammals. Proc Biol Sci 281, 20132995. https://doi.org/10.1098/rspb.2013.2995

Drescher, J.W., 1967. Environmental Influences on Initiation and Maintenance of Hibernation in the Arctic Ground Squirrel, Citellus Undulatus. Ecology 48, 962–966. https://doi.org/10.2307/1934541

Duffield, G.E., Best, J.D., Meurers, B.H., Bittner, A., Loros, J.J., Dunlap, J.C., 2002. Circadian Programs of Transcriptional Activation, Signaling, and Protein Turnover Revealed by Microarray Analysis of Mammalian Cells. Current Biology 12, 551–557. https://doi.org/10.1016/S0960-9822(02)00765-0

Earnest, D.J., Turek, F.W., 1983. Effect of One-Second Light Pulses on Testicular Function and Locomotor Activity in the Golden Hamster1. Biology of Reproduction 28, 557–565. https://doi.org/10.1095/biolreprod28.3.557

Ebihara, S., Tsuji, K., 1980. Entrainment of the circadian activity rhythm to the light cycle: effective light intensity for a Zeitgeber in the retinal degenerate C3H mouse and the normal C57BL mouse. Physiology & behavior 24, 523–527. https://doi.org/10.1016/0031-9384(80)90246-2

Eckel-Mahan, K., Sassone-Corsi, P., 2015. Phenotyping Circadian Rhythms in Mice. Current Protocols in Mouse Biology 5, 271–281. https://doi.org/10.1002/9780470942390.mo140229

Ecker, J.L., Dumitrescu, O.N., Wong, K.Y., Alam, N.M., Chen, S.-K., LeGates, T., Renna, J.M., Prusky, G.T., Berson, D.M., Hattar, S., 2010. Melanopsin-expressing retinal ganglion-cell photoreceptors: cellular diversity and role in pattern vision. Neuron 67, 49–60. https://doi.org/10.1016/j.neuron.2010.05.023

Edgar, D.M., Kilduff, T.S., Martin, C.E., Dement, W.C., 1991. Influence of running wheel activity on free-running sleep/wake and drinking circadian rhythms in mice. Physiology & Behavior 50, 373–378. https://doi.org/10.1016/0031-9384(91)90080-8

Edgar, R.S., Green, E.W., Zhao, Y., van Ooijen, G., Olmedo, M., Qin, X., Xu, Y., Pan, M., Valekunja, U.K., Feeney, K.A., Maywood, E.S., Hastings, M.H., Baliga, N.S., Merrow, M., Millar, A.J., Johnson, C.H., Kyriacou, C.P., O, J.S., Reddy, A.B., 2012. Peroxiredoxins are conserved markers of circadian rhythms. https://doi.org/10.1038/nature11088

Eleftheriou, C.G., Wright, P., Allen, A.E., Elijah, D., Martial, F.P., Lucas, R.J., 2020. Melanopsin Driven Light Responses Across a Large Fraction of Retinal Ganglion Cells in a Dystrophic Retina. Front Neurosci 14, 320. https://doi.org/10.3389/fnins.2020.00320

Emanuel, A.J., Kapur, K., Do, M.T.H., 2017. Biophysical Variation within the M1 Type of Ganglion Cell Photoreceptor. Cell Rep 21, 1048–1062. https://doi.org/10.1016/j.celrep.2017.09.095

Enright, J.T., 1970. Ecological Aspects of Endogenous Rhythmicity. Annual Review of Ecology and Systematics 1, 221–238.

Estévez, O., Spekreijse, H., 1982. The "silent substitution" method in visual research. Vision Research 22, 681–691. https://doi.org/10.1016/0042-6989(82)90104-3

Euler, T., Haverkamp, S., Schubert, T., Baden, T., 2014. Retinal bipolar cells: elementary building blocks of vision. Nat Rev Neurosci 15, 507–519. https://doi.org/10.1038/nrn3783

Evans, D.A., Stempel, A.V., Vale, R., Ruehle, S., Lefler, Y., Branco, T., 2018. A synaptic threshold mechanism for computing escape decisions. Nature 558, 590–594. https://doi.org/10.1038/s41586-018-0244-6

Fain, G.L., Hardie, R., Laughlin, S.B., 2010. Phototransduction and the Evolution of Photoreceptors. Current Biology 20, R114–R124. https://doi.org/10.1016/j.cub.2009.12.006

Feord, R.C., Gomoliszewska, A., Pienaar, A., Mouland, J.W., Brown, T.M., 2023. Colour opponency is widespread across the mouse subcortical visual system and differentially targets GABAergic and non-GABAergic neurons. Sci Rep 13, 9313. https://doi.org/10.1038/s41598-023-35885-z

Fernandez, D.C., Chang, Y.-T., Hattar, S., Chen, S.-K., 2016. Architecture of retinal projections to the central circadian pacemaker. Proc Natl Acad Sci U S A 113, 6047–6052. https://doi.org/10.1073/pnas.1523629113

Festing, M., Overend, P., Das, R., Cortina-Borja, M., Berdoy, M., 2002. The design of animal experiments: reducing the use of animals in research through better experimental design. Laboratory Animal Handbooks. No. 14. 1-16.

File, S.E., 2001. Factors controlling measures of anxiety and responses to novelty in the mouse. Behav Brain Res 125, 151–157. https://doi.org/10.1016/s0166-4328(01)00292-3

File, S.E., 1993. The interplay of learning and anxiety in the elevated plus-maze. Behavioural Brain Research 58, 199–202. https://doi.org/10.1016/0166-4328(93)90103-W

File, S.E., 1990. One-trial tolerance to the anxiolytic effects of chlordiazepoxide in the plus-maze. Psychopharmacology (Berl) 100, 281–282. https://doi.org/10.1007/BF02244419

File, S.E., 1985. What can be learned from the effects of benzodiazepines on exploratory behavior? Neurosci Biobehav Rev 9, 45–54. https://doi.org/10.1016/0149-7634(85)90031-4

File, S.E., Gonzalez, L.E., Gallant, R., 1998. Role of the Basolateral Nucleus of the Amygdala in the Formation of a Phobia. Neuropsychopharmacol 19, 397–405. https://doi.org/10.1016/S0893-133X(98)00035-9

Finger, A.-M., Kramer, A., 2021. Peripheral clocks tick independently of their master. Genes Dev 35, 304–306. https://doi.org/10.1101/gad.348305.121

Flôres, D.E.F.L., Jannetti, M.G., Valentinuzzi, V.S., Oda, G.A., 2016. Entrainment of circadian rhythms to irregular light/dark cycles: a subterranean perspective. Sci Rep 6, 34264. https://doi.org/10.1038/srep34264

Fonken, L.K., Finy, M.S., Walton, J.C., Weil, Z.M., Workman, J.L., Ross, J., Nelson, R.J., 2009. Influence of light at night on murine anxiety- and depressive-like responses. Behav Brain Res 205, 349–354. https://doi.org/10.1016/j.bbr.2009.07.001

Fontana, L., 2023. Effect of indoor surfaces' spectral reflectance on the environmental light spectrum modification and on objects perceived color. Results in Engineering 17, 100805. https://doi.org/10.1016/j.rineng.2022.100805

Forro, T., Volitaki, E., Malagon-Vina, H., Klausberger, T., Nevian, T., Ciocchi, S., 2022. Anxiety-related activity of ventral hippocampal interneurons. Prog Neurobiol 219, 102368. https://doi.org/10.1016/j.pneurobio.2022.102368

Fosbury, R.A.E., Jeffery, G., 2022. Reindeer eyes seasonally adapt to ozone-blue Arctic twilight by tuning a photonic tapetum lucidum. Proceedings of the Royal Society B: Biological Sciences 289, 20221002. https://doi.org/10.1098/rspb.2022.1002

Foster, R.G., Helfrich-Förster, C., 2001. The regulation of circadian clocks by light in fruitflies and mice. Philosophical Transactions of the Royal Society B: Biological Sciences 356, 1779–1789. https://doi.org/10.1098/rstb.2001.0962

Foster, R.G., Hughes, S., Peirson, S.N., 2020. Circadian photoentrainment in mice and humans. Biology 9, 1–45. https://doi.org/10.3390/biology9070180

Foster, R.G., Provencio, I., Hudson, D., Fiske, S., De Grip, W., Menaker, M., 1991. Circadian photoreception in the retinally degenerate mouse (rd/rd). Journal of Comparative Physiology A 169, 39–50. https://doi.org/10.1007/BF00198171

Freedman, M.S., Lucas, R.J., Soni, B., Von Schantz, M., Muñoz, M., David-Gray, Z., Foster, R., 1999. Regulation of Mammalian Circadian Behavior by Non-rod, Non-cone, Ocular Photoreceptors. Science (New York, N.Y.), 284(5413), 502–504. https://doi.org/10.1126/science.284.5413.502

Fu, Y., Yau, K.-W., 2007. Phototransduction in mouse rods and cones. Pflugers Arch - Eur J Physiol 454, 805–819. https://doi.org/10.1007/s00424-006-0194-y

Galindo-Romero, C., Norte-Muñoz, M., Gallego-Ortega, A., Rodríguez-Ramírez, K.T., Lucas-Ruiz, F., González-Riquelme, M.J., Vidal-Sanz, M., Agudo-Barriuso, M., 2022. The retina of the lab rat: focus on retinal ganglion cells and photoreceptors. Front. Neuroanat. 16. https://doi.org/10.3389/fnana.2022.994890

Gamlin, P.D.R., McDougal, D.H., Pokorny, J., Smith, V.C., Yau, K.-W., Dacey, D.M., 2007. Human and macaque pupil responses driven by melanopsin-containing retinal ganglion cells. Vision Res 47, 946–954. https://doi.org/10.1016/j.visres.2006.12.015

Garey, J., Goodwillie, A., Frohlich, J., Morgan, M., Gustafsson, J.-A., Smithies, O., Korach, K.S., Ogawa, S., Pfaff, D.W., 2003. Genetic contributions to generalized arousal of brain and behavior.

Proceedings of the National Academy of Sciences 100, 11019–11022. https://doi.org/10.1073/pnas.1633773100

Gaskill, B.N., Gordon, C.J., Pajor, E.A., Lucas, J.R., Davis, J.K., Garner, J.P., 2013. Impact of nesting material on mouse body temperature and physiology. Physiol Behav 110–111, 87–95. https://doi.org/10.1016/j.physbeh.2012.12.018

Gaskill, B.N., Rohr, S.A., Pajor, E.A., Lucas, J.R., Garner, J.P., 2011. Working with what you've got: Changes in thermal preference and behavior in mice with or without nesting material. Journal of Thermal Biology 36, 193–199. https://doi.org/10.1016/j.jtherbio.2011.02.004

Gattermann, R., Johnston, R.E., Yigit, N., Fritzsche, P., Larimer, S., Özkurt, S., Neumann, K., Song, Z., Colak, E., Johnston, J., McPhee, M.E., 2008. Golden hamsters are nocturnal in captivity but diurnal in nature. Biology Letters 4, 253–255. https://doi.org/10.1098/rsbl.2008.0066

Gause, G.F., 1934. Experimental Analysis of Vito Volterra's Mathematical Theory of the Struggle for Existence. Science 79, 16–17. https://doi.org/10.1126/science.79.2036.16.b

Geisler, W.S., 2008. Visual Perception and the Statistical Properties of Natural Scenes. Annu. Rev. Psychol. 59, 167–192. https://doi.org/10.1146/annurev.psych.58.110405.085632

Gerkema, M.P., Davies, W.I.L., Foster, R.G., Menaker, M., Hut, R.A., 2013. The nocturnal bottleneck and the evolution of activity patterns in mammals. Proceedings of the Royal Society B: Biological Sciences 280. https://doi.org/10.1098/rspb.2013.0508

Gerlai, R., Clayton, N.S., 1999. Analysing hippocampal function in transgenic mice: an ethological perspective. Trends in Neurosciences 22, 47–51. https://doi.org/10.1016/S0166-2236(98)01346-0

Gillette, M.U., 1986. The suprachiasmatic nuclei: circadian phase-shifts induced at the time of hypothalamic slice preparation are preserved in vitro. Brain Research 379, 176–181. https://doi.org/10.1016/0006-8993(86)90273-8

Glickman, G., Hanifin, J.P., Rollag, M.D., Wang, J., Cooper, H., Brainard, G.C., 2003. Inferior retinal light exposure is more effective than superior retinal exposure in suppressing melatonin in humans. J Biol Rhythms 18, 71–79. https://doi.org/10.1177/0748730402239678

Glover, L.R., Schoenfeld, T.J., Karlsson, R.-M., Bannerman, D.M., Cameron, H.A., 2017. Ongoing neurogenesis in the adult dentate gyrus mediates behavioral responses to ambiguous threat cues. PLOS Biology 15, e2001154. https://doi.org/10.1371/journal.pbio.2001154

Goldberg, A.F.X., Moritz, O.L., Williams, D.S., 2016. Molecular basis for photoreceptor outer segment architecture. Progress in Retinal and Eye Research 55, 52–81. https://doi.org/10.1016/j.preteyeres.2016.05.003

Golini, E., Rigamonti, M., Iannello, F., De Rosa, C., Scavizzi, F., Raspa, M., Mandillo, S., 2020. A Non-invasive Digital Biomarker for the Detection of Rest Disturbances in the SOD1G93A Mouse Model of ALS. Frontiers in Neuroscience 14, 1–12. https://doi.org/10.3389/fnins.2020.00896

Gordon, C.J., 2012. Thermal physiology of laboratory mice: Defining thermoneutrality. Journal of Thermal Biology 37, 654–685. https://doi.org/10.1016/j.jtherbio.2012.08.004

Gordon, C.J., Puckett, E.T., Repasky, E.S., Johnstone, A.F.M., 2017. A Device that Allows Rodents to Behaviorally Thermoregulate when Housed in Vivariums. J Am Assoc Lab Anim Sci 56, 173–176.

Govardovskii, V.I., Fyhrquist, N., Reuter, T., Kuzmin, D.G., Donner, K., 2000. In search of the visual pigment template. Visual Neuroscience 17, 509–528. https://doi.org/10.1017/S0952523800174036

Graham, A.L., 2021. Naturalizing mouse models for immunology. Nat Immunol 22, 111–117. https://doi.org/10.1038/s41590-020-00857-2

Güler, A.D., Ecker, J.L., Lall, G.S., Haq, S., Altimus, C.M., Liao, H.-W., Barnard, A.R., Cahill, H., Badea, T.C., Zhao, H., Hankins, M.W., Berson, D.M., Lucas, R.J., Yau, K.-W., Hattar, S., 2008. Melanopsin cells are the principal conduits for rod-cone input to non-image-forming vision. https://doi.org/10.1038/nature06829

Guo, H., Brewer, J.M., Lehman, M.N., Bittman, E.L., 2006. Suprachiasmatic regulation of circadian rhythms of gene expression in hamster peripheral organs: effects of transplanting the pacemaker. J Neurosci 26, 6406–6412. https://doi.org/10.1523/JNEUROSCI.4676-05.2006

Häfker, N.S., Connan-McGinty, S., Hobbs, L., McKee, D., Cohen, J.H., Last, K.S., 2022. Animal behavior is central in shaping the realized diel light niche. Commun Biol 5, 562. https://doi.org/10.1038/s42003-022-03472-z

Hagen, J.F.D., Roberts, N.S., Johnston, R.J., 2023. The evolutionary history and spectral tuning of vertebrate visual opsins. Developmental Biology 493, 40–66. https://doi.org/10.1016/j.ydbio.2022.10.014

Halle, S., Stenseth, N.C. (Eds.), 2000. Activity Patterns in Small Mammals, Ecological Studies. Springer, Berlin, Heidelberg. https://doi.org/10.1007/978-3-642-18264-8

Hammond, K.R., 1954. Representative vs. systematic design in clinical psychology. Psychol Bull 51, 150–159. https://doi.org/10.1037/h0063011

Hankins, M.W., Peirson, S.N., Foster, R.G., 2008. Melanopsin: an exciting photopigment. Trends in Neurosciences 31, 27–36. https://doi.org/10.1016/j.tins.2007.11.002

Hardin, G., 1960. The Competitive Exclusion Principle. Science 131, 1292–1297. https://doi.org/10.1126/science.131.3409.1292

Hastings, J.W., Sweeney, B.M., 1960. The Action Spectrum for Shifting the Phase of the Rhythm of Luminescence in Gonyaulax polyedra. Journal of General Physiology 43, 697–706. https://doi.org/10.1085/jgp.43.4.697

Hastings, M.H., Maywood, E.S., Brancaccio, M., 2018. Generation of circadian rhythms in the suprachiasmatic nucleus. Nature reviews. Neuroscience 19, 453–469. https://doi.org/10.1038/S41583-018-0026-Z

Hatori, M., Panda, S., 2010. The emerging roles of melanopsin in behavioral adaptation to light. Trends in Molecular Medicine 16, 435–446. https://doi.org/10.1016/j.molmed.2010.07.005

Hattar, S., Kumar, M., Park, A., Tong, P., Tung, J., Yau, K.-W., Berson, D.M., 2006. Central projections of melanopsin-expressing retinal ganglion cells in the mouse. Journal of Comparative Neurology 497, 326–349. https://doi.org/10.1002/cne.20970

Hattar, S., Liao, H.W., Takao, M., Berson, D.M., Yau, K.W., 2002. Melanopsin-containing retinal ganglion cells: architecture, projections, and intrinsic photosensitivity. Science (New York, N.Y.) 295, 1065–1070. https://doi.org/10.1126/SCIENCE.1069609

Hattar, S., Lucas, R.J., Mrosovsky, N., Thompson, S., Douglas, R.H., Hankins, M.W., Lem, J., Biel, M., Hofmann, F., Foster, R.G., Yau, K.W., 2003. Melanopsin and rod-cone photoreceptive systems account for all major accessory visual functions in mice. Nature 424, 76–81. https://doi.org/10.1038/NATURE01761

Hazlerigg, D.G., Appenroth, D., Tomotani, B.M., West, A.C., Wood, S.H., 2023. Biological timekeeping in polar environments: lessons from terrestrial vertebrates. J Exp Biol 226, jeb246308. https://doi.org/10.1242/jeb.246308

Heard, E., 2022. Molecular biologists: let's reconnect with nature. Nature 601, 9–9. https://doi.org/10.1038/d41586-021-03818-3

Helfrich-Förster, C., Bertolini, E., Menegazzi, P., 2020. Flies as models for circadian clock adaptation to environmental challenges. European Journal of Neuroscience 51, 166–181. https://doi.org/10.1111/ejn.14180

Helm, B., Visser, M.E., Schwartz, W., Kronfeld-Schor, N., Gerkema, M., Piersma, T., Bloch, G., 2017. Two sides of a coin: ecological and chronobiological perspectives of timing in the wild. https://doi.org/10.1098/rstb.2016.0246

Henderson, S.T., Hodgkiss, D., 1963. The spectral energy distribution of daylight. Br. J. Appl. Phys. 14, 125. https://doi.org/10.1088/0508-3443/14/3/307

Hendrickson, A., 2009. Fovea: Primate, in: Squire, L.R. (Ed.), Encyclopedia of Neuroscience. Academic Press, Oxford, pp. 327–334. https://doi.org/10.1016/B978-008045046-9.00920-7

Herzog, E.D., Aton, S.J., Numano, R., Sakaki, Y., Tei, H., 2004. Temporal precision in the mammalian circadian system: a reliable clock from less reliable neurons. J Biol Rhythms 19, 35–46. https://doi.org/10.1177/0748730403260776

Hildebrand, E., Schimz, A., 1986. Integration of photosensory signals in Halobacterium halobium. Journal of Bacteriology 167, 305–311. https://doi.org/10.1128/jb.167.1.305-311.1986

Hoban, T.M., Sulzman, F.M., 1985. Light effects on circadian timing system of a diurnal primate, the squirrel monkey. American Journal of Physiology-Regulatory, Integrative and Comparative Physiology 249, R274–R280. https://doi.org/10.1152/ajpregu.1985.249.2.R274

Hoc, J.-M., 2001. Towards ecological validity of research in cognitive ergonomics. Theoretical Issues in Ergonomics Science 2, 278–288. https://doi.org/10.1080/14639220110104970

Hoelter, S.M., Dalke, C., Kallnik, M., Becker, L., Horsch, M., Schrewe, A., Favor, J., Klopstock, T., Beckers, J., Ivandic, B., Gailus-Durner, V., Fuchs, H., Angelis, M.H. de, Graw, J., Wurst, W., 2008. "Sighted C3H" mice – a tool for analysing the influence of vision on mouse behaviour? FBL 13, 5810–5823. https://doi.org/10.2741/3118

Holleman, G.A., Hooge, I.T.C., Kemner, C., Hessels, R.S., 2020. The "Real-World Approach" and Its Problems: A Critique of the Term Ecological Validity. Front Psychol 11, 721. https://doi.org/10.3389/fpsyg.2020.00721

Hopwood, T.W., Hall, S., Begley, N., Forman, R., Brown, S., Vonslow, R., Saer, B., Little, M.C., Murphy, E.A., Hurst, R.J., Ray, D.W., MacDonald, A.S., Brass, A., Bechtold, D.A., Gibbs, J.E., Loudon, A.S., Else, K.J., 2018. The circadian regulator BMAL1 programmes responses to parasitic worm infection via a dendritic cell clock. Sci Rep 8, 3782. https://doi.org/10.1038/s41598-018-22021-5

Hossain, S.M., Wong, B.K.Y., Simpson, E.M., 2004. The dark phase improves genetic discrimination for some high throughput mouse behavioral phenotyping. Genes, Brain and Behavior 3, 167–177. https://doi.org/10.1111/j.1601-183x.2004.00069.x

Hovi, A., Rautiainen, M., 2020. Spectral composition of shortwave radiation transmitted by forest canopies. Trees 34, 1499–1506. https://doi.org/10.1007/s00468-020-02005-7

Hubbard, J., Ruppert, E., Gropp, C.-M., Bourgin, P., 2013. Non-circadian direct effects of light on sleep and alertness: lessons from transgenic mouse models. Sleep Med Rev 17, 445–452. https://doi.org/10.1016/j.smrv.2012.12.004

Hughes, A.T.L., Piggins, H.D., 2012. Chapter 18 - Feedback actions of locomotor activity to the circadian clock, in: Kalsbeek, A., Merrow, M., Roenneberg, T., Foster, R.G. (Eds.), Progress in Brain Research, The Neurobiology of Circadian Timing. Elsevier, pp. 305–336. https://doi.org/10.1016/B978-0-444-59427-3.00018-6

Hughes, M.E., DiTacchio, L., Hayes, K.R., Vollmers, C., Pulivarthy, S., Baggs, J.E., Panda, S., Hogenesch, J.B., 2009. Harmonics of Circadian Gene Transcription in Mammals. PLOS Genetics 5, e1000442. https://doi.org/10.1371/journal.pgen.1000442

Hughes, R.N., 1997. Intrinsic exploration in animals: motives and measurement. Behavioural Processes 41, 213–226. https://doi.org/10.1016/S0376-6357(97)00055-7

Hughes, S., Jagannath, A., Hankins, M.W., Foster, R.G., Peirson, S.N., 2015. Chapter Six - Photic Regulation of Clock Systems, in: Sehgal, A. (Ed.), Methods in Enzymology, Circadian Rhythms and Biological Clocks, Part B. Academic Press, pp. 125–143. https://doi.org/10.1016/bs.mie.2014.10.018

Hughes, S., Jagannath, A., Rodgers, J., Hankins, M.W., Peirson, S.N., Foster, R.G., 2016. Signalling by melanopsin (OPN4) expressing photosensitive retinal ganglion cells. Eye (Basingstoke) 30, 247–254. https://doi.org/10.1038/eye.2015.264

Hughes, S., Watson, T.S., Foster, R.G., Peirson, S.N., Hankins, M.W., 2013. Nonuniform distribution and spectral tuning of photosensitive retinal ganglion cells of the mouse retina. Current Biology 23, 1696–1701. https://doi.org/10.1016/j.cub.2013.07.010

Hulburt, E.O., 1953. Explanation of the Brightness and Color of the Sky, Particularly the Twilight Sky. J. Opt. Soc. Am., JOSA 43, 113–118. https://doi.org/10.1364/JOSA.43.000113

Hut, R.A., Pilorz, V., Boerema, A.S., Strijkstra, A.M., Daan, S., 2011. Working for Food Shifts Nocturnal Mouse Activity into the Day. PLOS ONE 6, e17527. https://doi.org/10.1371/journal.pone.0017527

Hut, R.A., Scheper, A., Daan, S., 2000. Can the circadian system of a diurnal and a nocturnal rodent entrain to ultraviolet light? J Comp Physiol A 186, 707–715. https://doi.org/10.1007/s003590000124

Hut, R.A., van Oort, B.E., Daan, S., 1999. Natural entrainment without dawn and dusk: the case of the European ground squirrel (Spermophilus citellus). J Biol Rhythms 14, 290–299. https://doi.org/10.1177/074873099129000704

Iannello, F., 2019. Non-intrusive high throughput automated data collection from the home cage. Heliyon 5, e01454. https://doi.org/10.1016/j.heliyon.2019.e01454

Ingram, N.T., Sampath, A.P., Fain, G.L., 2016. Why are rods more sensitive than cones? J Physiol 594, 5415–5426. https://doi.org/10.1113/JP272556

Inouye, S.-I.T., Kawamura, H., 1979. Persistence of circadian rhythmicity in a mammalian hypothalamic "island" containing the suprachiasmatic nucleus. Proceedings of the National Academy of Sciences of the United States of America, 76(11), 5962–5966. https://doi.org/10.1073/pnas.76.11.5962.

Ishida, A., Mutoh, T., Ueyama, T., Bando, H., Masubuchi, S., Nakahara, D., Tsujimoto, G., Okamura, H., 2005. Light activates the adrenal gland: Timing of gene expression and glucocorticoid release. Cell Metabolism 2, 297–307. https://doi.org/10.1016/j.cmet.2005.09.009

Jabbur, M.L., Dani, C., Spoelstra, K., Dodd, A.N., Johnson, C.H., 2024. Evaluating the Adaptive Fitness of Circadian Clocks and their Evolution. J Biol Rhythms 39, 115–134. https://doi.org/10.1177/07487304231219206

Jabbur, M.L., Zhao, C., Johnson, C.H., 2021. Insights into the Evolution of Circadian Clocks Gleaned from Bacteria, in: Johnson, C.H., Rust, M.J. (Eds.), Circadian Rhythms in Bacteria and Microbiomes. Springer International Publishing, Cham, pp. 111–135. https://doi.org/10.1007/978-3-030-72158-9_7

Jacobs, G.H., 2014. The Discovery of Spectral Opponency in Visual Systems and its Impact on Understanding the Neurobiology of Color Vision. Journal of the History of the Neurosciences 23, 287–314. https://doi.org/10.1080/0964704X.2014.896662

Jacobs, G.H., 1993. The distribution and nature of colour vision among the mammals. Biol Rev Camb Philos Soc 68, 413–471. https://doi.org/10.1111/j.1469-185x.1993.tb00738.x

Jacobs, G.H., Neitz, J., Deegan, J.F., 1991. Retinal receptors in rodents maximally sensitive to ultraviolet light. Nature 353, 655–656. https://doi.org/10.1038/353655a0

Jacquemoud, S., Ustin, S.L., 2019. Modeling Leaf Optical Properties: prospect. In: Leaf Optical Properties. Cambridge University Press; 2019:265-291.

Jagannath, A., Hughes, S., Abdelgany, A., Pothecary, C.A., Di Pretoro, S., Pires, S.S., Vachtsevanos, A., Pilorz, V., Brown, L.A., Hossbach, M., MacLaren, R.E., Halford, S., Gatti, S., Hankins, M.W., Wood, M.J.A., Foster, R.G., Peirson, S.N., 2015. Isoforms of Melanopsin Mediate Different Behavioral Responses to Light. Current Biology 25, 2430–2434. https://doi.org/10.1016/j.cub.2015.07.071

Jalali, M.S., Jones, J.R., Tural, E., Gibbons, R.B., 2024. Human-Centric Lighting Design: A Framework for Supporting Healthy Circadian Rhythm Grounded in Established Knowledge in Interior Spaces. Buildings 14, 1125. https://doi.org/10.3390/buildings14041125

Jannetti, M.G., Tachinardi, P., Valentinuzzi, V.S., Oda, G.A., 2023. Temporal Dissociation Between Activity and Body Temperature Rhythms of a Subterranean Rodent (Ctenomys famosus) in Field Enclosures. J Biol Rhythms 38, 278–289. https://doi.org/10.1177/07487304231154715

Jeon, C.-J., Strettoi, E., Masland, R.H., 1998. The Major Cell Populations of the Mouse Retina. J. Neurosci. 18, 8936–8946. https://doi.org/10.1523/JNEUROSCI.18-21-08936.1998

Joesch, M., Meister, M., 2016. A neuronal circuit for colour vision based on rod-cone opponency. Nature 532, 236–239. https://doi.org/10.1038/nature17158

Johnsen, S., 2011. Units and Geometry, in: Johnsen, S. (Ed.), The Optics of Life: A Biologist's Guide to Light in Nature. Princeton University Press, p. 0. https://doi.org/10.23943/princeton/9780691139906.003.0002

Johnson, C.H., Golden, S.S., Ishiura, M., Kondo, T., 1996. Circadian clocks in prokaryotes. Mol Microbiol 21, 5–11. https://doi.org/10.1046/j.1365-2958.1996.00613.x

Johnson, J., Wu, V., Donovan, M., Majumdar, S., Rentería, R.C., Porco, T., Van Gelder, R.N., Copenhagen, D.R., 2010. Melanopsin-dependent light avoidance in neonatal mice. Proc. Natl. Acad. Sci. U.S.A. 107, 17374–17378. https://doi.org/10.1073/pnas.1008533107

Jones, K.A., Hatori, M., Mure, L.S., Bramley, J.R., Artymyshyn, R., Hong, S.-P., Marzabadi, M., Zhong, H., Sprouse, J., Zhu, Q., Hartwick, A.T.E., Sollars, P.J., Pickard, G.E., Panda, S., 2013. Small-molecule antagonists of melanopsin-mediated phototransduction. Nat Chem Biol 9, 630–635. https://doi.org/10.1038/nchembio.1333

Jones, M.A., Covington, M.F., Ditacchio, L., Vollmers, C., Panda, S., Harmer, S.L., Kay, S.A., 2010. Jumonji domain protein JMJD5 functions in both the plant and human circadian systems. https://doi.org/10.1073/pnas.1014204108

Joshi, D., Chandrashekaran, M.K., 1985. White light of different spectral composition causes differential phase shifts of circadian rhythm of activity in a bat. Naturwissenschaften 72, 548–549. https://doi.org/10.1007/BF00367607

Jud, C., Schmutz, I., Hampp, G., Oster, H., Albrecht, U., 2005. A guideline for analyzing circadian wheel-running behavior in rodents under different lighting conditions. Biological procedures online 7, 101–116. https://doi.org/10.1251/BPO109

Judd, D.B., MacAdam, D.L., Wyszecki, G., Budde, H.W., Condit, H.R., Henderson, S.T., Simonds, J.L., 1964. Spectral Distribution of Typical Daylight as a Function of Correlated Color Temperature. Journal of the Optical Society of America 54, 1031. https://doi.org/10.1364/josa.54.001031

Judd, F.K., Burrows, G.D., Norman, T.R., 1985. The biological basis of anxiety: An overview. Journal of Affective Disorders 9, 271–284. https://doi.org/10.1016/0165-0327(85)90058-8

Juola, J., Hovi, A., Rautiainen, M., 2022. A spectral analysis of stem bark for boreal and temperate tree species. Ecol Evol 12, e8718. https://doi.org/10.1002/ece3.8718

Kale, K.V., Solankar, M.M., Nalawade, D.B., Dhumal, R.K., Gite, H.R., 2017. A Research Review on Hyperspectral Data Processing and Analysis Algorithms. Proc. Natl. Acad. Sci., India, Sect. A Phys. Sci. 87, 541–555. https://doi.org/10.1007/s40010-017-0433-y

Kale, K.V., Solankar, M.M., Nalawade, D.B., Kale, K.V., Solankar, M.M., Nalawade, D.B., 2019. Hyperspectral Endmember Extraction Techniques, in: Processing and Analysis of Hyperspectral Data. IntechOpen. https://doi.org/10.5772/intechopen.88910

Kallmyer, N.E., Shin, H.J., Brem, E.A., Israelsen, W.J., Reuel, N.F., 2019. Nesting box imager: Contact-free, real-time measurement of activity, surface body temperature, and respiratory rate applied to hibernating mouse models. PLoS Biology 17, 1–13. https://doi.org/10.1371/journal.pbio.3000406

Kalsbeek, A., Bruinstroop, E., Yi, C. x., Klieverik, L. p., La Fleur, S. e, Fliers, E., 2010. Hypothalamic control of energy metabolism via the autonomic nervous system. Annals of the New York Academy of Sciences 1212, 114–129. https://doi.org/10.1111/j.1749-6632.2010.05800.x

Kaneko, M., Kaneko, K., Shinsako, J., Dallman, M.F., 1981. Adrenal sensitivity to adrenocorticotropin varies diurnally. Endocrinology 109, 70–75. https://doi.org/10.1210/endo-109-1-70

Kautzky, M., Peterreins, V., Qiu, Y., Zhao, Z., Kotkat, A.H., Katzner, S., Euler, T., Busse, L., 2024. A hemispheric dome setup for naturalistic visual stimulation in head-fixed mice. https://doi.org/10.1101/2024.05.31.596599

Keidser, G., Naylor, G., Brungart, D.S., Caduff, A., Campos, J., Carlile, S., Carpenter, M.G., Grimm, G., Hohmann, V., Holube, I., Launer, S., Lunner, T., Mehra, R., Rapport, F., Slaney, M., Smeds, K., 2022. Comment on the Point of View "Ecological Validity, External Validity and Mundane Realism in Hearing Science." Ear Hear 43, 1601–1602. https://doi.org/10.1097/AUD.0000000000001241

Keidser, G., Naylor, G., Brungart, D.S., Caduff, A., Campos, J., Carlile, S., Carpenter, M.G., Grimm, G., Hohmann, V., Holube, I., Launer, S., Lunner, T., Mehra, R., Rapport, F., Slaney, M., Smeds, K., 2020. The Quest for Ecological Validity in Hearing Science: What It Is, Why It Matters, and How to Advance It. Ear Hear 41 Suppl 1, 5S-19S. https://doi.org/10.1097/AUD.0000000000000944

Kenagy, G.J., 1976. The periodicity of daily activity and its seasonal changes in free-ranging and captive kangaroo rats. Oecologia 24, 105–140. https://doi.org/10.1007/BF00572754

Khademagha, P., Aries, M.B.C., Rosemann, A.L.P., van Loenen, E.J., 2016. Implementing non-image-forming effects of light in the built environment: A review on what we need. Building and Environment 108, 263–272. https://doi.org/10.1016/j.buildenv.2016.08.035

Khalsa, S.B.S., Jewett, M.E., Cajochen, C., Czeisler, C.A., 2003. A phase response curve to single bright light pulses in human subjects. J Physiol 549, 945–952. https://doi.org/10.1113/jphysiol.2003.040477

Kopp, C., 2001. Locomotor activity rhythm in inbred strains of mice: implications for behavioural studies. Behavioural Brain Research 125, 93–96. https://doi.org/10.1016/S0166-4328(01)00289-3

Krakauer, J.W., Ghazanfar, A.A., Gomez-Marin, A., MacIver, M.A., Poeppel, D., 2017. Neuroscience Needs Behavior: Correcting a Reductionist Bias. Neuron 93, 480–490. https://doi.org/10.1016/j.neuron.2016.12.041

Kriegsfeld, L.J., Silver, R., 2006. The regulation of neuroendocrine function: Timing is everything. Horm Behav 49, 557–574. https://doi.org/10.1016/j.yhbeh.2005.12.011

Lall, G.S., Revell, V.L., Momiji, H., Al Enezi, J., Altimus, C.M., Güler, A.D., Aguilar, C., Cameron, M.A., Allender, S., Hankins, M.W., Lucas, R.J., 2010. Distinct contributions of rod, cone, and melanopsin photoreceptors to encoding irradiance. Neuron 66, 417–428. https://doi.org/10.1016/J.NEURON.2010.04.037

Lamb, T.D., 2016. Why rods and cones? Eye 30, 179–185. https://doi.org/10.1038/eye.2015.236

Lasko, T.A., Kripke, D.F., Elliot, J.A., 1999. Melatonin Suppression by Illumination of Upper and Lower Visual Fields. J Biol Rhythms 14, 122–125. https://doi.org/10.1177/074873099129000506

Latham, N., Mason, G., 2004. From house mouse to mouse house: the behavioural biology of free-living *Mus musculus* and its implications in the laboratory. Applied Animal Behaviour Science, International Society for Applied Ethology Special Issue: A selection of papers from the 36th ISAE International Congress. 86, 261–289. https://doi.org/10.1016/j.applanim.2004.02.006

Lawrence, S., Lau, E., Steutel, D., Stopar, J., Wilcox, B.B., Lucey, P., 2003. A New Measurement of the Absolute Spectral Reflectance of the Moon.

Leamey, C., Protti, D., Dreher, B., 2008. Comparative survey of the mammalian visual system with reference to the mouse. Eye, Retina and Visual System of the Mouse. 35-60.

Legates, T.A., Altimus, C.M., Wang, H., Lee, H.K., Yang, S., Zhao, H., Kirkwood, A., Weber, E.T., Hattar, S., 2012. Aberrant light directly impairs mood and learning through melanopsin-expressing neurons. Nature 491, 594–598. https://doi.org/10.1038/nature11673

Lezak, K.R., Missig, G., Carlezon Jr, W.A., 2017. Behavioral methods to study anxiety in rodents. Dialogues in Clinical Neuroscience 19, 181–191. https://doi.org/10.31887/DCNS.2017.19.2/wcarlezon

Lockard, R.B., Owings, D.H., 1974. Seasonal Variation in Moonlight Avoidance by Bannertail Kangaroo Rats. Journal of Mammalogy 55, 189–193. https://doi.org/10.2307/1379266

Lockwood, D.J., 2016. Rayleigh and Mie Scattering, in: Luo, M.R. (Ed.), Encyclopedia of Color Science and Technology. Springer, New York, NY, pp. 1097–1107. https://doi.org/10.1007/978-1-4419-8071-7_218

Lowrey, P.L., Shimomura, K., Antoch, M.P., Yamazaki, S., Zemenides, P.D., Ralph, M.R., Menaker, M., Takahashi, J.S., 2000. Positional syntenic cloning and functional characterization of the mammalian circadian mutation tau. Science 288, 483–492. https://doi.org/10.1126/science.288.5465.483

Lucas, R.J., Allen, A.E., Brainard, G.C., Brown, T.M., Dauchy, R.T., Didikoglu, A., Do, M.T.H., Gaskill, B.N., Hattar, S., Hawkins, P., Hut, R.A., McDowell, R.J., Nelson, R.J., Prins, J.-B., Schmidt, T.M., Takahashi, J.S., Verma, V., Voikar, V., Wells, S., Peirson, S.N., 2024. Recommendations for measuring and standardizing light for laboratory mammals to improve welfare and reproducibility in animal research. PLOS Biology 22, e3002535. https://doi.org/10.1371/journal.pbio.3002535

Lucas, R.J., Allen, A.E., Milosavljevic, N., Storchi, R., Woelders, T., 2020. Can We See with Melanopsin? Annual Review of Vision Science 6, 453–468. https://doi.org/10.1146/annurev-vision-030320-041239

Lucas, R.J., Douglas, R.H., Foster, R.G., 2001. Characterization of an ocular photopigment capable of driving pupillary constriction in mice. Nat Neurosci 4, 621–626. https://doi.org/10.1038/88443

Lucas, R.J., Freedman, M.S., Muñoz, M., Garcia-Fernández, J.-M., Foster, R.G., 1999. Regulation of the Mammalian Pineal by Non-rod, Non-cone, Ocular Photoreceptors. Science 284, 505–507. https://doi.org/10.1126/science.284.5413.505

Lucas, R.J., Lall, G.S., Allen, A.E., Brown, T.M., 2012. How rod, cone, and melanopsin photoreceptors come together to enlighten the mammalian circadian clock. Prog Brain Res 199, 1–18. https://doi.org/10.1016/B978-0-444-59427-3.00001-0

Lucas, R.J., Peirson, S.N., Berson, D.M., Brown, T., Cooper, H., Czeisler, C.A., Figueiro, M.G., Gamlin, P.D., Lockley, S.W., O'Hagan, J.B., Price, L.L.A., Provencio, I., Skene, D.J., Brainard, G.C., 2013. Irradiance Toolbox User Guide 1–19.

Lucas, R.J., Peirson, S.N., Berson, D.M., Brown, T.M., Cooper, H.M., Czeisler, C.A., Figueiro, M.G., Gamlin, P.D., Lockley, S.W., O'hagan, J.B., Price, L.L.A., Provencio, I., Skene, D.J., Brainard, G.C., 2014. Measuring and using light in the melanopsin age. Trends in Neurosciences 37, 1–9. https://doi.org/10.1016/j.tins.2013.10.004

Lupi, D., Oster, H., Thompson, S., Foster, R.G., 2008. The acute light-induction of sleep is mediated by OPN4-based photoreception. Nature Neuroscience 11, 1068–1073. https://doi.org/10.1038/nn.2179

Matusz, P.J., Dikker, S., Huth, A.G., Perrodin, C., 2019. Are we ready for real-world neuroscience? J Cogn Neurosci 31, 327–338. https://doi.org/10.1162/jocn_e_01276

Matynia, A., Parikh, S., Chen, B., Kim, P., McNeill, D.S., Nusinowitz, S., Evans, C., Gorin, M.B., 2012. Intrinsically photosensitive retinal ganglion cells are the primary but not exclusive circuit for light aversion. Exp Eye Res 105, 60–69. https://doi.org/10.1016/j.exer.2012.09.012

McGuire, R.A., Rand, W.M., Wurtman, R.J., 1973. Entrainment of the body temperature rhythm in rats: effect of color and intensity of environmental light. Science 181, 956–957. https://doi.org/10.1126/science.181.4103.956

Melyan, Z., Tarttelin, E.E., Bellingham, J., Lucas, R.J., Hankins, M.W., 2005. Addition of human melanopsin renders mammalian cells photoresponsive. Nature 433, 741–745. https://doi.org/10.1038/nature03344

Menaker, M., 1968. Extraretinal Light Perception in the Sparrow, I. Entrainment of the Biological Clock. Proceedings of the National Academy of Sciences of the United States of America 59, 414–421.

Mendez, A., Burns, M.E., Roca, A., Lem, J., Wu, L.W., Simon, M.I., Baylor, D.A., Chen, J., 2000. Rapid and reproducible deactivation of rhodopsin requires multiple phosphorylation sites. Neuron 28, 153–164. https://doi.org/10.1016/s0896-6273(00)00093-3

Milosavljevic, N., Cehajic-Kapetanovic, J., Procyk, C.A., Lucas, R.J., 2016. Chemogenetic Activation of Melanopsin Retinal Ganglion Cells Induces Signatures of Arousal and/or Anxiety in Mice. Current Biology 26, 2358–2363. https://doi.org/10.1016/j.cub.2016.06.057

Mitsui, A., Kumazawa, S., Takahashi, A., Ikemoto, H., Cao, S., Arai, T., 1986. Strategy by which nitrogen-fixing unicellular cyanobacteria grow photoautotrophically. Nature 323, 720–722. https://doi.org/10.1038/323720a0

Mochizuki, T., Crocker, A., McCormack, S., Yanagisawa, M., Sakurai, T., Scammell, T.E., 2004. Behavioral state instability in orexin knock-out mice. Journal of Neuroscience 24, 6291–6300. https://doi.org/10.1523/JNEUROSCI.0586-04.2004

Mohawk, J.A., Green, C.B., Takahashi, J.S., 2012. Central and Peripheral Circadian Clocks in Mammals. Annual Review of Neuroscience 35, 445–462. https://doi.org/10.1146/annurev-neuro-060909-153128

Mohawk, J.A., Takahashi, J.S., 2011. Cell Autonomy and Synchrony of Suprachiasmatic Nucleus Circadian Oscillators. Trends Neurosci 34, 349–358. https://doi.org/10.1016/j.tins.2011.05.003

Monecke, S., Sage-Ciocca, D., Wollnik, F., Pévet, P., 2013. Photoperiod Can Entrain Circannual Rhythms in Pinealectomized European Hamsters. J Biol Rhythms 28, 278–290. https://doi.org/10.1177/0748730413498561

Moore, R.Y., Eichler, V.B., 1972. Loss of a circadian adrenal corticosterone rhythm following suprachiasmatic lesions in the rat. Brain Res 42, 201–206. https://doi.org/10.1016/0006-8993(72)90054-6

Moore, R.Y., Lenn, N.J., 1972. A retinohypothalamic projection in the rat. Journal of Comparative Neurology 146, 1–14. https://doi.org/10.1002/cne.901460102

Moore, R.Y., Silver, R., 1998. Suprachiasmatic Nucleus Organization. Chronobiology International. https://doi.org/10.3109/07420529808998703

Morgenstern, Y., Murray, R.F., Harris, L.R., 2011. The human visual system's assumption that light comes from above is weak. Proceedings of the National Academy of Sciences 108, 12551–12553. https://doi.org/10.1073/pnas.1100794108

Morimoto, T., 2022. Hyperspectral characterization of natural lighting environments, in: Progress in Brain Research. Elsevier B.V., pp. 37–48. https://doi.org/10.1016/bs.pbr.2022.04.008

Morimoto, T., Kishigami, S., Linhares, J.M.M., Nascimento, S.M.C., Smithson, H.E., 2019. Hyperspectral environmental illumination maps: characterizing directional spectral variation in natural environments. Optics Express 27, 32277. https://doi.org/10.1364/OE.27.032277

Morin, L.P., Allen, C.N., 2006. The circadian visual system, 2005. Brain Research Reviews 51, 1–60. https://doi.org/10.1016/j.brainresrev.2005.08.003

Mouland, J.W., Brown, T.M., 2022. Beyond irradiance: Visual signals influencing mammalian circadian function, in: Progress in Brain Research. Elsevier B.V., pp. 145–169. https://doi.org/10.1016/bs.pbr.2022.04.010

Mouland, J.W., Martial, F., Watson, A., Lucas, R.J., Brown, T.M., 2019. Cones Support Alignment to an Inconsistent World by Suppressing Mouse Circadian Responses to the Blue Colors Associated with Twilight. Current Biology 29, 4260-4267.e4. https://doi.org/10.1016/j.cub.2019.10.028

Mouland, J.W., Martial, F.P., Lucas, R.J., Brown, T.M., 2021. Modulations in irradiance directed at melanopsin, but not cone photoreceptors, reliably alter electrophysiological activity in the suprachiasmatic nucleus and circadian behaviour in mice. Journal of Pineal Research 70, e12735. https://doi.org/10.1111/jpi.12735

Mouland, J.W., Stinchcombe, A.R., Forger, D.B., Brown, T.M., Lucas, R.J., 2017. Responses to Spatial Contrast in the Mouse Suprachiasmatic Nuclei. Current Biology 27, 1633-1640.e3. https://doi.org/10.1016/j.cub.2017.04.039

Mouland, J.W., Watson, A.J., Martial, F.P., Lucas, R.J., Brown, T.M., 2023. Colour and melanopsin mediated responses in the murine retina. Front. Cell. Neurosci. 17. https://doi.org/10.3389/fncel.2023.1114634

Mrosovsky, N., 1999. Masking: history, definitions, and measurement. Chronobiol Int 16, 415–429. https://doi.org/10.3109/07420529908998717

Mrosovsky, N., Hattar, S., 2003. Impaired masking responses to light in melanopsin-knockout mice. Chronobiol Int 20, 989–999. https://doi.org/10.1081/cbi-120026043

Münch, M., Wirz-Justice, A., Brown, S.A., Kantermann, T., Martiny, K., Stefani, O., Vetter, C., Wright, K.P., Wulff, K., Skene, D.J., 2020. The Role of Daylight for Humans: Gaps in Current Knowledge. Clocks Sleep 2, 61–85. https://doi.org/10.3390/clockssleep2010008

Mure, L.S., Rieux, C., Hattar, S., Cooper, H.M., 2007. Melanopsin-dependent nonvisual responses: evidence for photopigment bistability in vivo. J Biol Rhythms 22, 411–424. https://doi.org/10.1177/0748730407306043

Nakamura, T.J., Ebihara, S., Shinohara, K., 2011. Reduced light response of neuronal firing activity in the suprachiasmatic nucleus and optic nerve of cryptochrome-deficient mice. PLoS One 6, e28726. https://doi.org/10.1371/journal.pone.0028726

Nascimento, S.M.C., Amano, K., Foster, D.H., 2016. Spatial distributions of local illumination color in natural scenes. Vision Research, Vision and the Statistics of the Natural Environment 120, 39–44. https://doi.org/10.1016/j.visres.2015.07.005

Naumann, S., Byrne, M.L., de la Fuente, A., Harrewijn, A., Nugiel, T., Rosen, M., van Atteveldt, N., Matusz, P.J., 2022. Assessing the Degree of Ecological Validity of Your Study: Introducing the Multidimensional Assessment of Research in Context (MARC) Tool. Mind, Brain, and Education 16, 228–238. https://doi.org/10.1111/mbe.12318

Nelson, R.J., Zucker, I., 1981. Absence of extraocular photoreception in diurnal and nocturnal rodents exposed to direct sunlight. Comparative Biochemistry and Physiology Part A: Physiology 69, 145–148. https://doi.org/10.1016/0300-9629(81)90651-4

Nevala, N.E., Baden, T., 2019. A low-cost hyperspectral scanner for natural imaging and the study of animal colour vision above and under water. Sci Rep 9, 10799. https://doi.org/10.1038/s41598-019-47220-6

Newman, G.C., Hospod, F.E., 1986. Rhythm of suprachiasmatic nucleus 2-deoxyglucose uptake in vitro. Brain Res 381, 345–350. https://doi.org/10.1016/0006-8993(86)90086-7

Nilsson, D.E., Smolka, J., 2021. Quantifying biologically essential aspects of environmental light. Journal of the Royal Society Interface 18. https://doi.org/10.1098/rsif.2021.0184

Noda, H.M., Muraoka, H., Nasahara, K.N., 2021. Plant ecophysiological processes in spectral profiles: perspective from a deciduous broadleaf forest. J Plant Res 134, 737–751. https://doi.org/10.1007/s10265-021-01302-7

Northeast, R.C., Huang, Y., McKillop, L.E., Bechtold, D.A., Peirson, S.N., Piggins, H.D., Vyazovskiy, V.V., 2019. Sleep homeostasis during daytime food entrainment in mice. Sleep 42, 1–13. https://doi.org/10.1093/sleep/zsz157

Novak, C.M., Burghardt, P.R., Levine, J.A., 2012. The use of a running wheel to measure activity in rodents: Relationship to energy balance, general activity, and reward. Neurosci Biobehav Rev 36, 1001–1014. https://doi.org/10.1016/j.neubiorev.2011.12.012

Oda, G.A., Valentinuzzi, V.S., 2024. A clock for all seasons in the subterranean. J Comp Physiol A Neuroethol Sens Neural Behav Physiol 210, 677–689. https://doi.org/10.1007/s00359-023-01677-z

Okudaira, N., Kripke, D.F., Webster, J.B., 1983. Naturalistic studies of human light exposure. Am J Physiol 245, R613-615. https://doi.org/10.1152/ajpregu.1983.245.4.R613

Olde Engberink, A.H.O., Huisman, J., Michel, S., Meijer, J.H., 2020. Brief light exposure at dawn and dusk can encode day-length in the neuronal network of the mammalian circadian pacemaker. FASEB J 34, 13685–13695. https://doi.org/10.1096/fj.202001133RR

Oliver, P.L., Sobczyk, M.V., Maywood, E.S., Edwards, B., Lee, S., Livieratos, A., Oster, H., Butler, R., Godinho, S.I.H., Wulff, K., Peirson, S.N., Fisher, S.P., Chesham, J.E., Smith, J.W., Hastings, M.H., Davies, K.E., Foster, R.G., 2012. Disrupted circadian rhythms in a mouse model of schizophrenia. Current Biology li, 314–319. https://doi.org/10.1016/j.cub.2011.12.051

Ollinger, S.V., 2011. Sources of variability in canopy reflectance and the convergent properties of plants. New Phytologist 189, 375–394. https://doi.org/10.1111/j.1469-8137.2010.03536.x

Onishi, K.G., Maneval, A.C., Cable, E.C., Tuohy, M.C., Scasny, A.J., Sterina, E., Love, J.A., Riggle, J.P., Malamut, L.K., Mukerji, A., Novo, J.S., Appah-Sampong, A., Gary, J.B., Prendergast, B.J., 2020. Circadian and circannual timescales interact to generate seasonal changes in immune function. Brain Behav Immun 83, 33–43. https://doi.org/10.1016/j.bbi.2019.07.024

Ono, D., Weaver, D.R., Hastings, M.H., Honma, K.-I., Honma, S., Silver, R., 2024. The Suprachiasmatic Nucleus at 50: Looking Back, Then Looking Forward. J Biol Rhythms 39, 135–165. https://doi.org/10.1177/07487304231225706

Otto, C., Nilsson, L.M., 1981. Why Do Beech and Oak Trees Retain Leaves Until Spring? Oikos 37, 387–390. https://doi.org/10.2307/3544134

Ouyang, Y., Andersson, C.R., Kondo, T., Golden, S.S., Johnson, C.H., 1998. Resonating circadian clocks enhance fitness in cyanobacteria. Proc Natl Acad Sci U S A 95, 8660–8664. https://doi.org/10.1073/pnas.95.15.8660

Owens, L., Buhr, E., Tu, D.C., Lamprecht, T.L., Lee, J., Van Gelder, R.N., 2012. Effect of Circadian Clock Gene Mutations on Nonvisual Photoreception in the Mouse. Investigative Ophthalmology & Visual Science 53, 454–460. https://doi.org/10.1167/iovs.11-8717

Palmer, G., Johnsen, S., 2015. Downwelling spectral irradiance during evening twilight as a function of the lunar phase. Appl. Opt., AO 54, B85–B92. https://doi.org/10.1364/AO.54.000B85

Panda, S., Antoch, M.P., Miller, B.H., Su, A.I., Schook, A.B., Straume, M., Schultz, P.G., Kay, S.A., Takahashi, J.S., Hogenesch, J.B., 2002a. Coordinated Transcription of Key Pathways in the Mouse by the Circadian Clock. Cell 109, 307–320. https://doi.org/10.1016/S0092-8674(02)00722-5

Panda, S., Nayak, S.K., Campo, B., Walker, J.R., Hogenesch, J.B., Jegla, T., 2005. Illumination of the melanopsin signaling pathway. Science 307, 600–604. https://doi.org/10.1126/science.1105121

Panda, S., Provencio, I., Tu, D.C., Pires, S.S., Rollag, M.D., Castrucci, A.M., Pletcher, M.T., Sato, T.K., Wiltshire, T., Andahazy, M., Kay, S.A., Van Gelder, R.N., Hogenesch, J.B., 2003. Melanopsin is required for non-image-forming photic responses in blind mice. Science 301, 525–527. https://doi.org/10.1126/science.1086179

Panda, S., Sato, T.K., Castrucci, A.M., Rollag, M.D., DeGrip, W.J., Hogenesch, J.B., Provencio, I., Kay, S.A., 2002b. Melanopsin (Opn4) requirement for normal light-induced circadian phase shifting. Science 298, 2213–2216. https://doi.org/10.1126/science.1076848

Paranjpe, D.A., Anitha, D., Kumar, S., Kumar, D., Verkhedkar, K., Chandrashekaran, M.K., Joshi, A., Sharma, V.K., 2003. Entrainment of eclosion rhythm in Drosophila melanogaster populations reared for more than 700 generations in constant light environment. Chronobiol Int 20, 977–987. https://doi.org/10.1081/cbi-120025247

Paul, M.J., Zucker, I., Schwartz, W.J., 2007. Tracking the seasons: the internal calendars of vertebrates. Philosophical Transactions of the Royal Society B: Biological Sciences 363, 341–361. https://doi.org/10.1098/rstb.2007.2143

Peirson, S.N., Brown, L.A., Pothecary, C.A., Benson, L.A., Fisk, A.S., 2018. Light and the laboratory mouse. Journal of Neuroscience Methods 300, 26–36. https://doi.org/10.1016/j.jneumeth.2017.04.007

Peirson, S.N., Haiford, S., Foster, R.G., 2009. The evolution of irradiance detection: Melanopsin and the non-visual opsins. Philosophical Transactions of the Royal Society B: Biological Sciences 364, 2849–2865. https://doi.org/10.1098/rstb.2009.0050

Peirson, S.N., Thompson, S., Hankins, M.W., Foster, R.G., 2005. Mammalian photoentrainment: Results, methods, and approaches. Methods in Enzymology 393, 697–726. https://doi.org/10.1016/S0076-6879(05)93037-1

Pellow, S., Chopin, P., File, S.E., Briley, M., 1985. Validation of open:closed arm entries in an elevated plus-maze as a measure of anxiety in the rat. J Neurosci Methods 14, 149–167. https://doi.org/10.1016/0165-0270(85)90031-7

Penninx, B.W.J.H., Pine, D.S., Holmes, E.A., Reif, A., 2021. Anxiety disorders. Lancet 397, 914–927. https://doi.org/10.1016/S0140-6736(21)00359-7

Pernold, K., Iannello, F., Low, B.E., Rigamonti, M., Rosati, G., Scavizzi, F., Wang, J., Raspa, M., Wiles, M.V., Ulfhake, B., 2019. Towards large scale automated cage monitoring - Diurnal rhythm and

impact of interventions on in-cage activity of C57BL/6J mice recorded 24/7 with a non-disrupting capacitive-based technique. PLoS ONE 14, 1–20. https://doi.org/10.1371/journal.pone.0211063

Phifer-Rixey, M., Nachman, M.W., 2015. Insights into mammalian biology from the wild house mouse Mus musculus. eLife 4, e05959. https://doi.org/10.7554/eLife.05959

Pilorz, V., Tam, S.K.E., Hughes, S., Pothecary, C.A., Jagannath, A., Hankins, M.W., Bannerman, D.M., Lightman, S.L., Vyazovskiy, V.V., Nolan, P.M., Foster, R.G., Peirson, S.N., 2016. Melanopsin Regulates Both Sleep-Promoting and Arousal-Promoting Responses to Light. PLoS Biology 14, 1–24. https://doi.org/10.1371/journal.pbio.1002482

Pittendrigh, C.S., 1960. Circadian Rhythms and the Circadian Organization of Living Systems. Cold Spring Harb Symp Quant Biol 25, 159–184. https://doi.org/10.1101/SQB.1960.025.01.015

Pittendrigh, C.S., 1958. Perspectives in the study of biological clocks. In Perspectives in Marine Biology,AA Buzati-Traverso, ed, pp 239-268, University of California Press, Berkeley.https://doi.org/10.1525/9780520350281-020

Pittendrigh, C.S., Daan, S., 1976. A functional analysis of circadian pacemakers in nocturnal rodents. J. Comp. Physiol. 106, 291–331. https://doi.org/10.1007/BF01417859

Pittendrigh, C.S., Minis, D.H., 1964. The Entrainment of Circadian Oscillations by Light and Their Role as Photoperiodic Clocks. The American Naturalist 98, 261–294.

Pittler, S.J., Baehr, W., 1991. Identification of a nonsense mutation in the rod photoreceptor cGMP phosphodiesterase beta-subunit gene of the rd mouse. Proc. Natl. Acad. Sci. U.S.A. 88, 8322–8326. https://doi.org/10.1073/pnas.88.19.8322

Plaza, A., Martinez, P., Perez, R., Plaza, J., 2002. Spatial/spectral endmember extraction by multidimensional morphological operations. IEEE Transactions on Geoscience and Remote Sensing 40, 2025–2041. https://doi.org/10.1109/TGRS.2002.802494

Poehn, B., Krishnan, S., Zurl, M., Coric, A., Rokvic, D., Häfker, N.S., Jaenicke, E., Arboleda, E., Orel, L., Raible, F., Wolf, E., Tessmar-Raible, K., 2022. A Cryptochrome adopts distinct moon- and sunlight states and functions as sun- versus moonlight interpreter in monthly oscillator entrainment. Nat Commun 13, 5220. https://doi.org/10.1038/s41467-022-32562-z

Pratt, B.L., Goldman, B.D., 1986. Activity rhythms and photoperiodism of syrian hamsters in a simulated burrow system. Physiology & Behavior 36, 83–89. https://doi.org/10.1016/0031-9384(86)90078-8

Provencio, I., Foster, R.G., 1995. Circadian rhythms in mice can be regulated by photoreceptors with cone-like characteristics. Brain research 694, 183–190. https://doi.org/10.1016/0006-8993(95)00694-L

Provencio, Jiang, G., De Grip, W.J., Hayes, W.P., Rollag, M.D., 1998. Melanopsin: An opsin in melanophores, brain, and eye. Proceedings of the National Academy of Sciences 95, 340–345. https://doi.org/10.1073/pnas.95.1.340

Provencio, Rodriguez, I.R., Jiang, G., Hayes, W.P., Moreira, E.F., Rollag, M.D., 2000. A Novel Human Opsin in the Inner Retina. J. Neurosci. 20, 600–605. https://doi.org/10.1523/JNEUROSCI.20-02-00600.2000

Prut, L., Belzung, C., 2003. The open field as a paradigm to measure the effects of drugs on anxiety-like behaviors: a review. European Journal of Pharmacology, Animal Models of Anxiety Disorders 463, 3–33. https://doi.org/10.1016/S0014-2999(03)01272-X

Puller, C., Haverkamp, S., 2011. Bipolar cell pathways for color vision in non-primate dichromats. Vis Neurosci 28, 51–60. https://doi.org/10.1017/S0952523810000271

Qiu, Y., Zhao, Z., Klindt, D., Kautzky, M., Szatko, K.P., Schaeffel, F., Rifai, K., Franke, K., Busse, L., Euler, T., 2021. Natural environment statistics in the upper and lower visual field are reflected in mouse retinal specializations. Current Biology 31, 3233-3247.e6. https://doi.org/10.1016/j.cub.2021.05.017

Ralph, M.R., Foster, R.G., Davis, F.C., Menaker, M., 1990. Transplanted suprachiasmatic nucleus determines circadian period. Science 247, 975–978. https://doi.org/10.1126/science.2305266

Ralph, M.R., Menaker, M., 1988. A Mutation of the Circadian System in Golden Hamsters. Science 241, 1225–1227. https://doi.org/10.1126/science.3413487

Rångtell, F.H., Ekstrand, E., Rapp, L., Lagermalm, A., Liethof, L., Búcaro, M.O., Lingfors, D., Broman, J.-E., Schiöth, H.B., Benedict, C., 2016. Two hours of evening reading on a self-luminous tablet vs. reading a physical book does not alter sleep after daytime bright light exposure. Sleep Med 23, 111–118. https://doi.org/10.1016/j.sleep.2016.06.016

Rao, S., Chun, C., Fan, J., Kofron, J.M., Yang, M.B., Hegde, R.S., Ferrara, N., Copenhagen, D.R., Lang, R.A., 2013. A direct and melanopsin-dependent fetal light response regulates mouse eye development. Nature 494, 243–246. https://doi.org/10.1038/nature11823

Rattenborg, N.C., de la Iglesia, H.O., Kempenaers, B., Lesku, J.A., Meerlo, P., Scriba, M.F., 2017. Sleep research goes wild: new methods and approaches to investigate the ecology, evolution and functions of sleep. Philos Trans R Soc Lond B Biol Sci 372, 20160251. https://doi.org/10.1098/rstb.2016.0251

Rayleigh, Lord, 1899. XXXIV. On the transmission of light through an atmosphere containing small particles in suspension, and on the origin of the blue of the sky. The London, Edinburgh, and Dublin Philosophical Magazine and Journal of Science, 47(287), 375–384.https://doi.org/10.1080/14786449908621276

Rea, M., Figueiro, M., Bullough, J., 2002. Circadian photobiology: an emerging framework for lighting practice and research. Lighting Research & Technology 34, 177–187. https://doi.org/10.1191/1365782802lt057oa

Refinetti, R., 2004. Daily activity patterns of a nocturnal and a diurnal rodent in a seminatural environment. Physiology and Behavior 82, 285–294. https://doi.org/10.1016/j.physbeh.2004.03.015

Rezende, E.L., Cortés, A., Bacigalupe, L.D., Nespolo, R.F., Bozinovic, F., 2003. Ambient temperature limits above-ground activity of the subterranean rodent *Spalacopus cyanus*. Journal of Arid Environments 55, 63–74. https://doi.org/10.1016/S0140-1963(02)00259-8

Richter, C.P., 1965. Biological Clocks in Medicine and Psychiatry. Medical Journal of Australia 2, 500–500. https://doi.org/10.5694/j.1326-5377.1965.tb18974.x

Richter, C.P., 1922. A Behavioristic Study of the Activity of the Rat. Comparative Psychology Monographs 1, 2, 56–56.

Richter, S.H., Garner, J.P., Würbel, H., 2009. Environmental standardization: cure or cause of poor reproducibility in animal experiments? Nat Methods 6, 257–261. https://doi.org/10.1038/nmeth.1312

Riede, S.J., van der Vinne, V., Hut, R.A., 2017. The flexible clock: predictive and reactive homeostasis, energy balance and the circadian regulation of sleep–wake timing. Journal of Experimental Biology 220, 738–749. https://doi.org/10.1242/jeb.130757

Robbers, Y., Koster, E.A.S., Krijbolder, D.I., Ruijs, A., van Berloo, S., Meijer, J.H., 2015. Temporal behaviour profiles of *Mus musculus* in nature are affected by population activity. Physiology & Behavior 139, 351–360. https://doi.org/10.1016/j.physbeh.2014.11.020

Rodgers, R.J., Lee, C., Shepherd, J.K., 1992. Effects of diazepam on behavioural and antinociceptive responses to the elevated plus-maze in male mice depend upon treatment regimen and prior maze experience. Psychopharmacology (Berl) 106, 102–110. https://doi.org/10.1007/BF02253596

Roenneberg, T., Daan, S., Merrow, M., 2003. The art of entrainment. J Biol Rhythms 18, 183–194. https://doi.org/10.1177/0748730403018003001

Roenneberg, T., Foster, R.G., 1997. Twilight Times: Light and the Circadian System. Photochemistry and Photobiology 66, 549–561. https://doi.org/10.1111/j.1751-1097.1997.tb03188.x

Roenneberg, T., Hastings, J.W., 1988. Two photoreceptors control the circadian clock of a unicellular alga. Naturwissenschaften 75, 206–207. https://doi.org/10.1007/BF00735584

Roenneberg, T., Hut, R., Daan, S., Merrow, M., 2010. Entrainment Concepts Revisited. J Biol Rhythms 25, 329–339. https://doi.org/10.1177/0748730410379082

Roenneberg, T., Merrow, M., 2016. The Circadian Clock and Human Health. Curr Biol 26, R432-443. https://doi.org/10.1016/j.cub.2016.04.011

Roenneberg, T., Merrow, M., 2002. Life before the clock: modeling circadian evolution. J Biol Rhythms 17, 495–505. https://doi.org/10.1177/0748730402238231

Roenneberg, T., Merrow, M., 1999. Circadian Systems and Metabolism. J Biol Rhythms 14, 449–459. https://doi.org/10.1177/074873099129001019

Röhlich, P., van Veen, T., Szél, A., 1994. Two different visual pigments in one retinal cone cell. Neuron 13, 1159–1166. https://doi.org/10.1016/0896-6273(94)90053-1

Rosbash, M., 2009. The Implications of Multiple Circadian Clock Origins. PLoS Biology | www.plosbiology.org 7, 1000062. https://doi.org/10.1371/journal.pbio.1000062

Rosenwasser, A.M., Boulos, Z., Terman, M., 1983. Circadian feeding and drinking rhythms in the rat under complete and skeleton photoperiods. Physiology & Behavior 30, 353–359. https://doi.org/10.1016/0031-9384(83)90138-5

Ruby, N.F., Brennan, T.J., Xie, X., Cao, V., Franken, P., Heller, H.C., O'Hara, B.F., 2002. Role of Melanopsin in Circadian Responses to Light. Science 298, 2211–2213. https://doi.org/10.1126/science.1076701

Rüger, M., Gordijn, M.C.M., Beersma, D.G.M., de Vries, B., Daan, S., 2005. Nasal versus temporal illumination of the human retina: effects on core body temperature, melatonin, and circadian phase. J Biol Rhythms 20, 60–70. https://doi.org/10.1177/0748730404270539

Rupp, A.C., Ren, M., Altimus, C.M., Fernandez, D.C., Richardson, M., Turek, F., Hattar, S., Schmidt, T.M., 2019. Distinct ipRGC subpopulations mediate light's acute and circadian effects on body temperature and sleep. Elife 8, e44358. https://doi.org/10.7554/eLife.44358

Rushton, W. a. H., 1972. Review Lecture. Pigments and signals in colour vision. The Journal of Physiology 220, 1–31. https://doi.org/10.1113/jphysiol.1972.sp009719

Saini, C., Liani, A., Curie, T., Gos, P., Kreppel, F., Emmenegger, Y., Bonacina, L., Wolf, J.-P., Poget, Y.-A., Franken, P., Schibler, U., 2013. Real-time recording of circadian liver gene expression in freely moving mice reveals the phase-setting behavior of hepatocyte clocks. Genes Dev 27, 1526–1536. https://doi.org/10.1101/gad.221374.113

Sandi, C., Loscertales, M., Guaza, C., 1997. Experience-dependent facilitating effect of corticosterone on spatial memory formation in the water maze. Eur J Neurosci 9, 637–642. https://doi.org/10.1111/j.1460-9568.1997.tb01412.x

Sandi, C., Pinelo-Nava, M.T., 2007. Stress and Memory: Behavioral Effects and Neurobiological Mechanisms. Neural Plasticity 2007, 078970. https://doi.org/10.1155/2007/78970

Saper, C.B., Scammell, T.E., Lu, J., 2005. Hypothalamic regulation of sleep and circadian rhythms. Nature 437, 1257–1263. https://doi.org/10.1038/nature04284

Sato, T., Kawamura, H., 1984. Circadian rhythms in multiple unit activity inside and outside the suprachiasmatic nucleus in the diurnal chipmunk (Eutamias sibiricus). Neurosci Res 1, 45–52. https://doi.org/10.1016/0168-0102(84)90029-4

Sawant, O.B., Horton, A.M., Zucaro, O.F., Chan, R., Bonilha, V.L., Samuels, I.S., Rao, S., 2017. The Circadian Clock Gene Bmal1 Controls Thyroid Hormone-Mediated Spectral Identity and Cone Photoreceptor Function. Cell Rep 21, 692–706. https://doi.org/10.1016/j.celrep.2017.09.069

Schlaich, A.E., Bouten, W., Bretagnolle, V., Heldbjerg, H., Klaassen, R.H.G., Sørensen, I.H., Villers, A., Both, C., 2017. A circannual perspective on daily and total flight distances in a long-distance migratory raptor, the Montagu's harrier, Circus pygargus. Biol Lett 13, 20170073. https://doi.org/10.1098/rsbl.2017.0073

Schlangen, L.J.M., Price, L.L.A., 2021. The Lighting Environment, Its Metrology, and Non-visual Responses. Front. Neurol. 12. https://doi.org/10.3389/fneur.2021.624861

Schlichting, M., Grebler, R., Menegazzi, P., Helfrich-Förster, C., 2015. Twilight Dominates Over Moonlight in Adjusting Drosophila's Activity Pattern. J Biol Rhythms 30, 117–128. https://doi.org/10.1177/0748730415575245

Schmid, B., Helfrich-Förster, C., Yoshii, T., 2011. A new ImageJ plug-in "actogramJ" for chronobiological analyses. Journal of Biological Rhythms 26, 464–467. https://doi.org/10.1177/0748730411414264

Schmid-Holmes, S., Drickamer, L.C., Robinson, A.S., Gillie, L.L., 2001. Burrows and Burrow-Cleaning Behavior of House Mice (Mus musculus domesticus). amid 146, 53–62. https://doi.org/10.1674/0003-0031(2001)146[0053:BABCBO]2.0.CO;2

Schmidt, T.M., Chen, S.K., Hattar, S., 2011. Intrinsically photosensitive retinal ganglion cells: Many subtypes, diverse functions. Trends in Neurosciences 34, 572–580. https://doi.org/10.1016/j.tins.2011.07.001

Schmidt, T.M., Taniguchi, K., Kofuji, P., 2008. Intrinsic and extrinsic light responses in melanopsin-expressing ganglion cells during mouse development. J Neurophysiol 100, 371–384. https://doi.org/10.1152/jn.00062.2008

Schmuckler, M.A., 2001. What Is Ecological Validity? A Dimensional Analysis. Infancy 2, 419–436. https://doi.org/10.1207/S15327078IN0204_02

Schwartz, W.J., Gainer, H., 1977. Suprachiasmatic Nucleus: Use of 14C-Labeled Deoxyglucose Uptake as a Functional Marker. Science 197, 1089–1091. https://doi.org/10.1126/science.887940

Schwartz, W.J., Helm, B., Gerkema, M.P., 2017. Wild clocks: preface and glossary. https://doi.org/10.1098/rstb.2017.0211

Schwartz, W.J., Reppert, S.M., Eagan, S.M., Moore-Ede, M.C., 1983. In vivo metabolic activity of the suprachiasmatic nuclei: a comparative study. Brain Res 274, 184–187. https://doi.org/10.1016/0006-8993(83)90538-3

Sekaran, S., Foster, R.G., Lucas, R.J., Hankins, M.W., 2003. Calcium Imaging Reveals a Network of Intrinsically Light-Sensitive Inner-Retinal Neurons. Current biology : CB. 13. 1290-8. https://doi.org/10.1016/S0960-9822(03)00510-4.

Sekaran, S., Lupi, D., Jones, S.L., Sheely, C.J., Hattar, S., Yau, K.-W., Lucas, R.J., Foster, R.G., Hankins, M.W., 2005. Melanopsin-dependent photoreception provides earliest light detection in the mammalian retina. Curr Biol 15, 1099–1107. https://doi.org/10.1016/j.cub.2005.05.053

Selby, C.P., Thompson, C., Schmitz, T.M., Van Gelder, R.N., Sancar, A., 2000. Functional redundancy of cryptochromes and classical photoreceptors for nonvisual ocular photoreception in mice. Proc Natl Acad Sci U S A 97, 14697–14702. https://doi.org/10.1073/pnas.260498597

Semo, M., Gias, C., Ahmado, A., Sugano, E., Allen, A.E., Lawrence, J.M., Tomita, H., Coffey, P.J., Vugler, A.A., 2010. Dissecting a Role for Melanopsin in Behavioural Light Aversion Reveals a Response Independent of Conventional Photoreception. PLoS ONE 5, e15009. https://doi.org/10.1371/journal.pone.0015009

Shamay-Tsoory, S.G., Mendelsohn, A., 2019. Real-Life Neuroscience: An Ecological Approach to Brain and Behavior Research. Perspect Psychol Sci 14, 841–859. https://doi.org/10.1177/1745691619856350

Shand, J., Foster, R.G., 1999. The extraretinal photoreceptors of non-mammalian vertebrates, in: Archer, S.N., Djamgoz, M.B.A., Loew, E.R., Partridge, J.C., Vallerga, S. (Eds.), Adaptive Mechanisms in the Ecology of Vision. Springer Netherlands, Dordrecht, pp. 197–222. https://doi.org/10.1007/978-94-017-0619-3_7

Sharma, V.K., 2003. Adaptive Significance of Circadian Clocks. Chronobiology International 20, 901–919. https://doi.org/10.1081/CBI-120026099

Sharma, V.K., Chandrashekaran, M.K., Nongkynrih, P., 1997. Daylight and Artificial Light Phase Response Curves for the Circadian Rhythm in Locomotor Activity of the Field Mouse Mus booduga. Biological Rhythm Research 28, 39–49. https://doi.org/10.1076/brhm.28.3.5.39.13131

Sheeba, V., Sharma, V.K., Chandrashekaran, M.K., Joshi, A., 1999. Persistence of eclosion rhythm in Drosophila melanogaster after 600 generations in an aperiodic environment. Naturwissenschaften 86, 448–449. https://doi.org/10.1007/s001140050651

Shemesh, Y., Cohen, M., Bloch, G., 2007. Natural plasticity in circadian rhythms is mediated by reorganization in the molecular clockwork in honeybees; Natural plasticity in circadian rhythms is mediated by reorganization in the molecular clockwork in honeybees. The FASEB Journal, Research Communication J 21, 2304–2311. https://doi.org/10.1096/fj.06-8032com

Shiwen, L., Steel, L., Dahlsjö, C.A., Peirson, S.N., Shenkin, A., Morimoto, T., Smithson, H.E., Spitschan, M., 2021. Hyperspectral characterisation of natural illumination in woodland and forest environments 7. https://doi.org/10.1117/12.2595301

Siegel, J.M., 2020. Sleep under evolutionarily relevant conditions. Sleep Med 67, 244–245. https://doi.org/10.1016/j.sleep.2020.01.003

Signoroni, A., Savardi, M., Baronio, A., Benini, S., 2019. Deep Learning Meets Hyperspectral Image Analysis: A Multidisciplinary Review. J Imaging 5, 52. https://doi.org/10.3390/jimaging5050052

Sikka, G., Hussmann, G.P., Pandey, D., Cao, S., Hori, D., Park, J.T., Steppan, J., Kim, J.H., Barodka, V., Myers, A.C., Santhanam, L., Nyhan, D., Halushka, M.K., Koehler, R.C., Snyder, S.H., Shimoda, L.A., Berkowitz, D.E., 2014. Melanopsin mediates light-dependent relaxation in blood vessels. Proc Natl Acad Sci U S A 111, 17977–17982. https://doi.org/10.1073/pnas.1420258111

Simoncelli, E.P., Olshausen, B.A., 2001. Natural Image Statistics and Neural Representation. Annu. Rev. Neurosci. 24, 1193–1216. https://doi.org/10.1146/annurev.neuro.24.1.1193

Sinturel, F., Gos, P., Petrenko, V., Hagedorn, C., Kreppel, F., Storch, K.-F., Knutti, D., Liani, A., Weitz, C., Emmenegger, Y., Franken, P., Bonacina, L., Dibner, C., Schibler, U., 2021. Circadian hepatocyte clocks keep synchrony in the absence of a master pacemaker in the suprachiasmatic nucleus or other extrahepatic clocks. Genes Dev. 35, 329–334. https://doi.org/10.1101/gad.346460.120

Siraji, M.A., Lazar, R.R., van Duijnhoven, J., Schlangen, L.J.M., Haque, S., Kalavally, V., Vetter, C., Glickman, G.L., Smolders, K.C.H.J., Spitschan, M., 2023. An inventory of human light exposure behaviour. Sci Rep 13, 22151. https://doi.org/10.1038/s41598-023-48241-y

Sliney, D.H., 2016. What is light? the visible spectrum and beyond. Eye (Basingstoke) 30, 222–229. https://doi.org/10.1038/eye.2015.252

Smith, K., 2023. Lab mice go wild: making experiments more natural in order to decode the brain. Nature 618, 448–450. https://doi.org/10.1038/d41586-023-01926-w

Sokolove, P.G., Bushell, W.N., 1978. The chi square periodogram: Its utility for analysis of circadian rhythms. Journal of Theoretical Biology 72, 131–160. https://doi.org/10.1016/0022-5193(78)90022-X

Solessio, E., Engbretson, G.A., 1993. Antagonistic chromatic mechanisms in photoreceptors of the parietal eye of lizards. Nature 364, 442–445. https://doi.org/10.1038/364442a0

Somers, B., Asner, G.P., Tits, L., Coppin, P., 2011. Endmember variability in Spectral Mixture Analysis: A review. Remote Sensing of Environment 115, 1603–1616. https://doi.org/10.1016/j.rse.2011.03.003

Sonoda, T., Li, J.Y., Hayes, N.W., Chan, J.C., Okabe, Y., Belin, S., Nawabi, H., Schmidt, T.M., 2020. A noncanonical inhibitory circuit dampens behavioral sensitivity to light. Science 368, 527–531. https://doi.org/10.1126/science.aay3152

Spitschan, M., Aguirre, G.K., Brainard, D.H., Sweeney, A.M., 2016. Variation of outdoor illumination as a function of solar elevation and light pollution. Scientific reports, 6, 26756. https://doi.org/10.1038/srep26756

Spitschan, M., Jain, S., Brainard, D.H., Aguirre, G.K., 2014. Opponent melanopsin and S-cone signals in the human pupillary light response. Proceedings of the National Academy of Sciences 111, 15568–15572. https://doi.org/10.1073/pnas.1400942111

Spitschan, M., Lucas, R.J., Brown, T.M., 2017. Chromatic clocks: Color opponency in non-image-forming visual function. Neurosci Biobehav Rev 78, 24–33. https://doi.org/10.1016/j.neubiorev.2017.04.016

Spitschan, M., Woelders, T., 2018. The Method of Silent Substitution for Examining Melanopsin Contributions to Pupil Control. Front. Neurol. 9. https://doi.org/10.3389/fneur.2018.00941

Spoelstra, K., Wikelski, M., Daan, S., Loudon, A.S.I., Hau, M., 2016. Natural selection against a circadian clock gene mutation in mice. Proc Natl Acad Sci U S A 113, 686–691. https://doi.org/10.1073/pnas.1516442113

Stabio, M.E., Sabbah, S., Quattrochi, L.E., Ilardi, M.C., Fogerson, P.M., Leyrer, M.L., Kim, M.T., Kim, I., Schiel, M., Renna, J.M., Briggman, K.L., Berson, D.M., 2018. The M5 Cell: A Color-Opponent Intrinsically Photosensitive Retinal Ganglion Cell. Neuron 97, 150-163.e4. https://doi.org/10.1016/j.neuron.2017.11.030

Stangl, M., Maoz, S.L., Suthana, N., 2023. Mobile cognition: imaging the human brain in the 'real world.' Nat Rev Neurosci 24, 347–362. https://doi.org/10.1038/s41583-023-00692-y

Steel, L.C.E., Tir, S., Tam, S.K.E., Bussell, J.N., Spitschan, M., Foster, R.G., Peirson, S.N., 2022. Effects of Cage Position and Light Transmission on Home Cage Activity and Circadian Entrainment in Mice. Frontiers in neuroscience, 15, 832535. https://doi.org/10.3389/fnins.2021.832535.

Stehle, J.H., von Gall, C., Korf, H.-W., 2002. Organisation of the circadian system in melatonin-proficient C3H and melatonin-deficient C57BL mice: a comparative investigation. Cell Tissue Res 309, 173–182. https://doi.org/10.1007/s00441-002-0583-2

Stemmer, M., Schuhmacher, L.-N., Foulkes, N.S., Bertolucci, C., Wittbrodt, J., 2015. Cavefish eye loss in response to an early block in retinal differentiation progression. Development 142, 743–752. https://doi.org/10.1242/dev.114629

Stephan, F.K., 1983. Circadian rhythms in the rat: Constant darkness, entrainment to T cycles and to skeleton photoperiods. Physiology & Behavior 30, 451–462. https://doi.org/10.1016/0031-9384(83)90152-X

Stephan, F.K., Zucker, I., 1972. Circadian Rhythms in Drinking Behavior and Locomotor Activity of Rats Are Eliminated by Hypothalamic Lesions. Proc. Natl. Acad. Sci. U.S.A. 69, 1583–1586. https://doi.org/10.1073/pnas.69.6.1583

Stern, A., 2021. Ultraviolet Hyperspectral Imaging Opens New Research Opportunities. URL: https://www.electrooptics.com

Stokkan, K.-A., Folkow, L., Dukes, J., Neveu, M., Hogg, C., Siefken, S., Dakin, S.C., Jeffery, G., 2013. Shifting mirrors: adaptive changes in retinal reflections to winter darkness in Arctic reindeer. Proceedings of the Royal Society B: Biological Sciences 280, 20132451. https://doi.org/10.1098/rspb.2013.2451

Stokkan, K.-A., Yamazaki, S., Tei, H., Sakaki, Y., Menaker, M., 2001. Entrainment of the Circadian Clock in the Liver by Feeding. Science 291, 490–493. https://doi.org/10.1126/science.291.5503.490

Storch, K.-F., Lipan, O., Leykin, I., Viswanathan, N., Davis, F.C., Wong, W.H., Weitz, C.J., 2002. Extensive and divergent circadian gene expression in liver and heart. Nature 417, 78–83. https://doi.org/10.1038/nature744

Stothard, E.R., McHill, A.W., Depner, C.M., Birks, B.R., Moehlman, T.M., Ritchie, H.K., Guzzetti, J.R., Chinoy, E.D., LeBourgeois, M.K., Axelsson, J., Wright, K.P., 2017. Circadian Entrainment to the Natural Light-Dark Cycle across Seasons and the Weekend. Current Biology 27, 508–513. https://doi.org/10.1016/j.cub.2016.12.041

Strauss, O., 2005. The Retinal Pigment Epithelium in Visual Function. Physiological Reviews 85, 845–881. https://doi.org/10.1152/physrev.00021.2004

Sun, D., Gao, W., Hu, H., Zhou, S., 2022. Why 90% of clinical drug development fails and how to improve it? Acta Pharmaceutica Sinica B 12, 3049–3062. https://doi.org/10.1016/j.apsb.2022.02.002

Sun, H., Macke, J.P., Nathans, J., 1997. Mechanisms of spectral tuning in the mouse green cone pigment. Proceedings of the National Academy of Sciences of the United States of America, 94(16), 8860–8865. https://doi.org/10.1073/pnas.94.16.8860

Sutherland, D., Singleton, G., 2003. Monitoring activity patterns and social interactions of small mammals with an automated event recording system: Wild house mice (Mus domesticus) as a case study. pp. 159–164.

Svaetichin, G., MacNichol., E.F., 1958. Retinal Mechanisms for Chromatic and Achromatic Vision. Annals of the New York Academy of Sciences 74, 385–404. https://doi.org/10.1111/j.1749-6632.1958.tb39560.x

Sweeney, B.M., Hastings, J.W., 1960. Effects of Temperature upon Diurnal Rhythms. Cold Spring Harb Symp Quant Biol 25, 87–104. https://doi.org/10.1101/SQB.1960.025.01.009

Swetter, B.J., Karpiak, C.P., Cannon, J.T., 2011. Separating the effects of shelter from additional cage enhancements for group-housed BALB/cJ mice. Neurosci Lett 495, 205–209. https://doi.org/10.1016/j.neulet.2011.03.067

Szatko, K.P., Korympidou, M.M., Ran, Y., Berens, P., Dalkara, D., Schubert, T., Euler, T., Franke, K., 2020. Neural circuits in the mouse retina support color vision in the upper visual field. Nat Commun 11, 3481. https://doi.org/10.1038/s41467-020-17113-8

Takahashi, J.S., 2017. Transcriptional architecture of the mammalian circadian clock. Nat Rev Genet 18, 164–179. https://doi.org/10.1038/nrg.2016.150

Tam, S.K.E., Brown, L.A., Wilson, T.S., Tir, S., Fisk, S., Pothecary, C.A., Vinne, V.V.D., Foster, R.G., Vyazovskiy, V.V., Bannerman, D.M., Harrington, M.E., Peirson, S.N., 2021. Dim Light in the Evening Causes Coordinated Realignment of Circadian Rhythms , Sleep and Short-term Memory.

Tam, S.K.E., Hasan, S., Hughes, S., Hankins, M.W., Foster, R.G., Bannerman, D.M., Peirson, S.N., 2016. Modulation of recognition memory performance by light requires both melanopsin and classical photoreceptors. Proceedings of the Royal Society B: Biological Sciences 283. https://doi.org/10.1098/rspb.2016.2275

Tamayo, E., Mouland, J.W., Lucas, R.J., Brown, T.M., 2023. Regulation of mouse exploratory behaviour by irradiance and cone-opponent signals. BMC Biology 21, 178. https://doi.org/10.1186/s12915-023-01663-6

Tamotsu, S., Morita, Y., 1986. Photoreception in pineal organs of larval and adult lampreys, Lampetra japonica. J Comp Physiol A 159, 1–5. https://doi.org/10.1007/BF00612489

Tao, J., Zhang, X., Liu, Y., Jiang, Q., Zhou, Y., 2023. Estimating Agricultural Cropping Intensity Using a New Temporal Mixture Analysis Method from Time Series MODIS. Remote Sensing 15, 4712. https://doi.org/10.3390/rs15194712

Thompson, S., Foster, R.G., Stone, E.M., Sheffield, V.C., Mrosovsky, N., 2008. Classical and melanopsin photoreception in irradiance detection: negative masking of locomotor activity by light. Eur J Neurosci 27, 1973–1979. https://doi.org/10.1111/j.1460-9568.2008.06168.x

Tir, S., Steel, L.C.E., Tam, S.K.E., Semo, M., Pothecary, C.A., Vyazovskiy, V.V., Foster, R.G., Peirson, S.N., 2022. Chapter 6 - Rodent models in translational circadian photobiology, in: Santhi, N., Spitschan, M. (Eds.), Progress in Brain Research, Circadian and Visual Neuroscience. Elsevier, pp. 97–116. https://doi.org/10.1016/bs.pbr.2022.02.015

Tomotani, B.M., Flores, D.E.F.L., Tachinardi, P., Paliza, J.D., Oda, G.A., Valentinuzzi, V.S., 2012. Field and Laboratory Studies Provide Insights into the Meaning of Day-Time Activity in a Subterranean Rodent (Ctenomys aff. knighti), the Tuco-Tuco. PLoS ONE 7, e37918. https://doi.org/10.1371/journal.pone.0037918

Troxell-Smith, S.M., Tutka, M.J., Albergo, J.M., Balu, D., Brown, J.S., Leonard, J.P., 2016. Foraging decisions in wild versus domestic *Mus musculus*: What does life in the lab select for? Behavioural Processes 122, 43–50. https://doi.org/10.1016/j.beproc.2015.10.020

Tsai, J.W., Hannibal, J., Hagiwara, G., Colas, D., Ruppert, E., Ruby, N.F., Heller, H.C., Franken, P., Bourgin, P., 2009. Melanopsin as a sleep modulator: Circadian gating of the direct effects of light on sleep and altered sleep homeostasis in Opn4-/- mice. PLoS Biology 7. https://doi.org/10.1371/journal.pbio.1000125

Turner, P.V., Pang, D.S., Lofgren, J.L., 2019. A Review of Pain Assessment Methods in Laboratory Rodents. Comp Med 69, 451–467. https://doi.org/10.30802/AALAS-CM-19-000042

Twente, John W., 1955. Some Aspects of Habitat Selection and Other Behavior of Cavern-Dwelling Bats. Ecology 36, 706–732. https://doi.org/10.2307/1931308

Ueda, H.R., Matsumoto, A., Kawamura, M., Iino, M., Tanimura, T., Hashimoto, S., 2002. Genome-wide Transcriptional Orchestration of Circadian Rhythms inDrosophila. Journal of Biological Chemistry 277, 14048–14052. https://doi.org/10.1074/jbc.C100765200

Ueno, H., Takahashi, Y., Murakami, S., Wani, K., Matsumoto, Y., Okamoto, M., Ishihara, T., 2024. Effects of home-cage elevation on behavioral tests in mice. Brain and Behavior 14, e3269. https://doi.org/10.1002/brb3.3269

Underwood, H., Calaban, M., 1987. Pineal melatonin rhythms in the lizard Anolis carolinensis: II. Photoreceptive inputs. J Biol Rhythms 2, 195–206. https://doi.org/10.1177/074873048700200303

Underwood, H., Steele, C.T., Zivkovic, B., 2001. Circadian organization and the role of the pineal in birds. Microsc Res Tech 53, 48–62. https://doi.org/10.1002/jemt.1068

Ustin, S.L., Jacquemoud, S., 2020. How the Optical Properties of Leaves Modify the Absorption and Scattering of Energy and Enhance Leaf Functionality, in: Cavender-Bares, J., Gamon, J.A., Townsend, P.A. (Eds.), Remote Sensing of Plant Biodiversity. Springer International Publishing, Cham, pp. 349–384. https://doi.org/10.1007/978-3-030-33157-3_14

Usui, S., Takahashi, Y., Okazaki, T., 2000. Range of entrainment of rat circadian rhythms to sinusoidal light-intensity cycles. American Journal of Physiology-Regulatory, Integrative and Comparative Physiology 278, R1148–R1156. https://doi.org/10.1152/ajpregu.2000.278.5.R1148

van Bommel, W., van den Beld, G., 2004. Lighting for work: a review of visual and biological effects. Lighting Research & Technology 36, 255–266. https://doi.org/10.1191/1365782804li122oa

van der Horst, G.T., Muijtjens, M., Kobayashi, K., Takano, R., Kanno, S., Takao, M., de Wit, J., Verkerk, A., Eker, A.P., van Leenen, D., Buijs, R., Bootsma, D., Hoeijmakers, J.H., Yasui, A., 1999. Mammalian Cry1 and Cry2 are essential for maintenance of circadian rhythms. Nature 398, 627–630. https://doi.org/10.1038/19323

van der Kooi, C.J., Stavenga, D.G., Arikawa, K., Belušič, G., Kelber, A., 2021. Evolution of Insect Color Vision: From Spectral Sensitivity to Visual Ecology. Annu Rev Entomol 66, 435–461. https://doi.org/10.1146/annurev-ento-061720-071644

Van Der Veen, D.R., Riede, S.J., Heideman, P.D., Hau, M., Van Der Vinne, V., Hut, R.A., 2017. Flexible clock systems: adjusting the temporal programme. https://doi.org/10.1098/rstb.2016.0254

van der Vinne, V., Gorter, J.A., Riede, S.J., Hut, R.A., 2015. Diurnality as an energy-saving strategy: energetic consequences of temporal niche switching in small mammals. Journal of Experimental Biology 218, 2585–2593. https://doi.org/10.1242/jeb.119354

van der Vinne, V., Riede, S.J., Gorter, J.A., Eijer, W.G., Sellix, M.T., Menaker, M., Daan, S., Pilorz, V., Hut, R.A., 2014. Cold and hunger induce diurnality in a nocturnal mammal. Proceedings of the National Academy of Sciences 111, 15256–15260. https://doi.org/10.1073/pnas.1413135111

Van der Zee, E.A., Havekes, R., Barf, R.P., Hut, R.A., Nijholt, I.M., Jacobs, E.H., Gerkema, M.P., 2008. Circadian time-place learning in mice depends on Cry genes. Curr Biol 18, 844–848. https://doi.org/10.1016/j.cub.2008.04.077

van Diepen, H.C., Ramkisoensing, A., Peirson, S.N., Foster, R.G., Meijer, J.H., 2013. Irradiance encoding in the suprachiasmatic nuclei by rod and cone photoreceptors. FASEB J 27, 4204–4212. https://doi.org/10.1096/fj.13-233098

van Diepen, H.C., Schoonderwoerd, R.A., Ramkisoensing, A., Janse, J.A.M., Hattar, S., Meijer, J.H., 2021. Distinct contribution of cone photoreceptor subtypes to the mammalian biological clock. Proceedings of the National Academy of Sciences 118, e2024500118. https://doi.org/10.1073/pnas.2024500118

van Dorp, R., Rolleri, E., Deboer, T., 2024. Sleep and the sleep electroencephalogram in C57BL/6 and C3H/HeN mice. Journal of Sleep Research 33, e14062. https://doi.org/10.1111/jsr.14062

Van Gelder, R.N., Wee, R., Lee, J.A., Tu, D.C., 2003. Reduced Pupillary Light Responses in Mice Lacking Cryptochromes. Science 299, 222–222. https://doi.org/10.1126/science.1079536

Van Oosterhout, F., Fisher, S.P., Van Diepen, H.C., Watson, T.S., Houben, T., Vanderleest, H.T., Thompson, S., Peirson, S.N., Foster, R.G., Meijer, J.H., 2012. Ultraviolet light provides a major input to non-image-forming light detection in mice. Current Biology 22, 1397–1402. https://doi.org/10.1016/j.cub.2012.05.032

Van Someren, E.J.W., Swaab, D.F., Colenda, C.C., Cohen, W., McCall, W.V., Rosenquist, P.B., 1999. Bright light therapy: Improved sensitivity to its effects on rest- activity rhythms in Alzheimer patients by application of nonparametric methods. Chronobiology International 16, 505–518. https://doi.org/10.3109/07420529908998724

Viitala, J., Korplmäki, E., Palokangas, P., Koivula, M., 1995. Attraction of kestrels to vole scent marks visible in ultraviolet light. Nature 373, 425–427. https://doi.org/10.1038/373425a0

Visser, E.K., Beersma, D.G., Daan, S., 1999. Melatonin suppression by light in humans is maximal when the nasal part of the retina is illuminated. J Biol Rhythms 14, 116–121. https://doi.org/10.1177/074873099129000498

Voelkl, B., Altman, N.S., Forsman, A., Forstmeier, W., Gurevitch, J., Jaric, I., Karp, N.A., Kas, M.J., Schielzeth, H., Van de Casteele, T., Würbel, H., 2020. Reproducibility of animal research in light of biological variation. Nat Rev Neurosci 21, 384–393. https://doi.org/10.1038/s41583-020-0313-3

Võikar, V., Stanford, S.C., 2023. The Open Field Test, in: Harro, J. (Ed.), Psychiatric Vulnerability, Mood, and Anxiety Disorders: Tests and Models in Mice and Rats. Springer US, New York, NY, pp. 9–29. https://doi.org/10.1007/978-1-0716-2748-8_2

Völgyi, B., Chheda, S., Bloomfield, S.A., 2009. Tracer coupling patterns of the ganglion cell subtypes in the mouse retina. J Comp Neurol 512, 664–687. https://doi.org/10.1002/cne.21912

Voûte, A.M., Sluiter, J.W., Grimm, M.P., 1974. The influence of the natural light-dark cycle on the activity rhythm of pond bats (Myotis dasycneme Boie, 1825) during summer. Oecologia 17, 221–243. https://doi.org/10.1007/BF00344923

Walker, D.L., Toufexis, D.J., Davis, M., 2003. Role of the bed nucleus of the stria terminalis versus the amygdala in fear, stress, and anxiety. Eur J Pharmacol 463, 199–216. https://doi.org/10.1016/s0014-2999(03)01282-2

Walls, G.L., Walls, G.L., 1942. The vertebrate eye and its adaptive radiation. Cranbrook Institute of Science, Bloomfield Hills, Mich. https://doi.org/10.5962/bhl.title.7369

Walmsley, L., Hanna, L., Mouland, J., Martial, F., West, A., Smedley, A.R., Bechtold, D.A., Webb, A.R., Lucas, R.J., Brown, T.M., 2015. Colour As a Signal for Entraining the Mammalian Circadian Clock. PLOS Biology 13, e1002127. https://doi.org/10.1371/journal.pbio.1002127

Wang, J.-S., Kefalov, V.J., 2011. The Cone-specific visual cycle. Progress in Retinal and Eye Research 30, 115–128. https://doi.org/10.1016/j.preteyeres.2010.11.001

Wang, Q., Timberlake, M.A., Prall, K., Dwivedi, Y., 2017. The Recent Progress in Animal Models of Depression. Prog Neuropsychopharmacol Biol Psychiatry 77, 99–109. https://doi.org/10.1016/j.pnpbp.2017.04.008

Weaver, D.R., 1998. The Suprachiasmatic Nucleus: A 25-Year Retrospective. J Biol Rhythms 13, 100–112. https://doi.org/10.1177/074873098128999952

Webler, F.S., Spitschan, M., Foster, R.G., Andersen, M., Peirson, S.N., 2019. What is the "spectral diet" of humans? Curr Opin Behav Sci. 2019 Dec;30:80-86. doi: 10.1016/j.cobeha.2019.06.006. Epub 2019 Aug 13. PMID: 31431907; PMCID: PMC6701986.

Webster, M.A., Mizokami, Y., Webster, S.M., 2007. Seasonal variations in the color statistics of natural images. Network: Computation in Neural Systems 18, 213–233. https://doi.org/10.1080/09548980701654405

Wehr, T.A., 1991. The Durations of Human Melatonin Secretion and Sleep Respond to Changes in Daylength (Photoperiod). The Journal of Clinical Endocrinology & Metabolism 73, 1276–1280. https://doi.org/10.1210/jcem-73-6-1276

Weihe, W.H., Schidlow, J., Strittmatter, J., 1969. The effect of light intensity on the breeding and development of rats and golden hamsters. International Journal of Biometeorology 13, 69–79. https://doi.org/10.1007/BF02329580

Welsh, D.K., Logothetis, D.E., Meister, M., Reppert, S.M., 1995. Individual neurons dissociated from rat suprachiasmatic nucleus express independently phased circadian firing rhythms. Neuron 14, 697–706. https://doi.org/10.1016/0896-6273(95)90214-7

Weng, S., Estevez, M.E., Berson, D.M., 2013. Mouse Ganglion-Cell Photoreceptors Are Driven by the Most Sensitive Rod Pathway and by Both Types of Cones. PLOS ONE 8, e66480. https://doi.org/10.1371/journal.pone.0066480

West, A.C., Bechtold, D.A., 2015. The cost of circadian desynchrony: Evidence, insights and open questions. BioEssays 37, 777–788. https://doi.org/10.1002/bies.201400173

West, A.C., Smith, L., Ray, D.W., Loudon, A.S.I., Brown, T.M., Bechtold, D.A., 2017. Misalignment with the external light environment drives metabolic and cardiac dysfunction. Nat Commun 8, 417. https://doi.org/10.1038/s41467-017-00462-2

Wever, R., 1964. Zum Mechanismus der biologischen 24-Stunden-Periodik. Kybernetik 2, 127–144. https://doi.org/10.1007/BF00306797

Wiedenmayer, C., 1997. Causation of the ontogenetic development of stereotypic digging in gerbils. Animal Behaviour 53, 461–470. https://doi.org/10.1006/anbe.1996.0296

Williams, C.T., Barnes, B.M., Yan, L., Buck, C.L., 2017. Entraining to the polar day: circadian rhythms in arctic ground squirrels. J Exp Biol 220, 3095–3102. https://doi.org/10.1242/jeb.159889

Wisor, J.P., O'Hara, B.F., Terao, A., Selby, C.P., Kilduff, T.S., Sancar, A., Edgar, D.M., Franken, P., 2002. A role for cryptochromes in sleep regulation. BMC Neurosci 3, 20. https://doi.org/10.1186/1471-2202-3-20

Woelders, T., Wams, E.J., Gordijn, M.C.M., Beersma, D.G.M., Hut, R.A., 2018. Integration of color and intensity increases time signal stability for the human circadian system when sunlight is obscured by clouds. Sci Rep 8, 15214. https://doi.org/10.1038/s41598-018-33606-5

Woelfle, M.A., Ouyang, Y., Phanvijhitsiri, K., Johnson, C.H., 2004. The adaptive value of circadian clocks: an experimental assessment in cyanobacteria. Curr Biol 14, 1481–1486. https://doi.org/10.1016/j.cub.2004.08.023

Wong, J.C.Y., Smyllie, N.J., Banks, G.T., Pothecary, C.A., Barnard, A.R., Maywood, E.S., Jagannath, A., Hughes, S., van der Horst, G.T.J., MacLaren, R.E., Hankins, M.W., Hastings, M.H., Nolan, P.M., Foster, R.G., Peirson, S.N., 2018. Differential roles for cryptochromes in the mammalian retinal clock. FASEB J 32, 4302–4314. https://doi.org/10.1096/fj.201701165RR

Wright, K.P., McHill, A.W., Birks, B.R., Griffin, B.R., Rusterholz, T., Chinoy, E.D., 2013. Entrainment of the human circadian clock to the natural light-dark cycle. Current Biology 23, 1554–1558. https://doi.org/10.1016/j.cub.2013.06.039

Würbel, H., 2001. Ideal homes? Housing effects on rodent brain and behaviour. Trends Neurosci 24, 207–211. https://doi.org/10.1016/s0166-2236(00)01718-5

Xue, T., Do, M.T.H., Riccio, A., Jiang, Z., Hsieh, J., Wang, H.C., Merbs, S.L., Welsbie, D.S., Yoshioka, T., Weissgerber, P., Stolz, S., Flockerzi, V., Freichel, M., Simon, M.I., Clapham, D.E., Yau, K.-W., 2011. Melanopsin signalling in mammalian iris and retina. Nature 479, 67–73. https://doi.org/10.1038/nature10567

Xue, Y., Shen, S.Q., Corbo, J.C., Kefalov, V.J., 2015. Circadian and light-driven regulation of rod dark adaptation. Sci Rep 5, 17616. https://doi.org/10.1038/srep17616

Yamazaki, S., Numano, R., Abe, M., Hida, A., Takahashi, R., Ueda, M., Block, G.D., Sakaki, Y., Menaker, M., Tei, H., 2000. Resetting Central and Peripheral Circadian Oscillators in Transgenic Rats. Science 288, 682–685. https://doi.org/10.1126/science.288.5466.682

Yau, K.W., 1994. Phototransduction mechanism in retinal rods and cones. The Friedenwald Lecture. Invest Ophthalmol Vis Sci 35, 9–32.

Yilmaz, M., Meister, M., 2013. Rapid innate defensive responses of mice to looming visual stimuli. Curr Biol 23, 2011–2015. https://doi.org/10.1016/j.cub.2013.08.015

Yoo, S.-H., Yamazaki, S., Lowrey, P.L., Shimomura, K., Ko, C.H., Buhr, E.D., Siepka, S.M., Hong, H.-K., Oh, W.J., Yoo, O.J., Menaker, M., Takahashi, J.S., 2004. PERIOD2::LUCIFERASE real-time reporting of circadian dynamics reveals persistent circadian oscillations in mouse peripheral tissues. Proceedings of the National Academy of Sciences 101, 5339–5346. https://doi.org/10.1073/pnas.0308709101

Yoshimura, T., Ebihara, S., 1996. Spectral sensitivity of photoreceptors mediating phase-shifts of circadian rhythms in retinally degenerate CBA/J (rd/rd) and normal CBA/N (+ / +) mice. Journal of Comparative Physiology A: Sensory, Neural, and Behavioral Physiology 178, 797–802. https://doi.org/10.1007/BF00225828

Yoshimura, T., Nishio, M., Ebihara, S., Goto, M., 1994. Differences in circadian photosensitivity between retinally degenerate CBA/J mice (rd/rd) and normal CBA/N mice (+/+). Journal of biological rhythms 9, 51–60. https://doi.org/10.1177/074873049400900105

Zele, A.J., Feigl, B., Adhikari, P., Maynard, M.L., Cao, D., 2018. Melanopsin photoreception contributes to human visual detection, temporal and colour processing. Sci Rep 8, 3842. https://doi.org/10.1038/s41598-018-22197-w

Zhang, R., Lahens, N.F., Ballance, H.I., Hughes, M.E., Hogenesch, J.B., 2014. A circadian gene expression atlas in mammals: Implications for biology and medicine. Proceedings of the National Academy of Sciences 111, 16219–16224. https://doi.org/10.1073/pnas.1408886111

Zhang, X.Y., Diaz-delCastillo, M., Kong, L., Daniels, N., MacIntosh-Smith, W., Abdallah, A., Domanski, D., Sofrenovic, D., Yeung, T.P. (Skel), Valiente, D., Vollert, J., Sena, E., Rice, A.S., Soliman, N., 2023. A systematic review and meta-analysis of thigmotactic behaviour in the open field test in rodent models associated with persistent pain. PLOS ONE 18, e0290382. https://doi.org/10.1371/journal.pone.0290382